

# **Influence of Hofmeister Anions on the Krafft Temperature, Surface and Bulk Behaviour of Ionic Surfactants in Aqueous Solution**

**By**

**Khokan Chandra Sarker**

**Submitted for the partial fulfillment of the requirement for the Degree of  
Doctor of Philosophy (Ph.D)**




**Department of chemistry  
Bangladesh University of Engineering and Technology (BUET)  
Dhaka-1000, Bangladesh  
22 February, 2021**

## Certification of Thesis


The thesis titled 'Influence of Hofmeister Anions on the Krafft Temperature, Surface and Bulk behaviour of Ionic surfactants in aqueous solution' submitted by Khokan Chandra Sarker, Roll No.: 0412034203P, Session: April, 2012 has been accepted as satisfactory in partial fulfillment of the requirement for the degree of Doctor of Philosophy (Ph. D) on 22 February, 2021.

### BOARD OF EXAMINERS

1. Dr. Md. Nazrul Islam  
Professor  
Department of Chemistry, BUET, Dhaka.  
(Supervisor)

  
22/02/2021  
Chairman

2. Head (Dr. Md. Shakhsanul Hossain Firoz)  
Department of Chemistry, BUET, Dhaka.

  
Member (Ex-officio)

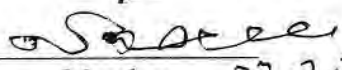
3. Dr. Md. Manwarul Islam  
Ex-Professor  
Department of Chemistry, BUET, Dhaka.

  
Member

4. Dr. Md. Rafique Ullah  
Professor  
Department of Chemistry, BUET, Dhaka.

  
Member

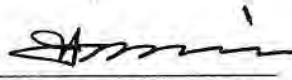
5. Dr. Nazrul Islam  
Ex-Professor  
Department of Chemistry, BUET, Dhaka.

  
Member 22.2.21

6. Dr. Mahbub Kabir  
Professor  
Department of Chemistry,  
Jahangirnagar University, Savar, Dhaka.

  
Member

7. Dr. Md. Mufazzal Hossain  
Professor  
Department of Chemistry,  
University of Dhaka.

  
Member (External)

## CANDIDATE'S DECLARATION

It is hereby declared that this thesis or any part of it has not been submitted elsewhere for the award of any degree or diploma.

Signature of the Candidate

*Khokan Chandra Sarker*

.....

Name of the Candidate: *Khokan Chandra Sarker*

## **DEDICATION**

**I dedicate this thesis to my Creator.**

# Table of Contents

Title	Page No.
Certification of Thesis	i
Candidate's declaration	ii
Dedication	iii
Table of Contents	iv
List of tables	ix
List of figures	x
List of Abbreviations of Technical Symbols and Terms	xiv
Layout of this thesis	xvi
Acknowledgements	xvii
Abstract	xviii
<b>Chapter one: Introduction</b>	
1.1 Introduction	1
1.2 Classification of surfactants	3
1.2.1 Anionic surfactants	4
1.2.2 Cationic surfactants	5
1.2.3 Nonionic surfactants	5
1.2.4 Zwitterionic surfactants	5
1.3 Krafft Temperature ( $T_K$ )	6
1.4 Micelle	7
1.4.1 Factors affecting the value of the CMC in aqueous solution	10
1.4.1.1 Structure of the surfactant	10
1.4.1.1.1 The hydrophobic group	10
1.4.1.1.2 The hydrophilic group	11
1.4.1.1.3 The counter-ion in ionic surfactants	12
1.4.1.2 The presence of added electrolyte in the solution	12
1.4.1.3 The presence of various organic compounds in the solution	13
1.4.1.4 Temperature of the solution	13

1.4.1.5	The effect of pH	14
1.5	Surface or interfacial tension	15
1.6	Thermodynamics of adsorption	16
1.7	Solubilization	19
1.8	Factors affecting the extent of solubilization	22
1.8.1	Structure of the surfactant	22
1.8.2	Structure of the solubilizate	22
1.8.3	Effect of electrolytes	23
1.8.4	Effect of organic additives	24
1.8.5	Effect of temperature	24
1.9	Applications of surfactants	25
1.9.1	Surfactants as detergents and cleaners	25
1.9.2	Surfactants in cosmetics, and personal care products	26
1.9.3	Surfactants in foods and food packaging	26
1.9.4	Surfactants in crop protection and pest control	27
1.9.5	Surfactants in chemical industry	27
1.9.6	Surfactants in textiles and fibers	28
1.9.7	Surfactants in leather and furs	28
1.9.8	Paints, lacquers, and other coating products	29
1.10	Aims and objectives of the present work	29

## **Chapter two: Chemicals and experimental procedures**

2.1	<b>Chemicals</b>	32
2.1.1	Surfactant	32
2.1.2	Salts	32

2.1.3	Dye	33
2.2	Experimental procedures	34
2.2.1	Krafft temperature measurement	34
2.2.2	CMC measurement	34
2.2.2.1	CMC measurement by conductometric method	34
2.2.2.2	CMC measurement by surface tensiometric method	35
2.2.3	The measurement of solubilization of water insoluble dye in the micellar system	35
2.2.4	The measurement of the metal-ligand complex in the micellar system	36
2.2.4.1	The measurement of the formation constant of the complex	37
2.2.5	UV–Vis. Spectrophotometric measurements	37
2.2.6	ATR–IR spectrophotometric measurement	38
2.2.7	Proton nuclear magnetic resonance ( $^1\text{H}$ NMR) spectroscopic measurement	39

### **Chapter three: Results and discussion**

3.1	Effect of potassium salts on the Krafft temperature ( $T_K$ ) of CPB and CPC in aqueous system	41
3.2	Effect of potassium salts on the critical micelle concentration (CMC) of CPC and CPB	48
3.2.1	Proton nuclear magnetic resonance ( $^1\text{H}$ NMR) spectra of CPB above and below the CMC	55
3.2.2	Proton nuclear magnetic resonance ( $^1\text{H}$ NMR) spectra of CPC above and below the CMC	57
3.3	Surface tension of aqueous solution of CPB and CPC in pure water and in the presence of different potassium salts	59
3.3.1	Surface excess concentration ( $\Gamma_{\text{max}}$ ) of CPB and CPC in aqueous system	63
3.4	Thermodynamic properties of CPB and CPC in aqueous system	66
3.5	Solubilization of PAN and curcumin in aqueous solution of CPB and CPC in pure water and in the presence of $5 \times 10^{-3}$ M $\text{KNO}_3$ and $1.66 \times 10^{-3}$ M $\text{K}_2\text{SO}_4$ respectively	72

3.5.1	The location of PAN solubilized in the micelle of CPB	76
3.5.2	The location of curcumin solubilized in the micelle of CPC	78
3.6	Complexation of Ni(II), Cu(II), Zn(II) with PAN in aqueous solution of CPB and Cu(II) with curcumin in aqueous solution of CPC	79
3.6.1	Stoichiometry of Cu(II)-PAN complex in aqueous solution of CPB	80
3.6.2	Effect of time on Cu(II)-PAN complex formation in aqueous solution of CPB	82
3.6.3	Calibration graph for Cu(II)-PAN complex in aqueous solution of CPB	82
3.6.4	The location of Cu(II)-PAN complex in the micelle of CPB in aqueous solution	83
3.7	Stoichiometry of Ni(II)-PAN complex in aqueous solution of CPB	84
3.7.1	Effect of time on Ni(II)-PAN complex formation in aqueous solution of CPB	86
3.7.2	Calibration graph for Ni(II)-PAN complex in aqueous solution of CPB	87
3.8	Stoichiometry of Zn(II)-PAN complex in aqueous solution of CPB	87
3.8.1	Effect of time on Zn(II)-PAN complex formation in aqueous solution of CPB	89
3.8.2	Calibration graph for Zn(II)-PAN complex in aqueous solution of CPB	89
3.9	Stoichiometry of Cu(II)-curcumin complex in aqueous solution of CPC	90
3.9.1	Calibration graph for Cu(II)-curcumin complex in aqueous solution of CPC	92
3.9.2	The location of Cu(II)-curcumin complex in the micelle of CPC in aqueous solution	93
3.10	ATR-IR spectra of CPC in aqueous solution in the presence of curcumin and Cu(II)-curcumin complex	94



<b>3.10.1</b>	ATR-IR spectra of CPB in aqueous solution, in the presence of PAN, and Cu(II)- PAN complex	<b>95</b>
<b>3.11</b>	Conclusions	<b>96</b>
	Scope of further work	<b>99</b>
	References	<b>100</b>
	Appendix	<b>111</b>
	Calculation	<b>148</b>

## List of tables

3.1	Degree of counter-ion binding, the CMC of CPB in pure water and in the presence of different potassium salts	53
3.2	Degree of counter-ion binding, the CMC of CPC in pure water and in the presence of different potassium salts	54
3.3	The surface tension of the solvent ( $\gamma_o$ ), surface tension of aqueous solution of CPC at CMC ( $\gamma_{CMC}$ ), and surface pressure ( $\pi_{CMC}$ ) of aqueous solution of CPC in pure water and in the presence of different potassium salts when ionic strength is $5 \times 10^{-3}$	62
3.4	The surface tension of the solvent ( $\gamma_o$ ), surface tension of aqueous solution of CPB at CMC ( $\gamma_{CMC}$ ), surface pressure ( $\pi_{CMC}$ ) of aqueous solution of CPB in pure water and in the presence of different potassium salts when ionic strength is $5 \times 10^{-3}$	63
3.5	The surface excess concentration ( $\Gamma_{max}$ ) of CPC in pure water and in the presence of different potassium salts when ionic strength is $5 \times 10^{-3}$	65
3.6	The surface excess concentration ( $\Gamma_{max}$ ) of aqueous solution of CPB in pure water and in the presence of different potassium salts when ionic strength is $5 \times 10^{-3}$	66
3.7	$\Delta G_{mic}^\circ$ , $\Delta G_{ad}^\circ$ , $\Delta H_{mic}^\circ$ , $\Delta H_{ad}^\circ$ , $\Delta S_{mic}^\circ$ , $\Delta S_{ad}^\circ$ for CPB and CPC in pure water at different temperatures	68
3.8	The values of the $T_c^*$ for CPB and CPC in aqueous solution	72

## List of figures

1.1	The basic structure of a cationic surfactant, cetylpyridinium bromide (CPB).	4
1.2	Schematic representation of the solubility curve for the ionic surfactants. (The Krafft temperature ( $T_K$ ) is the temperature at which surfactant solubility equals the CMC. Above the $T_K$ surfactant molecules form a dispersed phase; below the $T_K$ hydrated crystals are formed.	7
1.3	The structure of a spherical micelle.	8
1.4	Variation in physical properties of surfactant solutions below and above the CMC value.	9
1.5	Dependence of surface tension of solutions on solute concentration.	18
1.6	Different regions in the micelle on the basis of different solubilization sites which can be recognized.	19
1.7	Amount of material solubilized as a function of concentration of surfactant solution.	20
2.1	Structure of cetylpyridinium bromide (CPB)	32
2.2	Structure of cetylpyridinium chloride (CPC)	32
2.3	Structure of 1-(2-pyridylazo)-2-naphthal (PAN).	33
2.4	Structure of curcumin	33
3.1	Specific conductance ( $\mu\text{S}/\text{cm}$ ) versus temperature ( $^{\circ}\text{C}$ ) plot for (a) CPB in pure water; (b) CPC in pure water. (The arrow signs in the plots indicate the Krafft temperature)	41
3.1	Specific conductance ( $\mu\text{S}\text{cm}^{-1}$ ) versus temperature ( $^{\circ}\text{C}$ ) plots for (c) CPB (0.01 M); and (d) CPC (0.01 M) in pure water and in the presence of different potassium salts KF, KCl, KBr, KI, KSCN, $\text{KNO}_3$ , $\text{K}_2\text{SO}_4$ , $\text{K}_2\text{CO}_3$ , $\text{K}_2\text{HPO}_4$ and $\text{CuSO}_4$ when ionic strength of each salt is $2.5 \times 10^{-3}$	42
3.2	Surface tension (mN/m) versus temperature ( $^{\circ}\text{C}$ ) plot for (a) CPB (0.01 M) and (b) CPC (0.01 M) in pure water. (The arrow signs in the plots indicate the Krafft temperature.)	43
3.3	The Krafft Temperature ( $T_K$ ) versus salt concentration plots for (a) CPB (0.01M) in pure water and in the presence of different potassium salts (i) $\text{KNO}_3$ , (ii) $\text{K}_2\text{SO}_4$ , (iii) KCl, (iv) $\text{K}_2\text{HPO}_4$ , (v) $\text{K}_2\text{CO}_3$ , (vi) KF, (vii) KBr, (viii) KSCN, (ix) KI, and (x) $\text{CuSO}_4$ where ionic strengths of the salts are from $2.5 \times 10^{-3}$ to $12.5 \times 10^{-3}$ ; (b) CPC (0.01M) in pure water and in the presence of different potassium salts (i) $\text{K}_2\text{SO}_4$ , (ii) $\text{CuSO}_4$ , (iii) $\text{K}_2\text{HPO}_4$ , (iv) KF, (v) $\text{KNO}_3$ , (vi) KCl, (vii) $\text{K}_2\text{CO}_3$ , (viii) KBr, (ix) KSCN, and (x) KI where ionic strengths of the salts are from $2.5 \times 10^{-3}$ to $12.5 \times 10^{-3}$	44
3.4	Specific conductance versus concentration plots for (a) CPB in pure water at (i) $30^{\circ}\text{C}$ , (ii) $35^{\circ}\text{C}$ (iii) $40^{\circ}\text{C}$ , (iv) $45^{\circ}\text{C}$ ; (b) CPC in pure water at (i) $20^{\circ}\text{C}$ , (ii) $25^{\circ}\text{C}$ (iii) $30^{\circ}\text{C}$ , (iv) $35^{\circ}\text{C}$ , (v) $40^{\circ}\text{C}$ , (vi) $45^{\circ}\text{C}$	49
3.5	(a) Critical micelle concentration (CMC) versus temperature (K) plot for CPB in pure water; (b) Critical micelle concentration (mM) versus	49

temperature (°C) plot for CPC in pure water

3.6	Critical micelle concentration versus temperature (°C) plots for (a) CPB in the presence of $5 \times 10^{-3}$ M KBr and (b) in the presence of $5 \times 10^{-3}$ M KNO <sub>3</sub>	52
3.7	Critical micelle concentration versus temperature (°C) for CPC (a) in the presence of $5 \times 10^{-3}$ M KCl; (b) in the presence of K <sub>2</sub> SO <sub>4</sub> at $5 \times 10^{-3}$ ionic strength	52
3.8	<sup>1</sup> H NMR spectra of CPB in aqueous solution below the CMC ( $5 \times 10^{-3}$ M)	56
3.9	<sup>1</sup> H NMR spectra of CPB in aqueous solution above the CMC	57
3.10	<sup>1</sup> H NMR spectra of CPC in aqueous solution below the CMC	58
3.11	<sup>1</sup> H NMR spectra of CPC in aqueous solution above the CMC	58
3.12	Surface tension (mN/m) versus Log <sub>10</sub> C plots for aqueous solution of CPB (a) in pure water and (b) in the presence of K <sub>2</sub> CO <sub>3</sub> at 45 °C when ionic strength is $5 \times 10^{-3}$	60
3.13	Surface Tension versus Log <sub>10</sub> C plots for aqueous solution of CPC (a) in pure water and (b) in the presence of K <sub>2</sub> SO <sub>4</sub> at 45 °C when ionic strength is $5 \times 10^{-3}$	60
3.14	(a) Surface excess concentration of CPB (i) in pure water, (ii) in the presence of $5 \times 10^{-3}$ M KNO <sub>3</sub> , (iii) in the presence of $5 \times 10^{-3}$ M KBr; (b) Surface excess concentration of CPC (i) in pure water, (ii) in the presence of $5 \times 10^{-3}$ M KCl, (iii) in the presence of $1.66 \times 10^{-3}$ M K <sub>2</sub> SO <sub>4</sub> .	64
3.15	Enthalpy-Entropy compensation plots for CPB in aqueous solution (a) micellization, (b) adsorption	70
3.16	Enthalpy-Entropy compensation plots for CPC in aqueous solution (a) micellization, (b) adsorption	71
3.17	(a) Absorption spectra of PAN in aqueous solution of CPB where the concentrations of CPB are (i) pure water, (ii) 0.42 mM, (iii) 0.52 mM, (iv) 0.62 mM, (v) 0.72 mM, (vi) 0.82 mM, (vii) 0.92 mM, (viii) 1.23 mM, (ix) 2.23 mM, and (x) 3.23 mM; (b) Absorbance of PAN against the concentration of CPB (mM).	73
3.18	(a) Absorption spectra of PAN in aqueous solution of CPB in the presence of $5 \times 10^{-3}$ M KNO <sub>3</sub> ; where the concentrations of CPB are (i) aqueous solution of $5 \times 10^{-3}$ M KNO <sub>3</sub> , (ii) 0.01 mM, (iii) 0.05 mM, (iv) 0.1 mM, (v) 0.15 mM, (vi) 0.2 mM, (vii) 0.25 mM, (viii) 0.35 mM, and (ix) 0.4 mM; (b) Absorbance of PAN against the concentration of CPB in the presence of $5 \times 10^{-3}$ M KNO <sub>3</sub>	73
3.19	(a) Absorption spectra of curcumin in aqueous solution of CPC where the concentrations of CPC are (i) pure water, (ii) 0.06 mM, (iii) 0.1 mM, (iv) 0.12 mM, (v) 0.14 mM, (vi) 0.16 mM, (vii) 0.2 mM, (viii) 0.3 mM, (ix) 0.4 mM, and (x) 0.6 mM; (b) Absorbance of curcumin versus concentration of CPC (mM)	75
3.20	(a) Absorption spectra of curcumin in aqueous solution of CPC in the presence of K <sub>2</sub> SO <sub>4</sub> , ionic strength is $5 \times 10^{-3}$ , where the concentrations of CPC are (i) aqueous solution of $1.66 \times 10^{-3}$ M K <sub>2</sub> SO <sub>4</sub> , (ii) 0.14 mM, (iii) 0.15 mM, (iv) 0.16 mM, (v) 0.18 mM, (vi) 0.19 mM, (vii) 0.2 mM, and (viii) 0.22 mM; (b) Absorbance of curcumin versus concentration	75

of CPC (M) in the presence of  $1.66 \times 10^{-3}$  M  $K_2SO_4$

3.21	$^1H$ NMR spectra of CPB above the CMC in the presence of PAN	77
3.22	$^1H$ NMR spectra of CPC above the CMC in the presence of curcumin	78
3.23	(a) Absorption spectra of Cu(II)-PAN complex in aqueous solution of CPB where the concentrations of $CuSO_4$ are (i) 2 $\mu M$ , (ii) 4 $\mu M$ , (iii) 6 $\mu M$ , (iv) 8 $\mu M$ , (v) 10 $\mu M$ , (vi) 12 $\mu M$ , (vii) 16 $\mu M$ , and (viii) 18 $\mu M$ ; (b) Absorption spectra of Cu(ii)-PAN complex in aqueous solution of CPB where the concentrations of PAN are (i) 2 $\mu M$ , (ii) 4 $\mu M$ , (iii) 6 $\mu M$ , (iv) 8 $\mu M$ , (v) 10 $\mu M$ , (vi) 12 $\mu M$ , (vii) 14 $\mu M$ , and (viii) 16 $\mu M$	80
3.24	(i) Absorbance of Cu(II)-PAN complex versus concentration of PAN when concentration of $CuSO_4$ is constant (20 $\mu M$ ); (ii) Absorbance of Cu(II)-PAN complex versus concentration of $CuSO_4$ ( $\mu M$ ) when concentration of PAN is constant (20 $\mu M$ )	81
3.25	The absorbance of Cu(II)-PAN complex in aqueous solution of CPB versus time (hour)	82
3.26	Absorbance of Cu(II)-PAN complex versus concentration ( $\mu M$ ) of $CuSO_4$ when concentration of PAN is constant (250 $\mu M$ )	83
3.27	$^1H$ NMR spectra of CPB in aqueous solution above the CMC in the presence of Cu(II)-PAN complex	84
3.28	(a) Absorption spectra of Ni(II)-PAN complex in aqueous solution of CPB where the concentrations of PAN are (i) 4 $\mu M$ , (ii) 8 $\mu M$ , (iii) 12 $\mu M$ , (iv) 16 $\mu M$ , (v) 20 $\mu M$ ; (b) Absorption spectra of Ni(II)-PAN complex in aqueous solution of CPB where the concentrations of $NiSO_4$ are (i) 4 $\mu M$ , (ii) 8 $\mu M$ , (iii) 12 $\mu M$ , (iv) 16 $\mu M$ , (v) 18 $\mu M$	85
3.29	(i) Absorbance of Ni(II)-PAN complex versus concentration of PAN when concentration of $NiSO_4$ is 20 $\mu M$ ; (ii) Absorbance of Ni(II)-PAN complex versus concentration of $NiSO_4$ when concentration of PAN is 20 $\mu M$	85
3.30	The absorbance of Ni(II)-PAN complex in aqueous solution of CPB versus time (hour)	86
3.31	Absorbance of Ni(II)-PAN complex versus concentration of $NiSO_4$ ( $\mu M$ ) when concentration of PAN is 250 $\mu M$	87
3.32	(a) Absorption spectra of Zn(II)-PAN complex in aqueous solution of CPB where the concentrations of $ZnSO_4$ are (i) 4 $\mu M$ , (ii) 8 $\mu M$ , (iii) 12 $\mu M$ , (iv) 18 $\mu M$ , (v) 20 $\mu M$ , (vi) 24 $\mu M$ ; (b) Absorption spectra of Zn(II)-PAN complex in aqueous solution of CPB where the concentrations of PAN are (i) 8 $\mu M$ , (ii) 12 $\mu M$ , (iii) 16 $\mu M$ , (iv) 20 $\mu M$ , (v) 24 $\mu M$	88
3.33	(i) Absorbance of Zn(II)-PAN complex versus concentration of PAN when the concentration of $ZnSO_4$ is 20 $\mu M$ ; (ii) Absorbance of Zn(II)-PAN complex versus concentration of $ZnSO_4$ when the concentration of PAN is 20 $\mu M$	88
3.34	The absorbance of Zn(II)-PAN complex in aqueous solution of CPB versus time (hour)	89
3.35	Absorbance of Zn(II)-PAN complex versus concentration of $ZnSO_4$ ( $\mu M$ ) when the concentration of PAN is 250 $\mu M$	90

3.36	(a) Absorption spectra of Cu(II)-Curcumin complex in aqueous solution of CPC where the concentrations of curcumin are (i) 5.45 $\mu\text{M}$ , (ii) 10.91 $\mu\text{M}$ , (iii) 21.82 $\mu\text{M}$ , (iv) 32.73 $\mu\text{M}$ , (v) 43.64 $\mu\text{M}$ ; (b) Absorption spectra of Cu(II)-curcumin complex in aqueous solution of CPC where the concentrations of $\text{CuSO}_4$ are (i) 7.97 $\mu\text{M}$ , (ii) 9.31 $\mu\text{M}$ , (iii) 10.63 $\mu\text{M}$ , (iv) 11.96 $\mu\text{M}$ , (v) 13.29 $\mu\text{M}$	91
3.37	(a) Absorbance of Cu(II)-curcumin complex against the concentration of $\text{CuSO}_4$ in aqueous solution of CPC; (b) Absorbance of Cu(II)-curcumin complex against the concentration of curcumin in aqueous solution of CPC	91
3.38	Absorbance of Cu(II)-curcumin complex versus concentration of $\text{CuSO}_4$ ( $\mu\text{M}$ ) when the concentration of curcumin is 81.4 $\mu\text{M}$	92
3.39	$^1\text{H}$ NMR spectra of CPC in aqueous solution above the CMC in the presence of Cu(II)-curcumin complex	93
3.40	ATR-IR spectra of (i) CPC in aqueous solution, (ii) aqueous solution of CPC in the presence of curcumin, and (iii) aqueous solution of CPC in the presence of Cu(II)-curcumin complex	94
3.41	ATR-IR spectra of (i) CPB in aqueous solution, (ii) aqueous solution of CPB in the presence of PAN and (iii) aqueous solution of CPB in the presence of Cu(II)-PAN complex	95

## List of Abbreviations of Technical Symbols and Terms

Symble	Description
CPC	Cetylpyridinium chloride
CPB	Cetylpyridinium bromide
$T_k$	Krafft temperature
CMC	Critical micelle concentration
$\gamma$	Surface tension
$W_{\min.}$	Minimum amount of work
$\Gamma_{\max}$	Surface excess concentration
MSR	Molar solubilization ratio
$S_w$	Molar solubility of the solubilizate
$S_{CMC}$	Molar solubility at the CMC
$C_{\text{surf}}$	Molar concentration of the surfactant
$\epsilon$	Molar Absorptivity
$^1\text{H NMR}$	Proton Nuclear Magnetic Resonance
PAN	1-(2-pyridylazo)-2-naphthal
UV-Vis.	Ultraviolet and visible
ATR-IR	Attenuated total reflection and infrared
$\kappa$	Specific conductance
$\beta$	Counter-ion binding
$\alpha$	Degree of ionization or dissociation constant
$s_2$	Slope of post-micellar region
$s_1$	Slope of pre-micellar region
$\gamma_o$	Surface tension of the solvent
$\pi_{CMC}$	Surface pressure
$\gamma_{CMC}$	Surface tension of aqueous solution of surfactant at CMC
$\Gamma_{\max}$	Surface excess concentration
R	Gas constant
$\Delta G_{mic}^\circ$	Free energy changes of micellization

$\Delta S_{mic}^{\circ}$	Entropy changes of micellization
$\Delta H_{mic}^{\circ}$	Enthalpy changes of micellization
$\Delta H_{ad}^{\circ}$	Enthalpy changes of adsorption
$\Delta G_{ad}^{\circ}$	Free energy changes of adsorption
$\Delta S_{ad}^{\circ}$	Entropy change of adsorption



## **Layout of this dissertation**

**This thesis has been divided into three chapters**

- ✓ **Chapter one deals with a general introduction. Aims and objectives of the present work are also described at the end of this chapter.**
- ✓ **Chapter two describes chemicals and experimental procedures**
- ✓ **The experimental results and discussion are presented in chapter three.**
- ✓ **In chapter three, we report**
- ✓ **The Krafft temperature ( $T_K$ ) of CPB and CPC in pure water and in the presence of different potassium salts at different ionic strength.**
- ✓ **The Critical micelle concentration (CMC) of CPB and CPC in pure water and in the presence of different potassium salts.**
- ✓ **The surface tension of aqueous solution of CPB and CPC in pure water and in the presence of different potassium salts.**
- ✓ **The thermodynamic properties of CPB and CPC in aqueous solution.**
- ✓ **The solubilization of PAN in aqueous solution of CPB in pure water and in the presence of  $5 \times 10^{-3}$  M  $KNO_3$ .**
- ✓ **The solubilization of curcumin in aqueous solution of CPB in pure water and in the presence of  $1.66 \times 10^{-3}$  M  $K_2SO_4$ .**
- ✓ **Conclusions, scope of further work and references have also been presented at the end of this chapter.**
- ✓ **Appendix has also been included at the end of this thesis.**

## Acknowledgements

In the very outset of submitting this dissertation I can't but express my deepest sense of gratitude, wholehearted indebtedness and profound regard to my respected teacher and supervisor Professor **Dr. Md. Nazrul Islam**, Department of Chemistry, BUET for all of his indispensable guidance, invaluable advice and suggestion, extremely generous help, continuous encouragement, constant support and above all his amiable behavior and patience, enabled me to finish this gigantic task within the desired time. I must confess that without his monumental contribution, continuous inspiration, and constant supervision, it would have been difficult to complete and present this dissertation in such form.

I also feel a great pleasure to convey profound veneration and deep appreciation to my respected teachers, Professor Dr. Md. Nazrul Islam (Chairman), Professor Dr. Md. Shakhawat Hossain Firoz (Head, Department of Chemistry), Professor Dr. Manwarul Islam, Professor Dr. Nazrul Islam Professor Dr. Md. Rafique Ullah and all other teachers of the Department of Chemistry, BUET for their cordial co-operation and guidance specially for providing laboratory facilities to carry out my research work even at night. Specially, I give thanks to Urea Fertilizer Factory Limited (UFFL), Ghorashal, Narsingdi an enterprise of Bangladesh Chemical Industrise Corporation (BCIC) for their generous help to continue my research work and allow me to collect demineralised water from water treatment plant of UFFL.

I like to give thanks to Mr. Komol Kanta Sharker and Mr. Shuvo Das and other lab fellows for their effective co-operations and valuable information.

I am also very grateful to my wife and all of my relatives for their inspirations and encouragement during the period of my Ph. D. study.

In fine, my heartfelt thanks to all of my well-wishers in home and abroad.

*Khokan chandra sarker*  
.....

Khokan Chandra Sarker  
22 February, 2021

## Abstract

In the present work, the influence of Hofmeister anions on the Krafft Temperature ( $T_K$ ) of cetylpyridinium chloride (CPC) and cetylpyridinium bromide (CPB) has been investigated by means of conductometric, surface tensiometric methods, and visual inspection. The surface adsorption and bulk micellization as well as the solubilization of water insoluble 1-(2-pyridylazo)-2-naphthal (PAN) and curcumin in aqueous solution of surfactants CPB and CPC have been investigated. It was found that the  $T_K$  of these surfactants depends on the nature and ionic strength of the counter-ion present in the solution. The results show that the  $T_K$  of these surfactants decreases in the presence of stronger kosmotropes as well as moderate chaotropes but increases in the presence of stronger chaotropes and the common ion compared to that of CPB and CPC in pure water. Added electrolytes also affect the surface adsorption and bulk micellization of both these surfactants. It was found that in the presence of all the anions, the CMC of both these surfactants decrease more than the CMC of these surfactants in pure water due to the neutralization of the micelle surface charge by the associated counter-ions. The CMC of these surfactants in pure water and in the presence of potassium salts was found to increase gradually with increasing temperature. The surface excess concentration ( $\Gamma_{\max}$ ) of both these surfactants was found to decrease gradually with increasing temperature and the values are much lower in the presence of electrolyte than the corresponding values of these surfactants in pure water. The thermodynamic parameters such as free energy change ( $\Delta G_{mic}^\circ, \Delta G_{ad}^\circ$ ), enthalpy change ( $\Delta H_{mic}^\circ, \Delta H_{ad}^\circ$ ), and entropy change ( $\Delta S_{mic}^\circ, \Delta S_{ad}^\circ$ ) were calculated by measuring their CMC over a wide range of temperature. The values of  $\Delta G_{mic}^\circ, \Delta G_{ad}^\circ$  are found to be negative which indicates that both the processes are spontaneous. The enthalpy and entropy terms for both adsorption and micellization are found to compensate each other. In addition, the solubilization behavior of water-insoluble PAN and curcumin in micellar system of CPB and CPC respectively was examined at 30 °C as well as complexation of Cu(II), Ni(II), Zn(II) with the PAN and Cu(II) with the curcumin in the micellar system were also studied by the UV-visible spectrophotometric technique. The location of solubilized ligands and complexes has also been measured by  $^1\text{H}$ NMR spectra of CPC and CPB in aqueous solution. It has also been found that in the presence of potassium salt, the solubilization capacity is higher than that of the surfactant in pure water.

# **Chapter one: Introduction**

## **1.1 Introduction**

Surfactants, surface active agents are amphiphilic organic compound containing both nonpolar long-chain hydrocarbon and polar head group and play important roles in many areas, including chemistry, biology, and pharmacy [1]. This dual character of the amphiphile leads to self-association or micellization in polar solvent. The interior of the micelle has essentially the properties as a liquid hydrocarbon. So, the micelles have ability to solubilize many water-insoluble organic molecules, e.g. dyes, drugs, toxic waste and agrochemicals [2]. A noteworthy characteristic feature of ionic surfactants is their tendency to precipitate from aqueous solution as hydrated solid below a certain temperature and solubility increases markedly at or above this temperature. This phenomenon is generally termed as the Krafft phenomenon and the temperature is known as the Krafft temperature ( $T_k$ ) or the melting temperature of hydrated solid crystals of surfactant [3–11]. Below the  $T_k$  the surfactants lose many of its activities such as detergency, dispersing, emulsifying and micelle forming properties and cannot exhibit maximum degree of performance [12]. Under these circumstances, only monomer solubility governs their total solubility, and monomers are in equilibrium with the hydrated solid crystals. On the other hand, above the  $T_k$  surfactant dissolves in water markedly and the total solubility of the surfactant increases sharply [3]. The  $T_k$  is specific to each individual surfactant and differs depending on the nature of the counter-ion, the size of the head group, hydrophobic chain length, and added electrolytes [3, 10, 11].

Another characteristic feature of the surfactants is that they have strong tendency to adsorb onto the air water interface and reduce the surface tension of water because of their preferential surface activity. Consequently, in the presence of surfactant, the surface tension of water decreases gradually with increasing surfactant concentration and attain a nearly constant value at the critical micelle concentration (CMC). The most common technique for measuring the CMC is measuring the surface tension ( $\gamma$ ) at different concentration. The surface tension versus  $\log C$  plot shows a break at the CMC, after which it remains almost constant with further increase in concentration at a constant temperature. With the increase of concentration, the extent of lowering the surface tension is a measure of surface activity of amphiphilic molecules and increase in surface density of the adsorbed molecules. However, salt can also accelerate the diffusion of surface-active constituents from the bulk to the interface enhancing the adsorption of surfactant. The behavior of surfactants at the interface is dependent upon a number of forces,

including electrostatic attraction, hydrogen bonding, hydrophobic attraction, and solvation of various species.

In addition, the properties of surfactant change abruptly when micelle formation occurs in the bulk of the aqueous solution [13]. The concentration at which micelle formation starts is known as the critical micelle concentration (CMC). Each surfactant molecule has a characteristic CMC at a given temperature in pure water. Micelle formation depends on different factors such as temperature, dielectric constant of the medium, the length of alkyl chain, the presence of additives, relative size, charge of the head groups, and the extent of counter-ion binding [5, 14]. Furthermore, the valency of the counter-ion in ionic surfactants has a significant effect on the CMC. The CMC decreases with the increase of counter-ion valency. At or above the CMC, surfactants show an abrupt change in a number of physical properties [4]. Below the CMC most properties of surfactants are similar to those of simple electrolytes whereas above the CMC micelles and surfactant ions are thought to co-exist, the concentration of the latter changing very slightly. However, with increasing temperature, the disruption of the ice-berg structure of water surrounding the hydrophobic group increases, which disfavor micellization [15]. On the other hand, with increasing temperature the degree of hydration of the hydrophilic head group decreases, which favours micellization. Other major factor which plays an important role in micelle formation is the presence of electrolyte in aqueous solution of surfactant. The value of CMC decreases in the presence of added electrolyte because the electrostatic repulsion between the charged head groups decreases due to the neutralization of micellar surface charge.

The interior of the micelle has essentially the properties as a liquid hydrocarbon. This is why the micelles have strong ability to solubilize many water-insoluble organic molecules, e.g. dyes, drugs, toxic waste and agrochemicals [2]. The solubilization of water insoluble organic compounds in micellar system starts when the concentration of the surfactant is equal to the CMC and solubilization increases with increasing the surfactant concentration. Below the CMC surfactant molecule exist as monomers and have only little or no influence on the solubility of water insoluble organic compounds. This can be used to determine the CMC of surfactant [2]. With increasing the concentration of surfactant the extent of solubilization of hydrophobic solutes increases with increasing the number of micelle. It provides the basis for detergency, micellar

catalysis, extraction, and formation of microemulsion [16]. Depending on the polarity of the solubilize, the specific interactions between the solubilize and the surfactant, the solubilization may occur on the surface of the micelle or at the micelle-solvent interface, between hydrophilic head groups, in the so called palisade layer of micelle between the hydrophilic head group and the first few carbon of the hydrophobic group that comprise the outer core of micellar interior, more deeply in the palisade layer, in the inner core of micelle [16]. It has been demonstrated that the location of a dye in a micelle can be assessed from the  $^1\text{H}$  NMR spectra of the dye-containing surfactant solution [17]. The value of CMC decreases in the presence of added electrolytes which is very effective in solubilizing water insoluble compounds. In this case, the temperature of the analytical solution must be above the  $T_k$  because below the  $T_k$  surfactant does not form micelles. In that case, the solubilization of water insoluble compounds in aqueous solution of surfactant will be impossible.

One of the key themes of this thesis is to study the complexation of metal ions with water insoluble ligands in aqueous solution of surfactant. This complexation is very important in different practical fields because increasing industrialization has led to considerable pollution of the environment by toxic element. Thus, the monitoring of toxic elements and their species in aqueous systems has become very important. The UV-Vis. spectrophotometric method for estimation of metal ion in aqueous solution of surfactant is a direct, simple, fast, facile, sensitive, and environmentally friendly too. Besides, the solution of organic solvents is harmful and costlier than environmentally friendly aqueous solution of surfactant. These surface active agents play important roles in many areas, including chemistry, biology and pharmacy [1, 4].

### **1.2 Classification of surfactants**

Surfactants are amphiphilic in nature, which belong to a class of compounds that reduce the interfacial surface tension due to such amphiphilic structure by adsorbing to all available interfaces as a consequence dramatically change their free energy. The polar hydrophilic portion of the surfactant molecule is referred to as the “hydrophilic head group” while the nonpolar hydrophobic, portion is referred to as the “tail” which is shown in figure-1.1.





### 1.2.2 Cationic surfactants

Cationic surfactants carry a positive charge on the surface-active portion of the molecule. Pure cationic surfactants such as cetylpyridinium bromide (CPB) have been used extensively for research into the fundamental physical chemistry of their surface activity. Cationic surfactants play an important role as an antiseptic agent in cosmetics, as general fungicides and germicides, as fabric softeners and hair conditioners, and in a number of bulk chemical applications. The usage of cationic surfactants is much lesser than that of anionic and nonionic surfactants and costlier too. Some examples of cationic surfactants are

- (a) Laurylamine hydrochloride ( $\text{CH}_3(\text{CH}_2)_{11}\text{NH}_3^+ \text{Cl}^-$ ),
- (b) Tetradecyl trimethyl ammonium bromide ( $\text{CH}_3(\text{CH}_2)_{13}\text{N}^+(\text{CH}_3)_3\text{Br}^-$ ),
- (c) Trimethyl dodecyl ammonium chloride ( $\text{C}_{12}\text{H}_{25}\text{N}^+(\text{CH}_3)_3\text{Cl}^-$ ).

### 1.2.3 Nonionic surfactants

Nonionic surfactants carry no electrical charge, as their water solubility is derived from the presence of polar functionalities capable of significant hydrogen bonding interaction with water e.g., polyoxyethylenes, sugars, polyglycidols. They have either a polyether or a polyhydroxyl unit as the polar head group. They exhibit an inverse temperature-solubility relationship; that is, as the solution temperature is increased, their solubility in water decreases. At higher temperatures, they become more hydrophobic and less water soluble which is contrary to ionic compounds. Some examples of nonionic surfactants are

- (a) Alkylphenol ethoxylate ( $\text{C}_9\text{H}_{19}\text{-C}_6\text{H}_4\text{-(OCH}_2\text{CH}_2)_n\text{OH}$ ),
- (b) Polyoxyethylene (4) dodecanol ( $\text{CH}_3(\text{CH}_2)_{11}\text{-O-(CH}_2\text{CH}_2\text{O)}_4\text{H}$ ),
- (c) Polyoxyethylene (9) hexadecanol ( $\text{CH}_3(\text{CH}_2)_{15}\text{-O-(CH}_2\text{CH}_2\text{O)}_9\text{H}$ ).

### 1.2.4 Zwitterionic surfactants

This family of surfactants commonly referred to as „amphoterics“ that contain both positive and negative functional groups depending on the pH or other solution conditions. The positive charge is almost invariably ammonium, variation may occur in the source of negative charge, although carboxylate is by far the most common. With the variation of pH from low to high, an amphoteric surfactant changes from net cationic via zwitterionic to net anionic i.e. the compound is only zwitterionic over a certain pH range. At the isoelectric point the physicochemical behavior often resembles that of nonionic

surfactants. Below and above the isoelectric point there is a gradual shift towards the cationic and anionic character, respectively. Since this class of surfactant carries both positive and negative charges, they can adsorb onto both negatively charged and positively charged surfaces without changing the charge of the surface significantly. Some examples of zwitterionic surfactants are

- (a) Lauramidopropyl betaine ( $\text{C}_{11}\text{H}_{23}\text{CONH}(\text{CH}_2)_3\text{N}^+(\text{CH}_3)_2\text{CH}_2\text{COO}^-$ ),
- (b) Dodecyl betaine ( $\text{C}_{12}\text{H}_{25}\text{N}^+(\text{CH}_3)_2\text{CH}_2\text{COO}^-$ ),
- (c) Dodecyldimethyl ammonium acetate ( $\text{CH}_3(\text{CH}_2)_{11}(\text{CH}_3)_2\text{N}^+\text{CH}_2\text{COO}^-$ ).

### **1.3 Krafft Temperature ( $T_K$ )**

Surfactants are usually composed of a hydrocarbon chain and a polar head group. Depending on the system composition, a surfactant molecule can play different roles in terms of aggregation such as formation of micelles, liquid crystals, bilayers or vesicles, etc. While most common surfactants have a substantial solubility in water, this can change significantly with variations in hydrophobic tail length, head group nature, counter-ion valence, solution environment, and most importantly temperature. Below a certain temperature, the solubility of the surfactant is very limited and stay in the solution as hydrated solid due to the coagulation of the surfactant molecules [6]. and loses many of its activities such as detergency, dispersing, emulsifying and micelle forming properties [3, 12]. Surfactants in such a crystalline state will solubilize if the temperature increases, thus causing entropy to increase and encourage the crystalline structure to break apart. At or above this temperature the hydrated solid crystals become soluble enough to form micellar aggregates. This temperature is known as the Krafft point or Krafft temperature ( $T_K$ ). It is named after German chemist Friedrich Krafft. Below the Krafft temperature, the maximum solubility of the surfactant will be lower than the critical micelle concentration, meaning micelles will not form. The Krafft temperature is a point of phase change below which the surfactant remains in crystalline form, even in aqueous solution. The  $T_K$  may also be defined as the temperature at which the solubility of the monomeric surfactant is equivalent to its CMC; this is illustrated in figure-1.2. According to the model of Hato and Shinoda [18] the  $T_K$  is the melting point of the hydrated solid [1–8, 10–12, 15, 16, 19]. Below the  $T_K$  the solubility of the surfactant is too low and only monomers solubility governs their total solubility of the surfactant and surfactant monomers only exist in equilibrium with the hydrated crystals. On the other hand, above

the  $T_K$  micelles are formed and surfactants dissolve in water markedly and the total solubility of the surfactant increases abruptly [3]. The  $T_K$  of the surfactant differ depending on the nature of the counter-ion alkyl chain length, chain structure and the size of the head group etc. because it improves Van der Waals forces [10, 11]. Below the  $T_K$  surfactant cannot exhibit maximum degree of performance. This is why; the surfactants are usually employed well above their  $T_K$ .

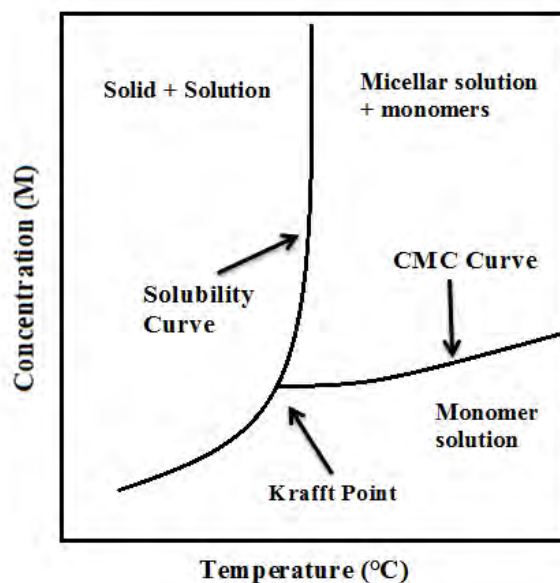


**Figure-1.2** Schematic representation of the solubility curve for the ionic surfactants (The Krafft temperature ( $T_K$ ) is the temperature at which surfactant solubility equals the CMC. Above  $T_K$  surfactant molecules form a dispersed phase; below the  $T_K$  hydrated crystals are formed.)

Moreover, above the  $T_K$  maximum reduction in surface or interfacial tension occurs at the CMC because the CMC then determines the surfactant monomer concentration. According to the pseudo phase separation model [12] the  $T_K$  is regarded as a triple point in the phase diagram of the surfactant-solvent system, at which a ternary equilibrium is established among the crystals, the surfactant micelle, and the monomeric surfactant.

## 1.4 Micelle

The word “micelle” has also been used in biology and in colloid chemistry. Micelles have become a subject of great interest to the chemist because of their similarity to biological membranes, globular proteins and their unusual catalysis of organic reactions. Micelle formation is a fundamental property of surfactants as their property of adsorption at

interfaces. Different properties such as detergency and solubilization depend on the existence of micelles in solution. For aqueous solutions of surfactant, the polar group is located in the solution while the nonpolar part seeks to avoid the aqueous environment by stretching into the gas phase or into an adjacent non-polar liquid phase. At higher concentrations when all the interfaces are occupied then surfactants self-assemble in the bulk in various aggregates: micelles, and vesicles. Surfactant in solution self-assembles at and above a particular concentration, and the self-association of an amphiphile occurs in a stepwise manner with one monomer added to the aggregate at a time. Micellar aggregates are short-lived dynamic species, which rapidly disassemble and reassemble [20]. The occurrence of micelles results from a delicate balance of favorable interaction between the hydrophobic alkyl chains and the opposing repulsive interaction between the head groups. The interaction between alkyl chains of the surfactant favours micellization and lead CMC to lower values by stabilizing micelles while the opposing repulsive interaction between the charged head groups disfavors micellization and leads CMC to higher values [14, 21]. Micelles are spontaneously formed clusters of surfactant molecules which are mostly spherical aggregates in water or organic solvents [22].

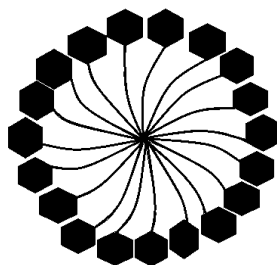


**Figure-1.3 The structure of a spherical micelle**

Figure-1.3 represents a spherical micelle formed in aqueous solution, where the hydrophobic chains are directed towards the interior of the aggregate, and the polar head-groups point towards water. The interior of micelle consist of mobile, non-stretched hydrophobic chains [23]. It needs to be mentioned here that water molecules can penetrate partially the micelle core to interact with surfactant hydrophobic tails [24]. The CMC is an important characteristic of a surfactant [25] because below this concentration surfactant molecules remain in the bulk as single molecule but above this concentration they aggregate as micelle [26].

At low concentration, an aqueous solution of ionic surfactant behaves essentially as a strong electrolyte. At the CMC, the interface is at nearly maximum coverage and to minimize further free energy molecules begin to aggregate in the bulk phase.

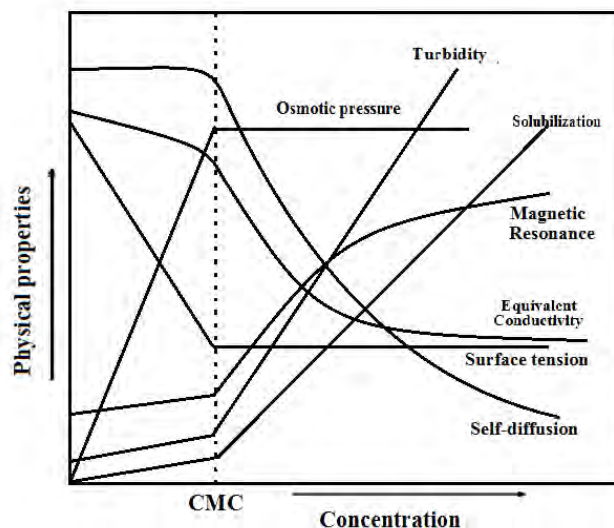


**Figure-1.4** Variation in Physical properties of surfactant solutions below and above the CMC value

On the other hand, with increasing the surfactant concentration the number of micelles increases while the monomer concentration stays roughly independent of concentration and the micelles maintain a dynamic equilibrium with the free surfactant monomers as well as the adsorbed monomolecular layer [27]. When surfactant aggregates or micelle formation commences the solution properties change dramatically (Figure-1.4). Several physical properties such as osmotic pressure, solubilization, surface tension, conductivity etc. are functions of concentration of an ionic surfactant. All the physico-chemical properties show an abrupt change in a narrow concentration range which indicates a highly cooperative association process is taking place. The general way of obtaining the CMC value of a surfactant is to plot an appropriate physico-chemical property versus the concentration of surfactant and observe the break in the plot which is shown in figure-1.4. The CMC value is an important point for surfactant applications from mineral processing to formulation of personal care products and foods, to drug delivery systems, and to new surfactant remediation technologies. In every formulation, the concentration of surfactant must be higher than the CMC.

### **1.4.1 Factors affecting the value of the CMC in aqueous solution**

Micelle formation occurs when surfactant spontaneously self-assemble in solution. The properties of solutions of surface-active agents change markedly when micelle formation commences. The factors affect the CMC in aqueous solution are

- (i) The structure of the surfactant,
- (ii) The presence of added electrolyte in the solution,
- (iii) The presence of various organic compounds in the solution,
- (iv) Temperature of the solution and
- (v) The Effect of pH.

#### **1.4.1.1 Structure of the surfactant**

In general, with the increase of hydrophobic character of the surfactant the CMC decreases and increases the aggregation number of micelle. Nonionic surfactants are better solubilizing agents than ionic surfactants in very dilute solutions because of their lower critical micelle concentrations. The different portion of surfactant such as hydrophilic head group, counter-ion and hydrophobic portion of surfactant which also affect the CMC in aqueous solution are given below-

##### **1.4.1.1.1 The hydrophobic group**

In aqueous medium, the CMC decreases as the number of carbon atoms in the hydrophobic group increases to about 16, and a general rule for ionic surfactants is that the CMC is halved by the addition of one methylene group to a straight-chain hydrophobic group attached to a single terminal hydrophilic group [1, 4, 10, 11]. For nonionics and zwitterionics the decrease with the increase in the hydrophobic group is somewhat larger, an increase by two methylene units reducing the CMC to about one-tenth its previous value [10, 11]. A phenyl group that is part of a hydrophobic group with a terminal hydrophilic group is equivalent to about three and one-half methylene groups [1, 4]. When the number of carbon atoms in a straight-chain hydrophobic group exceeds 16. However, the CMC no longer decreases so rapidly with increase in the length of the chain, and when the chain exceeds 18 carbons it may remain substantially unchanged with further increase in the chain length. This may be due to the coiling of these long chains in water. When the hydrophobic group is branched, the carbon atoms on the branches appear to have about one-half the effect of carbon atoms on a straight chain

[10]. When carbon-carbon double bonds are present in the hydrophobic chain, the CMC is generally higher than that of the corresponding saturated compound, with the cis isomer generally having a higher CMC than the trans isomer. This may be the result of a steric factor in micelle formation. Surfactants with either bulky hydrophobic or bulky hydrophilic groups have larger CMC values than those with similar, but less bulky, groups. The increase in the CMC upon introduction of a bulky hydrophobic group in the molecule is presumably due to the difficulty of incorporating the bulky hydrophobic group in the interior of a spherical or cylindrical micelle. The introduction of a polar group such as –OH into the hydrophobic chain generally causes a significant increase in the CMC in aqueous medium at room temperature, the carbon atoms between the polar group and the hydrophilic head appearing to have about one-half the effect on the CMC that they would have if the polar group were absent. When the polar group and the hydrophilic group are both attached to the same carbon atom, that carbon atom seems to have no effect on the value of the CMC.

#### **1.4.1.1.2 The hydrophilic group**

In aqueous medium, ionic surfactants have much higher CMCs than nonionic surfactants containing equivalent hydrophobic groups. Zwitterionics appear to have slightly smaller CMCs than ionics with the same number of carbon atoms in the hydrophobic group. As the hydrophilic group is moved from a terminal position to a more central position, the CMC increases [1, 4, 28]. The hydrophobic group seems to act as if it had become branched at the position of the hydrophilic group, with the carbon atoms on the shorter section of the chain having about half their usual effect on the CMC. This may be another example of the steric effect in micelle formation noted above. The CMC is higher when the charge on an ionic hydrophilic group is closer to the carbon atom of the hydrophobic group. This is explained as being due to an increase in electrostatic self-potential of the surfactant ion when the ionic head group moves from the bulk water to the vicinity of the nonpolar micellar core during the process of micellization; work is required to move an electric charge closer to a medium of lower dielectric constant. As expected, surfactants containing more than one hydrophilic group in the molecule show larger CMC than those with one hydrophilic group and the equivalent hydrophobic group. In quaternary cationics, pyridinium compounds have smaller CMC than the corresponding trimethylammonium compounds. This may be due to the greater ease of packing the

planar pyridinium, compared to the tetrahedral trimethylammonium, group into the micelle. However, the change per oxyethylene unit is much smaller than that per methylene unit in the hydrophobic chain.

#### **1.4.1.1.3 The counter-ion in ionic surfactants**

A plot of the specific conductivity ( $\kappa$ ) of an ionic surfactant versus its concentration, (C) in the aqueous phase is linear, with a break at the CMC. This break in the plot is due to the binding of some of the counter-ions of the ionic surfactant to the micelle. The degree of ionization ( $\alpha$ ), of the micelle near its CMC can be obtained from the ratio,  $S_2/S_1$ , of the slopes above and below the break indicative of the CMC. The degree of binding ( $\beta$ ) of the counter-ion to the micelle, for a surfactant with a single ionic head group in the molecule, is  $(1-\alpha)$ . The degree of counter-ion binding becomes weaker with the increase of radius of hydrated counter-ion. The degree of binding is related to the surface area per head group, with increasing the degree of binding the surface area per head group decreases. On the other hand, with increasing the surface area per head group, the degree of binding decreases [29]. The CMC in aqueous solution for a particular surfactant reflects the degree of binding of the counter-ion to the micelle. Increased binding of the counter-ion, in aqueous systems, causes a decrease in the CMC of the surfactant. The extent of binding of the counter-ion increases also with the increase in the polarizability and charge of the counter-ion and decreases with the increase in its hydrated radius. On the other hand, when comparing surfactants of different structural types, the value of the CMC does not always increase with the decrease in the degree of binding of the counter-ion. Thus, the degree of binding increases and the CMC decreases with the increase in the length of alkyl chain, the decrease in the CMC is due mainly to the increased hydrophobicity of the surfactant as a result of the increase in the alkyl chain length, and only to a minor extent due to the smaller area per head group.

#### **1.4.1.2 The presence of added electrolyte in the solution**

In aqueous solution, the presence of electrolyte causes a change in the CMC, the effect being more pronounced for anionic and cationic than for zwitterionic surfactants and more pronounced for zwitterionics than for nonionics. The depression of the CMC in these cases is due mainly to the decrease in the thickness of the ionic atmosphere surrounding the ionic head groups in the presence of the added electrolyte and the



consequent decreased electrical repulsion between them in the micelle. The change in the CMC of nonionics and zwitterionics has been attributed mainly to the „,salting-out“ or „,salting-in“ of the hydrophobic groups in the aqueous solvent by the added electrolyte, rather than to the effect of the latter on the hydrophilic groups of the surfactant. Salting in or salting out effect by an ion depends upon whether the ion is a water structure breaker or a water structure maker. Ions with a large ionic charge per radius ratio are water structure makers. These ions salt out the hydrophobic groups of the monomeric form of the surfactant and decrease the CMC. Ions with a small ionic charge per radius ratio are water structure breakers. These ions salt in the hydrophobic groups of the monomeric form of the surfactant and increase the CMC. Since the hydrophilic groups of the surfactant molecules are in contact with the aqueous phase in both the monomeric and micellar forms of the surfactant, while the hydrophobic groups are in contact with the aqueous phase only in the monomeric form, the effect of the electrolyte on the hydrophilic groups in the monomeric and micellar forms may cancel each other, leaving the hydrophobic groups in the monomers as the moiety most likely to be affected by the addition of electrolyte to the aqueous phase.

### **1.4.1.3 The presence of various organic compounds in the solution**

Small amounts of organic materials may produce remarkable changes in the CMC in aqueous media. Since some of these materials may be present as impurities or by-products of the manufacture of surfactants, their presence may cause significant differences in supposedly similar commercial surfactants. A knowledge of the effects of organic materials on the CMC of surfactants is therefore of great importance for both theoretical and practical purposes. To understand the effects produced, it is necessary to distinguish between two classes of organic materials that markedly affect the CMCs of aqueous solutions of surfactant: class I, materials that affect the CMC by being incorporated into the micelle; and class II, materials that change the CMC by modifying solvent-micelle or solvent-surfactant interactions.

### **1.4.1.4 Temperature of the solution**

In general, with the increase of temperature of the surfactant solution the value of CMC increases. With increasing temperature hydration of the hydrophilic group decreases which favors micellization. However, with increasing temperature disruption of the

structured water surrounding the hydrophobic group increases which disfavors micellization. Therefore, the relative magnitude of these two opposing effects determines whether the CMC increases or decreases over a particular temperature range. The effect of temperature on the CMC of surfactants in aqueous medium is complex. The value of CMC first decreases with temperature to some minimum and then increases with further increase in temperature. In some cases, CMC first increases with temperature to some extent and then decreases with further increase in temperature at a certain temperature.

### **1.4.1.5 The effect of pH**

Commonly, industrially important surfactants are consist of long-chain alkyl salts of strong acids, it might be expected that solution pH would have a relatively small effect, if any, on the CMC of the materials, an expectation generally borne out by experience. In solutions of sulfonate and sulfate salts, where the concentration of acid or base significantly exceeds that of the surfactant, the excess will act as if it were simply neutral electrolyte. Unlike the salts of strong acids, the carboxylate soap surfactants exhibit a significant sensitivity to pH. Since the carboxylate group is not fully ionized near or below the  $pK_a$ , the electrostatic interactions between head groups retarding micelle formation will vary with the solution pH, resulting in significant changes in the CMC. A similar result will be observed for the cationic alkylammonium salts near and above the  $pK_b$ , resulting in a decrease in the CMC. When the surfactant is in the fully ionized form, excess acid or base will act as neutral electrolyte. It is to be expected that pH will have no effect on the CMC of nonionic surfactants, and that is generally found. However, at very low pH it is possible that protonation of the ether oxygen of OE surfactants could occur. No doubt, such an event would alter the characteristics of the system. However, little can be found in the literature pertaining to such effects. A number of amphoteric surfactant systems show pH sensitivity related to the  $pK$  values of their substituent groups. At low pH, materials containing carboxyl and amine groups would act as cationic surfactants, while at high pH the activity would be anionic, by analogy to the action of amino acids. If the cation is a quaternary ammonium salt, no pH sensitivity would be expected, as would be the case for a strong-acid anionic group. Therefore, the pH sensitivity of amphoteric surfactants will vary according to the specific structure of the materials.

## **1.5 Surface or interfacial tension**

The properties of hydrophobic tails of surfactant and water are not same. The hydrophobic tail of the surfactant has more attraction to nonpolar group than polar group consequently nonpolar tails of surfactant monomer tends to adsorb to all the interfaces. Interface is referred the boundary between two immiscible phases. The phases may be solids, liquids, or vapours, although there cannot be an interface between two vapour phases. Mathematically, the interface is described as an infinitely thin line or plane separating the bulk phases at which there will be a sharp transition in properties from those of one phase to those of the other. Surface adsorption is one of the most fundamental interfacial phenomena. This adsorption has been studied to determine

- (a) The concentration of surfactant at the interface,
- (b) The orientation and packing of the surfactant at the interface,
- (c) The rate at which this adsorption occurs, and
- (d) The energy changes,  $\Delta G$ ,  $\Delta H$ , and  $\Delta S$ , in the system, resulting from the adsorption.

The relative adsorption of a surfactant at an interface can be determined from the measurement of the interfacial tension as a function of surfactant concentration. The environment of molecules located at an interface is different compared to those from either bulk phase. An interface is associated with the surface free energy which governs the transport of surfactant molecules from the bulk to the interface. The surface free energy is the minimum amount of work ( $W_{\min.}$ ) required to create new unit area of that interface ( $\Delta A$ ), so  $W_{\min} = \Delta A \times \gamma_0$ . The surface tension ( $\gamma_0$ ) is defined as the surface free energy per unit area or the force acting to the interface per unit length of the resulting thin film on the surface. Therefore, surface-active agent is a substance that adsorbs to the interface thereby change the amount of work required to expand that interface. Measurement of the surface or interfacial tension of liquid systems is accomplished by the Wilhelmy plate method which is the most useful and precise for solutions of surfactants. Reduction of surface or interfacial tension is one of the most commonly measured properties of surfactants in solution. It depends directly on the replacement of solvent molecules at the interface by surfactant molecules. The molecules at the surface of a liquid have potential energies greater than those of similar molecules in the interior of the liquid. We have seen in Figure-1.4 that the surface tension of a solution of an

individual surfactant decreases steadily as the bulk concentration of surfactant is increased until the concentration reaches a value known as the critical micelle concentration (CMC), above which the surface tension remains virtually unchanged. Further addition of stock solution the surfactant monomers in the bulk start to aggregate into micelles. In aqueous medium, the formation of a micelle depends on some environmental factors such as pH, temperature, additives, surface pressure, and counter-ion. In the micelle the hydrophobic tails are directed inwards or toward the core and the hydrophilic head groups are directed outwards, towards the bulk of water. If the CMC exceeds the solubility of the surfactant at a particular temperature, then the minimum surface tension will be achieved at the point of maximum solubility, rather than at the CMC [1, 4]. The temperature at which the solubility of an ionic surfactant becomes equal to the CMC is known as the Krafft point ( $T_K$ ). Here, it is noteworthy that the CMC could not be measured below the  $T_K$  because at this temperature surfactant stays in solution as hydrated solid crystals. In dilute solutions of surfactants, the amount of change in any interfacial phenomenon produced by the adsorption of surfactant at the interface is a function of the concentration of surfactant absorbed at the interface. The effect of a surfactant on an interfacial phenomenon is a function of the concentration of surfactant at the interface. We can define the effectiveness of a surfactant in adsorbing at an interface as the maximum concentration that the surfactant at that interface. The effectiveness of adsorption is related to the interfacial area occupied by the surfactant molecule. Moreover, added salt also affects the surface adsorption and bulk micelization of the surfactant. The surface excess concentration ( $\Gamma_{\max}$ ) was found to decrease gradually with increasing temperature and the values are much lower in the presence of the added counter-ions compared to that of the pure surfactant alone in aqueous solution.

### **1.6 Thermodynamics of adsorption**

In the consideration of adsorption processes, two aspects must be addressed: (1) the effect of the adsorbed species on the final equilibrium interfacial energy of the system and (2) the kinetics of the adsorption process. To understand and predict the role of surfactant adsorption, it is necessary to know the amount of material adsorbed at the interface. When considering a surfactant solution in equilibrium with vapor, the surface excess is defined as the concentration of surfactant molecules in a surface plane and the energy of the interface changes. The Gibbs equation, which relates changes in the interfacial energy of

a system to the degree of adsorption of a species at the interface and the compositions of the bulk phases, forms the basis for understanding the thermodynamics of the adsorption process.

Let us consider a system of bulk phases  $\alpha$  and  $\beta$  and a surface phase  $\sigma$ , and make an approximation for the location of interface using the ‘‘Gibbs dividing surface’’. This is a plane that is chosen such that the excess adsorption of solvent is zero. In this plane, the excess adsorption,  $\Gamma_i^\sigma$  of a solution component  $i$  is then given by

$$\Gamma_i^\sigma = \frac{n_i^\sigma}{A} \dots\dots\dots (1.1)$$

Here,  $A$  is the interfacial area. The term  $n_i^\sigma$  is the surface excess of component  $i$  in the surface phase  $\sigma$  compared with the bulk concentration if it had continued to the interface. The surface excess  $\Gamma_i^\sigma$  may be positive or negative, corresponding to surface enrichment or depletion of a solute, respectively.

The Gibbs adsorption equation is

$$d\gamma = -\sum_i \Gamma_i^\sigma d\mu_i \dots\dots\dots (1.2)$$

with  $\gamma$  the surface tension and  $\mu$  the chemical potential. For a system consisting only of a solvent, 1, and a solute, 2, such as a nonionic surfactant dissolved in water, then equation (1.2) becomes

$$d\gamma = -\Gamma_1^\sigma d\mu_1 - \Gamma_2^\sigma d\mu_2 \dots\dots\dots (1.3)$$

The choice of the Gibbs dividing surface is such that  $\Gamma_1^\sigma = 0$ , then equation (1.3) simplifies to

$$d\gamma = -\Gamma_2^\sigma d\mu_2 \dots\dots\dots (1.4)$$

Here,  $\Gamma_2^\sigma$  is the solute surface excess concentration. At constant temperature, the chemical potential is given by

$$d\mu_i = \text{const} + RT d \ln a_i \dots\dots\dots (1.5)$$

Therefore, applying to equation (1.4) gives the common form of the Gibbs equation for nondissociating materials

$$d\gamma = -\Gamma_2^\sigma RT d \ln a_2 \dots\dots\dots (1.6)$$

Or in rearranged form

$$\Gamma_2^\sigma = -\frac{1}{RT} \frac{d\gamma}{d \ln a_2} \dots\dots\dots (1.7)$$

For dissociating solutes, such as ionic surfactants of the form  $R^-M^+$ , and assuming ideal behavior below the CMC, equation (1.7) becomes

$$d\gamma = -\Gamma_R^\sigma d\mu_R - \Gamma_M^\sigma d\mu_M \dots\dots\dots (1.8)$$

For a system with no added electrolyte, the condition of electroneutrality at the interface requires  $\Gamma_R^\sigma = \Gamma_M^\sigma$ . Employing the mean ionic activities so that  $a_2 = (a_R a_M)^{1/2}$  and substituting into equation (1.8) gives the Gibbs equation for 1:1 dissociating compounds:

$$\Gamma_2^\sigma = -\frac{1}{2RT} \frac{d\gamma}{d \ln a_2} \dots \dots \dots (1.9)$$

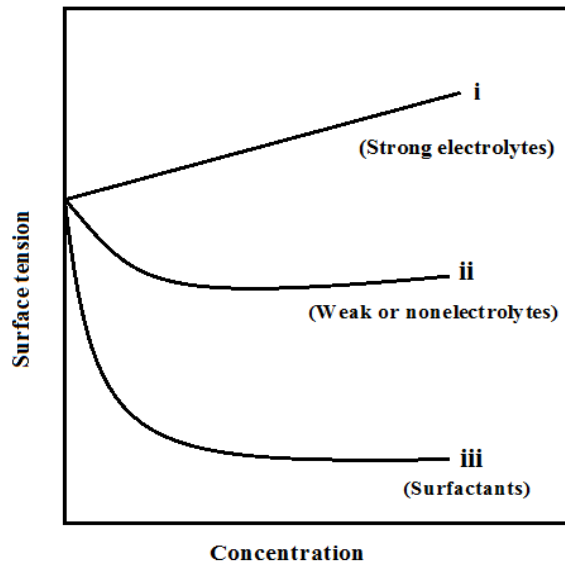


**Figure-1.5 Dependence of surface tension of solutions on solute concentration**

If sufficient salt is added to screen out electrostatic effects, and the same counter-ion  $M^+$  as the surfactant is present, then the activity of  $M^+$  is constant and the prefactor becomes unity, so that the surfactant ion behaves as a nondissociating solute and equation (1.7) can be used. For dilute systems, concentration can be employed rather than activity in equations (1.7) and (1.9). This equation directly tells us that when a solute adsorbs at the interface ( $\Gamma_2^\sigma > 0$ ), the surface tension decreases with the increase of solute concentration. This is also known as positive adsorption. Such a behavior is typical for weak or nonelectrolytes and surfactants in water, as shown in figure-1.5 (ii and iii). On the other hand, an increase in surface tension with the increase of solute concentration indicates that the solute avoids the interface ( $\Gamma_2^\sigma < 0$ ). This is called negative adsorption and such a behavior is typical for strong electrolytes in water, as shown in figure-1.5 (i).

## 1.7 Solubilization

One of the important properties of surfactants is solubilization of water insoluble organic compounds in micelles which is a colloidal phenomenon. This is defined as the spontaneous dissolving of a substance by reversible interaction with the micelles of a surfactant in a solvent to form a thermodynamically stable isotropic solution [10]. Moreover, solubilization is distinguished from emulsification by the fact that in solubilization, the solubilized material is in the same phase as the solubilizing solution and the system is consequently thermodynamically stable. This property depends on the easy penetration of solubilize inside the micelles without changing their chemical properties and protects them from any potential degradation. Solubilization of nonpolar organic compounds in micellar system is one of the most significant applications of surfactant. The extent of solubilization depends on many factors such as the structure of the surfactant, aggregation number, temperature, ionic strength of the medium, the nature of the solubilize, number of micelles and their shapes.

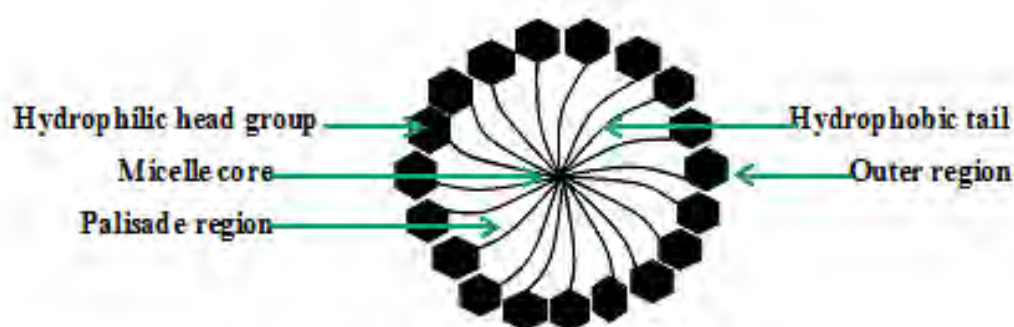


**Figure-1.6** Different regions in the micelle on the basis of different solubilization sites which can be recognized

However, below the CMC surfactant molecule exist as monomers and have only little or no influence on the solubility of organic compounds. In other words, solubilization in surfactant solution starts when the concentration of the surfactant is equal to the CMC and increases with increasing concentration. Depending on the nature of the solubilize, solubilization occurs at a number of different regions of micelle (figure-1.6) such as

- (a) On the surface of the micelle or at the micelle-solvent interface;
- (b) Between the hydrophilic head groups;

- (c) In the so-called palisade layer of the micelle between the hydrophilic groups and the first few carbon atoms of the hydrophobic groups that comprise the outer core of the micellar interior;
- (d) More deeply in the palisade layer; and
- (e) In the inner core of the micelle.

For example, non-polar molecules are solubilized in the core of the micelle and partially polar substances are distributed in the palisade of the micelles [16]. Studies of the solubilization of water insoluble compounds in micellar system have revealed a lot of application in the practical fields such as drug carrier [30], drug solubilization [13], separation, toxic waste removal [31] etc. If the solubility of a normally solvent-insoluble material is plotted against the concentration of the surfactant solution, we find that the solubility is very slight until a critical concentration is reached at which the solubility increases approximately linearly with the concentration of the surfactant which can be seen in figure-1.7. This is because micelles are formed which can accommodate the insoluble substance [32].

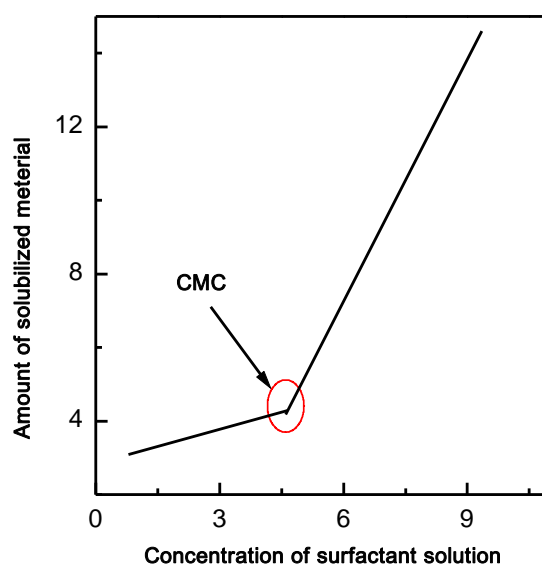


**Figure-1.7 Amount of material solubilized as a function of concentration of surfactant solution**

Moreover, below the CMC surfactant molecule exist as monomers and have only little or no influence on the solubility of water insoluble organic compounds. This indicates that



solubilization is a micellar phenomenon. Furthermore, dye solubilization can be used to determine the CMC of the surfactant based on the following observations such as the amount of dye solubilized below the CMC is very slight or zero and above the CMC solubilization increases with increasing the surfactant concentration. The solubilizing capacity or solubilization power (SP) of a surfactant is usually expressed quantitatively by a term known as molar solubilization ratio (MSR). The MSR is defined as the number of moles of solubilize per mole of micellized surfactant, given by the ratio  $(S_w - S_{CMC}) / (C_{surf} - CMC)$ , where  $S_w$  is the molar solubility of the solubilize in the aqueous system,  $S_{CMC}$  is molar solubility at the CMC, and  $C_{surf}$  is the molar concentration of the surfactant [13]. It often remains constant for a particular surfactant over a wide range of concentration above the CMC, although some surfactants show increasing solubilizing power at higher concentrations. In general, solubilization capacity is greater for polar solubilizes than for nonpolar ones, especially for spherical micelles because of the larger volume available at the surface of the micelle than in the interior and decreases with increase in the molar volume of the solubilize. The exact location in the micelle at which solubilization occurs, varies with the nature of the material solubilized and the type of interaction occurring between surfactant and solubilize. Diffraction studies measure changes in micellar dimensions on solubilization, whereas UV vis. spectroscopy, NMR and fluorescence spectra indicate changes in the environment of the solubilize on solubilization. Solubilization of water insoluble substance in aqueous solution of surfactant has major practical importance where it can replace the use of organic solvents or co-solvents; in detergency, where solubilization is believed to be one of the major mechanisms involved in the removal of oily soil; in micellar catalysis of organic reactions; in emulsion polymerization, where it appears to be an important factor in the initiation step; in the separation of materials for manufacturing or analytical purposes; and in enhanced oil recovery. Solubilization into nonaqueous media is of major importance in dry cleaning. The solubilization of materials in biological systems sheds light on the mechanisms of the interaction of drugs and other pharmaceutical materials with lipid bilayers and membranes. Separation processes based on micellar encapsulation [33, 34] have a great importance in the removal of contaminants from groundwater and industrial wastewater. Bio-based ionic surfactants are added to contaminated reservoirs at concentrations above the CMC. Such a process is both cost effective and environmentally friendly.

## **1.8 Factors affecting the extent of solubilization**

### **1.8.1 Structure of the surfactant**

Hydrocarbons and long-chain polar compounds are solubilized in the interior of the micelle or deep in the palisade layer. The amount of material solubilized generally increases with increasing the size of the micelles. The factors that cause an increase in either the diameter of the micelle or its aggregation number can produce an increase in the solubilization capacity. Solubilization capacity for hydrocarbons in the interior of the micelle in aqueous media increases with increasing the chain length of the hydrophobic portion of the surfactant. For examples, in aqueous solutions of POE nonionics, the extent of solubilization of aliphatic hydrocarbons at a given temperature appears to increase as the length of the hydrophobic group increases and as the length of the POE chain decreases reflecting the increase in the aggregation number of the micelles produced by these changes. In general, the order of solubilizing power for hydrocarbons and polar compounds that are solubilized in the inner core appears to be as follows: nonionics > cationics > anionics for surfactants with the same hydrophobic chain length [35]. The greater solubilizing power of cationics, compared to anionics of equivalent hydrophobic chain length, may be due to looser packing of the surfactant molecules in the micelles of the former. Moreover, bivalent metal alkyl sulfates appear to show greater solubilizing power than the corresponding sodium salts for hydrocarbons, probably reflecting the greater micellar aggregation numbers, asymmetry, and volumes of the former compared to the latter.

### **1.8.2 Structure of the solubilize**

The extent of solubilization in the micelle depends on the structure of solubilize. Crystalline solids generally show less solubility in micelles than liquids of similar structure. Short-chain alkyl-aryl hydrocarbons may be solubilized both at the micelle-water interface and in the core, the proportion in the core increase with increasing the concentration of the solubilize. For aliphatic and alky-laryl hydrocarbons, the extent of solubilization appears to decrease with increase in the chain length and to increase with unsaturation or cyclization if only one ring is formed. For condensed aromatic hydrocarbons, the extent of solubilization appears to decrease with increase in the molecular size. Branched-chain compounds appear to have approximately the same solubility as their normal chain isomers. For polar solubilizes, the situation is

complicated by the possibility of variation in the depth of penetration into the micelle as the structure of the solubilize is changed. If the micelle is more or less spherical in shape, we can expect that space will become less available as the micelle is penetrated more deeply. Thus, polar compounds that are solubilized close to the micelle-water interface should be solubilized to a greater extent than nonpolar solubilizes that are located in the inner core. This is generally the case, if the surfactant concentration is not high. We should also expect that polar compounds that are solubilized more deeply in the palisade layer would be less soluble than those whose locus of solubilization is closer to the micelle-water interface. Usually, the less polar the solubilize and the longer its chain length, the smaller its degree of solubilization; this may reflect its deeper penetration into the palisade layer.

### **1.8.3 Effect of electrolytes**

The addition of small amounts of neutral electrolyte to solutions of ionic surfactants appears to decrease the value of CMC which increase the extent of solubilization of hydrocarbons that are solubilized in the inner core of the micelle and to decrease that of polar compounds that are solubilized in the outer portion of the palisade layer. In the presence of neutral electrolyte in ionic surfactant solution the repulsion between the similarly charged ionic surfactant head groups decreases, thereby decreasing the CMC and increasing the aggregation number and volume of the micelles. The increase in aggregation number of the micelles presumably results in an increase in hydrocarbon solubilization in the inner core of the micelle. The decrease in mutual repulsion of the ionic head groups causes closer packing of the surfactant molecules in the palisade layer and a resulting decrease in the volume available there for solubilization of polar compounds. This may account for the observed reduction in the extent of solubilization of some polar compounds. For example, in the presence of  $5 \times 10^{-3}$  M NaSCN, the CMC of CPB decreases from  $83.9 \times 10^{-3}$  mM to  $7.35 \times 10^{-3}$  mM [36]. Furthermore, as the chain length of the polar compound increases, the reduction of solubility by electrolytes appears to decrease and the solubility of hydrocarbon is increased slightly by the addition of neutral electrolyte. The addition of neutral electrolyte to solutions of nonionic surfactants increases the extent of solubilization of hydrocarbons at a given temperature in those cases where electrolyte addition causes an increase in the aggregation number of the micelles [2].

#### **1.8.4 Effect of organic additives**

In general, the presence of solubilized hydrocarbon in the surfactant micelles, the solubility of polar compounds in the micelle increases. The solubilized hydrocarbon causes the micelle to swell, and this may make it possible for the micelle to incorporate more polar material in the palisade layer. On the other hand, the solubilization of such polar material as long-chain alcohols, amines, mercaptans, and fatty acids into the micelles of a surfactant appears to increase their solubilization of hydrocarbons. The solubilization power of hydrocarbons increases with the increase of the chain length of the polar compound and the less capability of hydrogen bonding, that is,  $RSH > RNH_2 > ROH$ . First explanation for this is that the increased chain length and lower polarity result in a lower degree of order in the micelle, with a consequent increase in solubilizing power for hydrocarbons. Second is that the additives with longer chain length and lesser hydrogen bonding power are solubilized more deeply in the interior of the micelle, and hence expand this region, producing the same effect as a lengthening of the hydrocarbon chain of the micelle-producing molecule. However, the addition of long-chain alcohols to aqueous solutions of sodium dodecyl sulfate decreased its solubilization of oleic acid. The extent of solubilization of the latter decreased as both the concentration and the chain length of the added alcohol increased. These effects are believed to be due to competition between oleic acid and added alcohol for sites in the palisade layer of the micelle.

#### **1.8.5 Effect of temperature**

For ionic surfactants, with increasing temperature generally the extent of solubilization for both polar and nonpolar solubilizates increases because increased thermal agitation increases the space available for solubilization in the micelle. On the other hand, for nonionic surfactants, the effect of temperature increase appears to depend on the nature of the solubilizate. Nonpolar materials which are solubilized in the inner core of the micelle show increased solubility as the temperature is raised, the increase becoming very rapid as the cloud point of the surfactant is approached. However, the solubility behavior of polar materials, whose locus of solubilization is the palisade layer of the micelle, appears to be very different, the amount of material solubilized generally going through a maximum as the temperature is increased to the cloud point. Further increase in temperature, the amount of material solubilized decrease because of increased dehydration and tighter coiling of the surfactant chains as a result the space available in

the palisade layer decrease. As the cloud point is approached, this decrease in the amount solubilized may become marked, particularly for short-chain polar compounds that are solubilized close to the surface of the micelle.

## **1.9 Applications of surfactants**

The surfactants have a wide variety of applications in our practical life. Work processes may be simplified, accelerated, or economized by the application of surfactants. Industrial applications include the use of surfactants as cleaning agents, emulsifiers and as process aids in the very important area. In the domestic sector, they are typically used as household cleaning agents and personal care products [37]. Some specific fields of application of surfactants are discussed below:

### **1.9.1 Surfactants as detergents and cleaners**

The primary application for surfactants is their use as soaps and detergents for a wide variety of cleaning processes which is the process of removing unwanted material from the surface of a solid by various physicochemical and mechanical means [37]. Three elements are present in every cleaning process: (1) the substrate, (2) the soil, and (3) the cleaning solution or bath. The substrate may vary from an impervious, smooth, hard surface like that of a glass plate to a soft, porous, complex surface like that of a piece of cotton or wool yarn. The soil may be liquid or solid, ionic or nonpolar, finely or coarsely ground, inert or reactive toward the cleaning bath. The bath used is generally a solution of various materials, collectively called the detergent in the cleaning liquid. In general, cleaning consists essentially of two processes: first is removal of the soil from the substrate and second is suspension of the soil in the bath and prevention of its redeposition. The second process is just as important as the first, since it prevents redeposition of the soil onto another part of the substrate.

Moreover, solubilization is a major factor to remove the oily soil from both hard and textile surfaces and its retention by the bath. When insufficient surfactant is present to solubilize all the oily soil, the remainder is probably suspended in the bath by macroemulsification antiredeposition agents. Organic polymers are called antiredeposition agents or soil release agents such as Sodium carboxymethylcellulose, Polyacrylates which are used in laundry detergents at low concentrations. Antiredeposition agents adsorb to the cellulosic material via H-bonding and thereby

produce a steric and sometimes also an electrical barrier (negatively charged) and prevent the redeposition of soil particles. Soaps are excellent detergents, but suffer from their sensitivity to pH and the presence of hardness in the water. The synthetic detergents have essentially replaced soaps. In practical situations, the complete efficiency of detergents is achieved by adding additives. Common additives include builders, antiredeposition agents, brighteners, and co-surfactants.

### **1.9.2 Surfactants in cosmetics, and personal care products**

An important field of application for surfactants is consumer products, these are detergents, dishwashing agents, cleaning agents, cosmetics and personal care products such as lipstick; rouge; mascara; and hair dyes, tints, and rinses [38]. Traditionally, such products have been made primarily from fats and oils. Natural surfactants and other amphiphilic materials have been used in cosmetics since their invention. An important aspect of such products is that it may produce an adverse reaction, in some cases, with the human skin, membranes, and other tissues or organs with which it will come into contact during use [39]. For safety reasons, we must study in depth about the possible adverse effects of surfactants in cosmetics and personal care products.

### **1.9.3 Surfactants in foods and food packaging**

Surfactants are used in food industry as cleaners and emulsifiers. There are at least two important aspects to the role of surfactants in food-related industries. One aspect is related to food handling and packaging and the other, to the quality and characteristics of the food itself. Bottles and similar containers must be cleaned before filling. These processes require some type of detergent; it must have special characteristics that usually include little or no foam formation. Low-foaming detergents and cleaners are also important for the cleaning of process tanks, piping, pumps, and flanges. The presence of foam will often restrict the access of cleaning and disinfecting agents to difficult areas, reducing their effectiveness at cleaning the entire system and leading to the formation of dangerous bacterial breeding grounds [40]. Surfactants are also involved in the production of many common food items such as whipped toppings, foam or sponge cakes, bread, mayonnaise and salad dressings, ice cream and sherbets, candies, chocolates, beverages, margarines, soups and sauces, coffee whiteners, and many more. It also involved in the extraction of cholesterol, solubilization of oils, essential nutrients, and liquor emulsification. Prime

examples are the monoglycerides and diglycerides derived from fats and oils, phospholipids such as lecithin and modified lecithins, reaction products of natural fatty acids or glycerides with natural lactic and fruit acids, reaction products of sugars or polyols with fatty acids, and a limited number of ethoxylated fatty acid and sugar derivatives. Surfactants are a key component in the manufacture of edible coatings and are also used in the production of margarine.

#### **1.9.4 Surfactants in crop protection and pest control**

Surfactants are critical components in agricultural formulations for the control of weeds, insects, and other pests in agricultural operations. Active substances for the protection of growing plants are offered as powder or liquid concentrates, which are diluted to so-called spray liquors for application. Surfactants are used as emulsifiers in spray preparations such as crop protection products; these are pesticides, herbicides, fungicides, and insecticides. Now a day, organosilicone surfactants have begun appearing in commercial spray-application products [41]. They easily break down, which is an environmental bonus, but the lack of stability poses difficulty in product storage as ready-to-use products. To prevent caking of fertilizers in mixers and to achieve uniform distribution of fertilizers in the soil, dilute solutions of fatty alcohol polyglycol ethers, alkylbenzene sulfonates or cationic surfactants are advantageous. Surfactants also improve application efficiency by facilitating the transport of the active components into the plant through pores and membrane walls. Foam formation during application can also be a problem since the presence of foam will, in most cases, significantly reduce the effectiveness of the applied material. It is vital to use a surfactant that is electrically compatible with that ingredient. If the active material is positively charged, the addition of an anionic surfactant will precipitate out directly before being applied due to the formation of a poorly soluble salt resulting in an unacceptable loss.

#### **1.9.5 Surfactants in chemical industry**

The surfactants are integral part of the chemical industry. The chemical processes utilize the wetting and dispersing power of surfactants. The systems which contain immiscible components, the reaction speed may be increased by the emulsification effect of surfactants. It is also necessary to mention that the surfactant micelles act as catalytic centers while few major industrial processes use the procedure to solve difficult process

problems. A newer catalytic system known as phase transfer catalysis uses amphiphilic molecules to transport reactants from one medium in which a reaction is slow or nonexistent into a contacting medium where the rate of reaction is high. Once reaction of a molecule is complete, the catalytic surfactant molecule returns to the nonreactive phase to bring over a new candidate for reaction. Surfactants may also be used to increase the yield in extraction processes.

### **1.9.6 Surfactants in textiles and fibers**

Surfactants have an important role in the manufacture and further processing of textiles as auxiliaries in a number of process steps. The dyeing of textiles is an obvious application of surfactants. In the manufacture of textiles, surfactants are applied to optimize individual processing steps such as drawing, spinning, and twisting, texturizing, coning, weaving and knitting. For natural fibers, the role of surfactants begins at the beginning with the washing and preparation of the crude fiber in preparation for spinning. Synthetic fibers also require surfactants at various steps in their evolution from monomeric organic chemicals to finished cloth. Depending on the type of polymer involved, the process may require surfactants beginning with the polymer synthesis. Even, it is common to apply a final treatment with a surface-active material to define the final characteristics of the product.

### **1.9.7 Surfactants in leather and furs**

Surfactants play important roles in manufacturing of leather and furs, from the original untreated skin or hide to the finished product. In leather tanning it is normal to treat the leather with a surfactant to produce a protective coating on the skin and hide fibers. This helps prevent the fibers from sticking together and keeps the fiber network flexible while increasing the tensile strength of the finished leather product. Surfactants also help the penetration of dyes and other components into the fiber network thereby improving the efficiency of various stages of the tanning process, saving time, energy, and materials while helping to guarantee a higher-quality, more uniform finished product. The leather goods are now commonly applied in the form of lacquer like polymer coatings that can be applied as emulsions and suspensions using suitable surfactants. Surfactants have similar applications in the fur industry.



### **1.9.8 Paints, lacquers, and other coating products**

Surfactants are required in the production of paints and lacquers, and in related coating systems. Pigment solids are far from smooth surfaces at the molecular level and the raw materials have small cracks and holes that serve as initiation points for the rupture of the structure. In the presence of the proper surfactant, the molecules penetrate into the cracks and crevices which facilitate the continued breaking of the large particles into smaller units. Surfactants, adsorbed onto the solid surface significantly reduce the surface energy of newly exposed solid. The adsorbed surfactant molecules also create a barrier like coating. In aqueous or latex paints, the surfactant is important in the preparation of the latex polymer. Surfactants are also of great importance in the manufacture of coating materials, paints, varnishes, lacquers, dyestuff pigments, binding materials, and binders. Surface active substances can speed up the preparation of dispersions, and improve the degree of dispersion and stability. Very few emulsion polymers are produced without the addition of surfactants.

### **1.10 Aims and objectives of the present work**

The surfactants are one of the most important groups of organic chemicals which are used in many domestic and industrial applications [42]. The applications of these compounds lie on their capacity of micelle formation [39]. This micelle formation starts at the CMC which is an important characteristic and specific to each individual surfactant. Below the CMC surfactant molecule exist as monomers and behaves as a simple electrolyte and loses many of its activities. Above the CMC the concentration of monomer remains almost same; the additional surfactants just form more and more micelles. The CMC values increase with temperature due to the destruction of ice-berg structure of water surrounding the hydrophobic tail and the degree of dehydration increases with increasing temperature which is unfavourable for micellization [2]. The opposing repulsive interaction between the polar or charged head groups of ionic surfactants increase the free energy of the system which also disfavour micellization and leads CMC to higher values limiting their applications. In the presence of every inorganic electrolyte, the CMC values of surfactants decreases [19] due to the screening of the effective charge of micelle [41]–[43] which favours their applications. For example, the CMC of cetylpyridinium bromide decreases from 0.84 mM to 0.074 mM in the presence of the NaSCN when the concentration of NaSCN is  $5 \times 10^{-3}$  M [19]. Generally, added salts lower the CMC, and

surface activity of surfactants, which is favorable for their industrial applications [19], [44]. On the other hand, in the presence of some electrolytes or additives the value of CMC increases [45] which limit their applications in different field.

Moreover, the surfactants are used in different products such as soap, detergent, shampoo, creams, shower-gel, and many other cosmetics. In spite of such fascinating applications, the surfactants do not work effectively below a certain temperature known as the critical micelle temperature or Krafft temperature ( $T_K$ ) [7]. Below the  $T_K$  the surfactant molecules remain in water as crystalline hydrated solids and lose many of its activities such as detergency, dispersing, emulsifying, and micelle forming properties. Therefore, it is essential to lower the  $T_K$  of surfactants below room temperature for their wider applications. Again, at or above the  $T_K$  the surfactant monomers become soluble enough in aqueous media and work effectively forming micellar aggregates at or above CMC. So, the  $T_K$  is the most important phenomenon of surfactant. The value of  $T_K$  increases in the presence of stronger chaotropes and common ion compared to that of the surfactant in pure water [9, 32]. At or above the  $T_K$  the solubility of surfactant increases due to the micelle formation and there is an establishment of equilibrium state between surfactant monomers and micelle formation [10, 11]. The  $T_K$  increases with increasing the concentration of the added electrolyte which limits their industrial applications [19]. In the case of ionic surfactant in aqueous system, the micelle has the core of very hydrophobic pseudo phase and there is a gradient of increasing polarity from the core towards the micelle surface [46]. These micelles have special characteristics of solubilizing the water insoluble organic compounds at or above the CMC and the solubility increases proportionally with increasing the concentration of surfactant above the CMC [17, 47]. Solubilization of water insoluble or sparingly soluble compounds in aqueous system have revealed a lot of application in the different practical fields such as drug formulations and drug carrier, drug solubilization, separation, toxic waste removal, metal ion estimation in aqueous system etc. [2, 48]. Some metal ions form complex with different ligands, in some cases these ligand and complex both are insoluble in water, or soluble in water at a specific condition such as low pH. These are also soluble in aqueous solution of surfactant. But, below the  $T_K$  both the ligand and complex become insoluble in aqueous solution of surfactant due to the absence of micelle and above the  $T_K$  surfactant stays in solution as monomers and micelle. From previous study it is found that

the Cu(II)-PAN complex is insoluble in aqueous solution at above the pH 2.5 [49] but soluble enough in the core of micelle above or below this pH. So, we aimed to

- 1) Lower the  $T_K$  and CMC of these surfactants.
- 2) Decrease the value of equilibrium surface tension.
- 3) Measure the extent of solubilization of organic ligands such as PAN and curcumin in aqueous solution of CPB and CPC respectively in pure water using UV-vis spectrophotometer at 30 °C.
- 4) Increase the capacity of solubilization of surfactant applying different potassium salts which will be favourable for their use in different practical purposes.
- 5) Solubilize the ligand and complex in aqueous solution of surfactant.
- 6) Measure the location of solubilized ligand and complex in the micelle which will be examined with the help of  $^1\text{H}$ NMR and ATR-IR spectroscopy. The  $^1\text{H}$  NMR technique plays an important role in characterization of micelle and locates the solubilize in micellar system.
- 7) Examine the possibilities of complex formation in micellar system and measuring the extent of metal ion in aqueous solution without using highly volatile organic solvent.

# **Chapter two: Chemicals and Experimental procedures**

## 2.1 Chemicals

### 2.1.1 Surfactants

#### Cetylpyridinium bromide (CPB)

##### Properties

Molecular Formula of CPB  $C_{21}H_{38}BrN$ ,

Molecular Weight 384.44g/mol,

Melting point 67-71 °C,

Water solubility soluble

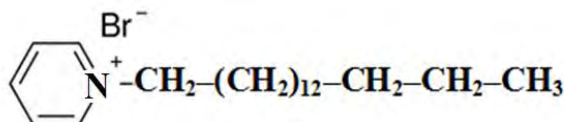


Figure-2.1 Structure of cetylpyridinium bromide (CPB)

#### Cetylpyridinium chloride (CPC)

##### Properties

Molecular Formula of CPC  $C_{21}H_{38}ClN$ ,

Molecular Weight 339.99g/mol,

Melting point 77 °C,

Water solubility soluble

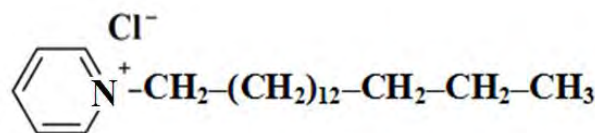


Figure-2.2 Structure of cetylpyridinium chloride (CPC)

Cetylpyridinium bromide (CPB) and Cetylpyridinium chloride (CPC) were collected from the Sigma-Aldrich with the purity of more than 98% and used as received.

### 2.1.2 Salts

- |                                  |  |
|----------------------------------|--|
| 1. Potassium fluoride (KF)       | 7. Potassium sulfate ( $K_2SO_4$ )             |
| 2. Potassium chloride (KCl)      | 8. Potassium hydrogen phosphate ( $K_2HPO_4$ ) |
| 3. Potassium bromide (KBr)       | 9. Potassium carbonate ( $K_2CO_3$ )           |
| 4. Potassium iodide (KI)         | 10. Nickel Sulphate ( $NiSO_4$ )               |
| 5. Potassium thiocyanate (KSCN)  | 11. Copper Sulphate ( $CuSO_4$ )               |
| 6. Potassium nitrate ( $KNO_3$ ) | 12. Zinc Sulphate ( $ZnSO_4$ )                 |

Salts were collected from Merck, Germany with the purity of more than 99% and used without further purification.



## **2.2 Experimental procedures**

### **2.2.1 Krafft temperature measurement**

The Krafft Temperature ( $T_K$ ) measurements were carried out using a Eutech-Cyber Scan-CON-510 conductivity meter equipped with a temperature-compensated cell having the cell constant  $1.0 \text{ cm}^{-1}$ . The meter was calibrated by measuring the conductivity of the potassium chloride solutions (Merck, Germany purity >99%) of different concentration such as 0.001, 0.01, and 0.1 M. To measure the  $T_K$  of the surfactant in pure water and in the presence of KF, KCl, KBr, KI, KSCN, KNO<sub>3</sub>, K<sub>2</sub>CO<sub>3</sub>, K<sub>2</sub>SO<sub>4</sub>, K<sub>2</sub>HPO<sub>4</sub>, and CuSO<sub>4</sub>; the solution was prepared in a volumetric flask and placed in a refrigerator for 24 hours at 2 °C. Upon refrigerating at 2 °C for 24 hours, precipitation of hydrated solid crystals was observed. The solution was taken out of the refrigerator 24 hours later. Then the beaker with solution placed in a water bath circulator, HAAKE F3-C, to maintain the temperature of the system. Thereafter, the temperature of this precipitated solution was gradually raised thermostatically and equilibrated at predetermined temperature for ten (10) minutes maintaining constant stirring. Upon temperature equilibrium the specific conductance ( $\kappa$ ) was measured using a Eutech-Cyber Scan-CON-510 conductivity meter at each temperature until it reached at a constant value. Plotting the values of conductivity against the temperature we found a curve. Then, the  $T_K$  was measured from the sharp break point of the curve [9].

### **2.2.2 CMC measurement**

#### **2.2.2.1 CMC measurement by conductometric method**

The values of CMC of CPC and CPB in pure water and in the presence of electrolytes were determined above the Krafft temperature where no precipitate was present. To measure the CMC in conductometric method, measurements were started with a dilute solution keeping in a 100 mL tall form beaker which was placed in a HAAKE F3-C water bath circulator to maintain the temperature of the system. Temperature equilibrium was maintained after thorough mixing. The subsequent concentrated solutions were made by adding a previously prepared stock solution into the vessel by a 1 mL graduated pipette into a 100 mL tall form beaker. The specific conductivity of the solution was measured for each concentration at a fixed temperature using Eutech-Cyber Scan-CON-510 conductivity meter. After each addition, the solution was stirred with a glass rod to make the solution homogeneous. Plotting the values of conductivity of the solution against the

concentrations we found a curve having a break and the CMC was determined from this break point of the curve. The CMC values were calculated from the change in the conductivity versus concentration plot. Data above and below the accent point were linearly fitted. To observe the effect of electrolytes on the CMC, surfactant solutions were prepared in various electrolytes solutions of desired concentration [19].

#### **2.2.2.2 CMC measurement by surface tensiometric method**

First a concentrated stock solution was prepared to measure the CMC in surface tensiometric method. A 100 mL crystallization disk was cleaned with dichromic acid, deionized water and then dried in an oven at 110 °C for half an hour. The surface tension of the solution of surfactant in pure water and in the presence of various electrolytes were measured by a surfacetensimeter (Kruss K9) equipped with a platinum plate. Before each measurement, the plate was thoroughly washed with double distilled water and was heated by the flame of Bunsen burner. Before starting experiment at a specific temperature, the surface tension of the double distilled water was confirmed to be in the range of  $\pm 0.2$  mN/m. A dilute solution was transferred into a vessel that was thermostated by circulating water at the desired temperature. Surface tension measurements were started with the dilute solution and the subsequent concentrated solutions were made by adding a previously prepared stock solution into the crystallization disk by a 1 mL graduated pipette and the surface tension is carefully measured. Care was taken that the platinum plate was properly wetted with the solution. The reading of surface tension was taken 10 minutes after the every addition in order to ensure the establishment of equilibrium. Moreover, the establishment of equilibrium was checked by repeated measurements at 10 minutes intervals until the surface tension readings reached a constant value. The deviation in taking a reading was  $\pm 0.2$  mN/m. The CMC was determined from the break point of surface tension ( $\gamma$ ) versus  $\log_{10}C$  plot where C is the concentration of the surfactant solution [2].

#### **2.2.3 The measurement of solubilization of water insoluble dye in the micellar system**

The solubilization study of PAN in aqueous solution of CPB and in the presence of  $5 \times 10^{-3}$  M  $\text{KNO}_3$  were carried out at 30 °C. For these experiments, the surfactant solutions of different concentrations were made in 100 mL reagent bottles, where the surfactant



concentrations in the first few were below the CMC and the last few were above the CMC. In every solution a fixed amount of solubilize but excess to that of solubilization equilibrium were used for solubilization study. To equilibrate the solutions, the bottles were continuously agitated using a shaker (Stuart Orbital shakers, SSL1) at 250 rpm for 48 hours held in a horizontal position. The temperature for the system was chosen above the  $T_K$  to ensure the micelle formation of the surfactants in aqueous solution. The residue was removed by means of centrifugation and then filtration by using Whatman 41, ashless Quantitative Filter Paper with a pore size of 2.5  $\mu\text{m}$  to separate the amount of dye that was not solubilized. The filtrate was then analyzed by using the UV visible spectrophotometer (Jenway Spectrophotometer-7315). The absorbance of each solution was measured by using a quartz cell of path length 1 cm. The concentration of solubilize in the micelle was calculated with the help of a calibration curve obtained from the absorption spectra of known concentrations of PAN in CPB and curcumin in CPC against a reagent blank. The strong absorbance at 472 nm ( $\lambda_{\text{max}}=472$  nm) for PAN in the micelles gave a satisfactory Beer's law plot. In the same way the solubilization of curcumin with CPC in aqueous solution and in the presence of  $1.66 \times 10^{-3}$  M  $\text{K}_2\text{SO}_4$  was studied at 30 °C. Furthermore, the CMC of CPB was measured by the solubilization of PAN in aqueous solution and in the presence of  $5 \times 10^{-3}$  M  $\text{KNO}_3$ . The CMC of CPC was also measured by solubilization of curcumin in aqueous solution of CPC and in the presence of  $1.66 \times 10^{-3}$  M  $\text{K}_2\text{SO}_4$  [2].

### **2.2.4 The measurement of the metal-ligand complex in the micellar system**

The complex formation study was conducted out using Jenway Spectrophotometer 7315, England to measure the intensity of colour of the complex in the surfactant solution. In this case, the stock solutions of  $\text{CuSO}_4$ ,  $\text{NiSO}_4$ ,  $\text{ZnSO}_4$ , and standard solution of PAN were prepared in the same concentration of CPB in pure water. Again the stock solution of  $\text{CuSO}_4$ , and curcumin were prepared in the same concentration of CPC. The environment of the each solution was kept same in every time. A 100 mL of stock solutions of  $\text{CuSO}_4$ ,  $\text{NiSO}_4$ ,  $\text{ZnSO}_4$  were prepared by dissolving required amount of AR crystallize  $\text{CuSO}_4$ ,  $\text{NiSO}_4$ ,  $\text{ZnSO}_4$  (Merck, Germany) in the surfactant solution prepared by doubly distilled de-ionized water. More dilute standard solutions were prepared by appropriate dilution of aliquots from the stock solution with surfactant solution when required. A set of solutions were prepared in the following way: the same amount of metal solution was placed in 25 mL volumetric flask and adequate amount of PAN was

added. The mixture was diluted to the mark with the aqueous solution of surfactant. The set of solutions prepared in 25 mL volumetric flask equilibrated by shaking with hand. The absorbance was measured against a corresponding reagent blank, as well as, that of blank test against water. The metal ion content in an unknown sample was determined using concurrently prepared calibration graph. The absorbance of each solution was measured using quartz cell of path length 1cm against blank test, as well as that of blank test against deionized water.

**2.2.4.1 The measurement of the formation constant of the complex**

Formation constant or stability constant is equilibrium constant for the formation of a complex in a solution which indicates the strength of interaction between the ligand and metal ion. It is very important to calculate the concentration of the complex in solution. The formation of a complex between a metal ion, M, and a ligand, L, is usually a substitution reaction. Metal ion stays in solution as hydrated, so the reaction for the formation of the complex is written as;



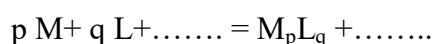
The equilibrium constant for this reaction is given by

$$\beta = \frac{[M(H_2O)_{n-1}L][H_2O]}{[M(H_2O)_n][L]} \dots\dots\dots (2.1)$$

In dilute solution the concentration of water is effectively constant. The expression becomes

$$\beta = \frac{[ML]}{[M][L]} \dots\dots\dots (2.2)$$

For the general equilibrium-



$$\beta_{pq} = \frac{[M_p L_q \dots\dots]}{[M]^p [L]^q \dots\dots} \dots\dots\dots (2.3)$$

**2.2.5 UV-Vis. spectrophotometric measurement**

Spectrophotometry is one of the most widely used methods of analysis, particularly in the visible region of the electromagnetic spectrum. Absorption spectrophotometry in the ultra-violet and visible regions is considered to be one of the valued techniques for the quantitative analysis. Visible light represents a very small part of electromagnetic spectrum and is generally considered to extend from 380-780 nm. It is very widely used in clinical chemistry and environmental laboratories [50]. UV-Vis. Spectrophotometer is

commonly used in the laboratory to analyze the colour compounds in the ultraviolet (UV) and visible (Vis.) regions of the electromagnetic spectrum. It allows one to determine the wavelength and absorbance. The following equation (2.4) is the common form of Beer's law.

$$A = \epsilon c l \dots\dots\dots (2.4)$$

The absorbance (A) is directly proportional to the concentration. The path length „l“ in equation (2.4) is expressed in centimeters; the concentration c is in moles/liter. The constant „ $\epsilon$ “ is known as Molar Absorptivity. Since A is unit less,  $\epsilon$  has the unit of  $L \text{ mol}^{-1} \text{ cm}^{-1}$ . Molar absorptivity and absorptivity are dependent on the nature of the absorbing material and the wavelength of measurement. Using this equation, we can determine the concentration of a sample to know the Molar extinction coefficient ( $\epsilon$ ) which is specific to a particular compound. In general, the Beer's law holds over a wide range of concentration if the structure of the coloured ion or of the coloured non-electrolyte in the dissolved state does not change with concentration.

### **2.2.6 ATR-IR spectrophotometric measurement**

Electromagnetic radiation can induce transitions among the vibrational energy levels only when the vibration of a molecule leads to an oscillating dipole moment and a vibrational spectrum can be expected. For example, molecules like  $H_2$ ,  $N_2$ ,  $O_2$  etc. will not give infrared spectrum whereas molecules like  $HCl$ ,  $H_2O$ ,  $NO_2$  etc. will give infrared spectrum. Infrared spectroscopy deals with the infrared region,  $14000 \text{ cm}^{-1}$  to  $10 \text{ cm}^{-1}$  of the electromagnetic spectrum. Furthermore, the IR portion of the electromagnetic spectrum is divided into three regions; near-infrared, mid-infrared and far-infrared. The near-infrared [51] energy, approximately in the region between  $14000$ - $4000 \text{ cm}^{-1}$  can excite overtone or harmonic vibrations. The mid-infrared [52] energy, approximately in the region between  $4000 \text{ cm}^{-1}$  to  $400 \text{ cm}^{-1}$ , can be used to study the fundamental vibrations of structures. The far-infrared region, approximately in the region between  $400$ - $10 \text{ cm}^{-1}$  can be used to study the rotations of structures. With IR spectroscopy, different functional groups adsorb at different IR bands or regions. Thus, this technique can help identify and even quantify organic and inorganic molecules. The infrared spectrum of a sample can be obtained by passing a beam of infrared light through the sample. A Fourier transform instrument [53] can be used to measure how much energy

was absorbed by the sample over the entire wavelength range. Attenuated total reflection (ATR) is a sampling technique used in conjunction with infrared spectroscopy which enables samples to be examined directly in the solid, vapour or liquid state without further preparation. The micellar solutions of CPB were studied in the presence of constant concentration of PAN to measure the effect of PAN and CuSO<sub>4</sub>-PAN complex on the alkyl chain of CPB. Here, it has been studied the effect of curcumin and CuSO<sub>4</sub>-curcumin complex on the alkyl chain of CPC at constant concentration of curcumin. The ATR-IR spectra were recorded on a SHIMADZU ATR-IR spectrophotometer and measurements were taken with 300 scans using a resolution of 1 cm<sup>-1</sup> by the attenuated total reflection technique. The incident angle employed for the sample was 45°.

### **2.2.7 Proton nuclear magnetic resonance (<sup>1</sup>H NMR) spectroscopic measurement**

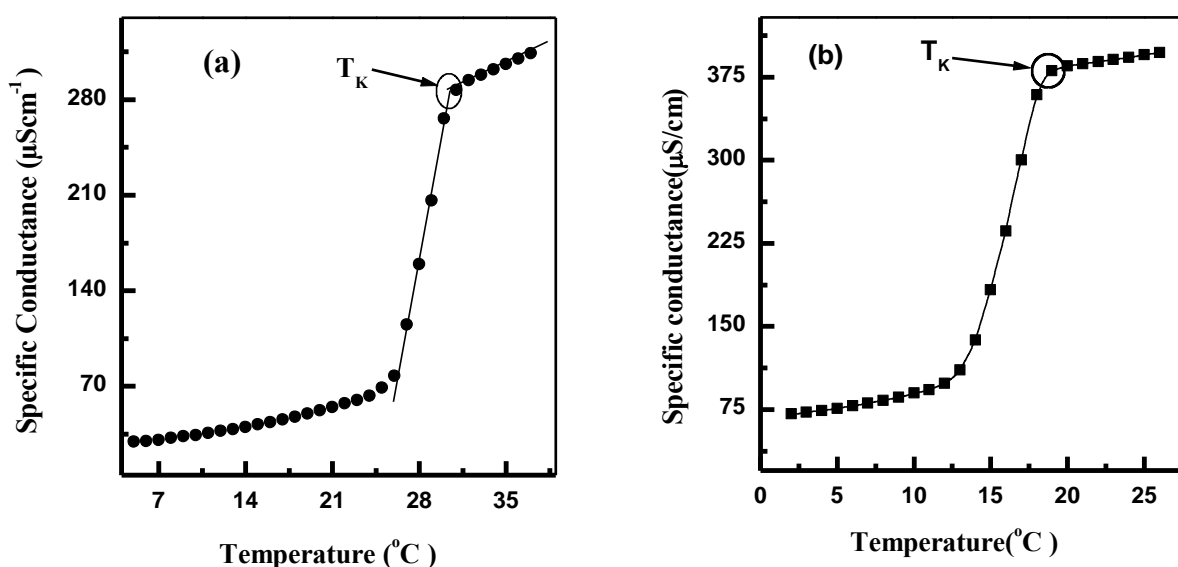
Surfactants lower the surface tension of the medium in which it is dissolved. At a certain concentration when the surface tension becomes lowest, these aggregate to each other and form micelle. Above this concentration when micelle formation starts, the physical properties of the solution change abruptly. The properties of these systems have been investigated by Proton nuclear magnetic resonance (<sup>1</sup>H NMR) spectroscopy. It plays an important role in characterization of micellization processes, physical properties of micelles, e.g. structure, size and shape, hydration of micelle, solubilization by micelles. It provides information at a molecular level that is not available by other spectroscopic methods. Chemical shift changes, relaxation experiments and NMR self diffusion measurements are almost used routinely. The first and obvious role of chemical shift is to distinguish among different molecules and different sites in the same molecule. Moreover, when it does not directly convey molecular information, chemical shift is essential to assign the information obtained by other NMR methods to the correct atomic location within the investigated system. NMR spectroscopy provides a deeper insight into the relative arrangement of surfactant molecules in the micelle. In the previous study [54–56] of NMR spectrum the chemical shift and relaxation time have been successfully utilized to understand the formation of micelle and relevant properties of surfactants. Below the CMC, the protons in the surfactant tail in solution are aqueous. On the other hand, above the CMC, the hydrocarbon chains are directed in the core of micelle

surrounded by other hydrophobic chain of micelle which may account for some chemical shifts [57]. The number of protons of  $^1\text{H}$  NMR signals is directly proportional to the area of that signals. Moreover, different kinds of protons have different electronic environments, and it is the electronic environment that determines just where in the spectrum a proton absorbs. The existence of the chemical shift can be attributed to the screening effect that the electrons about a nucleus exert. When a molecule is placed in a magnetic field, its electrons are caused to circulate and in circulating they generate secondary magnetic field and it opposes the applied field. The field felt by the proton is thus diminished and the proton is said to be shielded. Circulation of electrons, especially  $\pi$ -electrons, about nearby nuclei generates a field that can either oppose or reinforce the applied field at the proton depending on the location of the proton. If the induced field opposes the applied field, the proton is shielded and if the induced field reinforces the applied field then the field felt by the proton is augmented and the proton is said to be deshielded. For example, aromatic protons because of the powerful deshielding due to the circulation of the  $\pi$ -electrons consequently, aromatic protons absorb far down field; Ar-H ( $\delta=6.0-9.0$ ). The  $^1\text{H}$  chemical shifts of various protons in each of the two surfactants were monitored as a function of the surfactant concentration below and above its CMC. The micellar solutions of CPB were studied in the presence of constant concentration of PAN to measure the effect of PAN and Cu(II)-PAN complex on the protons of the alkyl chain. We also studied the effect of curcumin and Cu(II)-curcumin complex on the protons of the alkyl chain of CPC at constant concentration of curcumin. The NMR spectra were recorded on a BRUKER spectrometer operating at 400 MHz. Deuterium ( $^2\text{H}$ ) frequency-field lock is used to offset the effect of the natural drift of the NMR's magnetic field.

## **Chapter three: Results and discussion**

### 3.1 Effect of potassium salts on the Krafft temperature ( $T_K$ ) of CPB and CPC in aqueous system

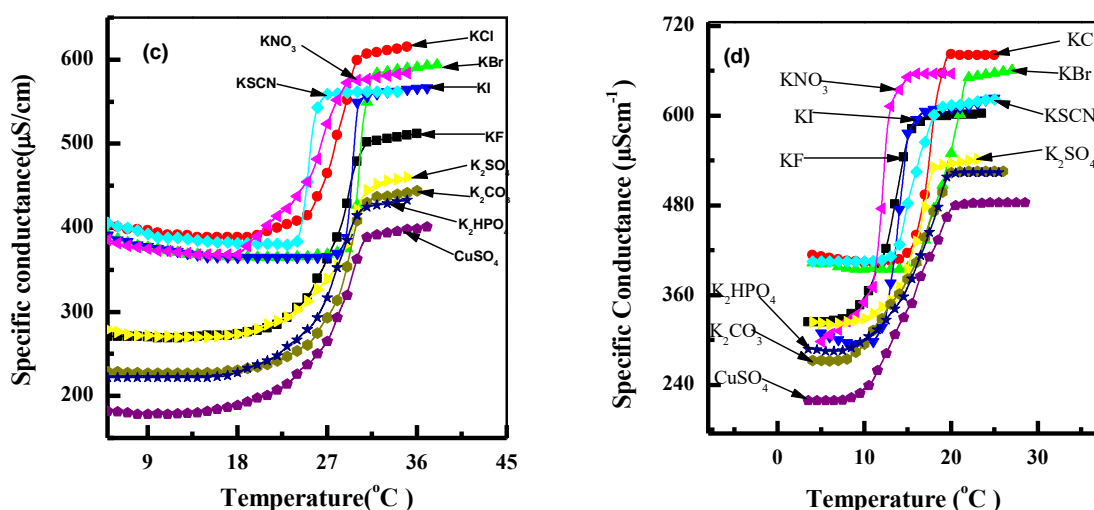
Krafft temperature ( $T_K$ ) is an important property of surfactant. To understand how surfactants work in cleaning, surface functionalization, foaming and emulsification it is important to know the  $T_K$  of the surfactant. The measurement of the  $T_K$  in pure water and in the presence of different potassium salts has been done by measuring the conductivity and surface tension of the solution at different temperature.



**Figures-3.1 Specific conductance ( $\mu\text{S}/\text{cm}$ ) versus temperature ( $^{\circ}\text{C}$ ) plot for (a) CPB in pure water; (b) CPC in pure water (The arrow signs in the plots indicate the Krafft temperature.)**

Figures-3.1(a) and (b) show the specific conductance ( $\mu\text{S}/\text{cm}$ ) versus temperature ( $^{\circ}\text{C}$ ) plots for CPB and CPC respectively in pure water. Figures-3.1(c) and (d) also show the specific conductance ( $\mu\text{S}/\text{cm}$ ) versus temperature ( $^{\circ}\text{C}$ ) plots for CPB and CPC respectively in the presence of different potassium salts at  $2.5 \times 10^{-3}$  ionic strength. These figures indicate that initially at low temperature conductivity increases very slowly upto a certain temperature because at low temperature surfactant molecules remain in water as hydrated solid crystals and the surfactant monomers. With increasing temperature, conductivity increases very sharply over a narrow temperature range because the hydrated solid start to ionize [19, 42]. But, at a certain temperature, the solution become transparent showing maximum conductivity, further increase in temperature the

conductivity increase very slowly or remain almost constant showing a break in the graph [10, 11]. The temperature at this break point is called the Krafft temperature ( $T_K$ ). Besides, the  $T_K$  is also narrated as the melting point of hydrated solid crystals in solution [12, 19, 42]. At or above this temperature the solubility of surfactant increases markedly due to the micelle formation and establishes an equilibrium state between surfactant monomers and micelle formation [36, 58]. Further increase in temperature, the conductivity increase very slowly due to the increase in the thermal motion of the charged species [59]. The values of  $T_K$  of CPB and CPC in pure water are found to be 30.15 and 18.53 °C respectively which are in good agreement with the literature value [19, 60].

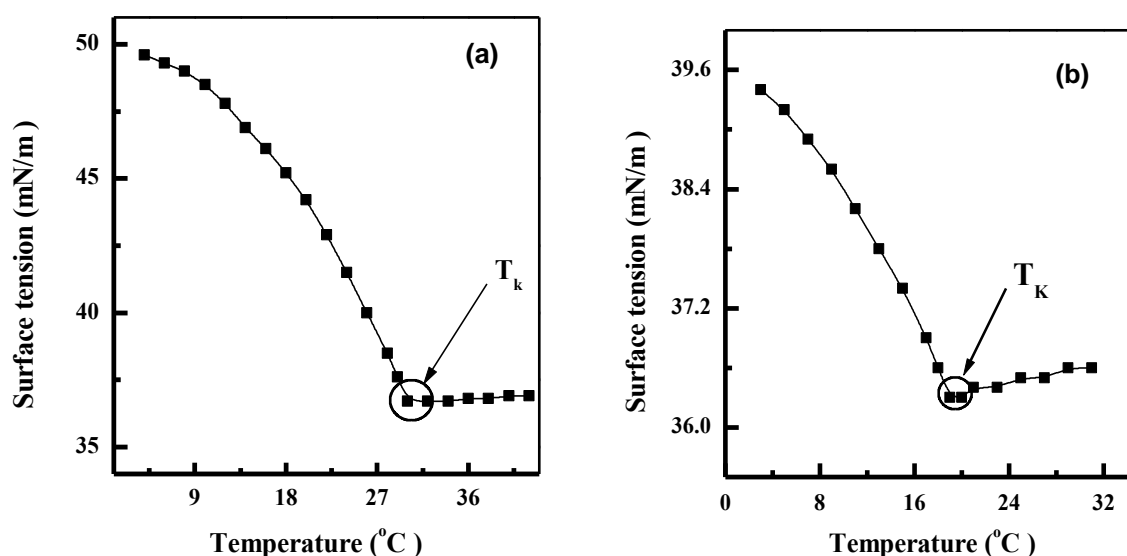


**Figures-3.1** Specific conductance( $\mu\text{Scm}^{-1}$ ) versus temperature ( $^{\circ}\text{C}$ ) plots for (c) CPB (0.01M); and (d) CPC (0.01 M) in pure water and in the presence of different potassium salts KF, KCl, KBr, KI, KSCN, KNO<sub>3</sub>, K<sub>2</sub>SO<sub>4</sub>, K<sub>2</sub>CO<sub>3</sub>, K<sub>2</sub>HPO<sub>4</sub> and CuSO<sub>4</sub> when ionic strength of each salt is  $2.5 \times 10^{-3}$

At and above the  $T_K$ , the surfactants attain maximum surface activity. To prove this phenomenon, surface tension of the surfactant was measured at different temperature. It is clear from figure-3.2(a) and 3.2(b) that the surfactants adsorb at the air-water interface due to their amphiphilic nature and breaks the cohesive force between the water molecules resulting in a decrease in the surface tension to stabilize the interface. With the increase of temperature the value of surface tension decreases and become minimum at a certain temperature, further increase in temperature the surface tension remains almost constant or increases very slowly. The temperature at the minimum surface tension is



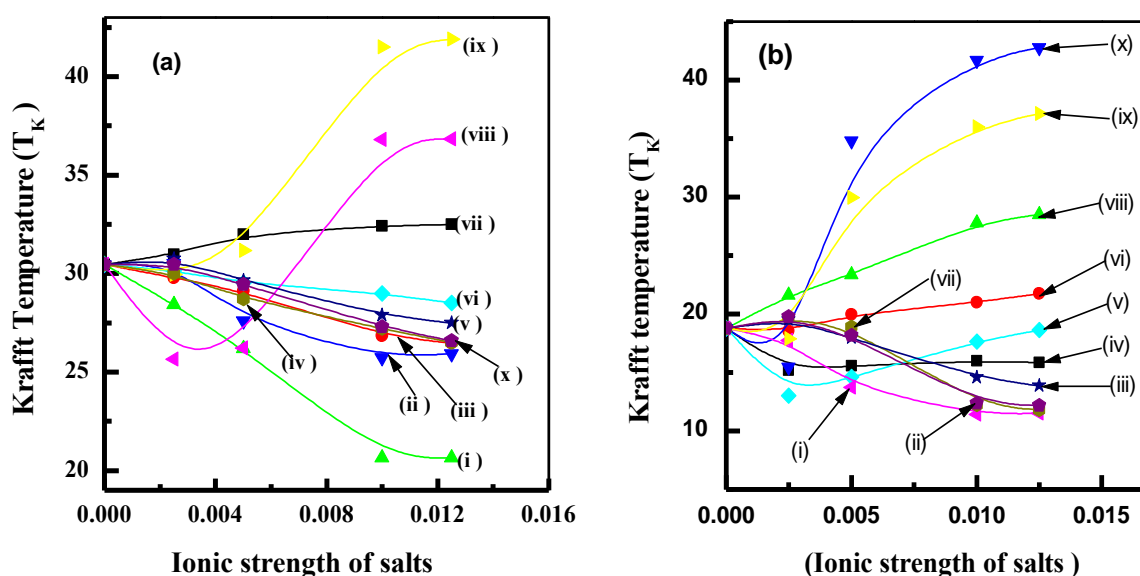
termed as Krafft temperature ( $T_K$ ). The  $T_K$  of aqueous solution of surfactant has also been measured measuring the surface tension of the solution at different temperature when the concentration of surfactant was above the CMC. Figures-3.2(a) and (b) represent the surface tension ( $\gamma$ ) versus temperature ( $T$ ) plots for CPB (0.01 M) and CPC (0.01 M) respectively in pure water. These figures show that surface tension decrease with increasing temperature and at a certain temperature the surface tensions of both the surfactants become the lowest and above this, the value of surface tension remains almost constant. The temperature at the break point is termed as krafft temperature ( $T_K$ ). The  $T_K$  values of these surfactants varies differently though the head groups, hydrophobic tails both of them are same [61].



**Figures-3.2 Surface tension (mN/m) versus temperature (°C) plot for (a) CPB (0.01 M) and (b) CPC (0.01 M) in pure water (The arrow signs in the plots indicate the Krafft temperature.)**

Figures-3.3(a) and (b) show the  $T_K$  of CPB and CPC respectively in aqueous solution in the presence of KF, KCl, KBr, KI, KSCN, KNO<sub>3</sub>, K<sub>2</sub>SO<sub>4</sub>, K<sub>2</sub>CO<sub>3</sub>, K<sub>2</sub>HPO<sub>4</sub> and CuSO<sub>4</sub> varying the concentration of these salts. It was observed that the  $T_K$  of CPB and CPC increase or decrease in the presence of added counter-ion depending on the size and charge density of these ions. It is evident from Figures-3.3(a) and (b) that stronger chaotropic ions SCN<sup>-</sup> and I<sup>-</sup> present in the extreme right side in the Hofmeister series cause an increase in the  $T_K$  due to the salting out effect. This is in line with the observation of a previous study that the  $T_K$  varies with the concentration of the added

electrolyte [62]. In the present work, the concentration of all the salt solutions have been kept within 0.1 M except for  $K_2SO_4$ ,  $K_2CO_3$ , and  $K_2HPO_4$  to investigate the salt effect on the  $T_K$  of CPB and CPC. The figures-3.3(a) and (b) show that the  $T_K$  increases in the presence of chaotropic anions ( $SCN^-$ ,  $I^-$ ) and common ions but decreases in the presence of kosmotropic anions ( $SO_4^{2-}$ ,  $CO_3^{2-}$ ,  $HPO_4^{2-}$ ,  $F^-$ ) and moderate chaotropic anions ( $Cl^-$  and  $NO_3^-$ ). Kosmotropes are small ions of high charge density or structure making ions since it induce a more organized structure of the water around the hydration sphere. This ions-water interaction is stronger than water-water interaction. So, the kosmotropic ions stay in water being strongly hydrated and decrease dielectric constant of the solution creating a more intense electrostatic field and they preferentially show higher negative adsorption behavior [63]. Consequently, in the presence of kosmotropic ion the aqueous solubility of nonpolar solutes decreases.



**Figures-3.3** The Krafft Temperature ( $T_K$ ) versus salt concentration plots for (a) CPB (0.01M) in pure water and in the presence of different potassium salts (i)  $KNO_3$ , (ii)  $K_2SO_4$ , (iii)  $KCl$ , (iv)  $K_2HPO_4$ , (v)  $K_2CO_3$ , (vi)  $KF$ , (vii)  $KBr$ , (viii)  $KSCN$ , (ix)  $KI$ , and (x)  $CuSO_4$  where ionic strengths of the salts are from  $2.5 \times 10^{-3}$  to  $12.5 \times 10^{-3}$ ; (b) CPC (0.01M) in pure water and in the presence of different potassium salts (i)  $K_2SO_4$ , (ii)  $CuSO_4$ , (iii)  $K_2HPO_4$ , (iv)  $KF$ , (v)  $KNO_3$ , (vi)  $KCl$ , (vii)  $K_2CO_3$ , (viii)  $KBr$ , (ix)  $KSCN$ , and (x)  $KI$  where ionic strengths of the salts are from  $2.5 \times 10^{-3}$  to  $12.5 \times 10^{-3}$

On the other hand, the aqueous solubility of polar solutes increases. From this study, it has been observed that the presence of kosmotropic ions such as  $SO_4^{2-}$ ,  $CO_3^{2-}$ ,  $HPO_4^{2-}$ ,

and  $F^-$  favour dispersion of the surfactants in the aqueous solution leading to an increase in solubility with a decrease in the  $T_K$ . However, with the increase of concentration of these ions the  $T_K$  decrease gradually with increasing the concentration of added electrolyte and found a minimum value when the concentration of these electrolytes become equal to the concentration of surfactant. Further increase in concentration of these electrolytes keeping the surfactant concentration constant, the  $T_K$  shows almost steady value. Among these kosmotropic ions, the behavior of  $F^-$  is somewhat exceptional. It cannot decrease the  $T_K$  of both the surfactants comparing with the other kosmotropic ions because the  $F^-$  ion remains in water being extensively hydrated due to high charge density and does not show any tendency to lose the hydration shell. Along with this hydration shell  $F^-$  ion acts as a single ion. So, its active charge density decreases and acts as a weak kosmotropic ion but cannot form a contact ion pair with the weakly hydrated cetylpyridinium ion. Hence, there exists a significant electrostatic repulsion between the charged surfactant molecules, which favors their dispersion in the aqueous solution leading to a decrease in the  $T_K$ .

On the contrary, ions with a low charge to radius ratio such as  $SCN^-$ ,  $I^-$  and  $Br^-$  are termed as chaotropic ion. In the case of these ions, the ion-water interaction is weaker than water-water interaction. Consequently, these ions do not bind to the adjacent water molecules strongly and remain in water being weakly hydrated [64] and have a preferential tendency to accumulate at the air-water or hydrocarbon-water interface [65]. This type of behavior of accumulation at the air-water interface is termed as positive adsorption behavior [66]. The chaotropic ions are water structure breaker and in the presence of these ions the aqueous solubility of nonpolar solutes increases. These ions form contact ion pair with the cationic part of both the surfactants effectively screening the electrostatic repulsion between the surfactant molecules and promote salting-out behavior, leading to an increase in the  $T_K$ .

Collins' „Law of matching water affinities“ [67, 68] suggest that interaction between ions in aqueous solution depends on charge density of these ions. This concept clarify that chaotropes form contact ion pair with chaotropes as well as kosmotropes do with other kosmotropes when water affinities of cation and anion become similar. Kosmotropes are

more strongly hydrated than the chaotropes as these ions can create a more intense electrostatic field. Consequently, the extent of distortion in the structure of free water surrounding the hydrated kosmotropes is much less than that in the case of weakly hydrated chaotropes. Kosmotropes do not come into close contact with chaotropes due to their large difference in water affinities. Such ions form a highly soluble solvent separated pairs since the weakly hydrated chaotropes cannot break through the hydration shell of the strongly hydrated kosmotropes.

Besides, the cetylpyridinium ion behaves as a chaotropic cation because the nitrogen of cetylpyridinium ion is  $sp^2$  hybridized which cannot accommodate tetrahedral structure of water. Consequently, cetylpyridinium ion remains in water being weakly hydrated [69]. Therefore, it can be expected that weakly hydrated chaotropes  $SCN^-$  and  $I^-$  will readily form contact ion pairs with the weakly hydrated cetylpyridinium ion and thus reduces the electrostatic repulsion between the surfactant molecules and improves Van der Waals forces. Such ion pairs are much less hydrated and show salting out behavior with a consequent increase in the  $T_K$  of both the surfactants. In the presence of stronger chaotropic anion such as  $I^-$  and  $SCN^-$ , the  $T_K$  of CPB increases from 30.15 °C to 41 °C and 36 °C, respectively and the  $T_K$  of CPC increases from 18.53 °C to 41 °C and 36 °C, respectively.

It is important to note here that  $SCN^-$  ion at  $2.5 \times 10^{-3}$  M and  $5 \times 10^{-3}$  M shows an irregular behaviour. At this ionic strength, the  $T_K$  was found to be lower than that of CPB in pure water when surfactant concentration is higher than that of  $SCN^-$  concentration. The  $T_K$  of CPB has been determined 25.64 °C and 26.22 °C when concentration of CPB is 0.01 M and concentrations of  $SCN^-$  are  $2.5 \times 10^{-3}$  M and  $5 \times 10^{-3}$  M, respectively. The vibrational sum frequency experiment revealed that the hydrogen atoms of water molecules are directed towards the bulk and the oxygen atom directed towards the gas phase [66]. Therefore, it is reasonable to expect a preferential accumulation of anions near the interface and the extent of accumulation of the anions at the interface are influenced by their relative tendency of hydration in the bulk. It is also observed that in the presence of different potassium salts,  $K_2SO_4$ , KF, KCl, KBr,  $KNO_3$ ,  $K_2HPO_4$ ,  $K_2CO_3$ , KSCN and KI, at 25 °C the increased surface tension of water were found to be 4.8, 1.4, 1.6, 1.2, 1.1, 0.4, 1.5, 0.3 and 0.7 (mN/m)/(M) respectively. Thus, it appears from the data that the

increase in surface tension for  $\text{SCN}^-$  is  $0.3 \text{ (mN/m)/(mol/L)}$  and this value is lower in compared to the other ions [2]. This is why, the  $\text{SCN}^-$  ion has the greatest ability to adsorb at the interface. When this ion adsorbs at the interface, the hydrogen bonding networks of water molecules at the interface are broken. As a result, the number of free water molecules increase which enhances the hydration of the surfactant monomers significantly. This gives the CPB molecules an increased solubility with a consequent decrease in the  $T_K$ . With increasing the concentration of  $\text{SCN}^-$  further adsorption does not occur because the interface is fully occupied. Under this condition, the contact ion pair formation occurs between  $\text{SCN}^-$  and cetylperidinium ion in the bulk and increase in the  $T_K$  of CPB.

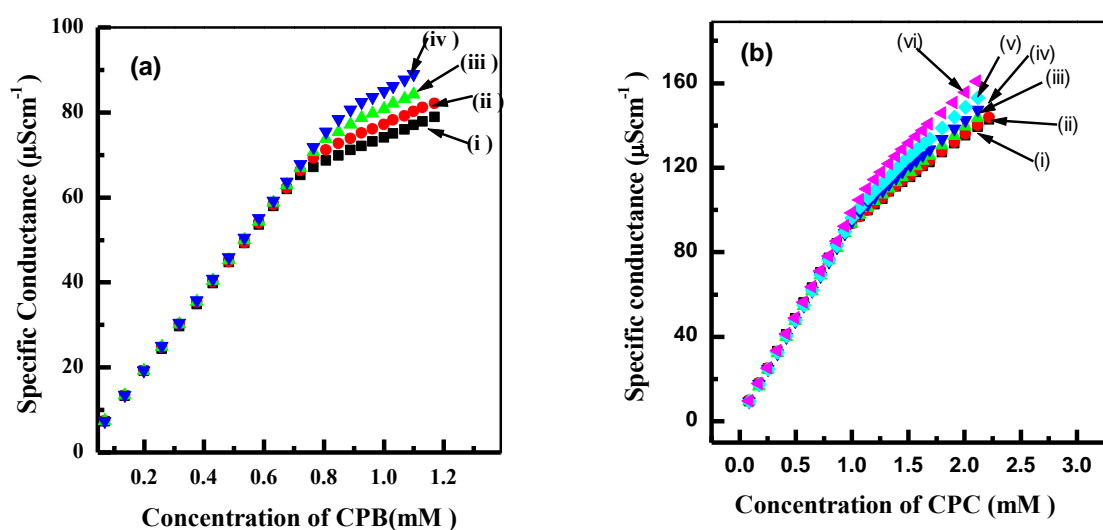
In addition, it is clear from the previously mentioned data that  $\text{SO}_4^{2-}$  has the greatest ability to increase the surface tension relative to the pure water. This observation indicates that more kosmotropic ions preferentially remain in the bulk of the aqueous solution being strongly hydrated. So, the kosmotropic ions show negative adsorption behavior according to the Gibbs adsorption equation [66]. However, it was shown by Levin and Santos that the kosmotropic ions remain hydrated near the interface and is repelled from it, while the chaotropic ions lose their hydration sheath and tend to accumulate at the air-water as well as low solvated hydrophobic interface [68, 70]. Water molecules interact with individual ions in the way which is dependent on the charge density and extent of hydration of the ions. The electrochemical process controls the behavior of the ions in the high dielectric regime of water. It was reported by Cremer and co-workers that the accumulation of the weakly hydrated chaotropes can interfere with hydrophobic hydration by increasing the surface tension of the hydrocarbon-water interface and exhibit salting out behavior of macromolecules [71]. Therefore, it is reasonable to expect that these ions will be preferentially accumulated at the surface of the hydrophobic chain of the surfactant. This directly disturbs the hydrophobic hydration of the surfactant resulting in salting out behavior with a consequent increase in the  $T_K$ .

Furthermore, it has been shown from neutron and X-ray diffraction experiments that considerably less hydrogen bonding exists in the presence of chaotropic ion than in pure water [24]. Nuclear magnetic resonance studies demonstrate that the water molecules adjacent to a chaotropic ions tumble more rapidly than in the bulk of the solution [72].

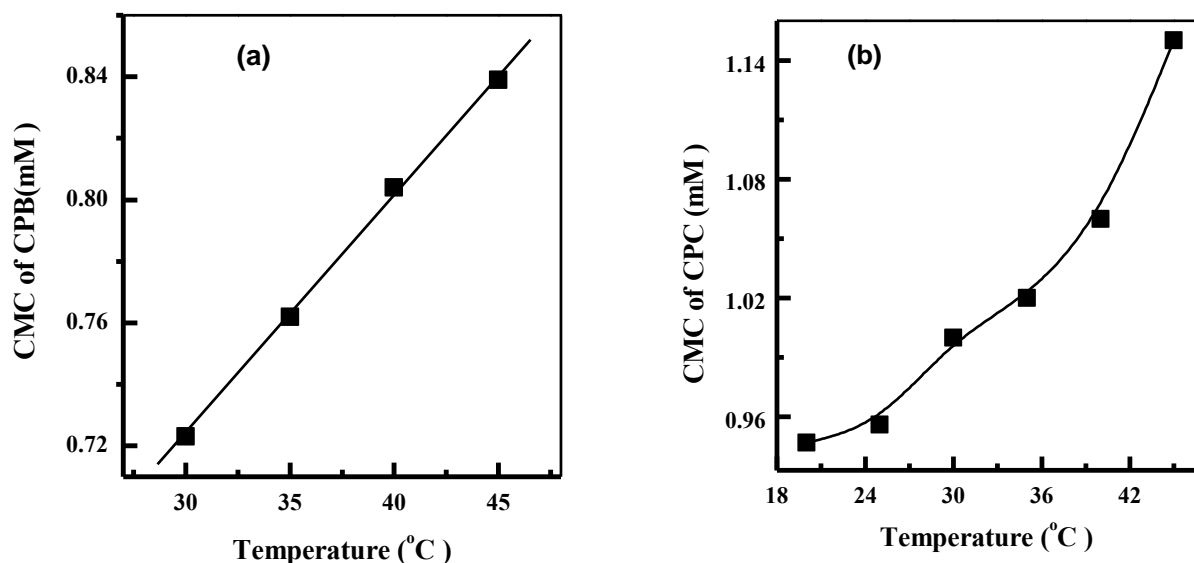
Therefore, it is expected that chaotropic ions do not form hydrogen bond with adjacent water molecules. These free water molecules promote hydration of the surfactant. Consequently, the solubility of the surfactant increases resulting in a decrease in the  $T_K$ . Besides, in the presence of KBr and KCl, the  $T_K$  of CPB and CPC respectively increases which can be attributed to the common ion effect [73]. In the presence of common ion, the solubility of weak or sparingly soluble salts decreases slightly to keep the solubility product constant. In spite of being moderate chaotropic ion,  $Cl^-$  and  $NO_3^-$  should exhibit higher tendency for hydration than more chaotropic  $SCN^-$  and  $I^-$  ions and decreases in the  $T_K$  of the surfactant. Since, the ion of smaller size having higher charge density has the capability to bind the water molecules more tightly around the hydration spheres than chaotropic ion. Thus, it appears that except for  $SCN^-$ ,  $I^-$ ,  $Br^-$  and common ion the rest of the anions such as  $NO_3^-$ ,  $SO_4^{2-}$ ,  $CO_3^{2-}$ ,  $HPO_4^{2-}$  and  $F^-$  are effective in lowering the  $T_K$  of CPC and CPB in aqueous solution.

### **3.2 Effect of potassium salts on the critical micelle concentration (CMC) of CPC and CPB**

The applications of surfactants lie on their capacity of micelle formation. So, it is important to know the CMC of CPB and CPC in aqueous system. The measurement of the CMC in pure water and in the presence of different potassium salts has been done by measuring the conductivity and surface tension of the solution at different concentration. Figures-3.4(a) and (b) show the specific conductance ( $\mu S/cm$ ) versus concentration (mM) of CPB and CPC respectively in pure water at different temperature. It is observed from each figure that the conductivity increases linearly with increasing the concentration of the surfactant upto a certain concentration and further increase in concentration the conductivity increase linearly showing a break in the graph. The break point in the specific conductance versus surfactant concentration plot is an indication of micelle formation. This evidence for micelle formation is explained as a sharp increase in the mass per unit charge of the micelle. The region below the break point is termed as pre-micellar region and above the break point is termed as post micellar region. The slope of the pre-micellar region is greater than that of the post-micellar region and the CMC is determined from the intersection point of two slopes of the two straight lines above and below the break point.



Figures-3.4 Specific conductance versus concentration plots for (a) CPB in pure water at (i) 30 °C, (ii) 35 °C (iii) 40 °C, (iv) 45 °C; (b) CPC in pure water at (i) 20 °C, (ii) 25 °C (iii) 30 °C, (iv) 35 °C, (v) 40 °C, (vi) 45 °C



Figures-3.5 (a) Critical micelle concentration (CMC) versus temperature (K) plot for CPB in pure water; (b) Critical micelle concentration (mM) versus temperature (°C) plot for CPC in pure water

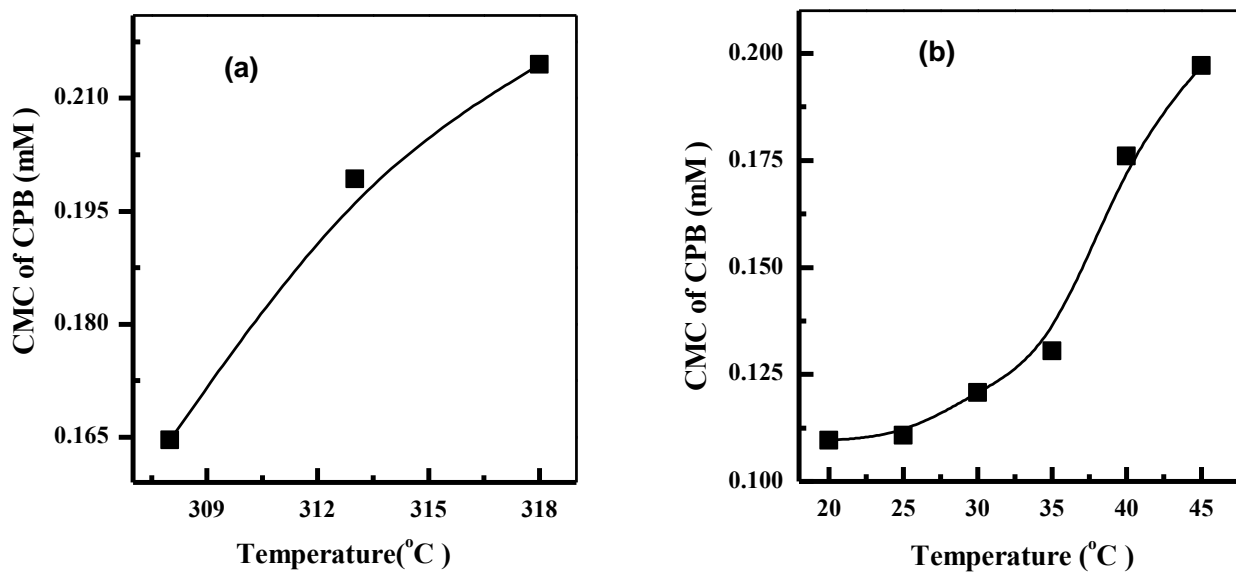
Figures-3.5 (a) and (b) show the CMC (mM) versus temperature (°C) plots for CPB and CPC, respectively in pure water. These figures indicate that CMC increase with increasing temperature of the system. The literatures contain examples of a continuous

increase in CMC with temperature [74, 75]. There are two opposing phenomena which govern the effect of temperature on the CMC of surfactant in aqueous solution [76, 77]. With the increase of temperature the degree of hydration of the hydrophilic head group decreases, which favours micellization and temperature increase of the solution also causes the disruption of ice-berg structure of water around the hydrophobic tail and this is unfavorable to micellization [78, 79]. These two factors determine whether the CMC will increase or decrease over a particular range of temperature. Our experimental results reveal that the CMC values of CPB and CPC in pure water show an increasing trend with increasing temperature which indicates that the second effect predominates over the first one. We have also investigated the effect of electrolytes on the CMC of CPB and CPC at 45 °C by conductometrically. This specific temperature was chosen to measure the CMC of each system because of the fact that the  $T_K$  of both the surfactants remains below 45 °C in the presence of all the electrolytes at ionic strength of  $5 \times 10^{-3}$ . Below the  $T_K$ , we could not measure the CMC because at this temperature the surfactant stays in water as hydrated solid crystals and above 45 °C the vaporization of water occurs which changes the concentration of solution and also the practical use of surfactant solution above this temperature are rather limited. The  $T_K$  can increase when the salt to surfactant concentration ratio is too high [62]. Below this temperature, we could not measure the CMC of these surfactants in the presence of  $5 \times 10^{-3}$  M  $SCN^-$  and  $\Gamma^-$  solutions because precipitation occurs. The  $T_K$  of the CPB and CPC remain below 45 °C in the presence of the most electrolytes studied in this work. A significant number of papers have dealt with the effect of electrolytes on the CMC of ionic surfactants [80–82]. Tables-3.4 and 3.5 show that the CMC obtained from the conductometric method is slightly higher than that obtained from the surface tensiometric method and is in good agreement with the literature values [81]. From these data it is observed that the CMC decreases in the presence of added electrolytes due to the neutralization of micellar surface charge by the excess counter-ions thereby electrostatic repulsion between the charged head groups decreases and favours micelle formation [83]. The weakly hydrated chaotropes preferentially adsorb at the hydrophobic surface and directly disturb hydrophobic hydration [64]. This phenomenon facilitates closer packing of surfactant in the micelle and thus decreases CMC. The chaotropes can form contact ion pair quickly with the surfactant head group as the cetylpyridinium ion behaves like a chaotrope. As a result, repulsion between the head groups decrease. Therefore, stronger chaotropic ions such as

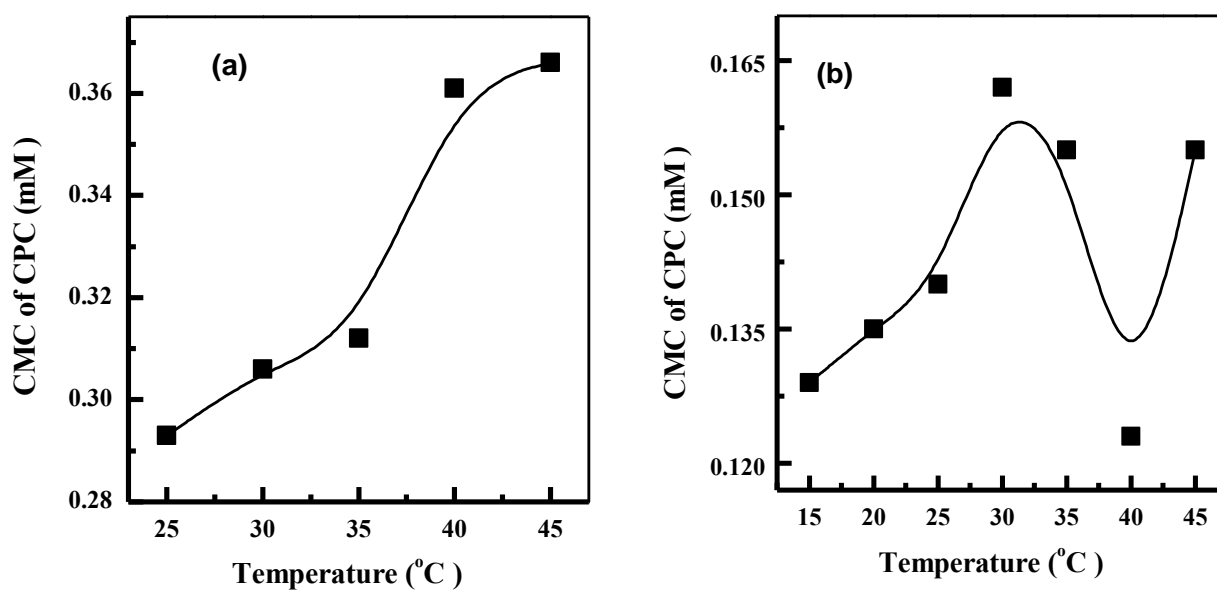


$\text{SCN}^-$  and  $\Gamma^-$  interact strongly and neutralize the micellar surface charge subsequently decrease the CMC of both the surfactants [83]. On the other hand, kosmotropic ions stay in water being strongly hydrated and do not show any tendency to lose their hydration shell. Therefore, they do not come into close contact with the micelle surface. Thus, chaotropes are more effective in lowering the CMC compared to kosmotropes. Among these ions,  $\text{F}^-$  is the least effective in lowering the CMC. The  $\text{F}^-$  ion stays in water being extensively hydrated and behaves as a single ion along with the hydration shell because of high charge density. As a result, the effective charge of this stronger kosmotrope decreases markedly and do not show any tendency to lose the hydration shell. But, it cannot approach at the close proximity of micelle surface to neutralize the micellar surface charge and stay in the bulk apart from cetylpyridinium ion. So, in the presence of  $\text{F}^-$  ion the CMC of both the surfactants decreases less than other kosmotropic ions.

In addition, different counter-ion present in solution competes with each other to adsorb onto the micelle surface and multivalent ions exhibit greater tendency for adsorption compared to the monovalent one [83–85]. Consequently, doubly charged kosmotropes screen the net positive charge of micelle surface double of singly charged ion [85]. In such a situation, in the presence of  $\text{SO}_4^{2-}$ ,  $\text{CO}_3^{2-}$ , and  $\text{HPO}_4^{2-}$  the values of CMC of both the surfactants decreases more compared to the rest of the monovalent ions ( $\text{Br}^-$ ,  $\text{Cl}^-$ , and  $\text{F}^-$ ). Among these ions  $\text{SCN}^-$  ion is the most effective in lowering the CMC of both the surfactants comparing the CMC in the presence of other ions. Where ionic strength of electrolytes used in every solution is  $5 \times 10^{-3}$ . A significant number of papers have dealt with the effect of electrolytes on the CMC values of ionic surfactants [59, 81, 86–88]. These studies have shown that in the presence of added electrolytes, the efficiency of lowering the CMC is dependent on the concentration of the added counter-ion and nature of them [83]. Figures-3.6(a) and (b) show the CMC versus temperature curves for CPB in the presence of  $5 \times 10^{-3}$  M KBr and  $\text{KNO}_3$  and Figures-3.7(a) and (b) show the CMC versus temperature curves for CPC in the presence of  $5 \times 10^{-3}$  M KCl and  $1.66 \times 10^{-3}$  M  $\text{K}_2\text{SO}_4$  respectively. From these Figures it is clearly observed that the CMC of the surfactant increases slightly with the increase of temperature in pure water even in the presence of salts over the studied temperature range.



Figures-3.6 Critical micelle concentration versus temperature (°C) plots for (a) CPB in the presence of  $5 \times 10^{-3}$  M KBr and (b) in the presence of  $5 \times 10^{-3}$  M KNO<sub>3</sub>



Figures-3.7 Critical micelle concentration versus temperature (°C) for CPC (a) in the presence of  $5 \times 10^{-3}$  M KCl; (b) in the presence of K<sub>2</sub>SO<sub>4</sub> at  $5 \times 10^{-3}$  ionic strength

**Table-3.1 Degree of counter-ion binding, the CMC of CPB in pure water and in the presence of different potassium salts**

Medium	Temperature (°C)	$\beta$	CMC (mM) (conductometric)	CMC (mM) (surface tensiometric)
Pure CPB	30	0.67	0.72	0.67
	35	0.65	0.76	0.69
	40	0.62	0.80	0.71
	45	0.57	0.84	0.81
$5 \times 10^{-3}$ M KNO <sub>3</sub>	20	0.61	0.11	0.11
	25	0.54	0.10	0.11
	30	0.52	0.12	0.12
	35	0.49	0.13	0.13
	40	0.48	0.18	0.13
	45	0.42	0.21	0.15
$5 \times 10^{-3}$ M KBr	35	0.39	0.16	0.17
	40	0.37	0.20	0.20
	45	0.36	0.23	0.21
$5 \times 10^{-3}$ M KF	45	0.38	0.60	0.57
$5 \times 10^{-3}$ M KCl	45	0.27	0.30	0.26
$5 \times 10^{-3}$ M KI	45	0.37	0.05	0.05
$5 \times 10^{-3}$ M KSCN	45	0.41	0.03	0.02
$1.66 \times 10^{-3}$ M K <sub>2</sub> SO <sub>4</sub>	45	0.66	0.20	0.09
$1.66 \times 10^{-3}$ M K <sub>2</sub> CO <sub>3</sub>	45	1	0.27	0.19
$1.66 \times 10^{-3}$ M K <sub>2</sub> HPO <sub>4</sub>	45	0.54	0.25	0.13

Generally, two interactions govern the CMC values: first is the Van der Waals interaction between the hydrophobic alkyl chains and second is the opposing repulsive interaction between the charged head groups. With the increase of temperature the degree of hydration of the hydrophilic head group decreases, which favours micellization and temperature increase of the solution also causes the disruption of ice-berg structure of water around the hydrophobic tail which is unfavorable to micellization. These two factors determines whether the CMC will increase or decrease with the change of temperature. The increase of CMC with increasing temperature indicates that the second effect predominates over the first one within the studied temperature range. From figure-3.7(b), it is also observed that in the presence of  $1.66 \times 10^{-3}$  M K<sub>2</sub>SO<sub>4</sub> the CMC of CPC initially increases and then decreases with increasing temperature, showing a maximum at 30 °C. This can be explained on the basis of fact that the thermal solubility of monomers which disfavors micellization and the dehydration of the head group favors micellization due to the increase in the hydrophobic character of the surfactant [5]. These two factors oppose each other depending on a number of factors [80] and determine whether the

CMC will decrease or increase with the change of temperature. Thus, the initial increase in the CMC can be attributed to the thermal solubility of the surfactant monomers with increasing temperature.

**Table-3.2 Degree of counter-ion binding, the CMC of CPC in pure water and in the presence of different potassium salts**

Medium	Temperature (°C)	$\beta$	CMC (mM) (conductometric)	CMC (mM) (surface tensiometric)
Pure CPC	20	0.56	0.95	0.73
	25	0.55	0.96	0.79
	30	0.54	0.1	0.91
	35	0.51	1.02	0.92
	40	0.44	1.06	1.03
	45	0.47	1.12	1.08
$1.66 \times 10^{-3}$ M $K_2SO_4$	20	0.56	0.14	0.10
	25	0.55	0.14	0.11
	30	0.55	0.16	0.14
	35	0.69	0.16	0.14
	40	0.56	0.12	0.12
	45	0.40	0.16	0.13
$5 \times 10^{-3}$ M KCl	25	0.54	0.29	0.28
	30	0.52	0.30	0.28
	35	0.56	0.34	0.28
	40	0.54	0.35	0.29
	45	0.26	0.36	0.29
$5 \times 10^{-3}$ M KF	45	0.33	0.75	0.74
$5 \times 10^{-3}$ M KBr	45	0.55	0.27	0.19
$5 \times 10^{-3}$ M KI	45	0.40	0.04	0.04
$5 \times 10^{-3}$ M KSCN	45	0.40	0.03	0.02
$5 \times 10^{-3}$ M $KNO_3$	45	0.54	0.18	0.14
$1.66 \times 10^{-3}$ M $K_2CO_3$	45	1	0.25	0.20
$1.66 \times 10^{-3}$ M $K_2HPO_4$	45	0.51	0.30	0.12

In the presence of  $K_2SO_4$  the CMC of CPC reaches at a maximum at 30 °C and then starts to decrease with further increase in temperature. Probably, the first effect exerts its limiting influence and then the dehydration of the head group dominates over the solubility effect. As a result, steric hindrance between the head groups decreases, showing

a gradual decrease in the CMC with increasing temperature. From thermodynamic considerations it has been quantitatively shown that micellization becomes more favorable with increasing temperature [11]. These phenomena have been attributed to an increase in the dehydration of the head group with increasing temperature. Our observation is in line with these phenomena. Further increase in temperature of the system, the CMC of CPC increase because the disruption of water structure around the hydrophobic chain increases and the degree of counter-ion binding decreases with increasing temperature which difavours micellization. The degree of counter-ion binding ( $\beta$ ) is obtained from the relationship  $\beta = (1-\alpha)$  where  $\alpha$  is the degree of ionization. The degree of ionization ( $\alpha$ ) of micelle was measured dividing the slope of post-micellar region ( $s_2$ ) by the slope of pre-micellar region ( $s_1$ ) i.e.  $\alpha = \left(\frac{s_2}{s_1}\right)$  [11, 81]. Tables-3.1 and 3.2 show the results of the degree of counter-ion binding ( $\beta$ ) for CPB and CPC. It is clear from these tables that  $\beta$  decreases with increasing temperature and the degree of ionization of the micelle increases due to the thermal agitation. This is in agreement with the observed values of the CMC in the presence of potassium electrolytes [81].

### **3.2.1 Proton nuclear magnetic resonance ( $^1\text{H}$ NMR) spectra of CPB above and below the CMC**

Surfactant aggregates in the bulk to form micelle when a specific concentration is exceeded and abrupt changes in physical properties of the solution can be observed. The properties of these systems have been investigated by proton nuclear magnetic resonance ( $^1\text{H}$  NMR). This technique plays an important role in characterization of micellization process, physical properties of micelles e.g. structure, size and shape, hydration of micelles, solubilization by micelles. It also provides information at a molecular level that is not available by other spectroscopic methods. Figure-3.8 shows the  $^1\text{H}$  NMR spectra for aqueous solution of CPB below the CMC. To understand the peak values of CPB, the hydrocarbon chain is differentiated as  $\alpha$ - $\text{CH}_2$ ,  $\beta$ - $\text{CH}_2$ , and  $-\text{CH}_3$ , group  $-\text{CH}_2$  and  $-\text{C}_5\text{H}_5\text{N}$ . The protons of group  $-\text{CH}_2$  in the aliphatic chain of CPB give a singlet, whose deconvolution and intregration reveals a signal at 1.230 ppm, the protons of  $-\text{CH}_3$  give a triplet at 0.827 ppm, the protons of  $\alpha$   $-\text{CH}_2$  give a triplet at 1.982 ppm, the protons of  $\beta$   $-\text{CH}_2$  give a doublet at 1.306 ppm, and the protons of  $-\text{C}_5\text{H}_5\text{N}$  give a multiplet from 8.018 to 8.816 ppm.

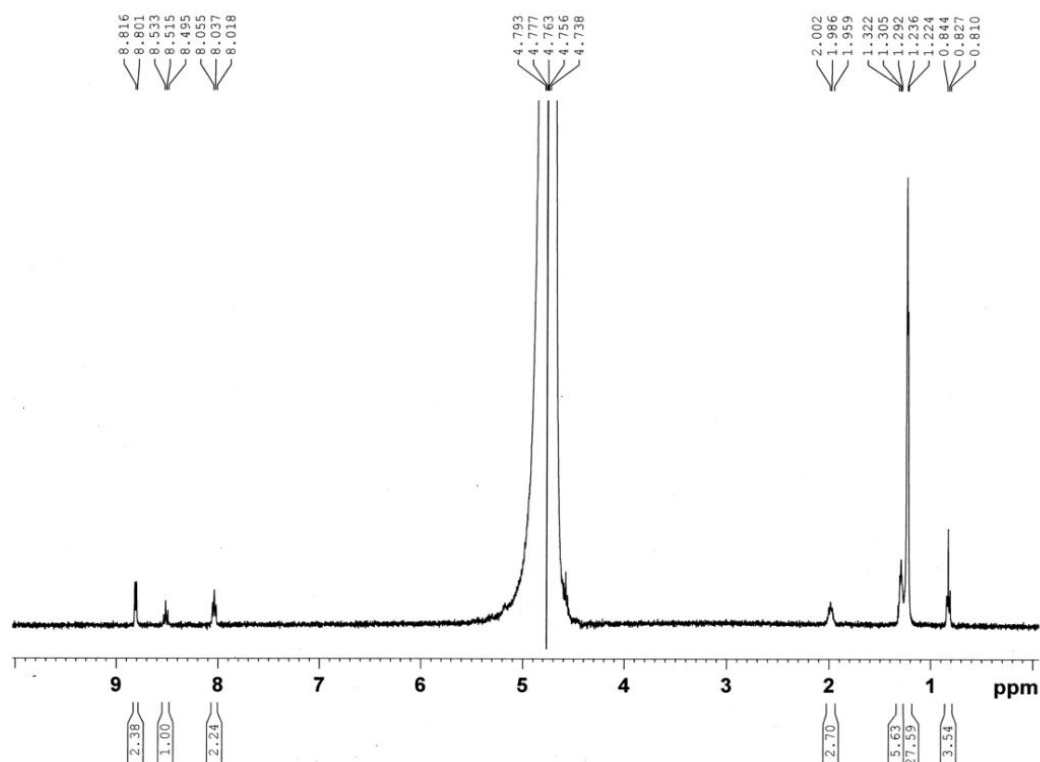


Figure-3.8  $^1\text{H}$  NMR spectra of CPB in aqueous solution below the CMC ( $5 \times 10^{-3}$  M)

Figure-3.9 shows the  $^1\text{H}$  NMR spectra for aqueous solution of CPB above the CMC, where the protons of  $-\text{CH}_2$  in the aliphatic chain of CPB give a singlet at 1.085 ppm, the protons of  $-\text{CH}_3$  give a triplet at 0.681 ppm, the protons of  $\alpha$   $-\text{CH}_2$  and  $\beta$   $-\text{CH}_2$  give a doublet and singlet at 1.986 and 1.305 ppm, respectively and the protons of  $-\text{C}_5\text{H}_5\text{N}$  give a multiplet from 8.075 to 9.020 ppm. From the comparison of  $^1\text{H}$  NMR signals of CPB above and below the CMC it is observed that the  $^1\text{H}$  NMR signals of  $\alpha$   $-\text{CH}_2$ ,  $\beta$   $-\text{CH}_2$ ,  $-\text{CH}_3$  and group  $-\text{CH}_2$  show upfield shifting due to the shielding effect. This analysis of chemical shifting revealed that the hydrophobic part of CPB plays a more significant role in the micellization. The change in chemical shift is an intrinsic tool to characterize the transition states during monomers to micelle formation [89, 90]. This chemical shifting suggests a structural transformation of CPB micelles in the sense of an hydrophobic core becoming more and more dense as the surfactants concentration increase [57, 91].

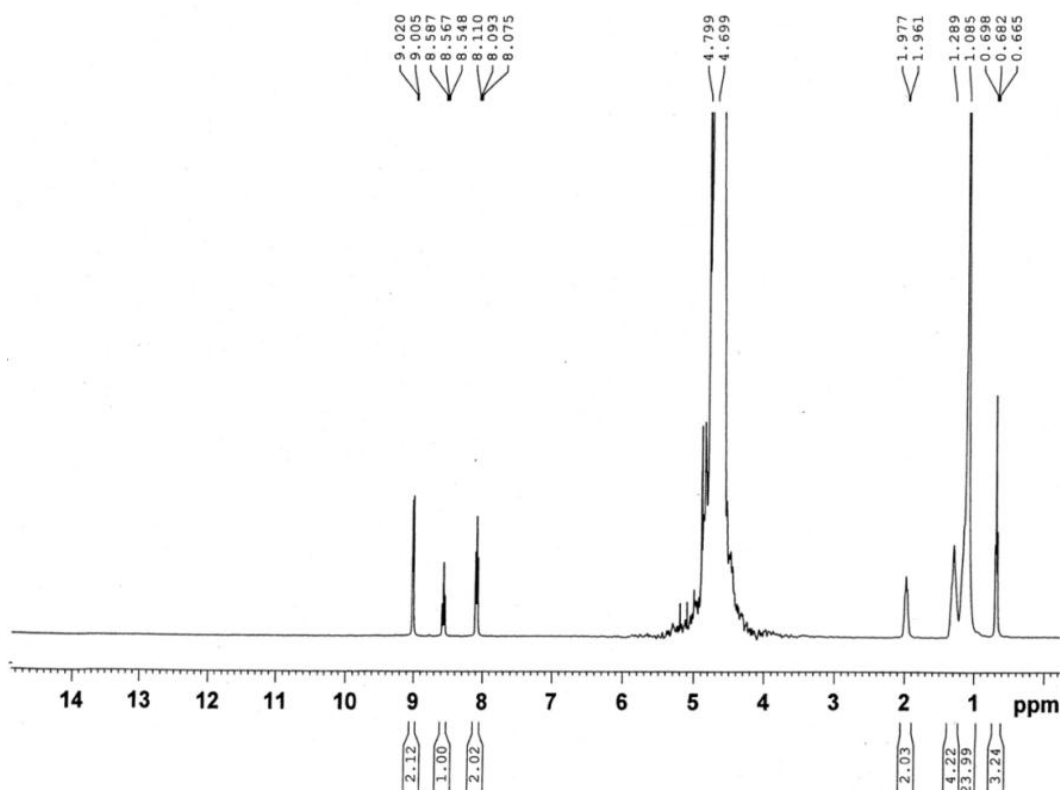


Figure-3.9  $^1\text{H}$  NMR spectra of CPB in aqueous solution above the CMC

### 3.2.2 Proton nuclear magnetic resonance ( $^1\text{H}$ NMR) spectra of CPC above and below the CMC

Figure-3.10 shows the  $^1\text{H}$  NMR spectra for aqueous solution of CPC below the CMC where the protons of group  $-\text{CH}_2$  in the aliphatic chain of CPC give two signals at 1.229 ppm, the protons of  $-\text{CH}_3$  give a triplet at 0.826 ppm, the protons of  $\alpha$   $-\text{CH}_2$  give a triplet at 1.985 ppm, the protons of  $\beta$   $-\text{CH}_2$  give a doublet at 1.298 ppm and the protons of  $-\text{C}_5\text{H}_5\text{N}$  give multiplet from 8.019 to 8.815 ppm. Figure-3.11 shows the  $^1\text{H}$  NMR spectra for aqueous solution of CPC above the CMC. This  $^1\text{H}$  NMR spectra shows that the protons of group  $-\text{CH}_2$  in the aliphatic chain give a doublet at 1.072 ppm, the protons of  $-\text{CH}_3$  give a triplet at 0.681 ppm, the protons of  $\alpha$   $-\text{CH}_2$  give a triplet at 1.985 ppm, the protons of  $\beta$   $-\text{CH}_2$  give a doublet at 1.298 ppm and the protons of  $-\text{C}_5\text{H}_5\text{N}$  give a multiplet from 8.037 to 8.866 ppm.

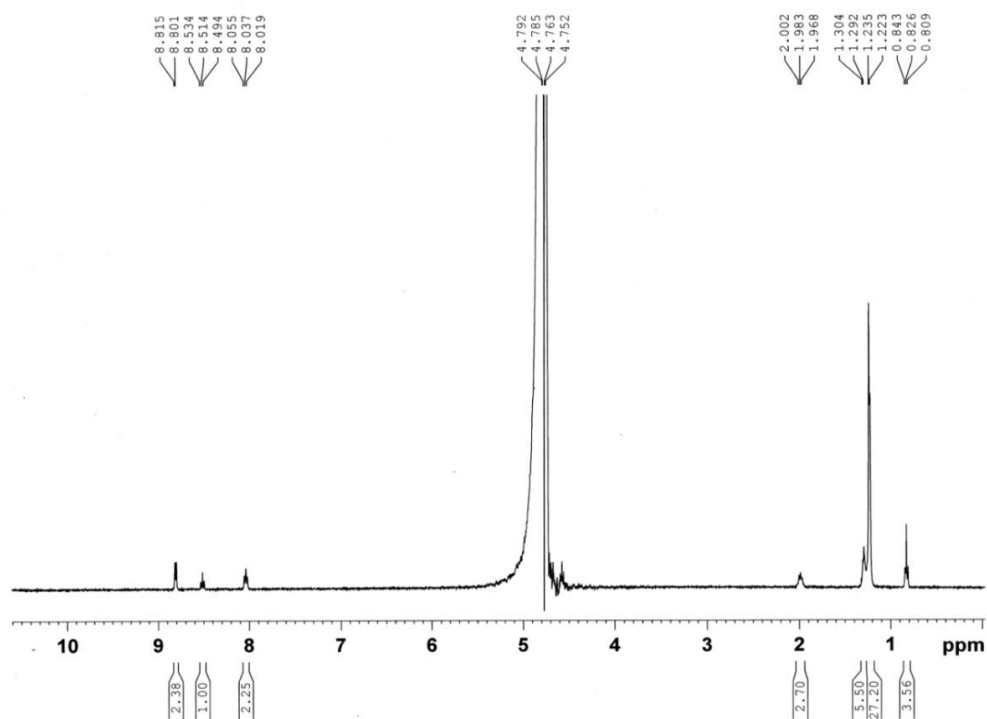


Figure-3.10  $^1\text{H}$  NMR spectra of CPC in aqueous solution below the CMC

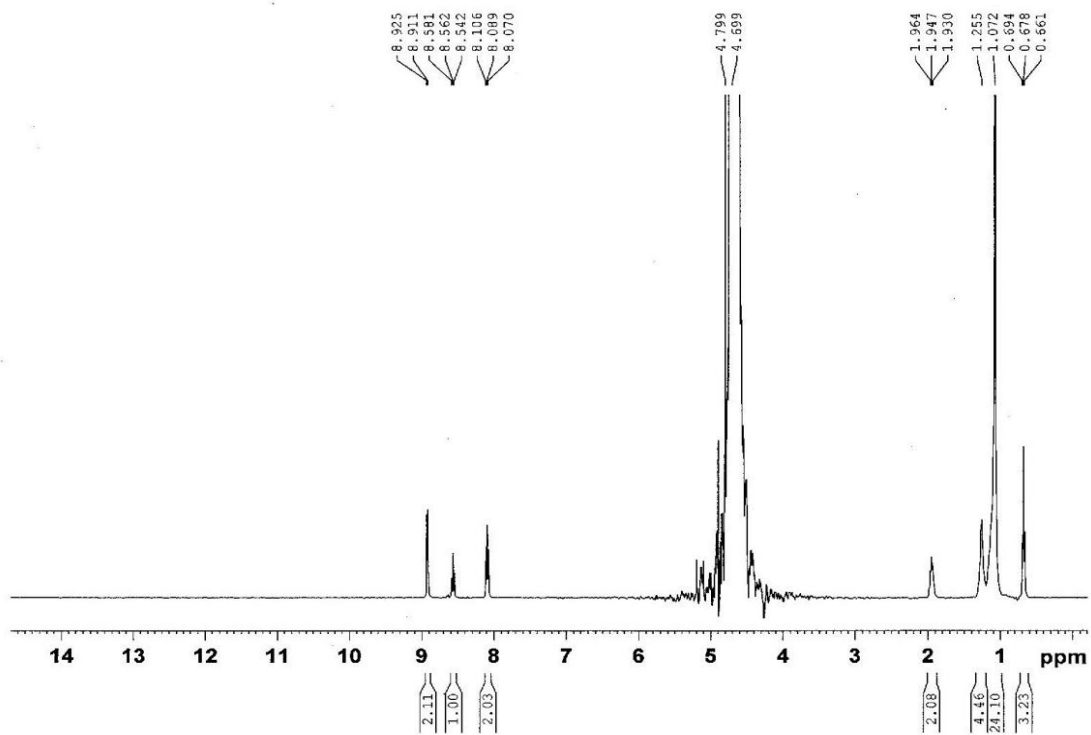


Figure-3.11  $^1\text{H}$  NMR spectra of CPC in aqueous solution above the CMC

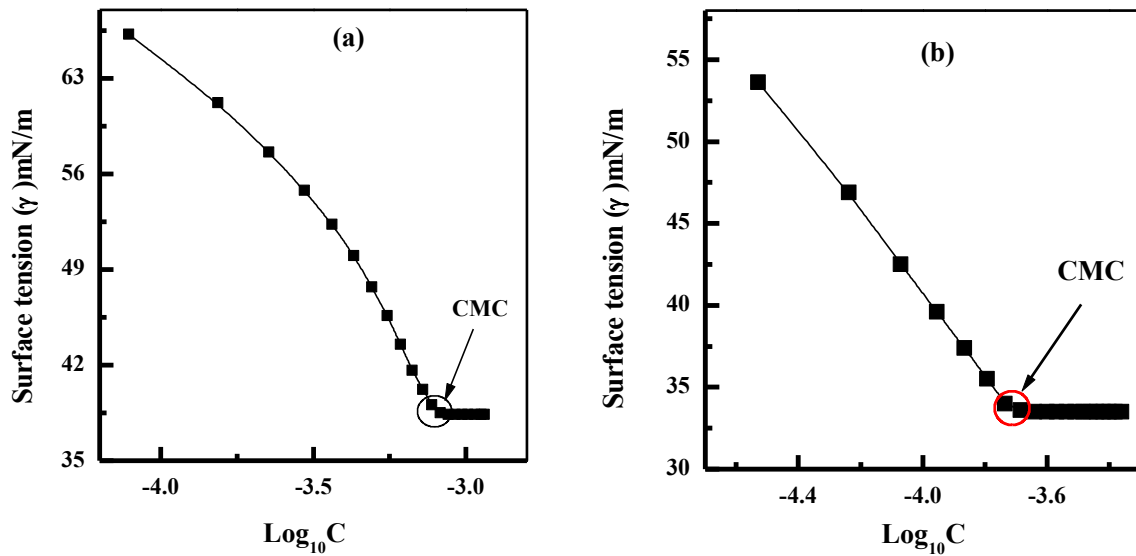


The analysis of proton NMR chemical shift of CPC above and below the CMC shows that the protons of  $-\text{CH}_3$  and group  $-\text{CH}_2$  show upfield shifting above the CMC due to the shielding effect. The protons of  $\text{C}_5\text{H}_5\text{N}-$  are deshielded above the CMC due to the interaction between the hydrophilic head groups in the micelle showing downfield shifting. This  $^1\text{H}$  NMR chemical shifting also suggests that the micelle formation occur due to the interaction among the hydrophobic tails and interaction among the hydrophilic head groups [54, 89]. Therefore, the core of the micelle constitutes a very hydrophobic pseudo phase and there is a gradient of increasing polarity from the core toward the micelle surface.

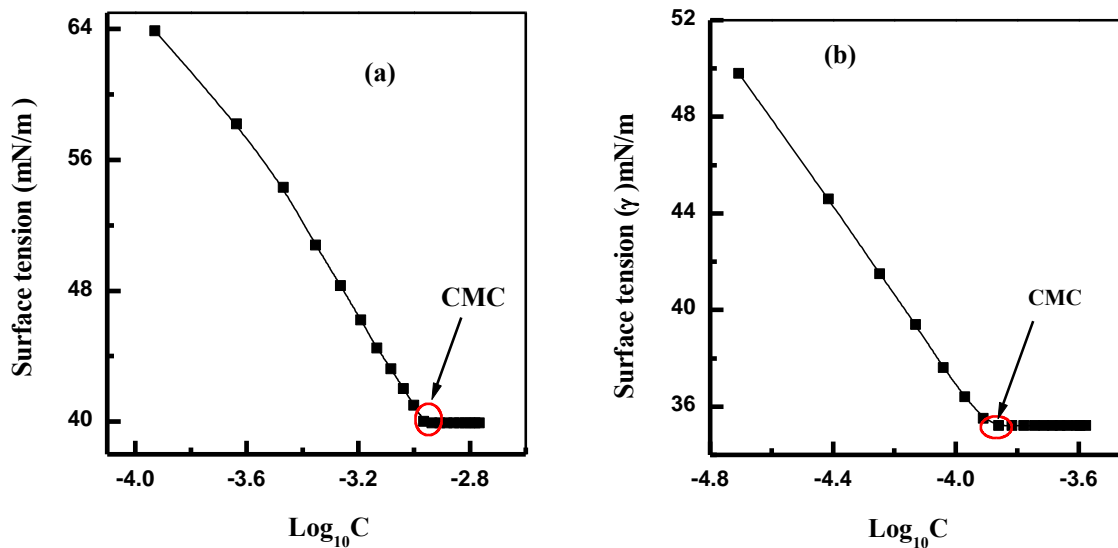
### **3.3 Surface tension of aqueous solution of CPB and CPC in pure water and in the presence of different potassium salts**

Surfactant is an amphiphilic organic compound which has a strong tendency to adsorb onto the air-water interface resulting in a decrease in the surface tension of water, thereby enhancing the interfacial properties and leading to the applications of surfactants in cleaning, surface functionalization, foaming and emulsification. Surface tension or surface free energy is the work or energy required to increase the surface area of a liquid. However, the addition of electrolyte has a remarkable effect on the surface tension [92]. Figure-3.12(a) and figure-3.13(a) show surface tension ( $\gamma$ ) versus  $\log_{10}C$  plots at 45 °C for both the surfactants CPB and CPC respectively in pure water where  $\log_{10}C$  is the logarithm of the surfactant concentration. Figure-3.12(b) and Figure-3.13(b) show surface tension ( $\gamma$ ) versus  $\log_{10}C$  plots at 45 °C for CPB and CPC in the presence of  $\text{K}_2\text{CO}_3$  and  $\text{K}_2\text{SO}_4$  respectively where ionic strength of these electrolytes is  $5 \times 10^{-3}$ . The gradual decrease in the surface tension ( $\gamma$ ) with increasing the surfactant concentration (C) for both the surfactants up to the CMC is a consequence of spontaneous adsorption of surfactant molecules from the bulk of the aqueous solution to the air-water interface and the extent of lowering of surface tension is a measure of surface activity of amphiphilic molecules. It is evident from Figures-3.12(a), (b) and Figures-3.13(a), (b) that the  $\gamma$  decreases up to the CMC and above this value the surface tension ( $\gamma$ ) remained almost constant and this is referred to as the equilibrium surface tension ( $\gamma_{\text{CMC}}$ ). At or above the CMC the interface is at maximum coverage and molecules begin to aggregate in the bulk to minimize further free energy change. These surface tension data show no minimum which indicates that the surfactant is free from surface active impurity [93]. Here, the

CMC is measured from the intersection point of the  $\gamma$  versus  $\log_{10}C$  plot. These is in good agreement with the literature value [13, 81].



**Figures-3.12** Surface tension (mN/m) versus  $\text{Log}_{10}C$  plots for aqueous solution of CPB (a) in pure water and (b) in the presence of  $\text{K}_2\text{CO}_3$  at  $45^\circ\text{C}$  when ionic strength is  $5 \times 10^{-3}$



**Figures-3.13** Surface Tension versus  $\text{Log}_{10}C$  plots for aqueous solution of CPC (a) in pure water and (b) in the presence of  $\text{K}_2\text{SO}_4$  at  $45^\circ\text{C}$  when ionic strength is  $5 \times 10^{-3}$

The CMC determined by different methods differs to some extent but data are obtained from an individual method has a good reproducibility [63]. The CMC obtained from the surface tensiometric method is slightly lower than that obtained from the conductometric

method. Tables-3.1 and 3.2 show the CMC of CPB and CPC measured by surface tensiometric method in pure water and in the presence of different potassium salts within the studied temperature range. Tables-3.3 and 3.4 also present the surface tension at the CMC of CPC and CPB, respectively in pure water and in the presence of different potassium salts. These results show that in the presence of potassium salt, the adsorbed molecules attain a close molecular packing due to the neutralization of positive surface charge which decrease the repulsion between the head groups showing a lower  $\gamma_{\text{CMC}}$  value compared to the corresponding value in pure water. Among these electrolytes, chaotropic ions can effectively accumulate at the air-water interface and screen the surface charge of the adsorbed molecules due to their large polarizability [63, 92]. These ions are more effective in lowering the  $\gamma_{\text{CMC}}$  compared to the kosmotropic ions. For example, the stronger chaotropic ions such as  $\text{SCN}^-$ ,  $\text{I}^-$  and  $\text{Br}^-$  are found to be significantly adsorbed to the interface due to their weakly hydration. The kosmotropic ions  $\text{SO}_4^{2-}$ ,  $\text{CO}_3^{2-}$ ,  $\text{HPO}_4^{2-}$ ,  $\text{F}^-$  and less chaotropic ions  $\text{Cl}^-$  and  $\text{NO}_3^-$  are found to be strongly hydrated and repel from interface [66, 94, 95]. In the presence of these ions the surface tension of the surfactants to be higher than the stronger chaotropic ions. Among these ions,  $\text{SCN}^-$  is the most effective in lowering the surface tension of aqueous solution of CPB and  $\text{I}^-$  is the most effective in lowering the surface tension of aqueous solution of CPC.

Moreover, the surface pressure ( $\pi_{\text{CMC}}$ ) of CPB and CPC in pure water and in the presence of potassium salts at ionic strength  $5 \times 10^{-3}$  were measured from the difference of surface tension of the solvent ( $\gamma_o$ ), and surface tension of the surfactant solution at CMC ( $\gamma_{\text{CMC}}$ ). The tables-3.3 and 3.4 show the values of CMC,  $\gamma_{\text{CMC}}$ ,  $\gamma_o$  and  $\pi_{\text{CMC}}$  of CPC and CPB respectively. From these data, it is observed that the surface pressure decreases with increasing temperature in every case which can be explained by the dehydration of the hydrophilic head-group and hydrophobic alkyl chain, additionally the thermal motions of the adsorbed molecules at the air-water interface [2]. With the increase of temperature the Van der Waals interaction between the alkyl chains of surfactants become weaker and head-group repulsion increases which inhibit the closer molecular packing of monolayer and the values of  $\gamma_{\text{CMC}}$  increase consequently, the values of  $\pi_{\text{CMC}}$  decrease.

**Table-3.3** The surface tension of the solvent ( $\gamma_0$ ), surface tension of aqueous solution of CPC at CMC ( $\gamma_{CMC}$ ), and surface pressure ( $\pi_{CMC}$ ) of aqueous solution of CPC in pure water and in the presence of different potassium salts when ionic strength is  $5 \times 10^{-3}$

Medium	Temperature (°C)	$\gamma_0$ (mN/m)	$\gamma_{CMC}$ (mN/m)	$\pi_{CMC}$ (mN/m)
CPC in pure water	20	73.6	42	38.4
	25	72.8	42.2	29.8
	30	72.0	42.5	29.5
	35	71.2	42.8	28.4
	40	69.6	43.0	26.6
	45	68.7	43.3	25.4
$1.66 \times 10^{-3}$ M $K_2SO_4$	20	73.6	37.8	35.8
	25	73.1	38.1	35.0
	30	71.6	38.3	33.3
	35	70.3	38.5	31.8
	40	69.8	38.8	31.0
	45	68.7	39.0	29.7
$5 \times 10^{-3}$ M KCl	25	72.6	35.6	37.0
	30	71.5	35.8	35.7
	35	70.8	36.0	34.8
	40	69.0	36.5	32.5
	45	68.7	36.8	31.9
$5 \times 10^{-3}$ M KF	45	67.9	38.9	29.0
$5 \times 10^{-3}$ M KBr	45	69.0	33.5	35.5
$5 \times 10^{-3}$ M KI	45	67.5	28.5	39.0
$5 \times 10^{-3}$ M KSCN	45	68.2	31.6	36.6
$5 \times 10^{-3}$ M $KNO_3$	45	69.0	31.8	37.2
$1.66 \times 10^{-3}$ M $K_2CO_3$	45	68.2	33.6	34.6
$1.66 \times 10^{-3}$ M $K_2HPO_4$	45	68.1	35.3	32.8

**Table-3.4** The surface tension of the solvent ( $\gamma_0$ ), surface tension of aqueous solution of CPB at CMC ( $\gamma_{CMC}$ ), surface pressure ( $\pi_{CMC}$ ) of aqueous solution of CPB in pure water and in the presence of different potassium salts when ionic strength is  $5 \times 10^{-3}$

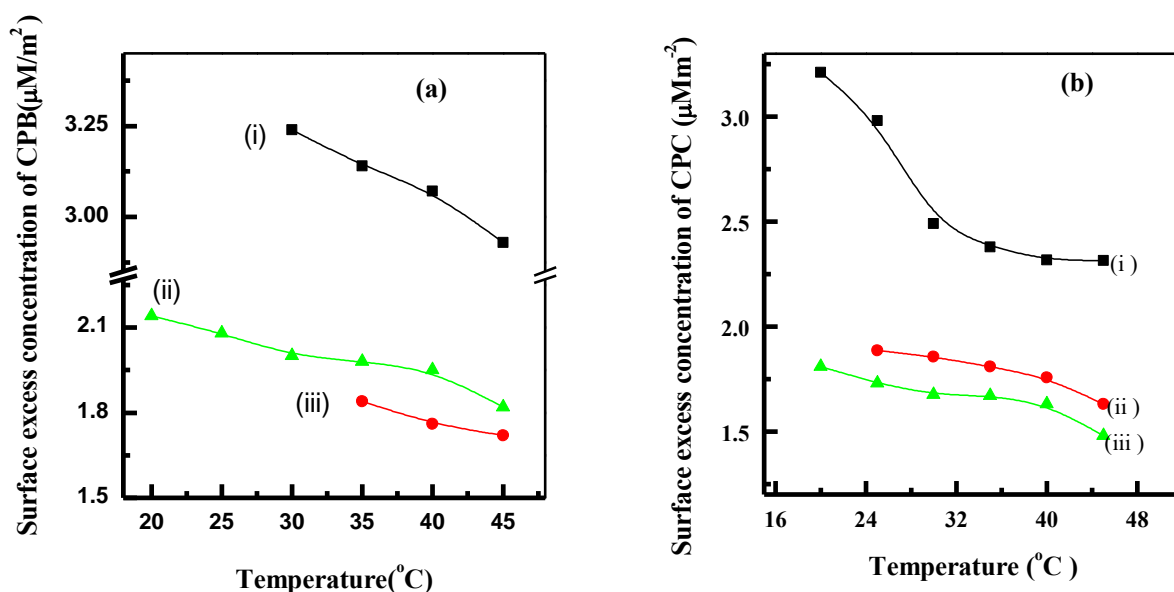
Medium	Temperature (°C)	$\gamma_0$ (mN/m)	$\gamma_{CMC}$ (mN/m)	$\pi_{CMC}$ (mN/m)
CPB in pure water	30	72.0	37.12	34.88
	35	71.2	37.23	33.97
	40	69.6	37.67	31.93
	45	68.7	38.34	30.35
$5 \times 10^{-3}$ M KNO <sub>3</sub>	20	73.6	31.90	41.70
	25	72.8	32.20	40.60
	30	72.4	32.50	39.90
	35	71.0	32.80	38.20
	40	70.0	33.30	36.70
	45	69.0	33.50	35.50
$5 \times 10^{-3}$ M KBr	35	70.8	33.47	37.43
	40	69.9	33.50	36.40
	45	69.0	33.52	35.47
$5 \times 10^{-3}$ M KF	45	67.9	36.30	31.60
$5 \times 10^{-3}$ M KCl	45	68.7	37.40	31.30
$5 \times 10^{-3}$ M KI	45	67.5	30.30	37.20
$5 \times 10^{-3}$ M KSCN	45	68.2	28.80	39.40
$1.66 \times 10^{-3}$ M K <sub>2</sub> SO <sub>4</sub>	45	68.7	37.30	31.40
$1.66 \times 10^{-3}$ M K <sub>2</sub> CO <sub>3</sub>	45	68.2	33.50	34.70
$1.66 \times 10^{-3}$ M K <sub>2</sub> HPO <sub>4</sub>	45	68.1	34.20	33.90

### 3.3.1 Surface excess concentration ( $\Gamma_{max}$ ) of CPB and CPC in aqueous system

The concentration of surfactant adsorbed at the air-water interface is termed as surface excess concentration ( $\Gamma_{max}$ ). The values of  $\Gamma_{max}$  were calculated from the slope of the straight line of the surface tension versus  $\log_{10}C$  plot before the CMC with the help of the following equation [72].

$$\Gamma_{max} = -\frac{1}{nRT} \left( \frac{\delta\gamma}{\delta \ln C} \right)_{T,P} \dots \dots \dots (1)$$

Where  $R$  is the gas constant ( $8.314 \text{ JK}^{-1}\text{mol}^{-1}$ ),  $T$  is the absolute temperature in  $\text{K}$ ,  $C$  is the surfactant concentration in the bulk,  $n$  is the number of species formed in the solution by the dissociation of the surfactant (for a non-ionic surfactant  $n=1$ , and for a ionic surfactant  $n=2$ ) and  $\left(\frac{\delta\gamma}{\delta\log C}\right)$  is the slope of the straight line of surface tension ( $\gamma$ ) versus  $\log C$  plot before CMC. Figures-3.14(a) and (b) show the variation of surface excess concentration ( $\Gamma_{\max.}$ ) of CPB and CPC at different temperatures in pure water and in the presence of  $5 \times 10^{-3} \text{ M KNO}_3$ ,  $\text{KBr}$  for CPB, and  $1.66 \times 10^{-3} \text{ M K}_2\text{SO}_4$ ,  $5 \times 10^{-3} \text{ M KCl}$  for CPC. The values of surface excess concentration of CPC and CPB are shown in the tables-3.5 and 3.6 respectively. From these tables it is observed that the values of surface excess concentration are positive which indicates that at the air water interface the surfactant has more concentration as compared to that in the bulk.



**Figures-3.14 (a) Surface excess concentration of CPB (i) in pure water, (ii) in the presence of  $5 \times 10^{-3} \text{ M KNO}_3$ , (iii) in the presence of  $5 \times 10^{-3} \text{ M KBr}$ ; (b) Surface excess concentration of CPC (i) in pure water, (ii) in the presence of  $5 \times 10^{-3} \text{ M KCl}$ , (iii) in the presence of  $1.66 \times 10^{-3} \text{ M}$  of  $\text{K}_2\text{SO}_4$**

Figure-3.14(a) shows the  $\Gamma_{\max.}$  values of CPB in pure water and in the presence of  $5 \times 10^{-3} \text{ M KNO}_3$  and  $\text{KBr}$ , and Figure-5.3(b) shows the  $\Gamma_{\max}$  values of CPC in pure water and in the presence of  $5 \times 10^{-3} \text{ M KCl}$  and  $1.66 \times 10^{-3} \text{ M K}_2\text{SO}_4$ . From these figures it is observed that the values of  $\Gamma_{\max}$  decrease gradually with increasing temperature. This can be

explained on the basis of thermal motion and disorganization of the adsorbed molecules. With the increase of temperature the kinetic energy and thermal motion of surfactant increases which brings about disturbance in the adsorbed molecules that dominates over the dehydration effect of the monolayer at the air-water interface. The disorganization of the adsorbed molecules at the air-water interface occurs with the increase of thermal motion and chain flexibility [96]. As a result, the Van der Waals interaction between the alkyl chains of surfactant become weaker and head group repulsion increases which also inhibit the close molecular packing of monolayer [97]. Consequently, the values of  $\Gamma_{\max}$  show a gradual decreasing trend with increasing temperature.

**Table-3.5 The surface excess concentration ( $\Gamma_{\max}$ ) of CPC in pure water and in the presence of different potassium salts when ionic strength is  $5 \times 10^{-3}$**

Medium	Temperature (°C)	$\Gamma_{\max}$ ( $\mu\text{M}/\text{m}^2$ )
CPC in pure water	20	3.21
	25	2.98
	30	2.49
	35	2.38
	40	2.32
	45	2.31
$1.66 \times 10^{-3}$ M $\text{K}_2\text{SO}_4$	20	1.81
	25	1.73
	30	1.68
	35	1.67
	40	1.63
	45	1.48
$5 \times 10^{-3}$ M KCl	25	1.89
	30	1.86
	35	1.81
	40	1.76
	45	1.63
$5 \times 10^{-3}$ M KF	45	2.68
$5 \times 10^{-3}$ M KBr	45	3.84
$5 \times 10^{-3}$ M KI	45	3.09
$5 \times 10^{-3}$ M KSCN	45	3.63
$5 \times 10^{-3}$ M $\text{KNO}_3$	45	6.06
$1.66 \times 10^{-3}$ M $\text{K}_2\text{CO}_3$	45	4.55
$1.66 \times 10^{-3}$ M $\text{K}_2\text{HPO}_4$	45	3.55

Besides, the charge of the head group of CPB and CPC is positive and thereby adsorbed monolayer creates a surface potential [98] which acts as hindrance for further adsorption from the bulk of the solution to the air-water interface. In the presence of electrolyte the surface potential is electrostatically screened at the air-water interface [82, 83].

Consequently, the obstruction for further adsorption of surfactant molecules is substantially reduced, giving higher surface excess concentration of the adsorbed molecules. But in the presence of  $5 \times 10^{-3}$  M  $\text{KNO}_3$ ,  $\text{KBr}$  for CPB and  $1.66 \times 10^{-3}$  M  $\text{K}_2\text{SO}_4$ ,  $5 \times 10^{-3}$  M  $\text{KCl}$  for CPC the surface excess concentration decrease compared to the CPB and CPC in pure water. Here, the decrease of the surface excess concentration of both surfactants can be explained by the counter-ion binding decrease or degree of ionization increase. In the presence of  $\text{KNO}_3$  and  $\text{KBr}$ , the surface potential increases due to the decrease of counter-ion binding ( $\beta$ ) of CPB than in the absence of these electrolytes which inhibit further adsorption of the surfactant monomer. Consequently, the surface excess concentration of CPB in the presence of these electrolytes becomes lower than that of CPB in pure water.

**Table-3.6** The surface excess concentration ( $\Gamma_{\max}$ ) of aqueous solution of CPB in pure water and in the presence of different potassium salts when ionic strength is  $5 \times 10^{-3}$

Medium	Temperature (°C)	$\Gamma_{\max}$ ( $\mu\text{M}/\text{m}^2$ )
CPB in pure water	30	3.56
	35	3.49
	40	3.30
	45	3.13
$5 \times 10^{-3}$ M $\text{KNO}_3$	20	2.14
	25	2.01
	30	1.95
	35	1.89
	40	1.86
	45	1.76
$5 \times 10^{-3}$ M $\text{KBr}$	35	1.78
	40	1.77
	45	1.72
$5 \times 10^{-3}$ M $\text{KF}$	45	1.59
$5 \times 10^{-3}$ M $\text{KCl}$	45	1.38
$5 \times 10^{-3}$ M $\text{KI}$	45	1.74
$5 \times 10^{-3}$ M $\text{KSCN}$	45	1.77
$1.66 \times 10^{-3}$ M $\text{K}_2\text{SO}_4$	45	1.23
$1.66 \times 10^{-3}$ M $\text{K}_2\text{CO}_3$	45	2.10
$1.66 \times 10^{-3}$ M $\text{K}_2\text{HPO}_4$	45	1.40

### 3.4 Thermodynamic properties of CPB and CPC in aqueous system

The thermodynamic properties of surfactants have been studied for a long time by measuring their CMC over a wide range of temperatures [14, 48, 96, 99, 100]. The free energy change ( $\Delta G_{mic}^\circ$ ), entropy change ( $\Delta S_{mic}^\circ$ ), and enthalpy change ( $\Delta H_{mic}^\circ$ ) for



micellization as well as enthalpy change ( $\Delta H_{ad}^{\circ}$ ), free energy change ( $\Delta G_{ad}^{\circ}$ ), entropy change ( $\Delta S_{ad}^{\circ}$ ) for surface adsorption have also been studied. The surface pressure, surface tension of the solvent, and the surface tension at CMC or above the CMC were calculated using the following equations.

$$\pi_{CMC} = \gamma_0 - \gamma_{CMC} \dots\dots\dots(2)$$

Where  $\pi_{CMC}$  is the surface pressure,  $\gamma_0$  is the surface tension of the solvent,  $\gamma_{CMC}$  is the surface tension at or above the CMC. On the other hand, the free energy ( $\Delta G_{mic}^{\circ}$ ), entropy ( $\Delta S_{mic}^{\circ}$ ) and enthalpy ( $\Delta H_{mic}^{\circ}$ ) changes for micellization and the surface activities of CPB and CPC in pure water were calculated using the following equations [63, 81, 101].

$$\Delta G_{mic}^{\circ} = (1 + \beta) RT \ln X_{CMC} \dots\dots\dots(3)$$

$$\Delta S_{mic}^{\circ} = - \left( \frac{\Delta G_{mic}^{\circ}}{\delta T} \right)_p \dots\dots\dots(4)$$

$$\Delta G_{mic}^{\circ} = \Delta H_{mic}^{\circ} - T \Delta S_{mic}^{\circ} \dots\dots\dots(5)$$

Where  $\beta$  is the counter-ion binding,  $X_{CMC}$  is the mole fraction of the surfactant at the CMC, R is the gas constant (R=8.314 J/K/mol) and T is the temperature in K. The percentage of error during the calculation of thermodynamic parameters lies within  $\pm 3\%$ . Moreover, the free energy of adsorption ( $\Delta G_{ad}^{\circ}$ ) is the energy required to adsorb one mole surfactant molecules from solution to the air-water interface at one atmospheric surface pressure, which was calculated using the following equation [10, 11, 81].

$$(\Delta G_{ad}^{\circ}) = (\Delta G_{mic}^{\circ}) - \frac{\pi_{CMC}}{\Gamma_{max}} \dots\dots\dots(6)$$

and  $\Delta H_{ad}^{\circ}$ ,  $\Delta S_{ad}^{\circ}$  were calculated with the help of following equations.

$$\Delta S_{ad}^{\circ} = - \left( \frac{\delta \Delta G_{ad}^{\circ}}{\delta T} \right)_p \dots\dots\dots(7)$$

$$\Delta G_{ad}^{\circ} = \Delta H_{ad}^{\circ} - T \Delta S_{ad}^{\circ} \dots\dots\dots(8)$$

Table-3.7 shows the thermodynamic parameters involved in the micellization and adsorption of CPB and CPC in pure water. It is seen from this table that the free energy terms for micellization and adsorption  $\Delta G_{mic}^{\circ}$  and  $\Delta G_{ad}^{\circ}$  for CPB and CPC in pure water

are negative within the studied temperature range. The negative values of  $\Delta G_{mic}^{\circ}$  indicate that the transfer of alkyl chain of surfactant from aqueous solution to the micelle core is a spontaneous process [2]. The free energy of adsorption ( $\Delta G_{ad}^{\circ}$ ) is the energy needed to transfer 1 mole of surfactant from solution to the surface at unit surface pressure [2]. The negative values of  $\Delta G_{ad}^{\circ}$  indicate that the surface adsorption at different temperatures is a spontaneous phenomenon [2]. With the increase of temperature, the values of  $\Delta G_{ad}^{\circ}$  become more negative which indicate that the surface adsorption become more spontaneous. This is consistent with the fact that with increasing temperature dehydration of the head groups increases and it results in the increase in the hydrophobicity of the molecules [96]. The value of  $\Delta G_{ad}^{\circ}$  at a given temperature is more negative than the corresponding value of  $\Delta G_{mic}^{\circ}$  which indicates the adsorption is more spontaneous than micelization. It can be explained with the consideration that when micelles are formed, work has to be done to transfer the monomeric surfactant molecules from the bulk to the micellar state in the bulk through the solvent medium. In most cases,  $\Delta G_{mic}^{\circ}$  become more negative with the increase of temperature up to 50 °C and then become more positive with further increase of temperature [1, 4]. It is evident from table-3.7 that the  $\Delta G_{mic}^{\circ}$  values of CPB are more negative than that of CPC with respective temperature. This suggests that CPB forms micelles more spontaneously than CPC.

**Table-3.7  $\Delta G_{mic}^{\circ}$ ,  $\Delta G_{ad}^{\circ}$ ,  $\Delta H_{mic}^{\circ}$ ,  $\Delta H_{ad}^{\circ}$ ,  $\Delta S_{mic}^{\circ}$ ,  $\Delta S_{ad}^{\circ}$  for CPB and CPC in pure water at different temperatures**

Medium	Temp. (°C)	$\Delta G_{mic}^{\circ}$ , kJmol <sup>-1</sup>	$\Delta G_{ad}^{\circ}$ , kJmol <sup>-1</sup>	$\Delta H_{mic}^{\circ}$ , kJmol <sup>-1</sup>	$\Delta H_{ad}^{\circ}$ , kJmol <sup>-1</sup>	$\Delta S_{mic}^{\circ}$ , kJmol <sup>-1</sup> K <sup>-1</sup>	$\Delta S_{ad}^{\circ}$ , kJmol <sup>-1</sup> K <sup>-1</sup>
CPB in pure water	30	-47.359	-57.103	-32.42	-36.923	0.0493	0.0666
	35	-47.398	-56.973	-62.08	-60.79	-0.0477	-0.0124
	40	-47.059	-56.882	-92.386	-85.48	-0.1447	-0.0914
	45	-46.167	-55.959	-123.03	-110.146	-0.2417	-0.1704
CPC in pure water	20	-32.975	-42.819	272.56	334.858	1.0428	1.289
	25	-33.201	-43.604	197.98	246.648	0.7758	0.974
	30	-42.465	-54.111	111.7	145.566	0.5088	0.659
	35	-42.11	-54.252	32.36	51.7	0.2418	0.344
	40	-40.609	-53.038	-48.496	-43.961	-0.0252	0.029
	45	-41.974	-54.376	-134.89	-145.324	-0.2922	-0.286

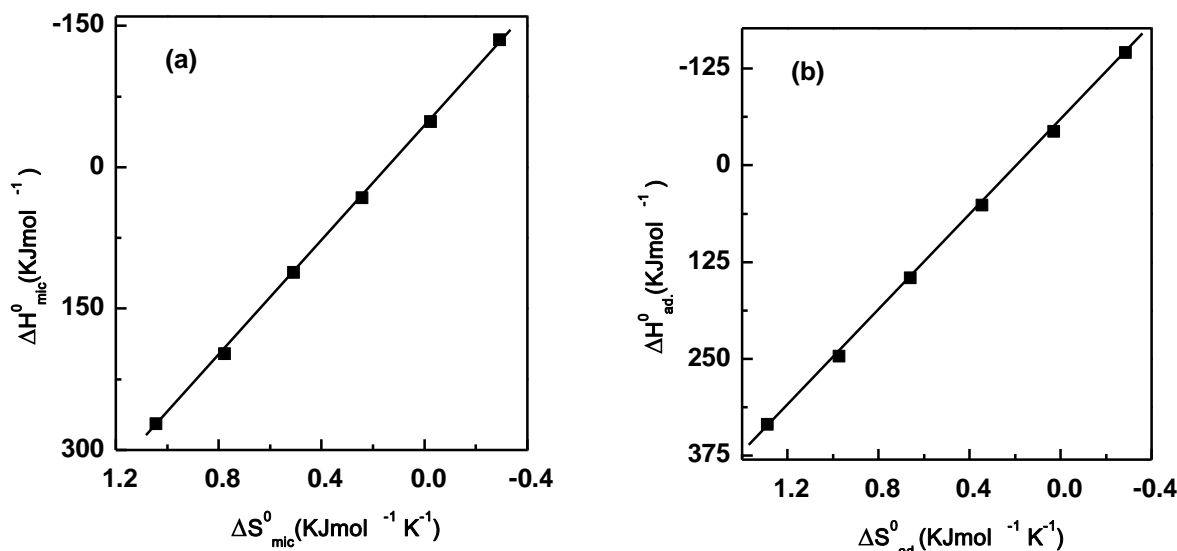
Table-3.7 shows that the values of  $\Delta H_{mic}^{\circ}$  for CPB are found to be negative and become more negative with increasing temperature. The negative value of  $\Delta H_{mic}^{\circ}$  indicates that

the micelle formation is an exothermic process. With the increase of temperature dehydration of hydrophilic head group increases which favour micellization at a given temperature. Consequently, the adsorption process and micellization become easier. The negative values of  $\Delta H_{mic}^{\circ}$  is associated with the favourable hydrophobic interaction in the interior of micelle and reduction of head group repulsion due to the neutralization of micellar surface charge in the presence of added electrolytes. The negative value of  $\Delta H_{mic}^{\circ}$  can also occur when a substantial number of water molecules surrounding small hydrophilic head groups become more important than destruction of the iceberg structure around alkyl chain [96, 102].

In addition, the negative values of  $\Delta H_{mic}^{\circ}$  can be taken as the evidence of London dispersion force, a major attractive force for micellization [103]. It is clear from table-3.7 that the negative value of  $\Delta H_{mic}^{\circ}$  for CPB decreases with increasing temperature. The hydrogen bond between the water molecules is diminished with the increases of temperature; consequently less energy is required to break up the ice-berg structure around hydrophobic alkyl chains. On the other hand, the values of  $\Delta H_{mic}^{\circ}$  and  $\Delta H_{ad}^{\circ}$  for CPC in pure water are positive at low temperature and decrease with increasing temperature due to the repulsion between the dehydrated head groups and destruction of the higher degree of hydrogen bonding of ice-berg water structure around the alkyl chain [63, 80, 96]. In the present study we have calculated the  $\Delta H_{ad}^{\circ}$  values for both the surfactants in pure water at different temperatures. The values of  $\Delta H_{ad}^{\circ}$  for CPB in pure water are negative and show a decreasing trend with increasing temperature. The surfactant is less hydrated at higher temperatures and requires less energy to adsorb at the air-water interface and thereby  $\Delta H_{ad}^{\circ}$  values show a decreasing trend and tend to become negative with increasing temperature. In the present study, the  $\Delta H_{ad}^{\circ}$  values for CPC in pure water at different temperatures have also been calculated. It has been observed that in the case of CPC in pure water, the initial  $\Delta H_{ad}^{\circ}$  values are positive and decrease gradually with the increase of temperature, finally the values become negative. At low temperatures, the surfactant remains much more hydrated and it needs more energy to adsorb at the air-water interface and it reflects in the initial higher positive values of  $\Delta H_{ad}^{\circ}$ .



organized monolayer and the concomitant loss of one degree of rotational freedom of the adsorbed molecules at the air-water interface [105]. Since, most of the iceberg structure is destroyed with increasing temperature; the second effect progressively dominates over the first one. As a result,  $\Delta S_{ad}^{\circ}$  values show a decreasing trend with increasing temperature.



**Figures-3.16 Enthalpy-Entropy compensation plots for CPC in aqueous solution (a) micellization, (b) adsorption**

In general, the entropy-enthalpy compensates each other for surface adsorption and bulk micellization to keep the negative value of Gibbs free energy nearly constant. This parameter is a characteristic of solute-solute and solute-solvent interactions, as suggested by Chen et. al. [77]. When the entropy term contributes less to the free energy, its counterpart, the enthalpy term contributes more to keep the negative free energy nearly constant. This kind of behavior has been observed for aqueous solutions of ionic surfactants previously [106, 107]. Figures-3.15(a), (b) and Figures-3.16(a), (b) shows the the linear relationship of enthalpy versus entropy of CPB and CPC respectively for both micelization and adsorption in pure water. This linear relationship is called the enthalpy-entropy compensation phenomenon [77, 108]. With the help of following equation, we can interpret the observed enthalpy-entropy linear relationship for both cases.

$$\Delta H_{mic./ad.} = T_c^* \Delta S_{mic./ad.} + \Delta H_{c mic./ad.}^* \dots \dots \dots (9)$$

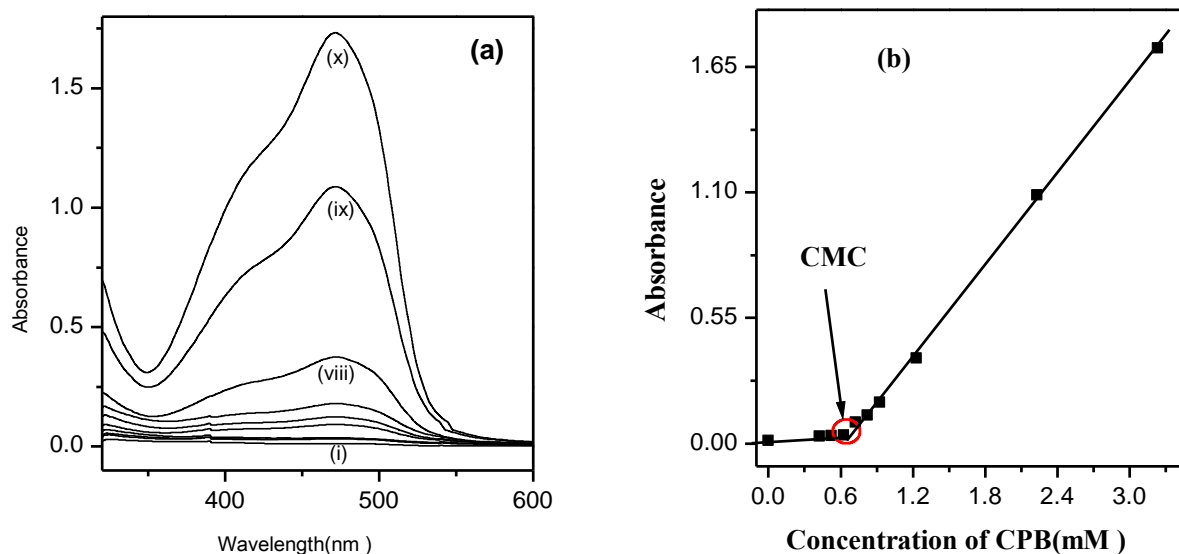
Where  $\Delta H_{c \text{ mic./ad.}}^*$  is the intercept of straight line which gives the information about the solute-solute interaction in micellar system [81]. In the case of micelization and adsorption, enthalpy entropy term compensate each other and slope of the straight line known as the compensation temperature ( $T_c^*$ ) having the dimension of the Kelvin temperature which is related with the interaction between the solute and solvent. Through this interaction, heat transfer from solvent to solute in the system. The  $T_c^*$  is found to be 252 to 311 K for the bulk micellization and 245 to 309 K for surface adsorption. The  $T_c^*$  values for surface adsorption and bulk micellization for CPB and CPC in pure water are given in table-3.8. In the previous report, it was found that the  $T_c^*$  lies in a relatively narrow range from about 250 to 315 K [109]. The values of  $T_c^*$  obtained in the present study are found within the suggested literature value.

**Table-3.8 The values of the  $T_c^*$  for CPB and CPC in aqueous solution**

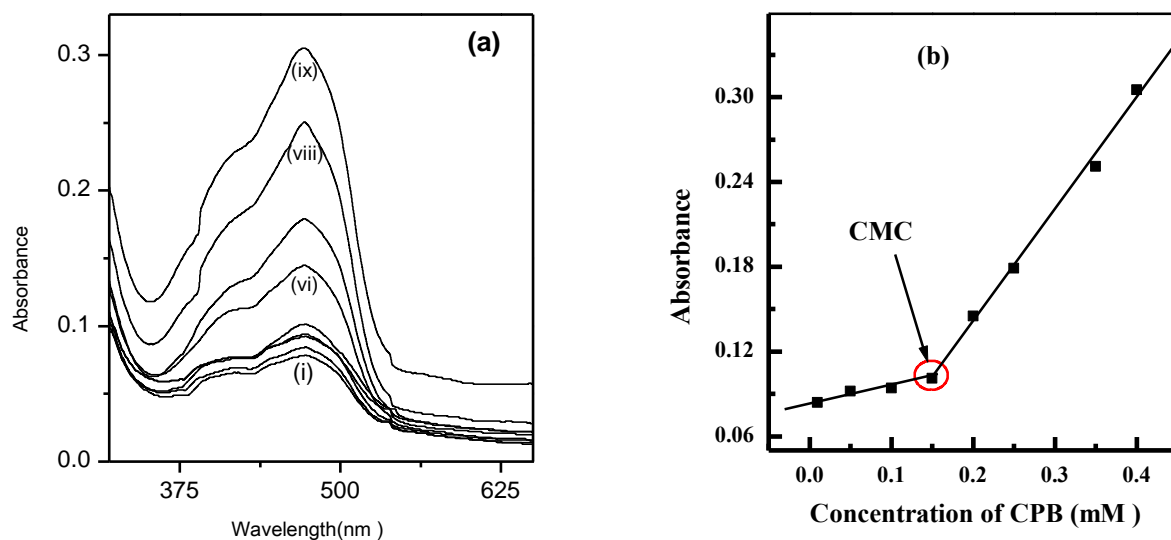
Surfactant solution	Process	Compensation Temperature ( $T_c^*$ )
CPB in pure water	Micelization	311 K
	Adsorption	309 K
CPC in pure water	Micelization	305 K
	Adsorption	305 K

### **3.5 Solubilization of PAN and curcumin in aqueous solution of CPB and CPC in pure water and in the presence of $5 \times 10^{-3}$ M $KNO_3$ and $1.66 \times 10^{-3}$ M $K_2SO_4$ respectively**

The solubilization capacity of surfactant depends on micelle formation because below the CMC solubilization of water insoluble substance is zero or nearly zero and above the CMC solubilization increase with increasing concentration of surfactant [2]. Based on this property the surfactants are used as drug carrier, toxic waste removal, solubilization of water insoluble dyes, ligands etc. The exact location of dye in the micelle varies with the nature of the material solubilized and the type of interaction occurring between surfactant and solubilize. Furthermore, the CMC of the surfactant has been measured based on the solubilization of dye in aqueous solution of surfactant.



Figures-3.17 (a) Absorption spectra of PAN in aqueous solution of CPB where the concentrations of CPB are (i) pure water, (ii) 0.42 mM, (iii) 0.52 mM, (iv) 0.62 mM, (v) 0.72 mM, (vi) 0.82 mM, (vii) 0.92 mM, (viii) 1.23 mM, (ix) 2.23 mM, and (x) 3.23 mM; (b) Absorbance of PAN against the concentration of CPB (mM)

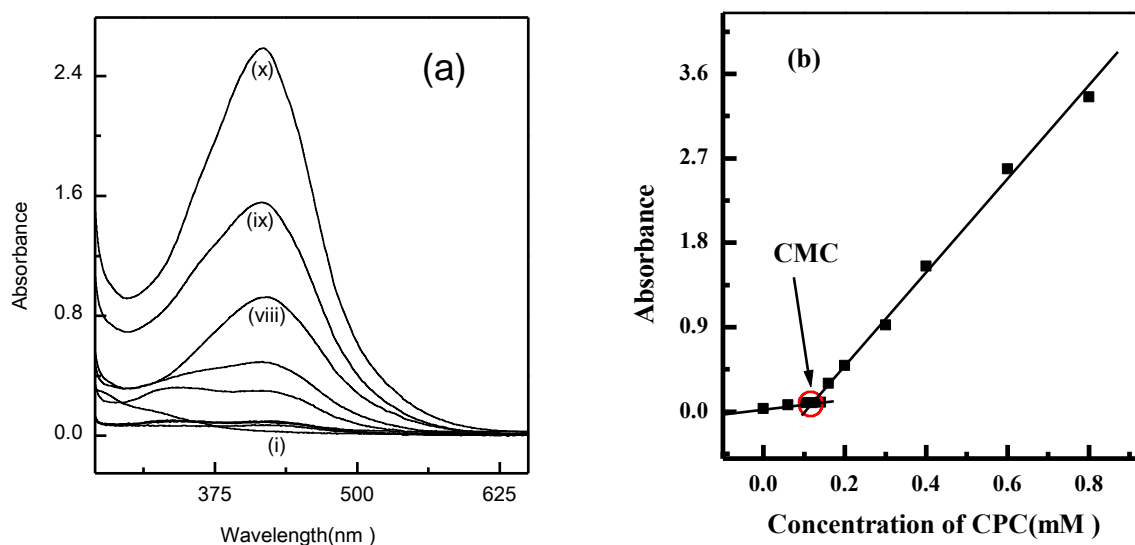


Figures-3.18 (a) Absorption spectra of PAN in aqueous solution of CPB in the presence of  $5 \times 10^{-3}$  M  $\text{KNO}_3$ ; where the concentrations of CPB are (i) aqueous solution of  $5 \times 10^{-3}$  M  $\text{KNO}_3$ , (ii) 0.01 mM, (iii) 0.05 mM, (iv) 0.1 mM, (v) 0.15 mM, (vi) 0.2 mM, (vii) 0.25 mM, (viii) 0.35 mM, and (ix) 0.4 mM; (b) Absorbance of PAN against the concentration of CPB (mM) in the presence of  $5 \times 10^{-3}$  M  $\text{KNO}_3$

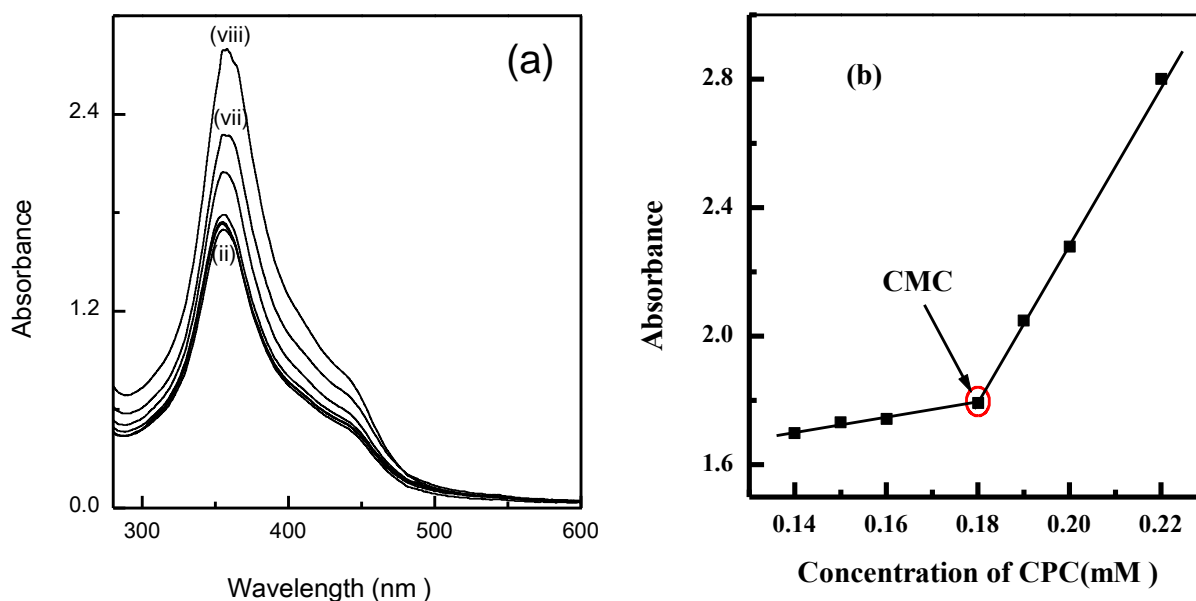
Figure-3.17(a) and Figure-3.18(a) show the absorption spectra of PAN solubilized in aqueous solution of pure CPB and in the presence of  $5 \times 10^{-3}$  M  $\text{KNO}_3$  respectively. The

solubilization of PAN were carried out at several surfactant concentrations ranging from 0.42 to 3.23 mM in aqueous solution of pure CPB and from 0.01 to 0.4 mM aqueous solution of CPB in the presence of  $5 \times 10^{-3}$  M  $\text{KNO}_3$ , some of which are below the CMC and some are above the CMC. Figures-3.19(a) and 3.20(a) show the absorption spectra of curcumin solubilized in aqueous solution of pure CPC and in the presence of  $1.66 \times 10^{-3}$  M  $\text{K}_2\text{SO}_4$  respectively. The solubilizations study was carried out at several concentration ranging from 0.06 to 0.6 mM CPC in pure water and from 0.14 to 0.22 mM aqueous solution of CPC in the presence of  $1.66 \times 10^{-3}$  M  $\text{K}_2\text{SO}_4$ , some of which are below the CMC and some are above the CMC. Here, it is noteworthy that no significant absorbance was found below the CMC. This indicates that below the CMC solubilization of water insoluble dye is zero or nearly zero. Figure-3.17(b), 3.18(b), 3.19(b) and 3.20(b) show that above the CMC the absorbance increases with increasing the concentration of surfactant which is in line with the previous observation [28]. This means that below the CMC there is no solubilization of PAN or curcumin molecules but above the CMC higher amount of these dyes are taken up by the surfactant micelles. Such a solution of nonpolar substance in a micellar system is thermodynamically stable [47]. At or above the CMC of CPB in pure water and in the presence of  $5 \times 10^{-3}$  M  $\text{KNO}_3$  the PAN absorb strongly at 472 nm. To quantify the effectiveness of a surfactant in solubilizing a given solubilizate, the molar solubilization ratio (MSR) is defined as the number of moles of organic compound solubilized per mole of surfactant added to the solution [110]. MSR can be determined from the slope of the linearly fitted line above the CMC when solute concentration is plotted against the concentration of surfactant. Figures-3.17(b) and 3.18(b) show the effect of CPB concentration on solubilization of PAN in pure water and in the presence of  $5 \times 10^{-3}$  M  $\text{KNO}_3$  respectively at 30 °C. The figures-3.19(b) and 3.20(b) show the effect of concentration of CPC on solubilization of curcumin in pure water and in the presence of  $1.66 \times 10^{-3}$  M  $\text{K}_2\text{SO}_4$  respectively at the same temperature. This specific temperature was chosen to measure the solubilization power of each system because of the fact that the  $T_K$  of both the surfactants in pure water and in the presence of strong electrolytes remain below 30 °C. The  $T_K$  of CPB in aqueous solution is 30.15 °C and in the presence of  $5 \times 10^{-3}$  M  $\text{KNO}_3$  the  $T_K$  is 26.2 °C. On the contrary, the  $T_K$  of CPC in pure water is 18.53 °C and in the presence of  $1.66 \times 10^{-3}$  M  $\text{K}_2\text{SO}_4$  the  $T_K$  is 13.75 °C. The values of molar solubilization ratio (MSR) of PAN in aqueous solution of CPB and in the presence of  $5 \times 10^{-3}$  M  $\text{KNO}_3$  were found to be 0.043 and 0.0501 respectively.





Figures-3.19 (a) Absorption spectra of curcumin in aqueous solution of CPC where the concentrations of CPC are (i) pure water, (ii) 0.06 mM, (iii) 0.1 mM, (iv) 0.12 mM, (v) 0.14 mM, (vi) 0.16 mM, (vii) 0.2 mM, (viii) 0.3 mM, (ix) 0.4 mM, and (x) 0.6 mM; (b) Absorbance of curcumin versus concentration of CPC (mM)



Figures-3.20 (a) Absorption spectra of curcumin in aqueous solution of CPC in the presence of  $K_2SO_4$ , ionic strength is  $5 \times 10^{-3}$  where the concentrations of CPC are (i) aqueous solution of  $1.66 \times 10^{-3}$  M  $K_2SO_4$ , (ii) 0.14 mM, (iii) 0.15 mM, (iv) 0.16 mM, (v) 0.18 mM, (vi) 0.19 mM, (vii) 0.2 mM, and (viii) 0.22 mM; (b) Absorbance of curcumin versus concentration of CPC (mM) in the presence of  $1.66 \times 10^{-3}$  M  $K_2SO_4$

On the other hand, the MSR values of curcumin in aqueous solution of CPC and in the presence of  $1.66 \times 10^{-3}$  M  $K_2SO_4$  were found to be 0.223 and 1.144 respectively. The

solubilizing powers of CPB and CPC in the presence of added electrolytes are found to be 1.17 and 5.13 fold higher than those of the respective surfactants in pure water. This clearly indicates that the solubilizing power of both the surfactants increase in the presence of electrolyte because the electrostatic repulsion between the charged head groups at the micelle surface decreases as a result aggregation number of micelle and the oil like environment of the micelle core increase which promote the solubilization capacity of both the surfactants [111, 112].

In addition, the CMC is determined from the intersection point of the absorbance versus surfactant concentration plot. Figures-3.17(b), 3.18(b), 3.19(b), and 3.20(b) show the absorbance versus surfactant concentration plot in both pre- and post-solubilization regions with a break. The concentration at the break point in the curve indicates the CMC of the surfactant. Here, the CMC is measured based on the rules of solubilization that below the CMC the extent of solubilization of water insoluble dye is zero or nearly zero and at or above the CMC solubilization increases with the increase of surfactant concentration due to the increase in the number of micelle. The CMC obtained from the solubilization method is slightly lower than that obtained from the conductometric method due to the hydrophobic attraction between the dye and surfactant in the micelle. The CMC of CPC is 0.12 mM in pure water and 0.17 mM in the presence of  $1.66 \times 10^{-3}$  M  $K_2SO_4$  determined by the solubilization of curcumin. On the other hand, the CMC of CPB is 0.72 mM in pure water and 0.14 mM in the presence of  $5 \times 10^{-3}$  M  $KNO_3$  determined by the solubilization of PAN.

### **3.5.1 The location of PAN solubilized in the micelle of CPB**

The shape and size of the micelles can influence various properties of a surfactant solution, e.g. solubilization. The proton NMR spectra play an important role in characterization of solubilization by micelle. The location of solubilized dye in the micelle was determined comparing the proton NMR spectra of aqueous solution of CPB above the CMC in the presence of PAN with the proton NMR spectra of aqueous solution of CPB above the CMC in the absence of PAN. In every case the concentration of CPB was same.

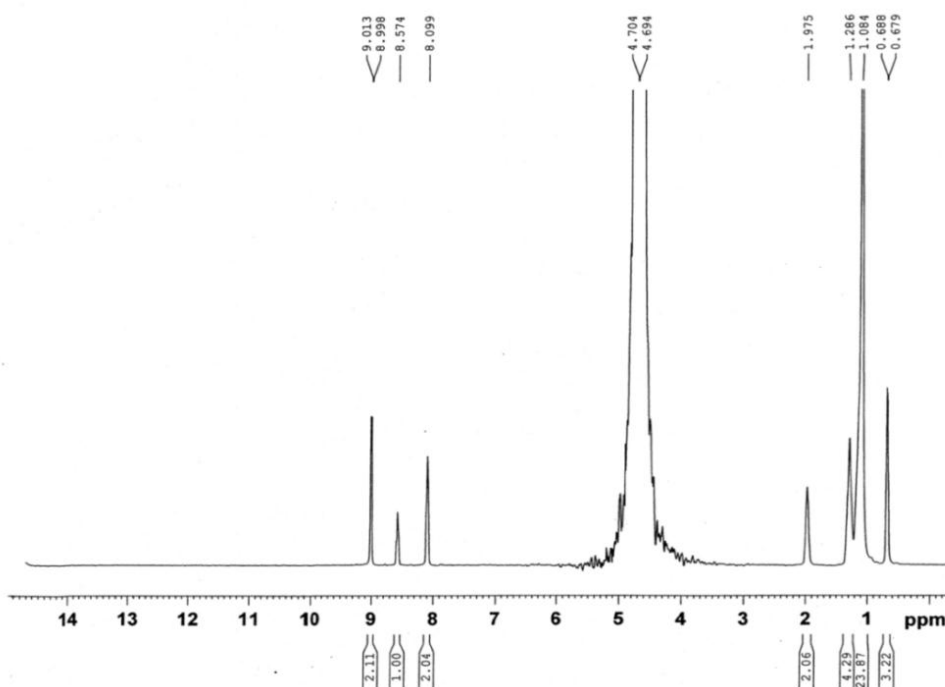


**Figure-3.21**  $^1\text{H}$  NMR spectra of CPB above the CMC in the presence of PAN

Figure-3.21 shows the chemical shifting of protons of CPB above the CMC in the presence of PAN. The signals will be upfield (shielding) or downfield (deshielding) shifted depending on the average disposition of the dye with respect to the surfactant segment [113]. The analysis of the  $^1\text{H}$  NMR chemical shifts shows that the protons of group  $-\text{CH}_2$  in the aliphatic chain of CPB give a singlet at 1.084 ppm, the protons of  $-\text{CH}_3$  give a doublet at 0.683 ppm, the protons of  $\alpha\text{-CH}_2$ , and  $\beta\text{-CH}_2$  give a singlet at 1.286 and 1.975 ppm, respectively and the protons of  $-\text{C}_5\text{H}_5\text{N}$  give a multiplet from 8.099 to 9.013 ppm. From the comparison of  $^1\text{H}$ NMR spectra of CPB in aqueous solution above the CMC (Figure-3.9), with the  $^1\text{H}$ NMR spectra of CPB in aqueous solution in the presence of PAN, (Figure-3.21), it is found that the proton NMR spectra of CPB show upfield shifting for the protons of  $\text{C}_5\text{H}_5\text{N}$ -,  $\alpha\text{-CH}_2$ , and  $\beta\text{-CH}_2$ . The protons of pyridinium ring show upfield shifting due to the interaction between the  $\pi$ -electron of PAN with  $\pi$ -electron of pyridinium ring and lone pair of nitrogen. This chemical shifting shows that it interacts to some extent with the polar head group of the surfactant. The analysis of the  $^1\text{H}$  NMR chemical shifts suggests that the sparingly soluble PAN, was solubilized in the interior of the surfactant micelles [54, 89, 90, 113].

### 3.5.2 The location of curcumin solubilized in the micelle of CPC

Figure-3.22 shows the  $^1\text{H}$  NMR spectra of CPC in aqueous solution at above the CMC in the presence of curcumin where the protons of group  $-\text{CH}_2$  in the aliphatic chain of CPC give a signal at 1.074 ppm, the protons of  $-\text{CH}_3$  give a triplet at 0.686 ppm, the protons of  $\alpha$   $-\text{CH}_2$  give a singlet at 1.887 ppm, the protons of  $\beta$   $-\text{CH}_2$  give a singlet at 1.204 ppm, and the protons of  $-\text{C}_5\text{H}_5\text{N}$  give a multiplet from 8.037 to 8.866 ppm. From the comparison of  $^1\text{H}$  NMR spectra of CPC in aqueous solution (Figure-3.11), with the  $^1\text{H}$  NMR spectra of CPC in aqueous solution in the presence of curcumin (Figure-3.22), it is found that the  $^1\text{H}$  NMR spectra of CPC show upfield shifting for the protons of group  $-\text{CH}_2$  and  $-\text{CH}_3$  due to the shielding effect. On the other hand, the protons of  $\alpha$   $-\text{CH}_2$  and  $\beta$   $-\text{CH}_2$  show downfield shifting due to the deshielding effect. The  $^1\text{H}$  NMR experiment led to the conclusion that the water insoluble curcumin was solubilized in the core and palisade layer of the micelle [89, 90].

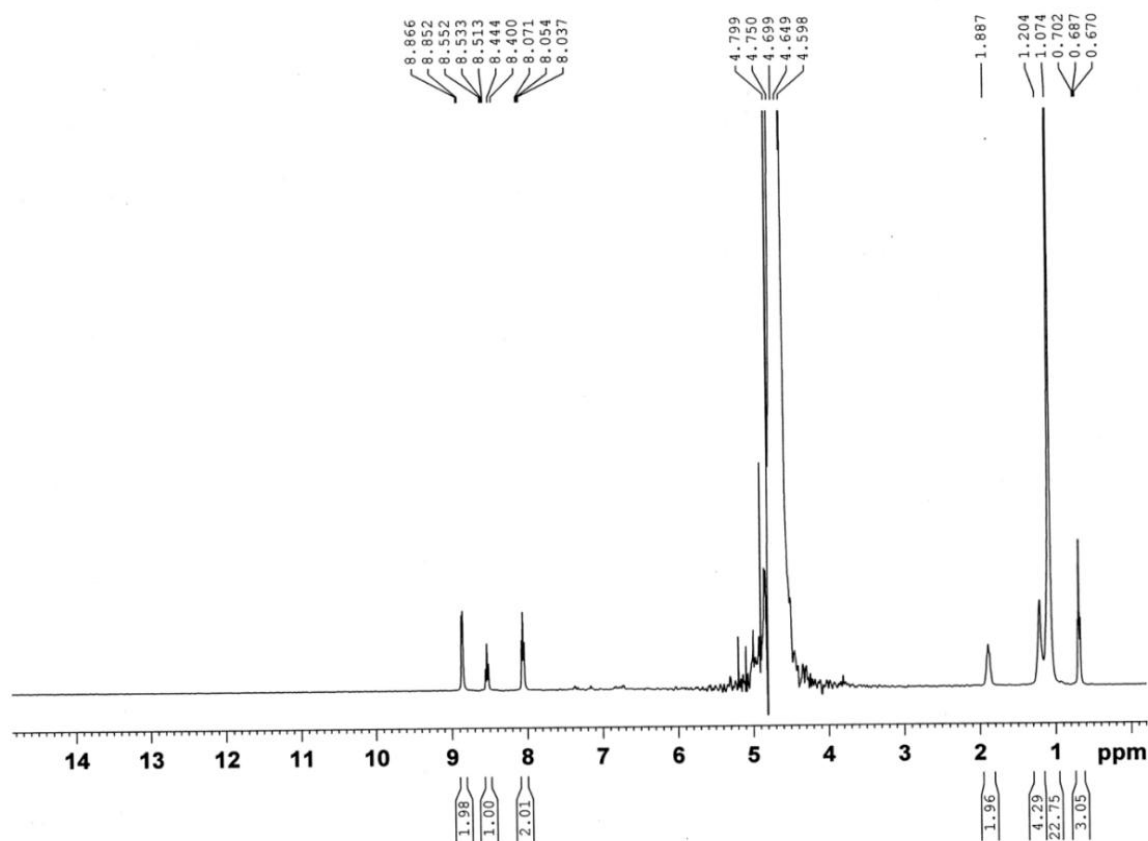


Figure-3.22  $^1\text{H}$  NMR spectra of CPC above the CMC in the presence of curcumin

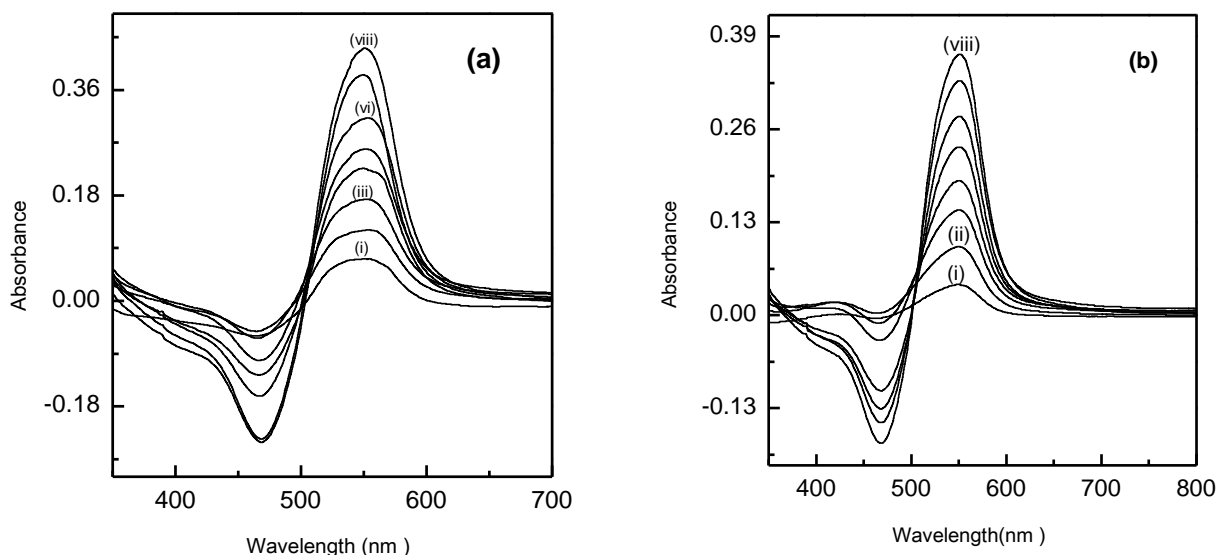
### **3.6 Complexation of Ni(II), Cu(II), Zn(II) with PAN in aqueous solution of CPB and Cu(II) with curcumin in aqueous solution of CPC**

The interactions of Cu(II) ion with PAN in aqueous solution of CPB has been studied by UV-visible spectrophotometric method. In all instances measurements were made against a reagent blank. The Cu(II)-PAN complex absorb strongly at 550 nm which is different from the absorbance of PAN in the same environment. The crucial fact of solubilization of water insoluble complex and ligand is the  $T_K$  of the surfactant because below the  $T_K$  surfactant remains in solution as hydrated solid crystals. Consequently, below the  $T_K$  both the ligand and complex become insoluble due to the absence of micelle. From previous study it is found that the Cu(II)-PAN complex is insoluble in aqueous solution at above the pH 2.5 [49] but soluble enough in the core of micelle above or below this pH and stable even at pH 6.9. Depending on the pH Cu(II) ion may bind with one or two ligands [49]. It has been found that at pH 1.5 Cu(II) ion form complex with PAN at 1:1 and Cu(II) ion form complex with PAN at 1:2 ratio at pH 2.5 showing maximum absorbance at 550 nm [49, 114]. In the micellar system, these metal ions unable to bind with two PAN molecules because micelle can not accommodate more than one molecule of PAN. The reaction of Cu(II) ion with PAN in micellar system is instantaneous but Ni(II) and Zn(II) react with PAN slowly. The Cu(II)-PAN complex absorbs strongly at 550 nm, the Ni(II)-PAN complex absorbs strongly at 566 nm with a shoulder centered apparently at 528 nm and Zn(II)-PAN complex absorbs strongly at 553 nm with a shoulder centered apparently at 521 nm which are fairly different from that of PAN. The PAN absorbs strongly at 472 nm in the identical micellar environment. On the other hand, the curcumin absorbs strongly at 417 nm and the Cu(II)-curcumin complex absorbs strongly at 364 nm which is fairly different from that of curcumin in the same environment (aqueous solution of CPC). This complex is insoluble in pure water, whereas soluble in aqueous solution of the surfactant and the composition of the complex remains same as in the solution of organic solvents [115]. Commonly, the metal to ligand ratio in the complex is determined using three different methods namely, mole ratio method, continuous variation method, and slope ratio method. Here, the slope ratio method has been applied to determine the ratio of metal to ligand in the complexes, Cu(II)-PAN, Ni(II)-PAN, Zn(II)-PAN, in aqueous solution of CPB and Cu(II)-curcumin complex in aqueous solution of CPC respectively. In every case, two series of solutions were prepared varying the amount of

one component in the complex and another component was added to a very large excess compared to the other. The stability constant can be the key for the investigation of equilibrium in solution. The stability of a complex in a particular environment may be referred in terms of thermodynamic stability and kinetic stability. The stability constant or formation constant is the equilibrium constant which measures the strength of the interaction between the ligands and metal ion [116, 117].

### **3.6.1 Stoichiometry of Cu(II)-PAN complex in aqueous solution of CPB**

The stoichiometry of Cu(II)-PAN complex has been investigated based on the slope ratio method [118–120] at pH 6.9 without adjusting the pH or adding buffer. In every case, two series of solutions of Cu(II)-PAN complex in aqueous solution of CPB have been prepared where one set of solutions contain fixed amount of Cu(II) ion varying the concentration of PAN. Another set of solutions which contain fixed amount of PAN varying the concentration of Cu(II) ion. The absorbance of these two series of solutions of Cu(II)-PAN complex have been measured by UV-Vis. spectrophotometer at 550 nm against the reagent blank at 30 °C.



**Figures-3.23 (a) Absorption spectra of Cu(II)-PAN complex in aqueous solution of CPB where the concentrations of CuSO<sub>4</sub> are (i) 2 μM, (ii) 4 μM, (iii) 6 μM, (iv) 8 μM, (v) 10 μM, (vi) 12 μM, (vii) 16 μM, and (viii) 18 μM; (b) Absorption spectra of Cu(II)-PAN complex in aqueous solution of CPB where the concentrations of PAN are (i) 2 μM, (ii) 4 μM, (iii) 6 μM, (iv) 8 μM, (v) 10 μM, (vi) 12 μM, (vii) 14 μM, and (viii) 16 μM**

The figure-3.23(a) shows the spectra of Cu(II)-PAN complex when the concentration of CuSO<sub>4</sub> is variable and the concentration of PAN (0.2 μM) is kept constant. Figure-3.23(b) shows the spectra of Cu(II)-PAN complex when the concentration of PAN is variable and concentration of CuSO<sub>4</sub> (0.2 μM) is kept constant. Figure-3.24(i) demonstrates a plot of absorbance of Cu(II)-PAN complex against the concentration of PAN when concentration of CuSO<sub>4</sub> is constant. Figure-3.24(ii) demonstrates a plot of absorbance of Cu(II)-PAN complex against the concentration of CuSO<sub>4</sub> when concentration of PAN is constant. These figures demonstrate that absorbance increases with the increase of concentration of ligand and metal ion.

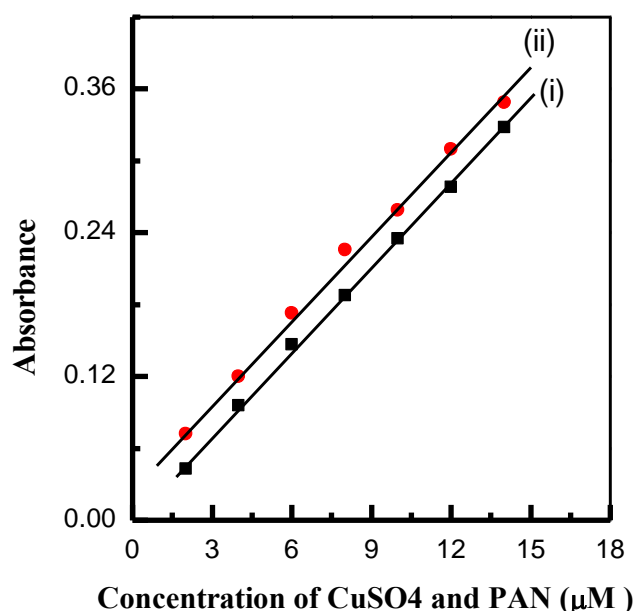


**Figure-3.24(i) Absorbance of Cu(II)-PAN complex versus concentration of PAN when concentration of CuSO<sub>4</sub> is constant (20 μM); (ii) Absorbance of Cu(II)-PAN complex versus concentration of CuSO<sub>4</sub> (μM) when concentration of PAN is constant (20 μM)**

The stoichiometry of the complex has been investigated based on the slope ratio method [118–120]. The slope ratio has been found to be 1.009 ( $\approx 1$ ) which is obtained from dividing the slope of one straight line by another. This slope ratio indicates that the mole ratio of metal ion to ligand is almost one. So, the maximum interaction may occur at 1:1 ratio of Cu(II) ion to PAN. In the presence of  $5 \times 10^{-3}$  M KNO<sub>3</sub>, the slope ratio of the Cu(II)-PAN complex in aqueous solution of CPB has also been found 1:1.

### 3.6.2 Effect of time on Cu(II)-PAN complex formation in aqueous solution of CPB

Cu(II)-PAN complex formation occurs spontaneously. The measurement of the amount of the complex has been done at pH 6.9 without adjusting the pH of the solution or adding buffer. Figure-3.25 shows the absorbance of Cu(II)-PAN complex versus time (hour). From this figure, it has been observed that the absorbance of the complex in aqueous solution of CPB become maximum just two hours after adding the reagent and the absorbance remains strictly unaltered for 10 hours. It has also been observed that the absorbance remains same for 48 hours at 30 °C.

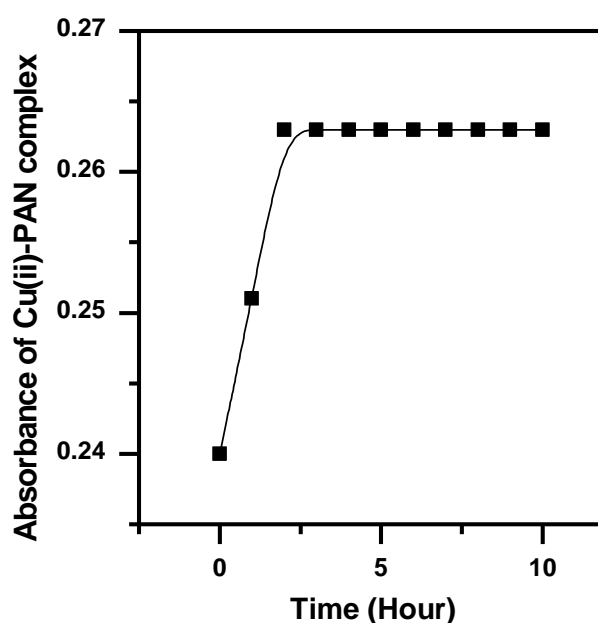


Figure-3.25 The absorbance of Cu(II)-PAN complex in aqueous solution of CPB versus time (hour)

### 3.6.3 Calibration graph for Cu(II)-PAN complex in aqueous solution of CPB

The effect of the concentration of  $\text{CuSO}_4$  has been studied over 0.6 to 40  $\mu\text{M}$  (or 0.04 to 2.54 ppm Cu(II) ion) at 30 °C. Figure-3.26 shows that the Cu(II)-PAN complex soluble in micellar system of the surfactant follows Beer's law from 0.8 to 20  $\mu\text{M}$   $\text{CuSO}_4$  (or 0.05 to 1.27 ppm Cu(II) ion). The formation constant ( $K_f$ ) of the complex has been found to be  $4.66 \times 10^5$  which indicates the strength of interaction between the ligand and metal ion. The Sandell's sensitivity [121] of the complex has been found to be  $2.84 \times 10^{-3} \mu\text{g cm}^{-2}$ . The Sandell's sensitivity is the concentration of the analyte ( $\mu\text{g mL}^{-1}$ ) which will give an absorbance of 0.001 in a cell of path length 1 cm. The molar absorptivity ( $\epsilon$ ) of Cu(II)-



PAN complex has been found to be  $2.32 \times 10^4$  L/mol/cm. The value of  $\epsilon$  has been calculated by the method of least squares as the slope of the straight line going through the origin. This indicates that how strongly Cu(II)-PAN complex absorbs light at 550 nm. This is an intrinsic property of chemical species that is dependent upon their chemical composition and structure.

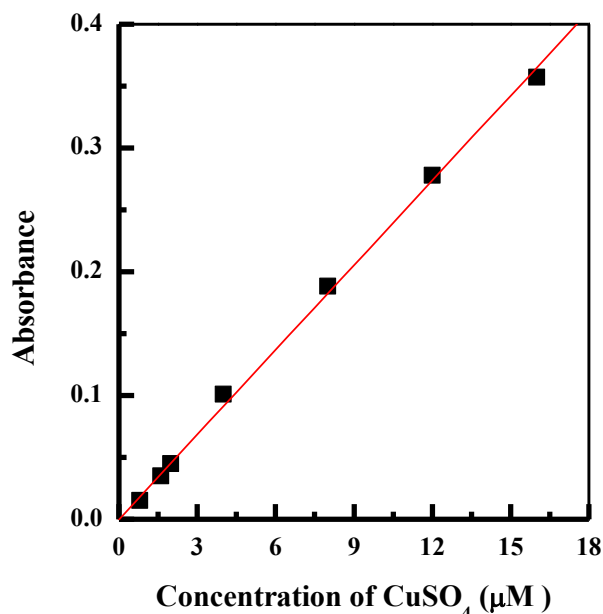


**Figure-3.26 Absorbance of Cu(II)-PAN complex versus concentration of CuSO<sub>4</sub> (µM) when concentration of PAN is constant (250 µM)**

#### **3.6.4 The location of Cu(II)-PAN complex in the micelle of CPB in aqueous solution**

Figure-3.27 shows the <sup>1</sup>H NMR spectra of CPB in the presence of Cu(II)-PAN complex in aqueous solution above the CMC. This figure shows that the protons of group -CH<sub>2</sub> in the aliphatic chain of CPB give a singlet at 1.081 ppm and the protons of -CH<sub>3</sub> give a doublet at 0.670 ppm, the protons of α-CH<sub>2</sub> and β-CH<sub>2</sub> give a singlet at 1.973 and 1.288 ppm, respectively and the protons of -C<sub>5</sub>H<sub>5</sub>N give a multiplet from 8.075 to 8.997 ppm. From the comparison of <sup>1</sup>H NMR spectra of CPB in aqueous solution in the presence of PAN (Figure-3.21), with the <sup>1</sup>H NMR spectra of CPB in aqueous solution in the presence of Cu(II)-PAN complex (Figure-3.27), it is observed that the protons of -CH<sub>3</sub> show upfield shifting due to the shielding effect which is attributed to the effect of complexation in the core of micelle and a downfield (deshielding) shifting is also

observed for the protons of pyridinium ring and  $\alpha$ -CH<sub>2</sub>. The analysis of the <sup>1</sup>H NMR chemical shifts suggests that the complex formation occurs from the core to micelle surface due to the polarity of the complex [89, 90].

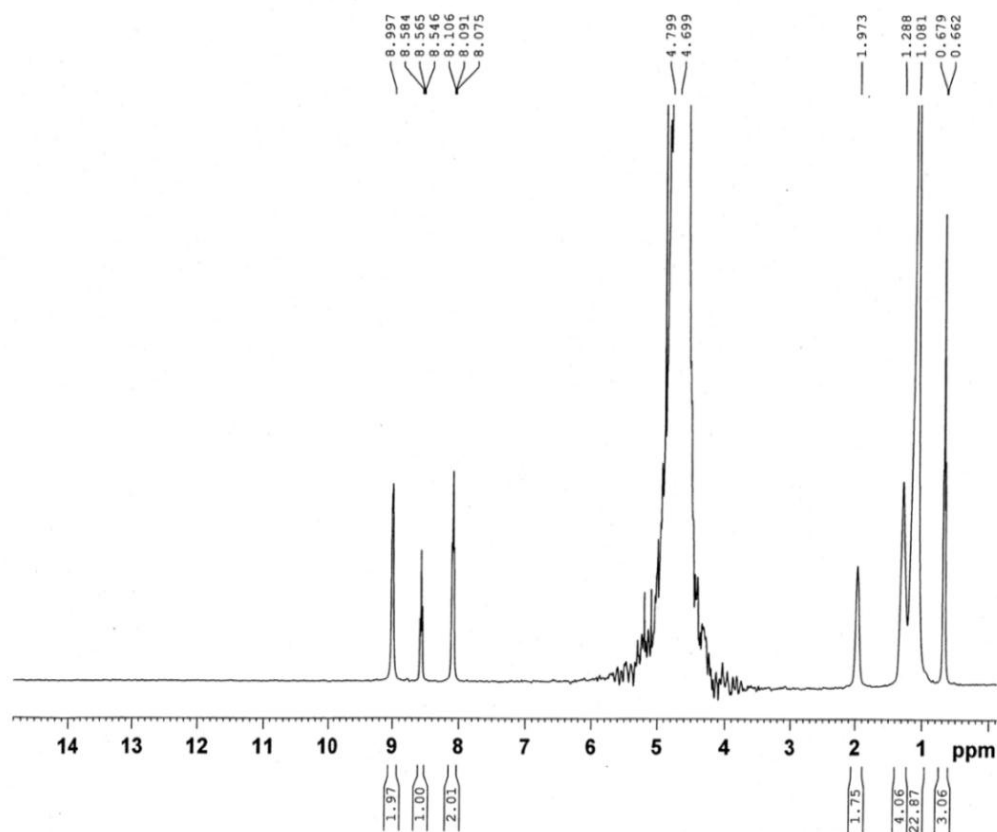
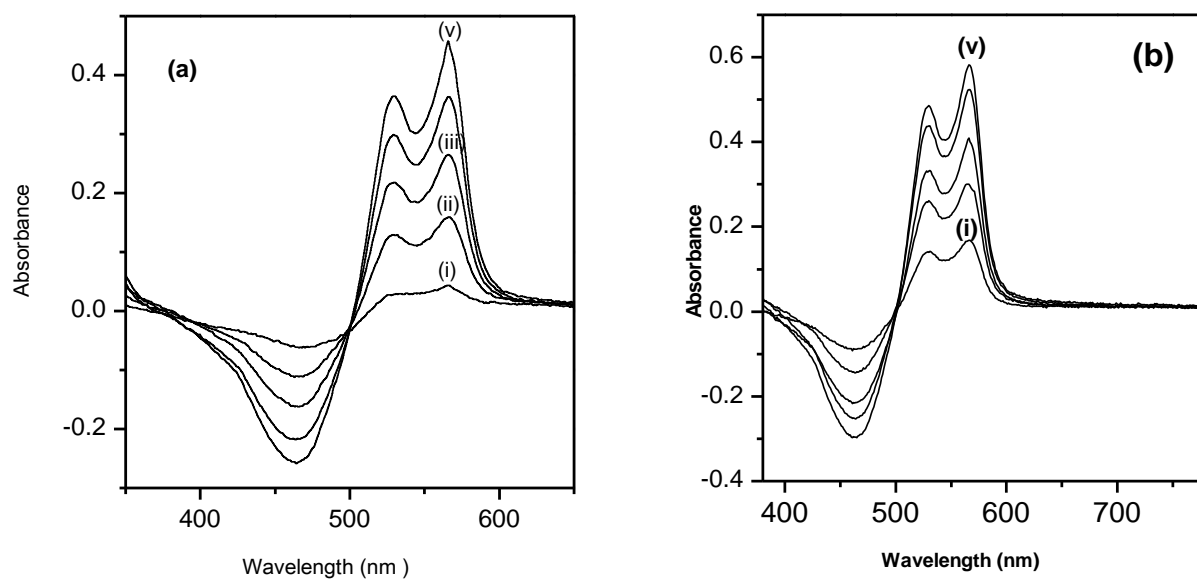


**Figure-3.27** <sup>1</sup>H NMR spectra of CPB in aqueous solution above the CMC in the presence of Cu(II)-PAN complex

### 3.7 Stoichiometry of Ni(II)-PAN complex in aqueous solution of CPB

Following the slope ratio method [118–120], two sets of solutions of Ni(II)-PAN complex in aqueous solution of CPB have been prepared where one set of solutions contain fixed amount of Ni(II) ion varying the concentration of PAN. Another set of solutions which contain fixed amount of PAN varying the concentration of Ni(II) ion. In all instances, absorbance of these two sets of solutions has been measured by UV-Vis. spectrophotometer at 566 nm against the reagent blank at 30 °C. Figure-3.28(a) shows the spectra of Ni(II)-PAN complex when the concentration of PAN is variable keeping the concentration of NiSO<sub>4</sub> (20 μM) constant. Figure-3.28(b) shows the spectra of Ni(II)-

PAN complex when the concentration of  $\text{NiSO}_4$  is variable keeping the concentration of PAN ( $20 \mu\text{M}$ ) constant.



Figures-3.28(a) Absorption spectra of Ni(II)-PAN complex in aqueous solution of CPB where the concentrations of PAN are (i)  $4 \mu\text{M}$ , (ii)  $8 \mu\text{M}$ , (iii)  $12 \mu\text{M}$ , (iv)  $16 \mu\text{M}$ , (v)  $20 \mu\text{M}$ ; (b) Absorption spectra of Ni(II)-PAN complex in aqueous solution of CPB where the concentrations of  $\text{NiSO}_4$  are (i)  $4 \mu\text{M}$ , (ii)  $8 \mu\text{M}$ , (iii)  $12 \mu\text{M}$ , (iv)  $16 \mu\text{M}$ , (v)  $18 \mu\text{M}$

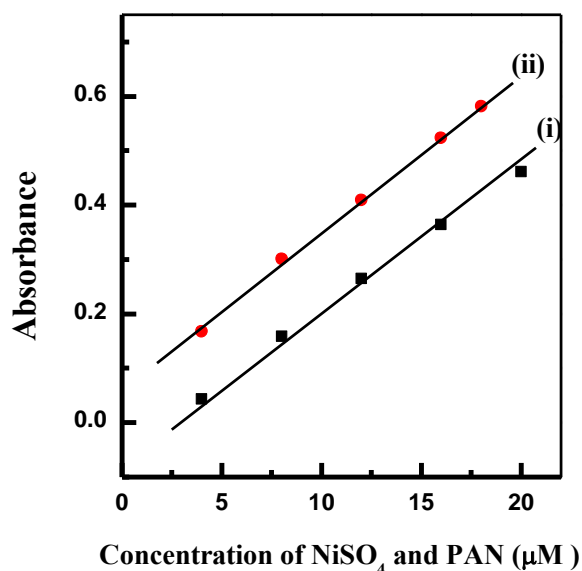
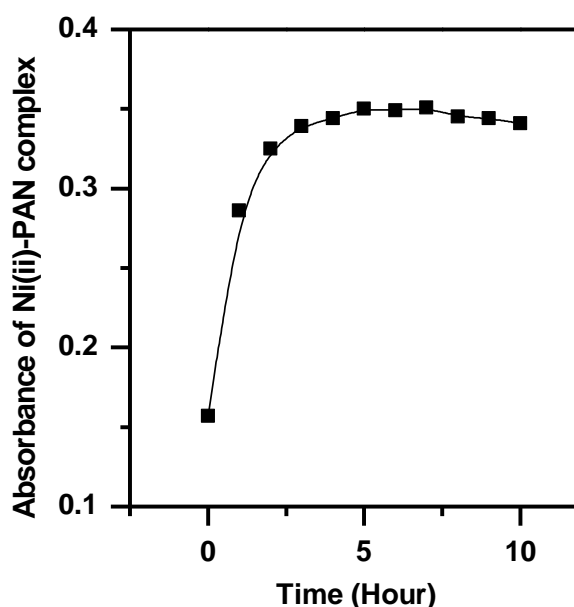


Figure-3.29(i) Absorbance of Ni(II)-PAN complex versus concentration of PAN when concentration of  $\text{NiSO}_4$  is  $20 \mu\text{M}$ ; (ii) Absorbance of Ni(II)-PAN complex versus concentration of  $\text{NiSO}_4$  when concentration of PAN is  $20 \mu\text{M}$

Figure-3.29(i) indicates a plot of absorbance of Ni(II)-PAN complex versus concentration of PAN when concentration of NiSO<sub>4</sub> is constant. Figure-3.29(ii) indicates a plot of absorbance of Ni(II)-PAN complex versus concentration of NiSO<sub>4</sub> when concentration of PAN is constant. Dividing the slope of one straight line by another, the ratio has been found to be 0.89 ( $\approx 1$ ). This slope ratio indicates that the mole ratio of metal ion to ligand in the Ni(II)-PAN complex is almost one. This indicates that the maximum interaction may occur at 1:1 ratio of Ni(II) ion to PAN in this complex in aqueous solution of CPB.

### 3.7.1 Effect of time on Ni(II)-PAN complex formation in aqueous solution of CPB

Ni(II) ion forms complex with PAN spontaneously in aqueous solution of CPB. Figure-3.30 shows the absorbance of Ni(II)-PAN complex versus time (hour). This figure indicates that the absorbance of Ni(II)-PAN complex in aqueous solution of CPB become maximum just three and half hours after diluting the solution upto the mark and the absorbance remains strictly unaltered for 10 hours. From the absorbance it has also been observed that the absorbance remains same for 48 hours at 30 °C.



**Figure-3.30** The absorbance of Ni(II)-PAN complex in aqueous solution of CPB versus time (hour)

### 3.7.2 Calibration graph for Ni(II)-PAN complex in aqueous solution of CPB

The Ni(II)-PAN complex soluble in aqueous solution of surfactant CPB which absorbs strongly at 566 nm. The effect of NiSO<sub>4</sub> concentration has been studied over 0.5 to 30 μM (or 0.03 to 1.76 ppm Ni(II) ion). Figure-3.31 shows that this complex follows Beer's law from 1.28 to 12.8 μM NiSO<sub>4</sub> (or 0.08 to 0.75 ppm Ni(II) ion) when the concentration of PAN is kept constant. The molar absorptivity ( $\epsilon$ ) of the complex has been found to be  $4.56 \times 10^4$  L/mol/cm and the formation constant ( $K_f$ ) of the complex has been found to be  $16.47 \times 10^5$ . The Sandell's sensitivity [121] is the concentration of the analyte in  $\mu\text{g mL}^{-1}$  which has been found to be  $1.36 \times 10^{-3} \mu\text{g cm}^{-2}$ .

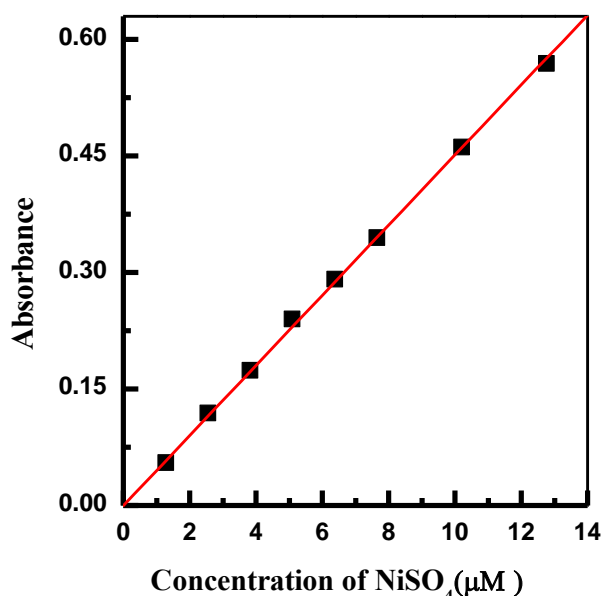
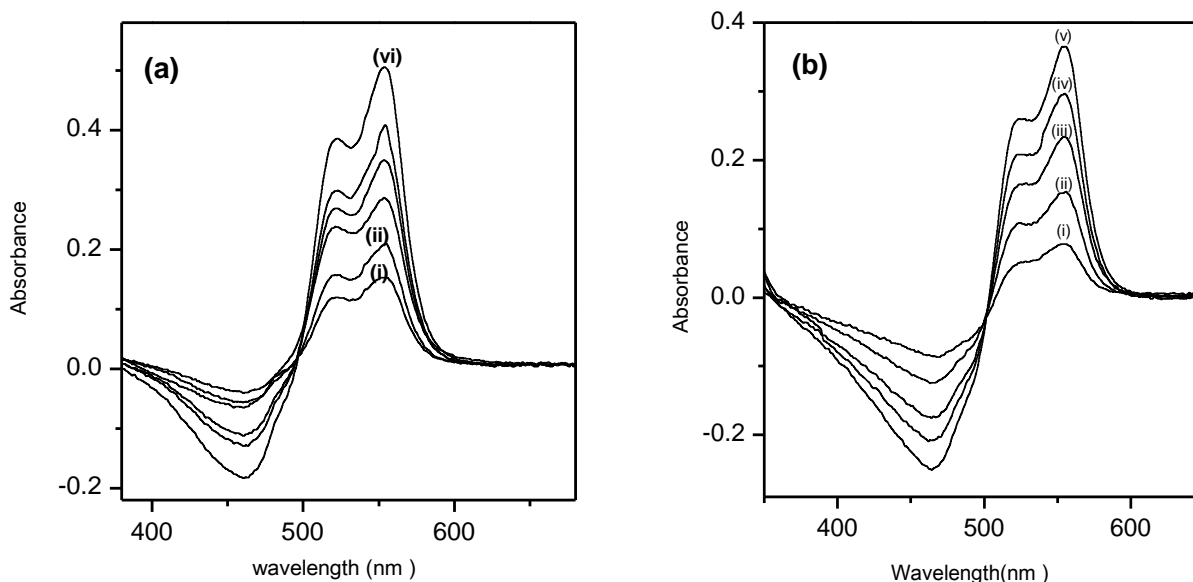


Figure-3.31 Absorbance of Ni(II)-PAN complex versus concentration of NiSO<sub>4</sub> (μM) when concentration of PAN is 250 μM

### 3.8 Stoichiometry of Zn(II)-PAN complex in aqueous solution of CPB

To measure the stoichiometry of Zn(II)-PAN complex two series of solutions of Zn(II)-PAN complex in aqueous solution of CPB have been prepared. The absorbance of these series of solutions have been measured by UV-Vis. spectrophotometer at 553 nm against the reagent blank when the concentration of ZnSO<sub>4</sub> is variable in the first series and the concentration of PAN is variable in the second series. Figure-3.32(a) shows the spectra of Zn(II)-PAN complex when the concentration of ZnSO<sub>4</sub> is variable keeping the concentration of PAN (20 μM) constant. Figure-3.32(b) shows the spectra of Zn(II)-PAN

complex when the concentration of PAN is variable keeping the concentration of  $ZnSO_4$  ( $20 \mu M$ ) constant.



**Figures-3.32 (a) Absorption spectra of Zn(II)-PAN complex in aqueous solution of CPB where the concentrations of  $ZnSO_4$  are (i) 4  $\mu M$ , (ii) 8  $\mu M$ , (iii) 12  $\mu M$ , (iv) 18  $\mu M$ , (v) 20  $\mu M$ , (vi) 24  $\mu M$ ; (b) Absorption spectra of Zn(II)-PAN complex in aqueous solution of CPB where the concentrations of PAN are (i) 8  $\mu M$ , (ii) 12  $\mu M$ , (iii) 16  $\mu M$ , (iv) 20  $\mu M$ , (v) 24  $\mu M$**

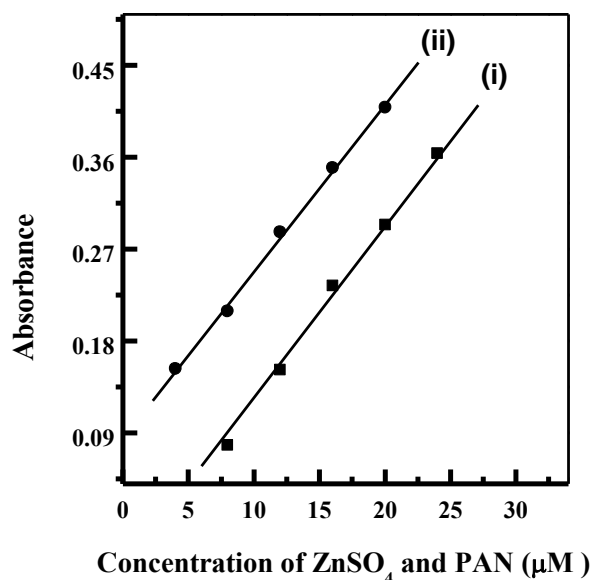


**Figure-3.33 (i) Absorbance of Zn(II)-PAN complex versus concentration of PAN when the concentration of  $ZnSO_4$  is 20  $\mu M$ ; (ii) Absorbance of Zn(II)-PAN complex versus concentration of  $ZnSO_4$  when the concentration of PAN is 20  $\mu M$**

Figure-3.33(i) shows a plot of absorbance of Zn(II)-PAN complex against the concentration of PAN when concentration of ZnSO<sub>4</sub> is constant. Figure-3.33(ii) shows a plot of absorbance of Zn(II)-PAN complex against the concentration of ZnSO<sub>4</sub> when concentration of PAN is constant. The stoichiometry of the complex has been investigated based on the slope ratio method [118–120]. The slope ratio of these straight lines has been found to be 1.09 ( $\approx 1$ ) which is obtained from dividing the slope of one straight line by another. This ratio indicates that the maximum interaction between Zn(II) ion and PAN in the complex may occur at 1:1 ratio.

### 3.8.1 Effect of time on Zn(II)-PAN complex formation in aqueous solution of CPB

Zn(II)-PAN complex formation occurs very slowly in aqueous solution of CPB. Figure-3.34 shows the absorbance of Zn(II)-PAN complex versus time (hour). From this figure, it is observed that the absorbance of Zn(II)-PAN complex in aqueous solution of CPB become maximum just twenty one hours after diluting the volume upto the mark and constant absorbance has been found which remains strictly unaltered for 30 hours.

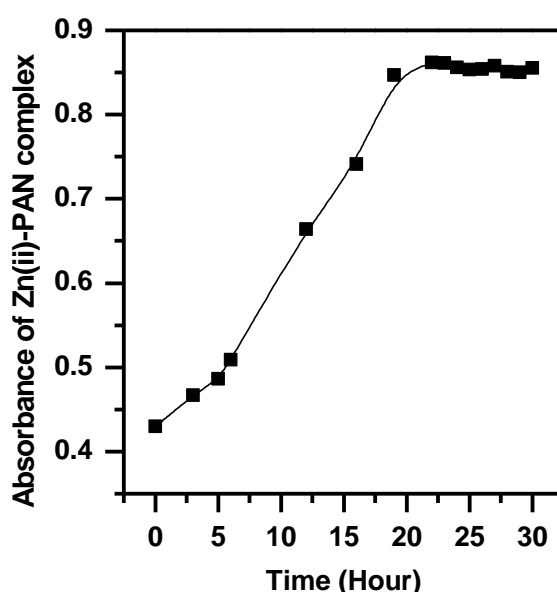


**Figure-3.34** The absorbance of Zn(II)-PAN complex in aqueous solution of CPB versus time (hour)

### 3.8.2 Calibration graph for Zn(II)-PAN complex in aqueous solution of CPB

The effect of ZnSO<sub>4</sub> concentration has been studied over 1 to 20  $\mu\text{M}$  (or 0.07 to 1.31 ppm Zn(II) ion) at 30 °C. Figure-3.35 shows that Zn(II)-PAN complex soluble in micellar

system follows Beer's law from 1.25 to 10  $\mu\text{M}$   $\text{ZnSO}_4$  (or 0.08 to 0.65 ppm  $\text{Zn(II)}$  ion) when the concentration of PAN (200  $\mu\text{M}$ ) is constant. The molar absorptivity ( $\epsilon$ ) of the complex has been found to be  $5.05 \times 10^4$  L/mol/cm and the formation constant ( $K_f$ ) has been found to be  $5.85 \times 10^5$ . The Sandell's sensitivity [121] is the concentration of the analyte in  $\mu\text{g mL}^{-1}$  which has been found to be  $1.29 \times 10^{-3}$   $\mu\text{g cm}^{-2}$ .

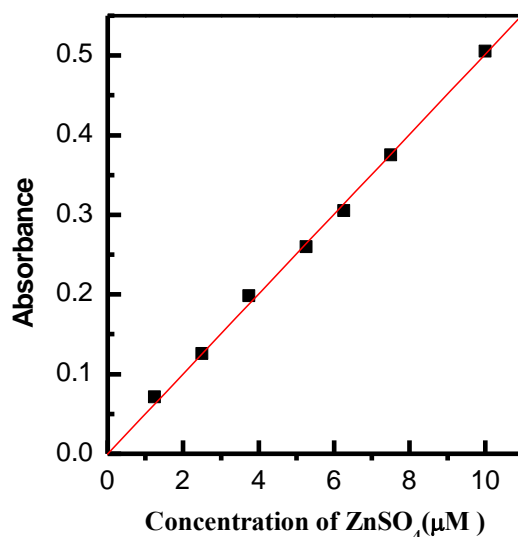


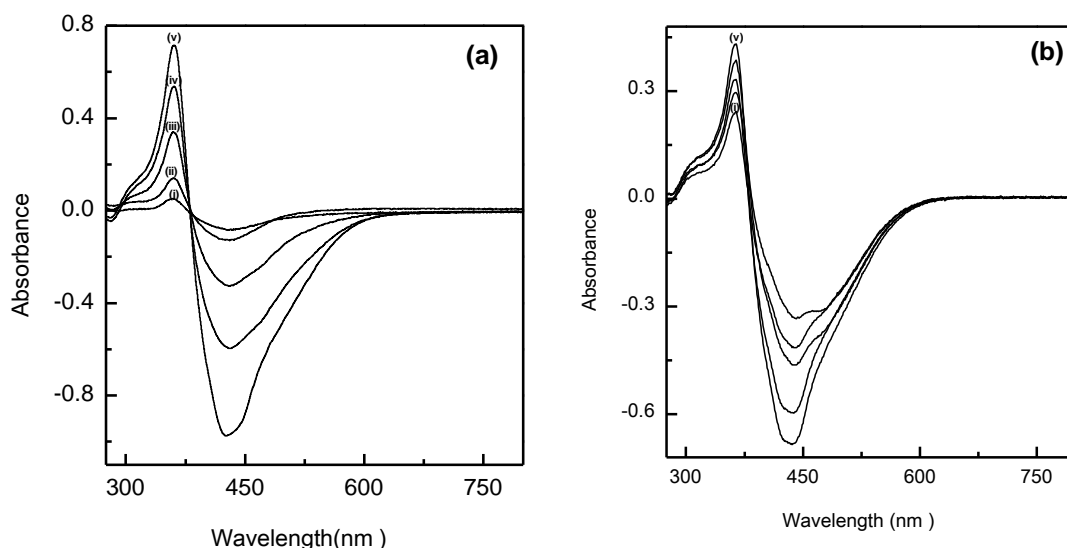
**Figure-3.35 Absorbance of Zn(II)-PAN complex versus concentration of  $\text{ZnSO}_4$  ( $\mu\text{M}$ ) when the concentration of PAN is 250  $\mu\text{M}$**

### **3.9 Stoichiometry of Cu(II)-curcumin complex in aqueous solution of CPC**

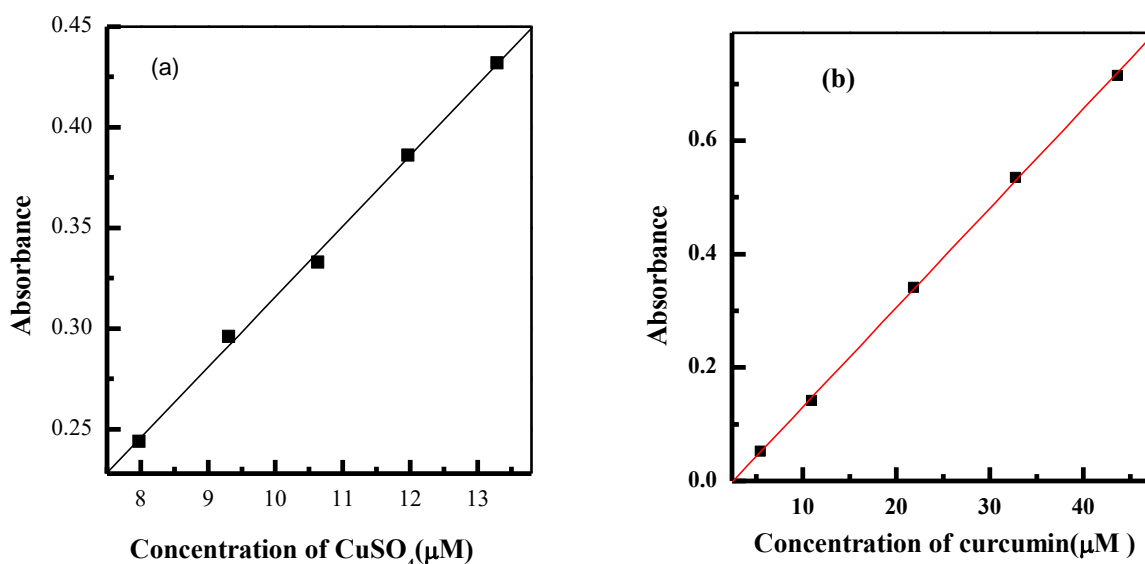
The stoichiometry of the Cu(II)-curcumin complex has been investigated based on the slope ratio method [118–120]. In all instances, the absorbance of the two series of Cu(II)-curcumin complex in aqueous solution of CPC has been measured by UV-Vis. spectrophotometer at 364 nm against the reagent blank. The concentration of  $\text{CuSO}_4$  is variable in one series and the concentration of curcumin is variable in the other series. The figure-3.36(a) shows the spectra of Cu(II)-curcumin complex when the concentration of  $\text{CuSO}_4$  is variable and the concentration of curcumin (7.97  $\mu\text{M}$ ) is constant. Figure-3.36(b) shows the spectra of Cu(II)-curcumin complex when the concentration of curcumin is variable and concentration of  $\text{CuSO}_4$  (54.2  $\mu\text{M}$ ) is constant. Figure-3.37(a) represents a plot of absorbance of Cu(II)-curcumin complex versus concentration of  $\text{CuSO}_4$  keeping the concentration of curcumin constant. Figure-3.37(b) represents a plot of absorbance of Cu(II)-curcumin complex versus concentration of curcumin keeping the concentration of  $\text{CuSO}_4$  constant. The slope of first straight line is 34631 (Figure-3.37a)



and the slope of second straight line is 17507 (Figure-3.37b). The slope ratio of these two straight lines is 2:1 which is obtained from dividing the slope of first straight line by another. This slope ratio indicates that the maximum interaction may occur at 2:1 ratio of Cu(II) ion to curcumin in the complex.



**Figures-3.36 (a) Absorption spectra of Cu(II)-curcumin complex in aqueous solution of CPC where the concentrations of curcumin are (i) 5.45  $\mu\text{M}$ , (ii) 10.91  $\mu\text{M}$ , (iii) 21.82  $\mu\text{M}$ , (iv) 32.73  $\mu\text{M}$ , (v) 43.64  $\mu\text{M}$ ; (b) Absorption spectra of Cu(II)-curcumin complex in aqueous solution of CPC where the concentrations of  $\text{CuSO}_4$  are (i) 7.97  $\mu\text{M}$ , (ii) 9.31  $\mu\text{M}$ , (iii) 10.63  $\mu\text{M}$ , (iv) 11.96  $\mu\text{M}$ , (v) 13.29  $\mu\text{M}$**



**Figures-3.37 (a) Absorbance of Cu(II)-curcumin complex against the concentration of  $\text{CuSO}_4$  in aqueous solution of CPC; (b) Absorbance of Cu(II)-curcumin complex against the concentration of curcumin in aqueous solution of CPC**

### 3.9.1 Calibration graph for Cu(II)-curcumin complex in aqueous solution of CPC

The effect of  $\text{CuSO}_4$  concentration has been studied over 0.75 to 33.6  $\mu\text{M}$  (or 0.05 to 2.13 ppm  $\text{Cu(II)}$  ion) in aqueous solution of CPC at 30 °C. Figure-3.38 shows that the  $\text{Cu(II)}$ -curcumin complex soluble in micellar system follows Beer's law from 8.4 to 16.8  $\mu\text{M}$   $\text{CuSO}_4$  or (0.53 to 1.07 ppm  $\text{Cu(II)}$  ion). The formation constant ( $K_f$ ) of the complex has been found to be  $8.87 \times 10^5$ . The molar absorptivity ( $\epsilon$ ) of  $\text{Cu(II)}$ -curcumin complex has been found to be  $3.82 \times 10^4$  L/mol/cm which is calculated by the method of least squares as the slope of the straight line going through the origin. The Sandell's sensitivity [121] is the concentration of the analyte in  $\mu\text{g mL}^{-1}$  which has been found to be  $1.72 \times 10^{-3}$   $\mu\text{g cm}^{-2}$ .

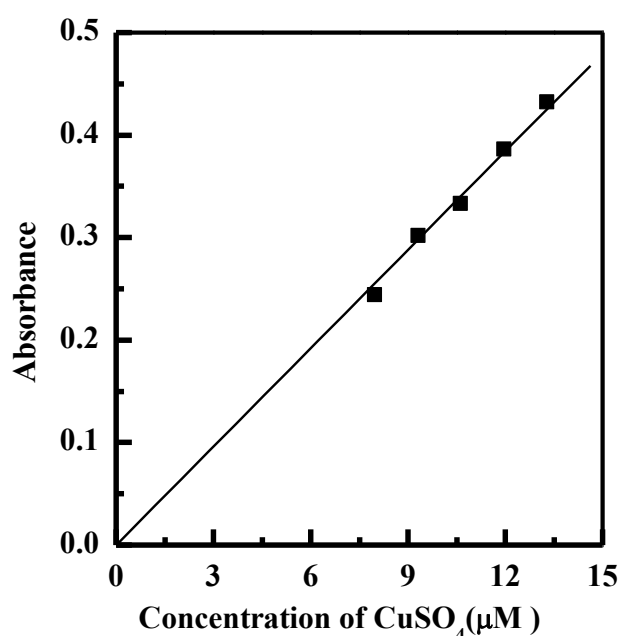
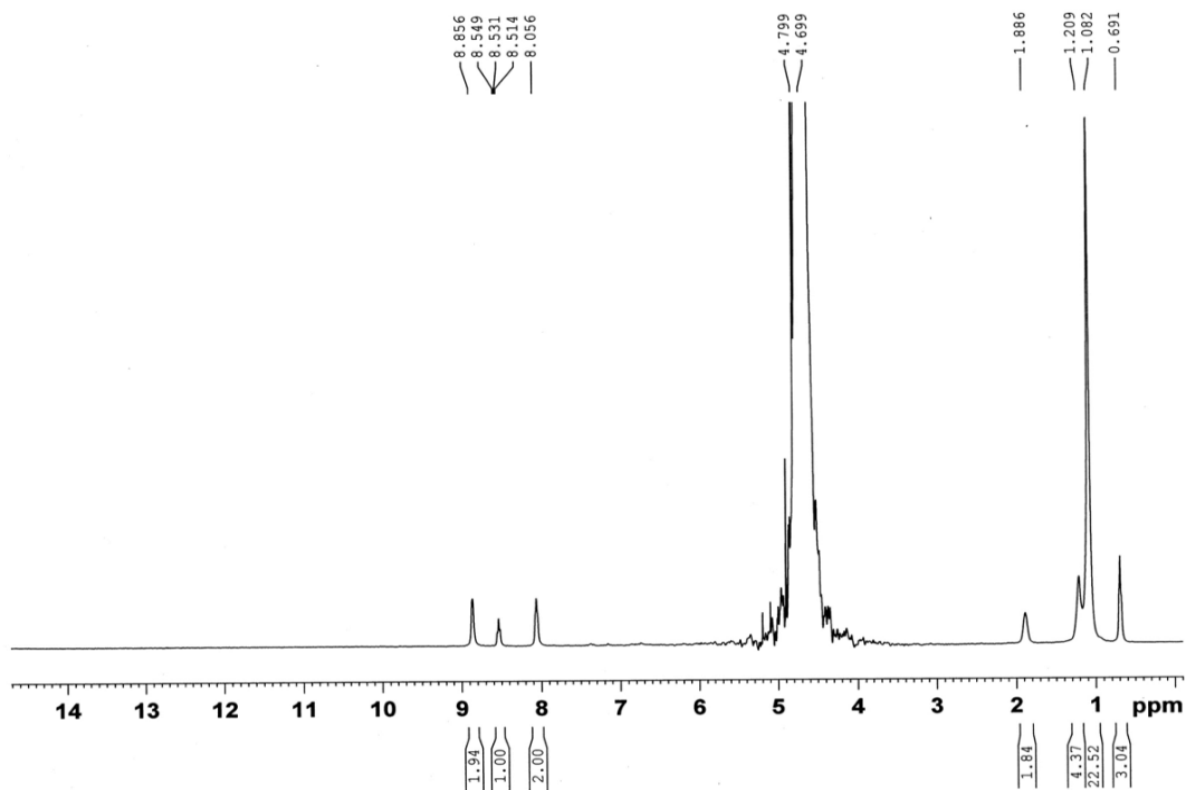


Figure-3.38 Absorbance of  $\text{Cu(II)}$ -curcumin complex versus concentration of  $\text{CuSO}_4$  ( $\mu\text{M}$ ) when the concentration of curcumin is 81.4  $\mu\text{M}$

### 3.9.2 The location of $\text{Cu(II)}$ -curcumin complex in the micelle of CPC in aqueous solution

Figure-3.21 shows the  $^1\text{H}$  NMR spectra of CPC in aqueous solution above the CMC in the presence of curcumin, where the protons of group  $-\text{CH}_2$  in the aliphatic chain of CPC give a signal at 1.074 ppm, the protons of  $-\text{CH}_3$  give a triplet at 0.686 ppm, the protons of

$\alpha$ -CH<sub>2</sub> give a singlet at 1.887 ppm, the protons of  $\beta$ -CH<sub>2</sub> give a singlet at 1.204 ppm, and the protons of C<sub>5</sub>H<sub>5</sub>N- give a multiplet from 8.037 to 8.866 ppm.



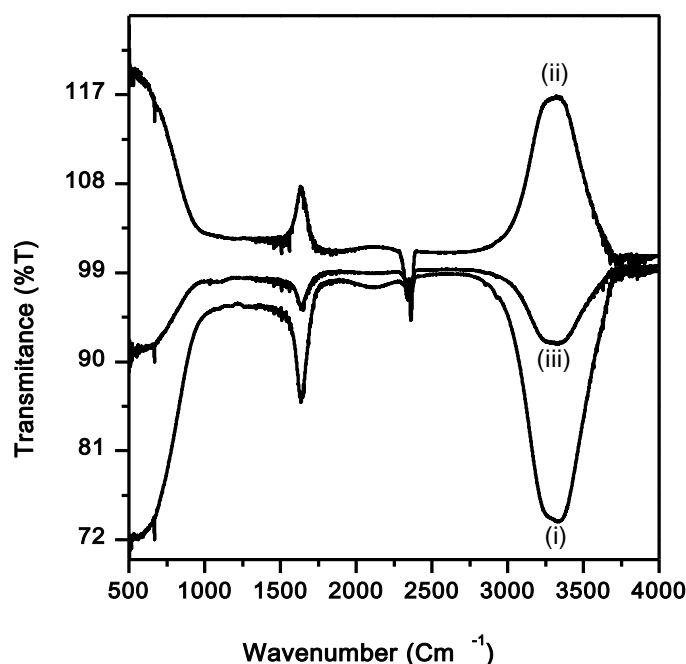
**Figure-3.39** <sup>1</sup>H NMR spectra of CPC in aqueous solution above the CMC in the presence of Cu(II)-curcumin complex

Figure-3.39 shows the <sup>1</sup>H NMR spectra and peak assignments of CPC in the presence of Cu(II)-curcumin complex in aqueous solution above the CMC. This figure shows that the protons of group -CH<sub>2</sub> in the aliphatic chain of CPC give a signal at 1.082 ppm, the protons of -CH<sub>3</sub> give a singlet at 0.691 ppm, the protons of  $\alpha$ -CH<sub>2</sub> give a singlet at 1.886 ppm, the protons of  $\beta$ -CH<sub>2</sub> give a singlet at 1.209 ppm, and the protons of C<sub>5</sub>H<sub>5</sub>N- give a multiplet from 8.056 to 8.856 ppm. From the comparison of <sup>1</sup>H NMR spectra of CPC in aqueous solution in the presence of curcumin (Figure-3.22), with the <sup>1</sup>H NMR spectra of CPC in aqueous solution in the presence of Cu(II)-curcumin complex (Figure-3.39), it has been found that a downfield (due to the deshielding effect) shifting is observed for the protons of -CH<sub>3</sub>,  $\alpha$ -CH<sub>2</sub>, group -CH<sub>2</sub> and C<sub>5</sub>H<sub>5</sub>N- which are attributed to the effect of complexation in the core of micelle. The examined results indicate that the

polarity of complex affects their solubilization site in the micelle solution [89, 90]. However, the analysis of the  $^1\text{H}$  NMR chemical shifts suggests that the water insoluble Cu(II)-curcumin complex has been solubilized in the palisade of the surfactant micelles and the solubilization site of the complex varies gradually from the palisade to the mantle of the surfactant micelle.

### 3.10 ATR-IR spectra of CPC in aqueous solution in the presence of curcumin and Cu(II)-curcumin complex

Figure-3.40 (i), (ii), and (iii) represent the ATR-IR spectra for CPC in pure water, curcumin in aqueous solution of CPC and Cu(II)-curcumin complex in aqueous solution of CPC respectively. We get bands from 3200 to 3350  $\text{cm}^{-1}$  for O–H stretching due to its tendency to absorb some moisture from the environment. The characteristic bands has been observed at 1625 and 2347  $\text{cm}^{-1}$  correspond to C=C stretching for aromatic ring and C=N stretching respectively.



**Figure-3.40 ATR-IR spectra of (i) CPC in aqueous solution, (ii) aqueous solution of CPC in the presence of curcumin, and (iii) aqueous solution of CPC in the presence of Cu(II)-curcumin complex**

### 3.10.1 ATR-IR spectra of CPB in aqueous solution, in the presence of PAN, and Cu(II)- PAN complex

Figure-3.41 (i), (ii), and (iii) represent the ATR-IR spectra for CPB in pure water, PAN in aqueous solution of CPB and Cu(II)-PAN complex in aqueous solution of CPB respectively. The bands have been appeared at 1625 and 2347  $\text{cm}^{-1}$  correspond to C=C stretching for aromatic ring and C=N stretching respectively. We get bands from 3200 to 3350  $\text{cm}^{-1}$  for O-H stretching due to its tendency to absorb some moisture from the system. The characteristic bands have been observed at 2820 and 2923  $\text{cm}^{-1}$  which are C-H stretching for the aliphatic chain (Figure-3.41(i)).

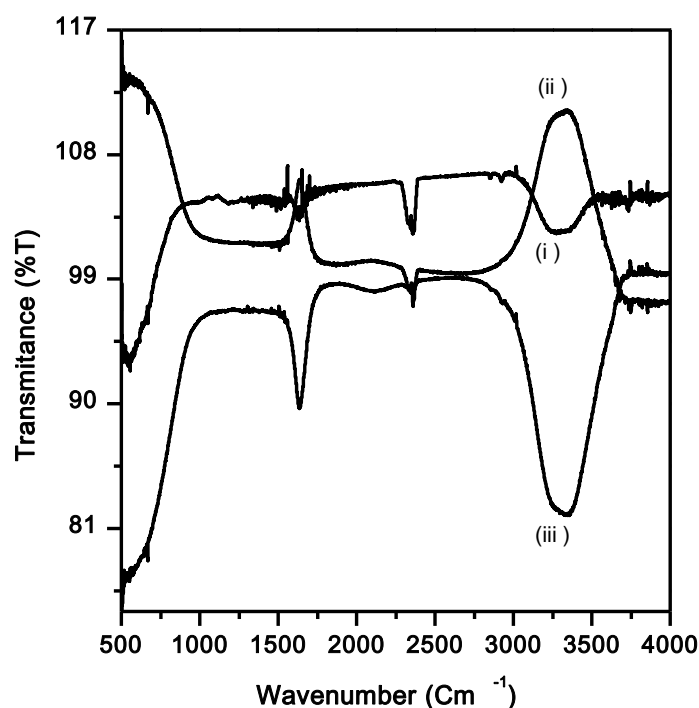


Figure-3.41 ATR-IR spectra of (i) CPB in aqueous solution, (ii) aqueous solution of CPB in the presence of PAN and (iii) aqueous solution of CPB in the presence of Cu(II)-PAN complex

### 3.11 Conclusions

In the present study, the effect of different potassium salts on the krafft temperature ( $T_K$ ), the critical micelle concentration (CMC), adsorption and bulk micellar behavior of CPC and CPB in aqueous solution have been shown. The solubilization of PAN in aqueous solution of CPB and in the presence of  $5 \times 10^{-3}$  M  $KNO_3$  as well as the solubilization of curcumin in aqueous solution of CPC and in the presence of  $1.66 \times 10^{-3}$  M  $K_2SO_4$  has also been observed. Along with this, the locations of solubilized ligand and complex formed with these ligands have been investigated with proton NMR spectroscopy. The results show the following observation;

1. The  $T_K$  of these surfactants can be modulated to lower or higher value depending on the nature of the electrolytes.
2. The  $T_K$  of both the surfactants increase in the presence of stronger chaotropic anions  $SCN^-$  and  $I^-$  due to the salting-out behavior and decrease in the presence of stronger kosmotropic ions  $SO_4^{2-}$ ,  $CO_3^{2-}$ ,  $HPO_4^{2-}$ , and  $F^-$  due to the salting-in effect.
3. The  $T_K$  of CPB decrease in the presence of moderate chaotropic ions  $NO_3^-$  and  $Cl^-$  and also found to be lower than the  $T_K$  of CPB in pure water in the presence of  $2.5 \times 10^{-3}$  M and  $5 \times 10^{-3}$  M  $SCN^-$  ion.
4. In the presence of  $Br^-$  and  $Cl^-$  the  $T_K$  of CPB and CPC respectively increase due to the common ion effect.
5. The order of anions in terms of decreasing the  $T_K$  of CPB is  $NO_3^- > SO_4^{2-} > Cl^- > HPO_4^{2-} > CO_3^{2-} > F^- > Br^- > SCN^- > I^-$ . On the other hand, the order of anions in terms of decreasing the  $T_K$  of CPC is  $SO_4^{2-} > NO_3^- > HPO_4^{2-} > CO_3^{2-} > F^- > Cl^- > Br^- > SCN^- > I^-$ .
6. The CMC of both the surfactants decreases with the addition of these electrolytes due to the neutralization of micellar surface charge by the associated counter-ion which is irrespective of the nature of these ions but in the presence of chaotropic ion the CMC decreases more than kosmotropic ion.
7. The propensity of the CMC of CPC follows the order:  $SCN^- > I^- > SO_4^{2-} > NO_3^- > CO_3^{2-} > Br^- > HPO_4^{2-} > Cl^- > F^- > \text{pure CPC at } 45^\circ\text{C}$ . On the other hand, the tendency of lowering the CMC of CPB follows the trend:  $SCN^- > I^- > SO_4^{2-} > NO_3^- > Br^- > CO_3^{2-} > HPO_4^{2-} > Cl^- > F^- > \text{pure CPB}$ .

8. The surface tension of aqueous solution of CPC and CPB decreases in the presence of these electrolytes. Among these electrolytes  $\text{SCN}^-$  is the most effective in lowering the surface tension of aqueous solution of CPB and in terms of decreasing the surface tension the ions follow the order:  $\text{SCN}^- > \Gamma^- > \text{NO}_3^- > \text{CO}_3^{2-} > \text{Br}^- > \text{HPO}_4^{2-} > \text{F}^- > \text{SO}_4^{2-} > \text{Cl}^- > \text{pure CPB}$ . On the other hand,  $\Gamma^-$  is the most effective in lowering the surface tension of aqueous solution of CPC and in terms of decreasing the surface tension the ions follow the order:  $\Gamma^- > \text{SCN}^- > \text{NO}_3^- > \text{CO}_3^{2-} > \text{Br}^- > \text{SO}_4^{2-} > \text{HPO}_4^{2-} > \text{Cl}^- > \text{F}^- > \text{pure CPC}$ .
9. The surface pressure of aqueous solutions of both the surfactants decreases with increasing temperature.
10. The value of surface excess concentration ( $\Gamma_{\text{max}}$ ) for CPB and CPC in pure water and in the presence of  $5 \times 10^{-3}$  M  $\text{KNO}_3$  and  $1.66 \times 10^{-3}$  M  $\text{K}_2\text{SO}_4$  respectively decreases gradually with increasing temperature.
11. The free energy change for micellization and adsorption ( $\Delta G_{\text{mic}}^\circ, \Delta G_{\text{ad}}^\circ$ ) of CPB and CPC in pure water were found to be negative. The negative values of free energy change indicate that both the processes are spontaneous.
12. The value of  $\Delta G_{\text{ad}}^\circ$  was found to be more negative than the respective value of  $\Delta G_{\text{mic}}^\circ$  which indicates that adsorption is more spontaneous than micellization.
13. With the increase of temperature, the values of  $\Delta H_{\text{mic}}^\circ, \Delta H_{\text{ad}}^\circ$  and the values of  $\Delta S_{\text{mic}}^\circ, \Delta S_{\text{ad}}^\circ$  decrease.
14. The solubilization of water insoluble organic compounds in micellar system increase in the presence of added electrolyte which is favourable for their use in different purposes.
15. The molar solubilization ratio (MSR) of PAN and curcumin in aqueous solution of CPB and CPC respectively increase in the presence of  $5 \times 10^{-3}$  M  $\text{KNO}_3$  and  $1.66 \times 10^{-3}$  M  $\text{K}_2\text{SO}_4$  respectively. Here, the surfactants have been used as a solubilizing agent which is an alternative of highly volatile and harmful organic solvent.
16. The CMC decreases in the presence of PAN and curcumin which is attributed to the electrostatic attraction between the  $\pi$ -electrons present in the aromatic ring of the dye and the cationic head of the surfactant in the micelle surface.

17. Chemically unchanged PAN and curcumin solubilized in micellar system form stable Cu(II)-PAN, Ni(II)-PAN, Zn(II)-PAN and Cu(II)-curcumin complexes with the formation constant  $4.66 \times 10^5$ ,  $16.47 \times 10^5$ ,  $5.85 \times 10^5$  and  $8.87 \times 10^5$  respectively.
18. The ratio of metal to ligand was found almost 1:1 for Cu(II)-PAN, Ni(II)-PAN, Zn(II)-PAN in aqueous solution of CPB and 2:1 for Cu(II)-curcumin complex in aqueous solution of CPC.
19. It is easy to estimate the Cu(II) from 0.05 to 1.27 ppm, Ni(II) from 0.08 to 0.75 ppm, and Zn(II) from 0.08 to 0.65 ppm in aqueous solution of surfactant through complex formation with the ligand PAN.
20. The estimation of Cu(II) ion from 8.4 to 16.8  $\mu\text{M}$   $\text{CuSO}_4$  or (0.53 to 1.07 ppm Cu(II) ion) in aqueous solution of CPC through complex formation with the ligand curcumin.
21. Here, the surfactants have been used as a solubilizing agent which is an alternative of highly volatile and harmful organic solvent. So, the estimation of metal ion in aqueous solution of surfactant will be cost effective, simple, easy, and environmentally friendly too.
22. Nuclear magnetic resonance spectroscopy yields information about micellization and the localization of the solubilized water insoluble dyes, ligands, complexes in aqueous solution of surfactant.

It is important to note here that except for  $\text{I}^-$ ,  $\text{SCN}^-$ ,  $\text{Br}^-$  and common ion, the rest of the anions used in this study are effective in lowering the  $T_K$  and all the anions are effective in lowering the CMC of both the surfactants. Many applications of the surfactants lie on their capacity to solubilize water insoluble organics which will increase in the presence of electrolytes through decreasing the  $T_K$ , and CMC. The effectiveness of the surfactants is usually governed by their maximum lowering of surface tension and ease of micelle formation in the bulk. So, it can be expected that the depression of the  $T_K$  and lowering of the CMC in the presence of the added electrolytes will favor wider industrial applications of CPC and CPB.



## **Scope of further work**

1. Research work may be carried out to observe the effect of different electrolytes and organic additives on the Krafft temperature, adsorption, micellization and relevant thermodynamic properties of these surfactants.
2. There is a scope to understand the solubilization and the location of different ligands in the micelle.
3. Research work may be carried out with the interaction between the ligand and surfactant.
4. There is a scope to understand the interaction between the ligands and metal ions in micellar system and the estimation of metal ion in aqueous solution without using any harmful and volatile organic solvent.

## References

- [1] Mayers, D., *Surfactant Science and Technology*, 3rd edition. John Wiley & Sons, Inc. Publication, 2006.
- [2] Roy, J.C., Islam, M.N., Aktaruzzaman, G., "The effect of NaCl on the Krafft temperature and related behavior of cetyltrimethylammonium bromide in aqueous solution," " *J. Surfact. Deterg.*, vol. 17, pp. 231–242, 2014.
- [3] Vautier-Giongo, C., Bales, B. L., "Estimate of the Ionization Degree of Ionic Micelles Based on Krafft Temperature Measurements," *J. Phys. Chem. B.*, vol. 107, no. 23, p. 5398–5403, 2003.
- [4] Myers, D., *Surfactant Science and Technology*, 3rd Edition. Wiley Interscience, N. J., 2004.
- [5] Islam, M. N.; Kato, T., "Temperature Dependence of the Surface Phase Behavior and Micelle Formation of Some Nonionic Surfactant," *J. Phys. Chem. B.*, vol. 107, pp. 965–971, 2003.
- [6] Chu, Z., Feng, Y. J., "Empirical Correlations between Krafft Temperature and Tail Length for Amidosulfobetaine Surfactants in the Presence of Inorganic Salt," *Langmuir*, vol. 28, pp. 1175–1181, 2011.
- [7] Banipal, T. S., Kaur, H., Banipal, P. K., Sood, A.K., "Effect of Head Groups, Temperature, and Polymer Concentration on Surfactant-Polymer Interactions," " *J. Surfact. Deterg.*, vol. 17, pp. 1181–1191, 2014.
- [8] Ballerat-Busserolles, K., Roux-Desgranges, G., Roux, A.H., "Thermodynamics in Micellar Solutions: Confirmation of Complex Foemation between Sodium Dodecyl Sulfate and polyethelene Glycol," *Langmuir*, vol. 13, no. 7, pp. 1946–1951, 1997.
- [9] Islam MN, Sarker KC, Akhtaruzzaman G, "Effect of electrolytes on the Krafft temperature of cetylpyridinium chloride in aqueous solution," *J Surfact Deterg*, vol. 17, pp. 525–530, 2014.
- [10] Rosen, M.J., *Surfactants and Interfacial Phenomena*, 3rd ed. John Wiley & Sons, Hoboken, 2004.
- [11] Rosen, M. J., *Surfactants and Interfacial Phenomena*, 3rd Edition. Wiley Interscience, N.Y., 2006.

- [12] Shinoda, K., Yamaguchi, N., Carlsson, A., "Physical meaning of the Krafft point: observation of melting phenomenon of hydrated solid surfactant at the Krafft point," " *J Phys Chem*, vol. 93, pp. 7216–7218, 1989.
- [13] Paria, S., Yuet, P. K., "Solubilization of Naphthalene by Pure and Mixed Surfactants," *Ind. Eng. Chem. Res.*, vol. 45, pp. 3552–3558, 2006.
- [14] Crook, E.H.; Trebbi, G.F.; Fordice, D.B., "Thermodynamic Properties of Solutions of Homogenous p,t-Octylphenoxyethoxyethanols (OPE1-10)," *J Phys. Chem.*, vol. 68, no. 12, pp. 3592–3599, 1964.
- [15] Varade, D., Joshi, T., Aswal, V. K., Goyal, P. S., Hassan, P. A., Bahadur, P., "Effect of salt on the micelles of cetyl pyridinium chloride," *Colloid Surf A.*, vol. 259, pp. 95–101, 2005.
- [16] Choucair, A., Eisenberg, A., "Interfacial solubilization of model amphiphilic molecules in block copolymer micelles," *J. Am. Chem. Soc.*, vol. 125, pp. 11993–12000, 2003.
- [17] Ali Reza Tehrani-Bagha 1,2 and Krister Holmberg 1, "Solubilization of Hydrophobic Dyes in Surfactant Solutions," *Materials*.
- [18] Masakatsu Hato, and Kozo Shinoda, "Krafft points of calcium and sodium dodecylpoly(oxyethylene) sulfates and their mixtures," *J. Phys. Chem.*, vol. 77, no. 3, pp. 378–381, 1973.
- [19] Islam, M. N., Sarker, K. C., Sharker, K. K., "Influence of Some Hofmeister Anions on the Krafft Temperature and Micelle Formation of Cetylpyridinium Bromide in Aqueous Solution," *J. Surfact. Deterg.*, vol. 18, pp. 9–16, 2014.
- [20] A. Patist, S.G. Oh, R. Leung, D.O. Shah, "Kinetics of micellization: its significance to technological processes," *Colloids and Surfaces A: Physicochem. Eng. Aspects*, vol. 176, pp. 3–16, 2001.
- [21] Lee, J. D., *Concise Inorganic chemistry*, 4th edn. ELBS, Singapore, 1991.
- [22] Jan Heyda, Mikael Lund, Milan Oncak, Petr Salvicek and Pavel Jungwirth, "Reversal of Hofmeister Ordering for pairing of NH<sub>4</sub><sup>+</sup> vs Alkylated Ammonium cations with Halide Anions in water," " *J. Phys. Chem. B.*, vol. 114, no. 33, pp. 10843–10852, Aug. 2010.
- [23] Yanjie Zhang and Paul S Cremer, "The inverse and direct Hofmeister series for lysozyme," vol. 106, no. 36, pp. 15249–15253, Sep. 2009.
- [24] Murcus, Y., "Effect of Ions on the Structure of Water: Structure Making and Breaking," *Chem. Rev.*, vol. 109, pp. 1346–1370, 2009.

- [25] Shchukin, E. D., "Colloid Chemistry: Textbook for Universities and High School," *Vysshaya, Shkola, Moscow*, 2004.
- [26] E. Ruckenstein, and R. Nagarajan, "Critical micelle concentration. Transition point for micellar size distribution," *J. Phys. Chem.*, vol. 79, no. 24, pp. 2622–2626, 1975.
- [27] Krassimir D. Danov a, , Peter A. Kralchevsky a, and ☐, Kavssery P. Ananthapadmanabhan, "Micelle–monomer equilibria in solutions of ionic surfactants and in ionic–nonionic mixtures: A generalized phase separation model," vol. 206, pp. 17–45, 2014.
- [28] Holmberg, K.; Jonsson, B.; Kronberg, B.; Lindman, B., *Surfactant and Polymers in Aqueous Solution*, 2nd ed. Wiley, Chichester, 2003.
- [29] Sujata Shinha and P Bhahadur, "Effect of organic counter-ions on the surface activity, micellar formation and dye solubilization behaviour of cationic surfactants," vol. 41A, pp. 914–920, 2002.
- [30] Francis MF, Piredda M, Winnik FM, "Solubilization of poorly water soluble drugs in micelles of hydrophobically modified hydroxypropylcellulose copolymers," " *J Controlled Release*, vol. 93, pp. 59–68, 2003.
- [31] Lee J, Moroi Y, "Solubilization of n-alkylbenzenes in aggregates of sodium dodecyl sulfate and a cationic polymer of high charge density (II).," *Langmuir*, vol. 20, pp. 6116–6119, 2004.
- [32] Tadros, T.F., *Applied Surfactants: Principles and Applications*. Wiley, New York, 2005.
- [33] Hiemenz, P.C.; Rajagopalan, R., *Biosurfactants and Biotechnology*. Marcel Dekker, 1997.
- [34] Fanun, M., *Colloids in Drug Delivery*. CRC Press, 2010.
- [35] "The surface chemistry of polyurethane foam formation: I. Equilibrium surface tensions of polysiloxane-polyether block copolymer solutions," *Journal of Colloid and Interface Science*, vol. 24, no. 2, pp. 135–140, 1967.
- [36] Jalali-Heravi, M., Konouz, E., "Use of Quatitative Structure-Property Relationships in Predicting the Krafft point of Anionic Surfactants," *Internet Electron. J. Mol. Des.*, vol. 1, pp. 410–417, 2002.
- [37] Schramm, L.L., *Dictionary of Colloid and Interface Science*. John Wiley & Sons, New York, 2001.
- [38] Umbach, W., "The importance of colloid chemistry in industrial practice," *progr. colloid polym. Sci.*, vol. 111, pp. 9–16, 1998.

- [39] R. Schueller and P. Romanowski, "The science of reactive hair-care products: a review of changing natural hair appearances," *Cosmetics and toiletries*, vol. 113, no. 5, pp. 39–44, 1998.
- [40] Romanowski, P. and Schueller, R., "Micro-organisms and personal-care products. *Cosmetics and Toiletries*," vol. 110, no. 11, pp. 71–78, 1995.
- [41] Knoche, M., "Effect of droplet size and carrier volume on performance of foliage-applied herbicides. *Crop Protection*," vol. 13, pp. 163–178, 1994.
- [42] Islam, M. N., Sharker, K. K., Sarker, K. C., "Salt-induced modulation of the Krafft temperature and critical micelle concentration of benzyl dimethyl hexadecyl ammonium Chloride," *J Surfact Deterg.*, vol. 18, pp. 651–659, 2015.
- [43] McCabe AJ, Wilcox DT, Holm BA, Glick PL., "Surfactant - a review for pediatric surgeons," *J Pediatr Surg*, vol. 35, pp. 1687–1700, 2000.
- [44] Hailu Demissie\*, Ramesh Duraisamy, "Effects of electrolytes on the surface and micellar characteristics of Sodium dodecyl sulphate surfactant solution," *Journal of Scientific and Innovative Research*, vol. 5, pp. 208–214, Dec. 2016.
- [45] Xue-Gong Lei, "Effects of additives on the aggregation of surfactants: Binding domination," vol. 10, no. 3, pp. 237–244, May 1992.
- [46] *Interaction Between Ionic Liquids and Gemini Surfactant: A Detailed Investigation into the Role of Ionic Liquids in Modifying Properties of Aqueous Gemini Surfactant - More - 2016 - Journal of Surfactants and Detergents - Wiley Online Library.*  
<https://aocs.onlinelibrary.wiley.com/doi/abs/10.1007/s11743-015-1747-x>, 2019.
- [47] Ali Reza Tehrani-Bagha, RG Singh, Krister Holmberg, "Solubilization of two organic dyes by anionic, cationic and nonionic surfactants," *Colloids and Surfaces A: Physicochemical and Engineering Aspects*, vol. 417, no. 1, pp. 133–139, 2013.
- [48] Farías T, de Ménorval LC, Zajac J, Rivera A., "Solubilization of drugs by cationic surfactants micelles: Conductivity and <sup>1</sup>H NMR experiments," *Colloids Surface A.*, vol. 345, pp. 51–57, 2009.
- [49] Coo, L. dIc., Cardwell, T. J., Cattrall, R.W., Kolev, S. D., "Study on the Formation Constant of the 1-(2-Pyridylazo)-2-Naphthol-Copper(ii) Complex in Acidic Aqueous solutions," *Comptes Rendus de l'Academie Bulgare des Sciences*, vol. 54, pp. 53–56, 2001.

- [50] Gray D. Christian, *Spectrometry in "Analytical Chemistry"*, 4th edn. John Wiley and Sons, New York, 1986.
- [51] J. Workman Jr., *Interpretive spectroscopy for near-infrared, The Hand book of Organic Compounds*. Academic Press: California, 2001.
- [52] Heise, H. M.; Kupper, L.; Butvina, L. N., "Attenuated total reflection mid-infrared spectroscopy for clinical chemistry applications using silver halide fibers," *Sensors and Actuators B: Chemical*, vol. 51, no. 1–3, pp. 84–91, 1998.
- [53] Smith, B.C., *Fundamentals of Fourier Transform Infrared Spectroscopy*. CRC Press: London, 1996.
- [54] Soderman O, Stilbs P, Price WS., "NMR studies of surfactants," *Concepts Magnetic Resonance*, vol. 23A, pp. 121–135, 2004.
- [55] Persson BO, Drakenberg T, Lindman B., "Amphiphile aggregation number and conformation from carb-13 nuclear magnetic resonance chemical shifts," *J Phys. Chem.*, vol. 80, p. 2124-2125, 1976.
- [56] Furo I., "NMR spectroscopy of micelles and related systems," *J. Mol. Liq.*, vol. 117, p. 117-137, 2005.
- [57] Budavari S., "The Merk Index – An Encyclopedia of Chemicals, Drugs and Biologicals," *ed., merk and Co., Inc., New Jersey*, 1989.
- [58] Malik, N. A., Ali, A., "Krafft temperature and thermodynamic study of interaction of glycine, diglycine, and triglycine with hexadecylpyridinium chloride and hexadecylpyridinium bromide: A conductometric approach," *Journal of Molecular Liquids*, vol. 213, pp. 213–220, 2016.
- [59] Mehta, S. K., Bhasin, K. K., Chauhan, R., Dham, S., "Effect of temperature on critical micelle concentration and thermodynamic behavior of dodecyldimethylammonium bromide and dodecyltrimethylammonium chloride in aqueous media," *A Colloids Surf. A.*, vol. 255, pp. 153–157, 2005.
- [60] Bakshi, M. S., Sood, R., "Cationic surfactant-poly (amido amine) dendrimer interactions studied by Krafft temperature measurements," *Colloids and Surfaces A.*, vol. 233, p. 203–210, 2004.
- [61] Tsujii, K., Okahashi, K., Takeuchi, T., "Addition-compound formation between anionic and zwitter-ionic surfactant in water," *J. Phys. Chem.*, vol. 86, p. 1437, 1982.

- [62] Carolina V-G, and Bales BL., "Estimate of the Ionization Degree of Ionic Micelles Based on Krafft Temperature Measurements," *J. Phys. Chem. B.*, vol. 107, pp. 5398–5403, 2003.
- [63] Moulik SP, Haque ME, Jana PK, Das AR, "Micellar properties of cationic surfactants in pure and mixed states," *J Phys Chem.*, vol. 100, pp. 701–708, 1996.
- [64] Nishikido N, Matsuura R., "The effect of added inorganic salts on the micelle formation of micelle formation in aqueous solution," *Bull Chem Soc.*, vol. 50, pp. 1690–1694, 1977.
- [65] Giulio Tesei , Vidar Aspelin , and Mikael Lund, "Specific Cation Effects on SCN<sup>-</sup> in Bulk Solution and at the Air–Water Interface," *J. Phys. Chem. B.*, vol. 122, no. 19, pp. 5094–5105, 2018.
- [66] Pegram, L. M., Record, M. T., "Hofmeister Salt Effects on Surface Tension Arise from Partitioning of Anions and Cations between Bulk Water and the Air-Water Interface," *J. Phys. Chem.*, vol. 111, pp. 5411–5417, 2007.
- [67] Collins, K. D., Neilson G. W., Enderby J. E., "Ions in water: Characterizing the forces that control chemical processes and biological structure," *Biophys. Chem.*, vol. 128, pp. 95–104, 2007.
- [68] Collins, K. D., "Why continuum electrostatics theories cannot explain biological structure, polyelectrolytes or ionic strength effects in ion-protein interactions," *Biophys. Chem.*, vol. 167, pp. 43–59, 2012.
- [69] Mason PE, Neilson GW, Dempsey CE, Barnes AC, Cruickshank and JM, "The hydration structure of guanidinium and thiocyanate ions: implications for protein stability in aqueous solution," *Proc Natl Acad Sci.*, vol. 100, pp. 4557–4561, 2003.
- [70] Dos Santos, A. P., Diehl, A., Levin, Y., "Surface Tensions, Surface Potentials, and the Hofmeister Series of Electrolyte Solutions," *Langmuir*, vol. 26, no. 13, pp. 10778–10783, 2010.
- [71] ZShang, Y., Furyk, S., Bergbreiter, D. E., Cremer, P. S., "Specific Ion Effects on the Water Solubility of Macromolecules: PNIPAM and the Hofmeister Series," *J. Am. Chem. Soc.*, vol. 127, no. 41, pp. 14505–14510, 2005.
- [72] Endom, L., Hertz, H. G., Thul, B., Zeidler, M. D., "A microdynamic model of electrolyte solutions as derived from nuclear relaxation and self-diffusion data," *Dtsch Bunsenges Phys. Chem.*, vol. 71, p. 1008–1031, 1967.

- [73] Nakayama, H., Shinoda, K., "The effect of added salts on the solubilities and Krafft points of sodium dodecyl sulfate and potassium perfluoro-octanoate," *Bull Chem. Soc. Jpn.*, vol. 40, pp. 1797–1799, 1967.
- [74] Chanchal Das and Bijan Das, "Thermodynamic and Interfacial Adsorption Studies on the Micellar Solutions of Alkyltrimethylammonium Bromides in Ethylene Glycol (1) + Water (2) Mixed Solvent Media," *J. Chem. Eng. Data*, vol. 54, no. 2, pp. 559–565, 2009.
- [75] C. Carnero Ruiz, L. Díaz-López, J. Aguiar, "Self-assembly of tetradecyltrimethylammonium bromide in glycerol aqueous mixtures: A thermodynamic and structural study," *Journal of Colloid and Interface Science*, vol. 305, no. 2, pp. 293–300, 2007.
- [76] Hunter, R.J., *Foundations of Colloid Science*, vol. 01. Oxford University Press, New York, 1989.
- [77] Chen L., Shi-yowl, Chiung-chang H., Enming C., "Temperature dependence of critical micelle concentration of polyoxyethylenated non-ionic surfactants," *Colloids Surf. A Physicochem Eng. Aspects*, vol. 135, pp. 175–181, 1998.
- [78] Mata, J., Varade, D., Bahadur, P., "Aggregation behavior of quarternary salt based cationic surfactants," *Thermochim Acta.*, vol. 428, pp. 147–155, 2005.
- [79] Islam, M. M., Rahman, M. R., Islam, M. N., "Micellization Behavior and Thermodynamic Properties of N-Alkyl Trimethylammonium Bromide Surfactants in aqueous media at different temperatures," *International Journal of Scientific & Engineering Research.*, vol. 6, p. 1508, 2015.
- [80] Mukerjee, P., Mysels, K., Kapauan, J., "Counterion specificity in the formation of ionic micelles-size, hydration, and hydrophobic bonding effects," *J. Phys. Chem.*, vol. 71, pp. 4166–4175, 1967.
- [81] Michele, A. D., Brinchi, L., Profio, P. D., Germani, R., Sawelli, G., Onori, G., "Effect of head group size, temperature and counterion specificity on cationic micelles," *J. Colloid Interface Sci.*, vol. 358, pp. 160–166, 2011.
- [82] Bojan, S., Marija, B. R., "Temperature and salt-induced micellization of dodecyltrimethylammonium chloride in aqueous solution: a thermodynamic study," *J. Colloid Interface Sci.*, vol. 338, pp. 216–221, 2009.
- [83] Abezgauz, L., Kuperkar, K., Hassan, P. A., Ramon, O., Bahadur, P., Danino, D., "Effect of Hofmeister anions on micellization and micellar growth of the surfactant cetylpyridinium chloride," *J. Colloid Interface Sci.*, vol. 342, pp. 83–92, 2010.



- [84] Srinivasan, V., Blankschtein, D., "Effect of Counterion Binding on Micellar Solution Behavior: 1. Molecular-Thermodynamic Theory of Micellization of Ionic Surfactants," *Langmuir*, vol. 19, pp. 9932–9945, 2003.
- [85] Srinivasan, V., Blankschtein, D., "Effect of Counterion Binding on Micellar Solution Behavior: 2. Prediction of Micellar Solution Properties of Ionic Surfactant-Electrolyte Systems," *Langmuir*, vol. 19, pp. 9946–9961, 2003.
- [86] M. D. Zeidler, *In Water: A Comprehensive Treatise*, F. Franks, ed., 2 vols. Plenum Press, New York, 1973.
- [87] Narten, A.H. ; and Levy, H.A., *Water—A Comprehensive Treatise*, Franks, ed., vol. 1. Plenum Press, New York, 1973.
- [88] Clifford, J., and Pethica, B.A., "Properties of micellar solutions. Part 3.—Spin lattice relaxation times of water protons in solutions of sodium alkyl sulphates," *Trans. Faraday Soc.*, vol. 61, p. 182, 1965.
- [89] "An <sup>1</sup>H NMR investigation into the loci of solubilization of 4-nitrotoluene, 2,6-dinitrotoluene, and 2,4,6-trinitrotoluene in nonionic surfactant micelles," *Colloids and Surfaces A Physicochemical and Engineering Aspects*, vol. 375, pp. 12–22, Feb. 2011.
- [90] Xi-Lian Wei, Bao-Lin Yin, Jie Liu, and De-Zhi Sun, "H NMR Study on Solubilization of Aromatic Solutes in Gemini Cationic Surfactant Micelles," *Journal of Dispersion Science and Technology*, vol. 28, pp. 291–295, 2007.
- [91] Okano LT, El Seound OA, Healstead TK., "A proton NMR study on aggregation of cationic surfactants in water, effects of the structure of the head group," *Colloid Polym. Sci.*, vol. 275, p. 138-145, 1997.
- [92] Lijuan Han Zhongbin Ye Hong Chen Pingya Luo, "The Interfacial Tension Between Cationic Gemini Surfactant Solution and Crude Oil," *J Surfact Deterg.*, vol. 12, no. 3, pp. 185–190, 2009.
- [93] Williams, F., Woodberry, N. T., Dixon, J. K., "Purification and surface tension properties of alkyl sodium sulfosuccinates," *J Colloid Sci.*, vol. 12, pp. 452–459, 1957.
- [94] Lund M, Vacha R, Jungwirth P., "Specific ion binding to macromolecules: effects of hydrophobicity and ion pairing," *Langmuir*, vol. 24, pp. 3387–3391, 2008.
- [95] Jarvis NL, Schelman MA, "Surface potentials of aqueous electrolyte solutions.," *J Phys Chem.*, vol. 72, pp. 74–78, 1968.

- [96] Md. Nazrul Islam, and Teiji Kato, "Thermodynamic Study on Surface Adsorption and Micelle Formation of Poly(ethylene glycol) Mono-n-tetradecyl Ethers," *Langmuir*, vol. 19, pp. 7201–7205, 2003.
- [97] Lu, J. R., Li, Z. X., Thomas, R. K., Staples, E. J., Thompson, L., Tucker, I., Penfold, J., "Neutron Reflection from a Layer of Monododecyl Octaethylene Glycol Adsorbed at the Air-Liquid Interface: The Structure of the Layer and the Effects of Temperature," *J. Phys. Chem.*, vol. 98, pp. 6559–6567, 1994.
- [98] Ritacco, H., Langevin, D., Diamant, H., Andelman, D., "Dynamic surface tension of aqueous solutions of ionic surfactants: role of electrostatics," *Langmuir*, vol. 27, pp. 1009–1014, 2011.
- [99] Zheng O, Zhao JX, "Solubilization of pyrene in aqueous micellar solutions of gemini surfactants C12-s-C12.2Br," *Journal of Colloid and Interface Science*, vol. 300, no. 2, pp. 749–754, May 2006.
- [100] Joon-Hyung Kim, Michael M. Domach, and Robert D. Tilton, "Effect of Electrolytes on the Pyrene Solubilization Capacity of Dodecyl Sulfate Micelles," *Langmuir*, vol. 16, no. 26, pp. 10037–10043, 2000.
- [101] Chatteraj DK, Birdi KS, *Adsorption and the Gibbs surface excess*. Plenum Press, New York, 1984.
- [102] F. Franks, M. D. Zeidler, *In Water, a Comprehensive Treatise*, vol. 2. Plenum Press, New York, 1973.
- [103] Lei Zhang, P. Somasundaran\*, and C. Maltesh†, "Electrolyte Effects on the Surface Tension and Micellization of n-Dodecyl  $\beta$ -d-Maltoside Solutions," *Langmuir*, vol. 12, no. 10, pp. 2371–2373, 1996.
- [104] Allison Callaghan, Ronald Doyle, Edward Alexander, and R. Palepu, "Thermodynamic properties of micellization and adsorption and electrochemical studies of hexadecylpyridinium bromide in binary mixtures of 1,2-ethanediol with water," *Langmuir*, vol. 9, no. 12, pp. 3422–3426, 1993.
- [105] A. M. Mankowich, "The energetics of surfactant adsorption at the air-water interface," *Journal of the American Oil Chemists Society*, vol. 43, no. 11, pp. 615–619, Nov. 1966.
- [106] K Kabir-ud-Din, AP Koya, ZA Khan, "Conductometric studies of micellization of Gemini surfactant pentamethylene-1,5-bis (tetradecyl dimethyl ammonium bromide) in water

- and water-organic solvent mixed media," *J Colloid Interface Sci.*, vol. 342, no. 2, pp. 340–347, 2010.
- [107] Björn Lindman, Bernard Brun, "Translational motion in aqueous sodium n-octanoate solutions," *Journal of Colloid and Interface Science*, vol. 42, no. 2, pp. 388–399, Feb. 1973.
- [108] Rajan Patel, Abbul Bashar Khan, Neeraj Dohare, Mohd Maroof Ali, Hament Kumar Rajor, "Mixed micellization and interfacial properties of ionic liquid-type imidazolium gemini surfactant with amphiphilic drug amitriptyline hydrochloride and its thermodynamics," *Springer Berlin Heidelberg*, vol. 18, no. 5, pp. 719–728, Sep. 2015.
- [109] Lumry R, Rajender S., "Enthalpy-entropy compensation phenomena in water solutions of proteins and small molecules: a ubiquitous property of water," *Biopolymers*, vol. 9, no. 10, pp. 1125–227, 1970.
- [110] santanu Paria and Pak K. Yuet, "Effects of Chain Length and Electrolyte on the Adsorption of n-Alkylpyridinium Bromide Surfactants at Sand–Water Interfaces," *Ind. Eng. Chem. Res.*, vol. 45, pp. 712–718, 2006.
- [111] Sivaram Harendra and Cumaraswamy Vipulanandan, "Effects of Surfactants on Solubilization of Perchloroethylene (PCE) and Trichloroethylene (TCE)," *Ind. Eng. Chem. Res.*, vol. 50, no. 9, pp. 5831–5837, 2011.
- [112] Hans Schott, "Solubilization of a water-insoluble dye. II," *J. Phys. Chem.*, vol. 71, no. 11, pp. 3611–3617, 1967.
- [113] Shimazu S., Pires PAR, El Seound OA., "1H and 13C NMR study on the aggregation of (2- acylaminoethyl) trimethyl ammonium chloride surfactant in D2O," *Langmuir*, vol. 19, p. 9645-9652, 2003.
- [114] Sarker K.C., Rafique Ullah Md., "Determination of Trace Amount of Cu(II) Using UV-Vis. Spectrophotometric Method," *chemijournal*, vol. 1, no. 1, Sep. 2019.
- [115] Burton, F., Pease, Max., Williams, B., "Spectrophotometric investigation of the analytical reagent 1-(2-pyridylazo)-2-naphthal and its copper chelate," *Analytical chemistry*, vol. 31, no. 6, pp. 1044–1047.
- [116] Ahmed E. Fazary, Ahmed M. Ramadan, "Stability constants and complex formation equilibria between iron, calcium, and zinc metal ions with vitamin B9 and glycine," pp. 139–148, Sep. 2014.

- [117] A. E. Martell and R. D. Hancock, Eds. Boston, MA., "Stability Constants and Their Measurement," in *Metal Complexes in Aqueous Solutions*," Springer US, pp. 217–244, 1996.
- [118] Harvey, E., Delmer, J. R., Manning, L., *Spectrophotometric methods of Establishing Empirical Formulas of Colored Complexes in Solution*, vol. 72. Department of the University of Lousvilies.
- [119] Job, P., "Formation and Stability of Inorganic Complexes in Solution," *Ann. Chim.*, vol. 9, pp. 113–203, 1928.
- [120] Yoe, J. A., Jones, A. L., "Colorimetric Determination of Iron with Disodium-1,2-dihydroxybenzene-3,5-disulphonate," *Ind. Eng. Chem., Anal, Ed.*, vol. 16, pp. 111–115, 1944.
- [121] E. B. sandell, *Colourimetric determination of traces of metals*, 3rd. Wiley Inter science, 1962.

# Appendix

## Data of CPC and CPB

Table-4.1 Krafft temperature data for pure CPC and CPB in aqueous solution

CPC (0.01M)				CPB (0.01M)			
Temp. (°C)	Specific conductance (μS/cm)	Temp. (°C)	Specific conductance (μS/cm)	Temp. (°C)	Specific conductance (μS/cm)	Temp. (°C)	Specific conductance (μS/cm)
2	71.1	20	385	5	29.5	23	59.8
2.5	71.3	20.5	386	5.5	29.8	23.5	61.3
3	72.5	21	387	6	30	24	63.1
3.5	73.3	21.5	388	6.5	30.6	24.5	65.4
4	74.2	22	389	7	30.8	25	69
4.5	75.2	22.5	390	7.5	31.6	25.5	73.1
5	76	23	391	8	32.1	26	77.8
5.5	77.2	23.5	392	8.5	33	26.5	91.7
6	78.2	24	393	9	33.5	27	117.1
6.5	79.5	24.5	394	9.5	33.9	27.5	142
7	80.9	25	395	10	34.3	28	158.4
7.5	82.3	25.5	396	10.5	35.4	28.5	183.7
8	83.3	26	397	11	36	29	206
8.5	84.5			11.5	36.7	29.5	234
9	86.1			12	37.3	30	266
9.5	87.7			12.5	38.1	30.5	285
10	89.9			13	38.7	31	287
10.5	91.1			13.5	39.6	31.5	291
11	92.7			14	40.2	32	294
11.5	95.7			14.5	41.1	32.5	296
12	98.6			15	42.2	33	298
12.5	103			15.5	42.9	33.5	300
13	110.6			16	43.9	34	302
13.5	123.2			16.5	45	34.5	304
14	137.6			17	45.7	35	306
14.5	161.4			17.5	46.7	35.5	308
15	183.2			18	47.5	36	310
15.5	212			18.5	48.7	36.5	312
16	236			19	50.1	37	314
16.5	272			19.5	51.1	37.5	315
17	300			20	52.5	38	316
17.5	333			20.5	53.4	38.5	318
18	359			21	54.6	39	319
18.5	375			21.5	55.8	39.5	320
19	381			22	57.4	40	321
19.5	383			22.5	58.9		

Table-4.2 Krafft temperature data for aqueous solution of CPB in the presence of KNO<sub>3</sub>

CPB (0.01M)- KNO <sub>3</sub>							
0.0125M KNO <sub>3</sub>		0.01 M KNO <sub>3</sub>		0.005 M KNO <sub>3</sub>		0.0025 M KNO <sub>3</sub>	
Temp. (°C)	Specific conductance (μS/cm)	Temp. (°C)	Specific conductance (μS/cm)	Temp. (°C)	Specific conductance (μS/cm)	Temp. (°C)	Specific conductance (μS/cm)
5	1744	5	1381	5	728	5	386
5.5	1737	5.5	1372	5.5	723	5.5	384
6	1732	6	1364	6	718	6	382
6.5	1726	6.5	1361	6.5	716	6.5	380
7	1718	7	1358	7	714	7	379
7.5	1711	7.5	1354	7.5	712	7.5	378
8	1704	8	1350	8	710	8	377
8.5	1697	8.5	1346	8.5	708	8.5	376
9	1688	9	1340	9	706	9	375
9.5	1684	9.5	1335	9.5	704	9.5	374
10	1680	10	1332	10	702	10	373
10.5	1674	10.5	1330	10.5	700	10.5	372
11	1667	11	1328	11	697	11	372
11.5	1662	11.5	1325	11.5	696	11.5	372
12	1655	12	1321	12	694	12	371
12.5	1650	12.5	1318	12.5	692	12.5	370

13	1644	13	1316	13	689	13	370
13.5	1639	13.5	1313	13.5	687	13.5	369
14	1636	14	1310	14	685	14	368
14.5	1632	14.5	1307	14.5	682	14.5	369
15	1628	15	1304	15	679	15	368
15.5	1627	15.5	1302	15.5	679	15.5	367
16	1626	16	1301	16	679	16	368
16.5	1625	16.5	1300	16.5	679	16.5	368
17	1624	17	1299	17	680	17	368
17.5	1623	17.5	1298	17.5	680	17.5	367
18	1622	18	1297	18	680	18	368
18.5	1621	18.5	1298	18.5	683	18.5	372
19	1625	19	1302	19	688	19	378
19.5	1636	19.5	1313	19.5	715	19.5	386
20	1658	20	1401	20	733	20	390
20.5	1833	20.5	1518	20.5	751	20.5	397
21	1840	21	1525	21	768	21	403
21.5	1843	21.5	1529	21.5	777	21.5	409
22	1842	22	1534	22	785	22	414
22.5	1841	22.5	1540	22.5	794	22.5	419
23	1840	23	1542	23	803	23	423
23.5	1839	23.5	1542	23.5	817	23.5	429
24	1838	24	1542	24	823	24	438
24.5	1837	24.5	1542	24.5	832	24.5	447
25	1836	25	1542	25	849	25	455
25.5	1835	25.5	1542	25.5	863	25.5	465
26	1834	26	1542	26	883	26	482
26.5	1833	26.5	1542	26.5	890	26.5	505
27	1834	27	1542	27	890	27	524
				27.5	891	27.5	538
				28	892	28	552
				28.5	892	28.5	563
				29	893	29	573
				29.5	894	29.5	575
				30	895	30	576
				30.5	896	30.5	576
				31	896	31	577
						31.5	578
						32	579
						32.5	580
						33	581
						33.5	582
						34	583
						34.5	583
						35	584

Table-4.3 Krafft temperature data for aqueous solution of CPB in the presence of  $K_2CO_3$ 

CPB (0.01M)- $K_2CO_3$							
0.004166M $K_2CO_3$		0.00333 M $K_2CO_3$		0.001666 M $K_2CO_3$		0.0008333 M $K_2CO_3$	
Temp. (°C)	Specific conductance ( $\mu S/cm$ )	Temp. (°C)	Specific conductance ( $\mu S/cm$ )	Temp. (°C)	Specific conductance ( $\mu S/cm$ )	Temp. (°C)	Specific conductance ( $\mu S/cm$ )
5	1049	4	843	3.5	466	5	229
5.5	1048	4.5	838	4	464	5.5	229
6	1046	5	835	4.5	462	6	229
6.5	1045	5.5	833	5	461	6.5	228
7	1044	6	830	5.5	460	7	228
7.5	1043	6.5	827	6	459	7.5	228
8	1042	7	825	6.5	458	8	228
8.5	1041	7.5	823	7	457	8.5	228
9	1040	8	821	7.5	456	9	227
9.5	1038	8.5	820	8	455	9.5	227
10	1036	9	819	8.5	454	10	227
10.5	1034	9.5	818	9	453	10.5	227
11	1033	10	816	9.5	452	11	227
11.5	1032	10.5	815	10	451	11.5	227

12	1030	11	815	10.5	450	12	227
12.5	1029	11.5	815	11	449	12.5	227
13	1028	12	815	11.5	448	13	227
13.5	1028	12.5	815	12	448	13.5	227
14	1029	13	815	12.5	447	14	227
14.5	1030	13.5	815	13	447	14.5	227
15	1031	14	815	13.5	447	15	228
15.5	1032	14.5	816	14	447	15.5	228
16	1033	15	817	14.5	447	16	228
16.5	1035	15.5	818	15	447	16.5	229
17	1037	16	819	15.5	448	17	230
17.5	1039	16.5	822	16	448	17.5	231
18	1041	17	823	16.5	449	18	231
18.5	1043	17.5	825	17	449	18.5	232
19	1045	18	826	17.5	449	19	233
19.5	1048	18.5	828	18	450	19.5	234
20	1051	19	830	18.5	451	20	235
20.5	1055	19.5	833	19	453	20.5	236
21	1059	20	838	19.5	456	21	238
21.5	1063	20.5	842	20	458	21.5	240
22	1067	21	847	20.5	460	22	242
22.5	1073	21.5	853	21	462	22.5	244
23	1081	22	859	21.5	464	23	247
23.5	1088	22.5	869	22	467	23.5	250
24	1094	23	876	22.5	471	24	254
24.5	1102	23.5	885	23	476	24.5	258
25	1114	24	893	23.5	480	25	261
25.5	1121	24.5	901	24	487	25.5	266
26	1131	25	908	24.5	491	26	275
26.5	1142	25.5	915	25	497	26.5	285
27	1149	26	924	25.5	506	27	293
27.5	1156	26.5	931	26	516	27.5	302
28	1158	27	938	26.5	525	28	314
28.5	1158	27.5	947	27	537	28.5	329
29	1158	28	955	27.5	548	29	354
29.5	1158	28.5	956	28	562	29.5	381
30	1158	29	956	28.5	578	30	409
30.5	1158	29.5	956	29	591	30.5	421
31	1158	30	956	29.5	603	31	430
31.5	1158	30.5	956	30	606	31.5	435
32	1158	31	956	30.5	608	32	437
32.5	1158	31.5	956	31	609	32.5	437
33	1158	32	956	31.5	610	33	438
33.5	1158	32.5	956	32	610	33.5	439
34	1158	33	956	32.5	611	34	440
34.5	1158	33.5	956	33	612	34.5	441
35	1158	34	956	33.5	613	35	442
35.5	1158	34.5	956	34	614	35.5	443
36	1158	35	956	34.5	615	36	444
36.5	1158	35.5	956	35	616	36.5	445
37	1159	36		35.5	616	37	
37.5		36.5		36	616	37.5	
38		37		36.5	617	38	
38.5		37.5		37	617	38.5	
39		38		37.5	617	39	
39.5		38.5		38	618	39.5	

Table-4.4 Krafft temperature data for aqueous solution of CPB in the presence of  $K_2SO_4$ 

CPB (0.01M)- $K_2SO_4$							
0.004166M $K_2SO_4$		0.00333 M $K_2SO_4$		0.001666 M $K_2SO_4$		0.000833 M $K_2SO_4$	
Temp. (°C)	Specific conductance ( $\mu S/cm$ )	Temp. (°C)	Specific conductance ( $\mu S/cm$ )	Temp. (°C)	Specific conductance ( $\mu S/cm$ )	Temp. (°C)	Specific conductance ( $\mu S/cm$ )
5	1221	4	--	3.5		5	279
5.5	1212	4.5	--	4	--	5.5	277
6	1202	5	998	4.5	--	6	276
6.5	1196	5.5	988	5	533	6.5	275



7	1191	6	981	5.5	531	7	273
7.5	1189	6.5	977	6	528	7.5	272
8	1186	7	973	6.5	526	8	272
8.5	1183	7.5	970	7	524	8.5	272
9	1180	8	966	7.5	523	9	272
9.5	1177	8.5	963	8	522	9.5	271
10	1173	9	961	8.5	521	10	271
10.5	1169	9.5	958	9	520	10.5	271
11	1167	10	956	9.5	519	11	271
11.5	1166	10.5	954	10	518	11.5	271
12	1165	11	953	10.5	517	12	270
12.5	1165	11.5	953	11	516	12.5	270
13	1165	12	952	11.5	515	13	270
13.5	1165	12.5	952	12	514	13.5	270
14	1165	13	951	12.5	513	14	270
14.5	1165	13.5	950	13	512	14.5	270
15	1165	14	949	13.5	512	15	270
15.5	1165	14.5	949	14	512	15.5	270
16	1165	15	949	14.5	513	16	271
16.5	1165	15.5	949	15	513	16.5	271
17	1167	16	949	15.5	514	17	272
17.5	1169	16.5	950	16	515	17.5	272
18	1171	17	951	16.5	516	18	274
18.5	1174	17.5	953	17	517	18.5	275
19	1177	18	954	17.5	518	19	276
19.5	1181	18.5	957	18	520	19.5	277
20	1186	19	961	18.5	522	20	280
20.5	1189	19.5	965	19	525	20.5	283
21	1192	20	969	19.5	527	21	285
21.5	1199	20.5	974	20	530	21.5	287
22	1205	21	978	20.5	532	22	289
22.5	1213	21.5	982	21	535	22.5	292
23	1218	22	986	21.5	539	23	294
23.5	1225	22.5	991	22	543	23.5	298
24	1235	23	998	22.5	547	24	303
24.5	1242	23.5	1004	23	553	24.5	307
25	1249	24	1014	23.5	557	25	313
25.5	1254	24.5	1026	24	564	25.5	320
26	1256	25	1035	24.5	572	26	327
26.5	1258	25.5	1046	25	579	26.5	333
27	1259	26	1053	25.5	588	27	339
27.5	1260	26.5	1060	26	597	27.5	346
28	1259	27	1060	26.5	614	28	355
28.5	1258	27.5	1060	27	629	28.5	366
29	1257	28	1060	27.5	642	29	381
29.5	1256	28.5	1060	28	649	29.5	395
30	1255	29	1060	28.5	649	30	421
30.5	1254	29.5	1060	29	650	30.5	436
31	1253	30	1060	29.5	651	31	445
31.5	1252	30.5	1060	30	652	31.5	448
32	1251	31	1060	30.5	653	32	452
32.5	1250	31.5	1060	31	654	32.5	454
33	1251	32	1060	31.5	655	33	456
				32	656	33.5	457
				32.5	657	34	458
				33	657	34.5	459
				33.5	658	35	460
				34	658		
				34.5	659		
				35	660		

Table-4.5 Krafft temperature data for aqueous solution of CPB in the presence of  $K_2HPO_4$ 

CPB (0.01M)- $K_2HPO_4$							
0.004166M $K_2HPO_4$		0.00333 M $K_2HPO_4$		0.001666 M $K_2HPO_4$		0.000833 M $K_2HPO_4$	
Temp. (°C)	Specific conductance ( $\mu S/cm$ )	Temp. (°C)	Specific conductance ( $\mu S/cm$ )	Temp. (°C)	Specific conductance ( $\mu S/cm$ )	Temp. (°C)	Specific conductance ( $\mu S/cm$ )
5	963	4	--	3.5		5	222
5.5	962	4.5	--	4		5.5	222
6	960	5	810	4.5		6	222
6.5	958	5.5	806	5	428	6.5	222
7	956	6	803	5.5	425	7	222
7.5	953	6.5	800	6	423	7.5	222
8	950	7	796	6.5	421	8	222
8.5	948	7.5	792	7	420	8.5	222
9	945	8	789	7.5	420	9	222
9.5	943	8.5	787	8	420	9.5	222
10	941	9	785	8.5	420	10	222
10.5	938	9.5	786	9	420	10.5	222
11	938	10	785	9.5	420	11	222
11.5	938	10.5	785	10	420	11.5	222
12	938	11	784	10.5	420	12	222
12.5	938	11.5	785	11	420	12.5	222
13	939	12	784	11.5	420	13	222
13.5	940	12.5	785	12	420	13.5	222
14	941	13	786	12.5	420	14	222
14.5	942	13.5	787	13	420	14.5	222
15	944	14	788	13.5	420	15	222
15.5	947	14.5	790	14	420	15.5	223
16	949	15	791	14.5	421	16	223
16.5	952	15.5	792	15	422	16.5	223
17	955	16	794	15.5	423	17	224
17.5	960	16.5	796	16	425	17.5	226
18	965	17	798	16.5	427	18	228
18.5	970	17.5	802	17	429	18.5	230
19	974	18	805	17.5	431	19	233
19.5	977	18.5	808	18	433	19.5	235
20	981	19	812	18.5	435	20	237
20.5	989	19.5	817	19	437	20.5	239
21	997	20	822	19.5	440	21	242
21.5	1003	20.5	827	20	443	21.5	245
22	1010	21	833	20.5	446	22	248
22.5	1017	21.5	838	21	450	22.5	253
23	1027	22	846	21.5	455	23	259
23.5	1038	22.5	856	22	460	23.5	263
24	1047	23	866	22.5	465	24	267
24.5	1059	23.5	876	23	471	24.5	273
25	1071	24	887	23.5	476	25	279
25.5	1085	24.5	898	24	483	25.5	284
26	1098	25	908	24.5	489	26	293
26.5	1111	25.5	920	25	498	26.5	305
27	1115	26	929	25.5	510	27	317
27.5	1115	26.5	940	26	520	27.5	334
28	1115	27	948	26.5	535	28	353
28.5	1115	27.5	954	27	551	28.5	367
29	1115	28	960	27.5	562	29	385
29.5	1115	28.5	961	28	574	29.5	404
30	1115	29	961	28.5	583	30	415
30.5	1115	29.5	961	29	594	30.5	423
31	1115	30	961	29.5	597	31	425
31.5	1115	30.5	961	30	599	31.5	426
32	1115	31	961	30.5	600	32	427
32.5	1115	31.5	961	31	601	32.5	428
33	1115	32	961	31.5	602	33	429
33.5		32.5	961	32	603	33.5	430
34		33	961	32.5	604	34	431
34.5		33.5		33	605	34.5	432
35		34		33.5	606	35	433
35.5		34.5		34	607	35.5	--

36		35		34.5	608	36	
36.5		35.5		35	609	36.5	
37		36		35.5	610	37	
37.5		36.5		36		37.5	
38		37		36.5		38	
38.5		37.5		37		38.5	
39		38		37.5		39	
39.5		38.5		38		39.5	
40		39		38.5		40	
40.5		39.5		39		40.5	
41		40		39.5		41	
41.5		40.5		40		41.5	
42		41		40.5		42	
42.5		41.5		41		42.5	

Table 4.6 Krafft temperature data for aqueous solution of CPB in the presence of CuSO<sub>4</sub>

CPB (0.01M)- CuSO <sub>4</sub>							
0.004166M CuSO <sub>4</sub>		0.00333 M CuSO <sub>4</sub>		0.001666 M CuSO <sub>4</sub>		0.000833 M CuSO <sub>4</sub>	
Temp. (°C)	Specific conductance (μS/cm)	Temp. (°C)	Specific conductance (μS/cm)	Temp. (°C)	Specific conductance (μS/cm)	Temp. (°C)	Specific conductance (μS/cm)
5	625	4	524	3.5	--	5	182
5.5	624	4.5	523	4	310	5.5	181
6	623	5	522	4.5	309	6	181.3
6.5	622	5.5	521	5	308	6.5	180.9
7	621	6	520	5.5	307	7	180.3
7.5	620	6.5	519	6	306	7.5	179.3
8	619	7	518	6.5	305	8	178.2
8.5	618	7.5	517	7	306	8.5	178.3
9	617	8	516	7.5	305	9	178.5
9.5	616	8.5	515	8	304	9.5	179.2
10	615	9	514	8.5	303	10	179
10.5	616	9.5	513	9	303	10.5	178.7
11	617	10	512	9.5	303	11	178.2
11.5	618	10.5	511	10	303	11.5	178.4
12	619	11	511	10.5	303	12	179
12.5	620	11.5	511	11	303	12.5	179.1
13	621	12	512	11.5	303	13	179.5
13.5	622	12.5	513	12	304	13.5	179.9
14	623	13	514	12.5	304	14	180.1
14.5	625	13.5	516	13	305	14.5	181.2
15	627	14	518	13.5	306	15	182
15.5	631	14.5	520	14	307	15.5	183.3
16	634	15	524	14.5	308	16	184.2
16.5	638	15.5	527	15	309	16.5	185.4
17	641	16	530	15.5	310	17	186.5
17.5	644	16.5	534	16	312	17.5	187.8
18	648	17	537	16.5	314	18	189
18.5	651	17.5	540	17	316	18.5	191.6
19	655	18	543	17.5	319	19	193.3
19.5	660	18.5	547	18	321	19.5	195.4
20	668	19	550	18.5	324	20	197.9
20.5	675	19.5	553	19	327	20.5	199.3
21	684	20	557	19.5	329	21	201
21.5	691	20.5	562	20	331	21.5	205
22	697	21	567	20.5	334	22	207
22.5	707	21.5	572	21	337	22.5	210
23	717	22	578	21.5	342	23	214
23.5	731	22.5	584	22	346	23.5	219
24	745	23	592	22.5	354	24	226
24.5	756	23.5	602	23	359	24.5	233
25	766	24	615	23.5	366	25	237
25.5	785	24.5	625	24	374	25.5	242
26	797	25	637	24.5	383	26	250
26.5	818	25.5	650	25	390	26.5	256
27	819	26	661	25.5	397	27	265
27.5	820	26.5	679	26	408	27.5	276

28	821	27	693	26.5	417	28	293
28.5	822	27.5	703	27	430	28.5	308
29	823	28	706	27.5	448	29	320
29.5	824	28.5	709	28	460	29.5	343
30	825	29	710	28.5	474	30	363
30.5	826	29.5	711	29	485	30.5	381
31	827	30	712	29.5	495	31	389
31.5	828	30.5	713	30	500	31.5	391
32	829	31	714	30.5	501	32	392
32.5	830	31.5	715	31	502	32.5	393
		32	716	31.5	503	33	394
		32.5	717	32	504	33.5	395
		33	718	32.5	505	34	396
		33.5	718	33	506	34.5	397
		34	719	33.5	507	35	398
		34.5	719	34	508	35.5	399
		35	719	34.5	508	36	399
				35	509	36.5	400
						37	401

Table-4.7 Krafft temperature data for aqueous solution of CPB in the presence of KSCN

CPB (0.01M)- KSCN							
0.0125M KSCN		0.01 M KSCN		0.005 M KSCN		0.0025 M KSCN	
Temp. (°C)	Specific conductance (μS/cm)	Temp. (°C)	Specific conductance (μS/cm)	Temp. (°C)	Specific conductance (μS/cm)	Temp. (°C)	Specific conductance (μS/cm)
5	1802	4	--	3.5		5	406
5.5	1797	4.5	--	4		5.5	404
6	1789	5	1440	4.5		6	402
6.5	1778	5.5	1436	5	652	6.5	401
7	1763	6	1430	5.5	643	7	400
7.5	1758	6.5	1422	6	635	7.5	398
8	1752	7	1413	6.5	629	8	397
8.5	1745	7.5	1408	7	624	8.5	395
9	1739	8	1400	7.5	619	9	393
9.5	1734	8.5	1388	8	617	9.5	391
10	1727	9	1385	8.5	615	10	389
10.5	1721	9.5	1380	9	614	10.5	388
11	1714	10	1377	9.5	612	11	388
11.5	1708	10.5	1374	10	610	11.5	388
12	1701	11	1371	10.5	608	12	388
12.5	1698	11.5	1369	11	606	12.5	388
13	1693	12	1367	11.5	603	13	387
13.5	1689	12.5	1365	12	602	13.5	386
14	1684	13	1362	12.5	600	14	385
14.5	1679	13.5	1359	13	599	14.5	384
15	1673	14	1355	13.5	598	15	384
15.5	1669	14.5	1350	14	597	15.5	384
16	1663	15	1346	14.5	596	16	383
16.5	1660	15.5	1343	15	595	16.5	383
17	1658	16	1340	15.5	594	17	383
17.5	1655	16.5	1338	16	593	17.5	383
18	1651	17	1335	16.5	593	18	382
18.5	1648	17.5	1333	17	592	18.5	382
19	1645	18	1331	17.5	591	19	382
19.5	1642	18.5	1329	18	590	19.5	382
20	1638	19	1327	18.5	590	20	381
20.5	1635	19.5	1325	19	590	20.5	381
21	1632	20	1323	19.5	589	21	381
21.5	1628	20.5	1320	20	588	21.5	381
22	1625	21	1316	20.5	588	22	381
22.5	1623	21.5	1313	21	588	22.5	381
23	1621	22	1312	21.5	588	23	380
23.5	1620	22.5	1311	22	588	23.5	382
24	1618	23	1311	22.5	588	24	384
24.5	1617	23.5	1311	23	587	24.5	400
25	1616	24	1311	23.5	587	25	455

25.5	1615	24.5	1311	24	589	25.5	520
26	1614	25	1311	24.5	604	26	543
26.5	1613	25.5	1311	25	620	26.5	554
27	1613	26	1311	25.5	684	27	559
27.5	1613	26.5	1311	26	723	27.5	559
28	1613	27	1311	26.5	735	28	560
28.5	1613	27.5	1311	27	738	28.5	561
29	1613	28	1311	27.5	742	29	561
29.5	1613	28.5	1311	28	744	29.5	561
30	1613	29	1311	28.5	745	30	562
30.5	1613	29.5	1312	29	745	30.5	562
31	1613	30	1313	29.5	745	31	562
31.5	1612	30.5	1314	30	746	31.5	562
32	1612	31	1315	30.5	746	32	562
32.5	1612	31.5	1316	31	747	32.5	562
33	1611	32	1318	31.5	748	33	562
33.5	1610	32.5	1321	32	749	33.5	562
34	1612	33	1329	32.5	749	34	562
34.5	1615	33.5	1342	33	750		
35	1625	34	1348				
35.5	1642	34.5	1357				
36	1678	35	1365				
36.5	1705	35.5	1373				
37	1712	36	1383				
37.5	1714	36.5	1405				
38	1713	37	1404				
38.5	1712	37.5	1402				
39	1711	38	1400				
39.5	1710	38.5	1398				
40	1709	39	1396				
40.5	1708	39.5	1393				
41	1707	40	1390				
41.5	1706	40.5	1388				
42	1705	41	1385				
42.5	1704	41.5	1382				
43	1703	42	1380				
43.5	1702	42.5	1378				

Table-4.8 Krafft temperature data for aqueous solution of CPB in the presence of KF

CPB (0.01M)- KF							
0.0125M KF		0.01 M KF		0.005 M KF		0.0025 M KF	
Temp. (°C)	Specific conductance (μS/cm)	Temp. (°C)	Specific conductance (μS/cm)	Temp. (°C)	Specific conductance (μS/cm)	Temp. (°C)	Specific conductance (μS/cm)
5	1152	4	--	3.5		5	271
5.5	1148	4.5	--	4	--	5.5	271
6	1143	5	1030	4.5	--	6	271
6.5	1136	5.5	1025	5	550	6.5	271
7	1133	6	1020	5.5	550	7	271
7.5	1130	6.5	1015	6	550	7.5	271
8	1126	7	1013	6.5	549	8	271
8.5	1123	7.5	1011	7	547	8.5	271
9	1120	8	1008	7.5	545	9	270
9.5	1118	8.5	1004	8	543	9.5	269
10	1116	9	1002	8.5	540	10	269
10.5	1113	9.5	1002	9	539	10.5	269
11	1109	10	1002	9.5	538	11	269
11.5	1107	10.5	1002	10	537	11.5	269
12	1105	11	1002	10.5	536	12	269
12.5	1103	11.5	1002	11	535	12.5	269
13	1101	12	1002	11.5	534	13	270
13.5	1100	12.5	1002	12	534	13.5	270
14	1102	13	1002	12.5	534	14	271
14.5	1103	13.5	1002	13	534	14.5	272
15	1102	14	1002	13.5	534	15	272
15.5	1102	14.5	1002	14	534	15.5	272
16	1102	15	1002	14.5	534	16	272

16.5	1102	15.5	1002	15	535	16.5	272
17	1102	16	1002	15.5	536	17	272
17.5	1103	16.5	1002	16	537	17.5	273
18	1103	17	1003	16.5	538	18	274
18.5	1104	17.5	1003	17	539	18.5	275
19	1105	18	1004	17.5	540	19	276
19.5	1106	18.5	1005	18	542	19.5	277
20	1108	19	1006	18.5	543	20	278
20.5	1111	19.5	1007	19	544	20.5	279
21	1117	20	1009	19.5	545	21	281
21.5	1124	20.5	1012	20	547	21.5	283
22	1134	21	1015	20.5	552	22	285
22.5	1140	21.5	1018	21	555	22.5	288
23	1145	22	1022	21.5	564	23	293
23.5	1151	22.5	1032	22	567	23.5	299
24	1158	23	1047	22.5	571	24	305
24.5	1166	23.5	1057	23	575	24.5	310
25	1181	24	1065	23.5	579	25	316
25.5	1197	24.5	1075	24	585	25.5	327
26	1214	25	1083	24.5	597	26	340
26.5	1243	25.5	1093	25	611	26.5	350
27	1259	26	1108	25.5	617	27	363
27.5	1273	26.5	1124	26	634	27.5	377
28	1295	27	1137	26.5	656	28	389
28.5	1305	27.5	1149	27	665	28.5	405
29	1315	28	1167	27.5	682	29	429
29.5	1325	28.5	1182	28	704	29.5	463
30	1329	29	1201	28.5	717	30	479
30.5	1328	29.5	1219	29	732	30.5	492
31	1328	30	1222	29.5	746	31	502
31.5	1328	30.5	1223	30	753	31.5	503
32	1329	31	1223	30.5	757	32	504
32.5	1329	31.5	1224	31	759	32.5	505
33	1329	32	1225	31.5	761	33	506
33.5	1329	32.5	1226	32	763	33.5	507
34	1328	33	1227	32.5	765	34	508
34.5	1328	33.5	1228	33	767	34.5	509
35	1328	34	1229	33.5	770	35	510
35.5	1328	34.5	1230	34	773	35.5	511
36	1328	35	1231	34.5	776	36	512
36.5		35.5	1232	35	779	36.5	

Table-4.9 Krafft temperature data for aqueous solution of CPB in the presence of KCl

CPB (0.01M)- KCl							
0.0125M KCl		0.01 M KCl		0.005 M KCl		0.0025 M KCl	
Temp. (°C)	Specific conductance (μS/cm)	Temp. (°C)	Specific conductance (μS/cm)	Temp. (°C)	Specific conductance (μS/cm)	Temp. (°C)	Specific conductance (μS/cm)
5	1882	4	--	3.5		5	403
5.5	1858	4.5	--	4		5.5	402
6	1846	5	1522	4.5	--	6	401
6.5	1828	5.5	1506	5	769	6.5	398
7	1815	6	1496	5.5	766	7	398
7.5	1808	6.5	1485	6	764	7.5	398
8	1802	7	1477	6.5	760	8	398
8.5	1799	7.5	1470	7	757	8.5	398
9	1795	8	1462	7.5	755	9	397
9.5	1791	8.5	1454	8	753	9.5	395
10	1786	9	1446	8.5	751	10	394
10.5	1782	9.5	1444	9	749	10.5	393
11	1778	10	1441	9.5	746	11	392
11.5	1774	10.5	1436	10	742	11.5	392
12	1770	11	1432	10.5	740	12	392
12.5	1766	11.5	1427	11	740	12.5	392
13	1759	12	1426	11.5	739	13	391
13.5	1755	12.5	1424	12	738	13.5	389
14	1750	13	1422	12.5	737	14	389

14.5	1744	13.5	1419	13	736	14.5	389
15	1739	14	1416	13.5	735	15	389
15.5	1734	14.5	1412	14	734	15.5	389
16	1730	15	1408	14.5	732	16	389
16.5	1727	15.5	1404	15	730	16.5	389
17	1725	16	1403	15.5	728	17	389
17.5	1723	16.5	1402	16	727	17.5	389
18	1721	17	1400	16.5	726	18	389
18.5	1719	17.5	1396	17	725	18.5	389
19	1717	18	1395	17.5	724	19	389
19.5	1715	18.5	1393	18	723	19.5	390
20	1714	19	1391	18.5	722	20	391
20.5	1713	19.5	1389	19	722	20.5	393
21	1714	20	1389	19.5	722	21	396
21.5	1717	20.5	1388	20	724	21.5	398
22	1725	21	1387	20.5	725	22	400
22.5	1735	21.5	1391	21	726	22.5	402
23	1748	22	1394	21.5	727	23	404
23.5	1769	22.5	1400	22	728	23.5	406
24	1798	23	1415	22.5	731	24	408
24.5	1813	23.5	1429	23	739	24.5	411
25	1840	24	1442	23.5	748	25	415
25.5	1856	24.5	1466	24	751	25.5	422
26	1879	25	1495	24.5	757	26	437
26.5	1893	25.5	1532	25	775	26.5	448
27	1900	26	1573	25.5	788	27	465
27.5	1900	26.5	1584	26	803	27.5	481
28	1901	27	1595	26.5	827	28	510
28.5	1900	27.5	1605	27	840	28.5	530
29	1900	28	1607	27.5	858	29	552
29.5	1901	28.5	1609	28	883	29.5	586
30	1902	29	1610	28.5	908	30	599
30.5	1902	29.5	1611	29	923	30.5	606
		30	1612	29.5	936	31	607
		30.5	1613	30	937	31.5	608
		31	1614	30.5	937	32	609
		31.5	1615	31	937	32.5	610
		32	1616	31.5	937	33	611
		32.5	1617	32	937	33.5	612
		33	1617	32.5	938	34	613
		33.5	1618	33	939	34.5	614
		34	1619	33.5	939	35	615
		34.5		34	940	35.5	
				34.5	940	36	
				35	941	36.5	

Table-4.10 Krafft temperature data for aqueous solution of CPB in the presence of KBr

CPB (0.01M)- KBr							
0.0125M KBr		0.01 M KBr		0.005 M KBr		0.0025 M KBr	
Temp. (°C)	Specific conductance (μS/cm)	Temp. (°C)	Specific conductance (μS/cm)	Temp. (°C)	Specific conductance (μS/cm)	Temp. (°C)	Specific conductance (μS/cm)
5	1877	4	--	3.5		5	393
5.5	1870	4.5	--	4	--	5.5	390
6	1862	5	1479	4.5	--	6	387
6.5	1855	5.5	1469	5	760	6.5	385
7	1847	6	1461	5.5	755	7	383
7.5	1839	6.5	1455	6	749	7.5	381
8	1831	7	1451	6.5	745	8	379
8.5	1823	7.5	1445	7	742	8.5	378
9	1815	8	1438	7.5	738	9	377
9.5	1810	8.5	1431	8	736	9.5	376
10	1802	9	1424	8.5	734	10	375
10.5	1793	9.5	1419	9	732	10.5	374
11	1781	10	1415	9.5	730	11	373
11.5	1776	10.5	1411	10	728	11.5	372
12	1771	11	1408	10.5	725	12	371

12.5	1766	11.5	1403	11	722	12.5	370
13	1761	12	1398	11.5	721	13	369
13.5	1755	12.5	1394	12	719	13.5	369
14	1751	13	1389	12.5	717	14	369
14.5	1748	13.5	1385	13	715	14.5	368
15	1744	14	1384	13.5	714	15	367
15.5	1743	14.5	1383	14	712	15.5	367
16	1742	15	1382	14.5	710	16	367
16.5	1740	15.5	1380	15	709	16.5	366
17	1738	16	1378	15.5	708	17	366
17.5	1736	16.5	1376	16	707	17.5	366
18	1734	17	1373	16.5	706	18	366
18.5	1730	17.5	1371	17	705	18.5	366
19	1726	18	1369	17.5	704	19	366
19.5	1722	18.5	1366	18	703	19.5	366
20	1718	19	1363	18.5	702	20	365
20.5	1712	19.5	1360	19	701	20.5	365
21	1708	20	1358	19.5	700	21	365
21.5	1706	20.5	1356	20	699	21.5	365
22	1705	21	1353	20.5	699	22	365
22.5	1704	21.5	1352	21	699	22.5	365
23	1703	22	1351	21.5	699	23	365
23.5	1702	22.5	1350	22	699	23.5	366
24	1701	23	1349	22.5	699	24	366
24.5	1700	23.5	1348	23	699	24.5	366
25	1699	24	1347	23.5	700	25	366
25.5	1698	24.5	1345	24	700	25.5	367
26	1697	25	1344	24.5	700	26	368
26.5	1696	25.5	1342	25	701	26.5	369
27	1695	26	1340	25.5	702	27	369
27.5	1694	26.5	1340	26	703	27.5	370
28	1692	27	1340	26.5	704	28	371
28.5	1689	27.5	1340	27	706	28.5	372
29	1687	28	1340	27.5	707	29	375
29.5	1686	28.5	1340	28	708	29.5	395
30	1688	29	1340	28.5	709	30	427
30.5	1692	29.5	1340	29	710	30.5	524
31	1700	30	1340	29.5	712	31	550
31.5	1745	30.5	1343	30	716	31.5	582
32	1799	31	1351	30.5	739	32	584
32.5	1880	31.5	1388	31	751	32.5	585
33	1894	32	1492	31.5	828	33	586
33.5	1895	32.5	1563	32	899	33.5	587
34	1896	33	1563	32.5	907	34	588
34.5	1896	33.5	1563	33	907	34.5	589
35	1896	34	1563	33.5	908	35	590
35.5	1896	34.5	1563	34	909	35.5	590
36	1896	35	1563	34.5	910	36	591
36.5	1896	35.5	1563	35	912	36.5	592
37	1896	36	1563	35.5	913	37	593
37.5	--	36.5	1563	36	914	37.5	593
38	--	37	1564	36.5	916	38	594
38.5		37.5	1563	37	917	38.5	--
39		38	1563	37.5	918	39	
39.5		38.5		38	919	39.5	
40		39		38.5	919	40	
40.5		39.5		39		40.5	
41		40		39.5		41	
41.5		40.5		40		41.5	



Table4.11 Krafft temperature data for aqueous solution of CPB in the presence of KI

CPB (0.01M)- KI							
0.0125M KI		0.01 M KI		0.005 M KI		0.0025 M KI	
Temp. (°C)	Specific conductance (μS/cm)	Temp. (°C)	Specific conductance (μS/cm)	Temp. (°C)	Specific conductance (μS/cm)	Temp. (°C)	Specific conductance (μS/cm)
5	1907	4	--	3.5		5	392
5.5	1897	4.5	--	4	--	5.5	389
6	1889	5	1532	4.5	--	6	386
6.5	1879	5.5	1523	5	789	6.5	385
7	1868	6	1515	5.5	784	7	384
7.5	1859	6.5	1508	6	782	7.5	382
8	1851	7	1504	6.5	780	8	380
8.5	1843	7.5	1496	7	774	8.5	379
9	1835	8	1484	7.5	772	9	378
9.5	1829	8.5	1480	8	769	9.5	377
10	1824	9	1476	8.5	767	10	376
10.5	1819	9.5	1472	9	763	10.5	375
11	1813	10	1466	9.5	760	11	374
11.5	1807	10.5	1460	10	755	11.5	373
12	1802	11	1455	10.5	753	12	372
12.5	1797	11.5	1452	11	751	12.5	371
13	1791	12	1449	11.5	750	13	370
13.5	1786	12.5	1445	12	749	13.5	369
14	1781	13	1440	12.5	748	14	368
14.5	1775	13.5	1436	13	747	14.5	367
15	1770	14	1430	13.5	745	15	366
15.5	1765	14.5	1426	14	742	15.5	366
16	1759	15	1423	14.5	740	16	366
16.5	1756	15.5	1419	15	737	16.5	366
17	1754	16	1414	15.5	736	17	366
17.5	1751	16.5	1412	16	734	17.5	365
18	1747	17	1410	16.5	732	18	365
18.5	1744	17.5	1408	17	730	18.5	365
19	1740	18	1406	17.5	729	19	365
19.5	1737	18.5	1404	18	728	19.5	365
20	1734	19	1401	18.5	727	20	365
20.5	1731	19.5	1397	19	726	20.5	365
21	1728	20	1395	19.5	725	21	365
21.5	1725	20.5	1393	20	724	21.5	365
22	1722	21	1392	20.5	723	22	365
22.5	1719	21.5	1391	21	722	22.5	365
23	1717	22	1390	21.5	722	23	365
23.5	1715	22.5	1389	22	722	23.5	365
24	1714	23	1388	22.5	722	24	365
24.5	1713	23.5	1387	23	721	24.5	365
25	1712	24	1385	23.5	720	25	365
25.5	1710	24.5	1383	24	719	25.5	365
26	1708	25	1380	24.5	718	26	365
26.5	1706	25.5	1379	25	717	26.5	365
27	1704	26	1377	25.5	716	27	366
27.5	1702	26.5	1375	26	715	27.5	368
28	1700	27	1373	26.5	715	28	370
28.5	1698	27.5	1374	27	715	28.5	375
29	1696	28	1375	27.5	716	29	389
29.5	1695	28.5	1374	28	717	29.5	458
30	1694	29	1375	28.5	718	30	550
30.5	1694	29.5	1374	29	719	30.5	554
31	1694	30	1373	29.5	725	31	557
31.5	1694	30.5	1375	30	748	31.5	559
32	1694	31	1377	30.5	810	32	560

32.5	1694	31.5	1380	31	842	32.5	561
33	1694	32	1382	31.5	873	33	562
33.5	1693	32.5	1385	32	877	33.5	563
34	1692	33	1387	32.5	878	34	563
34.5	1691	33.5	1390	33	879	34.5	564
35	1690	34	1393	33.5	880	35	565
35.5	1689	34.5	1399	34	881	35.5	565
36	1688	35	1404	34.5	882	36	566
36.5	1687	35.5	1408	35	883	36.5	566
37	1689	36	1414	35.5	884	37	567
37.5	1690	36.5	1418	36	885	37.5	567
38	1692	37	1422	36.5	886	38	567
38.5	1695	37.5	1426	37	887		
39	1699	38	1434	37.5	888		
39.5	1708	38.5	1441	38	889		
40	1723	39	1453				
40.5	1736	39.5	1460				
41	1753	40	1468				
41.5	1773	40.5	1475				
42	1795	41	1481				
42.5	1796	41.5	1484				
43	1797	42	1486				
43.5	1798	42.5	1488				
44	1799	43	1490				
44.5	1800	43.5	1492				
45	1801	44	1494				
45.5	1802	44.5	1495				
46	1803	45	1496				
46.5	1804	45.5	1497				
47	1805	46	1498				
47.5	1806	46.5	1498				
48	1807	47	1499				
		47.5	1500				
		48	1501				

Table-4.12 Krafft temperature data for aqueous solution of CPC in the presence of KNO<sub>3</sub>

CPC (0.01M)- KNO <sub>3</sub>							
0.0125M KNO <sub>3</sub>		0.01 M KNO <sub>3</sub>		0.005 M KNO <sub>3</sub>		0.0025 M KNO <sub>3</sub>	
Temp. (°C)	Specific conductance (μS/cm)	Temp. (°C)	Specific conductance (μS/cm)	Temp. (°C)	Specific conductance (μS/cm)	Temp. (°C)	Specific conductance (μS/cm)
3.5		3.5		3.5		3.5	
4	--	4	1546	4	679	4	--
4.5	--	4.5	1540	4.5	684	4.5	--
5	1691	5	1533	5	687	5	298
5.5	1685	5.5	1521	5.5	691	5.5	302
6	1678	6	1517	6	695	6	307
6.5	1670	6.5	1508	6.5	698	6.5	311
7	1663	7	1504	7	702	7	314
7.5	1658	7.5	1498	7.5	704	7.5	320
8	1653	8	1492	8	706	8	325
8.5	1642	8.5	1488	8.5	706	8.5	329
9	1635	9	1485	9	706	9	333
9.5	1630	9.5	1481	9.5	706	9.5	340
10	1627	10	1474	10	706	10	351
10.5	1624	10.5	1471	10.5	707	10.5	363
11	1622	11	1464	11	713	11	371
11.5	1619	11.5	1460	11.5	719	11.5	413
12	1616	12	1456	12	727	12	476
12.5	1612	12.5	1450	12.5	755	12.5	577
13	1608	13	1450	13	814	13	613
13.5	1605	13.5	1451	13.5	862	13.5	628
14	1602	14	1451	14	925	14	635
14.5	1601	14.5	1451	14.5	953	14.5	643
15	1604	15	1451	15	968	15	652
15.5	1611	15.5	1454	15.5	972	15.5	654

16	1619	16	1460	16	972	16	656
16.5	1627	16.5	1489	16.5	972	16.5	656
17	1654	17	1543	17	971	17	656
17.5	1687	17.5	1589	17.5	971	17.5	656
18	1779	18	1597	18	970	18	656
18.5	1867	18.5	1594	18.5	970	18.5	657
19	1891	19	1592	19	970	19	657
19.5	1890	19.5	1590	19.5	969	19.5	656
20	1888	20	1588	20	969	20	656
20.5	1886	20.5	1586	20.5	969		
21	1884	21	1583	21	968		
21.5	1882	21.5	1580	21.5	967		
22	1880	22	1577	22	967		
22.5	1878	22.5	1576				
23	1876	23	1575				
23.5	1874						
24	1872						

Table-4.13 Krafft temperature data for aqueous solution of CPC in the presence of  $K_2CO_3$ 

CPC (0.01M)- $K_2CO_3$							
0.004166M $K_2CO_3$		0.00333 M $K_2CO_3$		0.00166 M $K_2CO_3$		0.000833 M $K_2CO_3$	
Temp. (°C)	Specific conductance ( $\mu S/cm$ )	Temp. (°C)	Specific conductance ( $\mu S/cm$ )	Temp. (°C)	Specific conductance ( $\mu S/cm$ )	Temp. (°C)	Specific conductance ( $\mu S/cm$ )
3.5	1086	3.5	875	3.5	475	3.5	274
4	1081	4	870	4	475	4	273
4.5	1075	4.5	865	4.5	474	4.5	273
5	1070	5	859	5	474	5	273
5.5	1065	5.5	855	5.5	473	5.5	272
6	1061	6	853	6	473	6	272
6.5	1058	6.5	850	6.5	473	6.5	272
7	1054	7	849	7	473	7	273
7.5	1054	7.5	848	7.5	473	7.5	274
8	1061	8	850	8	473	8	275
8.5	1076	8.5	855	8.5	473	8.5	278
9	1099	9	869	9	473	9	284
9.5	1120	9.5	887	9.5	478	9.5	287
10	1142	10	912	10	495	10	295
10.5	1171	10.5	937	10.5	512	10.5	304
11	1198	11	969	11	529	11	313
11.5	1226	11.5	1008	11.5	554	11.5	323
12	1235	12	1030	12	585	12	329
12.5	1235	12.5	1040	12.5	610	12.5	339
13	1234	13	1046	13	639	13	348
13.5	1233	13.5	1044	13.5	655	13.5	355
14	1232	14	1042	14	656	14	362
14.5	1231	14.5	1041	14.5	657	14.5	370
15	1230	15	1040	15	657	15	382
15.5	1229	15.5	1039	15.5	657	15.5	392
16	1228	16	1038	16	657	16	404
16.5	1227	16.5	1037	16.5	658	16.5	417
17	1226	17	1036	17	659	17	438
17.5		17.5	1035	17.5	663	17.5	457
18		18	1034	18	674	18	472
18.5		18.5		18.5	680	18.5	483
19		19		19	688	19	498
19.5		19.5		19.5	689	19.5	518
20		20		20	689	20	524
20.5		20.5		20.5	689	20.5	525
21		21		21	689	21	525
21.5		21.5		21.5	689	21.5	525
22		22		22	689	22	526
22.5		22.5		22.5	689	22.5	526
23		23		23	689	23	526
23.5		23.5		23.5	689	23.5	526
24		24		24	689	24	526
24.5		24.5		24.5	689	24.5	526

25		25		25	689	25	526
25.5		25.5		25.5		25.5	526
26		26		26		26	526

Table-4.14 Krafft temperature data for aqueous solution of CPC in the presence of  $K_2SO_4$ 

CPC (0.01M)- $K_2SO_4$							
0.004166M $K_2SO_4$		0.00333M $K_2SO_4$		0.00166M $K_2SO_4$		0.000833M $K_2SO_4$	
Temp. (°C)	Specific conductance ( $\mu S/cm$ )	Temp. (°C)	Specific conductance ( $\mu S/cm$ )	Temp. (°C)	Specific conductance ( $\mu S/cm$ )	Temp. (°C)	Specific conductance ( $\mu S/cm$ )
3.5	1277	3.5		3.5		3.5	
4	1270	4	--	4	541	4	324
4.5	1263	4.5	1056	4.5	538	4.5	324
5	1256	5	1054	5	536	5	323
5.5	1253	5.5	1052	5.5	534	5.5	322
6	1250	6	1051	6	532	6	321
6.5	1248	6.5	1051	6.5	531	6.5	321
7	1248	7	1051	7	530	7	322
7.5	1248	7.5	1052	7.5	529	7.5	323
8	1249	8	1053	8	528	8	324
8.5	1253	8.5	1055	8.5	527	8.5	325
9	1263	9	1059	9	526	9	326
9.5	1272	9.5	1065	9.5	530	9.5	327
10	1288	10	1073	10	536	10	329
10.5	1302	10.5	1084	10.5	549	10.5	331
11	1323	11	1112	11	557	11	335
11.5	1336	11.5	1124	11.5	578	11.5	341
12	1341	12	1124	12	603	12	344
12.5	1340	12.5	1125	12.5	643	12.5	347
13	1339	13	1126	13	662	13	353
13.5	1338	13.5	1126	13.5	696	13.5	362
14	1337	14	1126	14	702	14	371
14.5	1336	14.5	1127	14.5	707	14.5	381
15	1335	15	1127	15	709	15	395
15.5	1334	15.5	1127	15.5	712	15.5	418
16	1333	16	1127	16	713	16	432
16.5	1332	16.5	1127	16.5	713	16.5	449
17	1331	17	1127	17	713	17	478
17.5	1330	17.5		17.5	714	17.5	513
18	1329	18		18	714	18	531
18.5	1328	18.5		18.5	715	18.5	532
19	1327	19		19	715	19	534
19.5		19.5		19.5	715	19.5	535
20		20		20	715	20	536
20.5		20.5		20.5		20.5	537
21		21		21		21	538
						21.5	539
						22	540
						22.5	541
						23	542

Table-4.15 Krafft temperature data for aqueous solution of CPC in the presence of  $K_2HPO_4$ 

CPC (0.01M)- $K_2HPO_4$							
0.004166M $K_2HPO_4$		0.00333M $K_2HPO_4$		0.00166M $K_2HPO_4$		0.000833M $K_2HPO_4$	
Temp. (°C)	Specific conductance ( $\mu S/cm$ )	Temp. (°C)	Specific conductance ( $\mu S/cm$ )	Temp. (°C)	Specific conductance ( $\mu S/cm$ )	Temp. (°C)	Specific conductance ( $\mu S/cm$ )
3.5	1073	3.5	892	3.5		3.5	288
4	1073	4	892	4	473	4	288
4.5	1073	4.5	891	4.5	476	4.5	287
5	1073	5	891	5	480	5	286
5.5	1073	5.5	892	5.5	483	5.5	285
6	1074	6	894	6	489	6	285
6.5	1075	6.5	896	6.5	493	6.5	285
7	1078	7	897	7	498	7	285

7.5	1082	7.5	899	7.5	502	7.5	286
8	1086	8	901	8	507	8	287
8.5	1090	8.5	904	8.5	513	8.5	290
9	1098	9	908	9	516	9	293
9.5	1109	9.5	914	9.5	520	9.5	297
10	1122	10	919	10	523	10	301
10.5	1130	10.5	925	10.5	528	10.5	305
11	1140	11	932	11	530	11	309
11.5	1150	11.5	939	11.5	533	11.5	314
12	1163	12	947	12	536	12	320
12.5	1175	12.5	955	12.5	539	12.5	327
13	1187	13	966	13	542	13	336
13.5	1193	13.5	986	13.5	548	13.5	342
14	1197	14	1003	14	557	14	351
14.5	1198	14.5	1014	14.5	569	14.5	358
15	1197	15	1020	15	589	15	371
15.5	1196	15.5	1022	15.5	605	15.5	382
16	1195	16	1022	16	617	16	398
16.5	1194	16.5	1022	16.5	627	16.5	413
17	1193	17	1022	17	639	17	426
17.5	1192	17.5	1022	17.5	654	17.5	444
18	1191	18	1022	18	662	18	459
18.5	1190	18.5	1022	18.5	669	18.5	478
19	1189	19	1022	19	670	19	502
19.5	1188			19.5	670	19.5	518
20	1187			20	669	20	522
20.5	1186			20.5	668	20.5	523
				21	668	21	524
				21.5	668	21.5	524
				22	668	22	524
				22.5	668	22.5	524
				23	668	23	524
				23.5	668	23.5	524
				24	668	24	524
						24.5	524
						25	524
						25.5	524
						26	524

Table-4.17 Krafft temperature data for aqueous solution of CPC in the presence of  $\text{CuSO}_4$ 

CPC (0.01M)- $\text{CuSO}_4$							
0.004166M $\text{CuSO}_4$		0.00333M $\text{CuSO}_4$		0.00166M $\text{CuSO}_4$		0.000833M $\text{CuSO}_4$	
Temp. ( $^{\circ}\text{C}$ )	Specific conductance ( $\mu\text{S}/\text{cm}$ )	Temp. ( $^{\circ}\text{C}$ )	Specific conductance ( $\mu\text{S}/\text{cm}$ )	Temp. ( $^{\circ}\text{C}$ )	Specific conductance ( $\mu\text{S}/\text{cm}$ )	Temp. ( $^{\circ}\text{C}$ )	Specific conductance ( $\mu\text{S}/\text{cm}$ )
3.5	702	3.5	611	3.5	358	3.5	219
4	701	4	611	4	357	4	219
4.5	700	4.5	611	4.5	357	4.5	219
5	698	5	611	5	357	5	219
5.5	696	5.5	612	5.5	356	5.5	219
6	695	6	613	6	355	6	219
6.5	694	6.5	613	6.5	354	6.5	219
7	693	7	613	7	353	7	219
7.5	692	7.5	613	7.5	354	7.5	220
8	693	8	614	8	355	8	221
8.5	700	8.5	615	8.5	356	8.5	223
9	711	9	619	9	356	9	225
9.5	742	9.5	635	9.5	358	9.5	229
10	760	10	649	10	361	10	235
10.5	791	10.5	680	10.5	366	10.5	239
11	822	11	703	11	372	11	245
11.5	840	11.5	736	11.5	385	11.5	259
12	865	12	756	12	396	12	270
12.5	875	12.5	771	12.5	414	12.5	282
13	879	13	778	13	438	13	294
13.5	879	13.5	778	13.5	452	13.5	307
14	878	14	778	14	469	14	321

14.5	877	14.5	778	14.5	480	14.5	330
15	877	15	778	15	489	15	342
15.5	876	15.5	778	15.5	497	15.5	349
16	876	16	778	16	502	16	368
16.5	876	16.5	778	16.5	512	16.5	385
17	876	17	778	17	528	17	401
17.5	876	17.5	778	17.5	541	17.5	411
18	876	18	778	18	576	18	421
18.5	875	18.5	778	18.5	583	18.5	434
19	875	19		19	589	19	451
19.5		19.5		19.5	588	19.5	464
20		20		20	588	20	477
20.5		20.5		20.5	589	20.5	480
21		21		21	589	21	481
21.5		21.5		21.5	589	21.5	482
22		22		22	589	22	483
22.5		22.5		22.5	589	22.5	483
23		23		23	589	23	483
23.5		23.5		23.5	589	23.5	483
24		24		24	589	24	484
24.5		24.5		24.5	589	24.5	484
25		25		25	589	25	484
25.5		25.5		25.5	589	25.5	484
26		26		26	589	26	484
26.5		26.5		26.5	589	26.5	484
27		27		27		27	484
27.5		27.5		27.5		27.5	484
28		28		28		28	484
28.5		28.5		28.5		28.5	484
34.5		34.5		34.5		34.5	
35		35		35		35	
35.5		35.5		35.5		35.5	

Table-4.18 Krafft temperature data for aqueous solution of CPC in the presence of KSCN

CPC (0.01M)- KSCN							
0.0125M KSCN		0.01 M KSCN		0.005 M KSCN		0.0025 M KSCN	
Temp. (°C)	Specific conductance (μS/cm)	Temp. (°C)	Specific conductance (μS/cm)	Temp. (°C)	Specific conductance (μS/cm)	Temp. (°C)	Specific conductance (μS/cm)
5	1808	5	1474	5	736	3.5	405
5.5	1798	5.5	1466	5.5	734	4	405
6	1786	6	1458	6	732	4.5	405
6.5	1778	6.5	1450	6.5	731	5	405
7	1772	7	1442	7	730	5.5	405
7.5	1768	7.5	1431	7.5	728	6	405
8	1763	8	1428	8	726	6.5	405
8.5	1756	8.5	1424	8.5	724	7	405
9	1750	9	1422	9	722	7.5	405
9.5	1745	9.5	1420	9.5	720	8	405
10	1739	10	1418	10	718	8.5	405
10.5	1733	10.5	1415	10.5	716	9	405
11	1725	11	1413	11	713	9.5	405
11.5	1716	11.5	1410	11.5	710	10	405
12	1709	12	1407	12	710	10.5	406
12.5	1705	12.5	1402	12.5	710	11	406
13	1700	13	1398	13	712	11.5	406
13.5	1696	13.5	1393	13.5	712	12	407
14	1693	14	1385	14	712	12.5	409
14.5	1691	14.5	1379	14.5	717	13	412
15	1688	15	1377	15	724	13.5	418
15.5	1685	15.5	1375	15.5	729	14	428
16	1682	16	1373	16	734	14.5	453
16.5	1678	16.5	1370	16.5	744	15	483
17	1675	17	1366	17	756	15.5	505
17.5	1671	17.5	1361	17.5	773	16	525
18	1667	18	1358	18	797	16.5	551
18.5	1664	18.5	1355	18.5	821	17	565

19	1661	19	1353	19	835	17.5	584
19.5	1658	19.5	1352	19.5	841	18	601
20	1655	20	1351	20	842	18.5	610
20.5	1651	20.5	1350	20.5	844	19	612
21	1648	21	1349	21	846	19.5	613
21.5	1645	21.5	1348	21.5	847	20	614
22	1642	22	1347	22	848	20.5	614
22.5	1640	22.5	1346	22.5	849	21	615
23	1638	23	1345	23	850	21.5	616
23.5	1636	23.5	1344	23.5	851	22	617
24	1635	24	1343	24	852	22.5	618
24.5	1634	24.5	1342	24.5	854	23	619
25	1633	25	1341	25	855	23.5	620
25.5	1632	25.5	1340	25.5	856	24	621
26	1631	26	1340	26	858	24.5	621
26.5	1630	26.5	1340	26.5	860	25	622
27	1629	27	1340	27	862	25.5	
27.5	1628	27.5	1340	27.5	864	26	
28	1627	28	1339	28	865	26.5	
28.5	1626	28.5	1340	28.5	867	27	
29	1625	29	1339	29	869	27.5	
29.5	1624	29.5	1340	29.5	872	28	
30	1623	30	1340	30	874	28.5	
30.5	1622	30.5	1340	30.5	876	29	
31	1621	31	1341	31	876	29.5	
31.5	1620	31.5	1344	31.5	876	30	
32	1619	32	1347	32	876	30.5	
32.5	1620	32.5	1351	32.5	876	31	
33	1621	33	1354	33	876	31.5	
33.5	1624	33.5	1357	33.5	876	32	
34	1627	34	1368	34	876		
34.5	1631	34.5	1373	34.5	876		
35	1636	35	1393	35	876		
35.5	1641	35.5	1405				
36	1652	36	1425				
36.5	1663	36.5	1426				
37	1695	37	1427				
37.5	1716	37.5	1429				
38	1715	38	1430				
38.5	1714	38.5	1431				
39	1713	39	1432				
39.5	1712	39.5	1433				
40	1711	40	1434				
40.5	1710	40.5	1434				
41	1709	41	1435				
41.5	1708						
42	1707						
42.5	1706						
43	1705						

Table-4.19 Krafft temperature data for aqueous solution of CPC in the presence of KF

CPC (0.01M)- KF							
0.0125M KF		0.01 M KF		0.005 M KF		0.0025 M KF	
Temp. (°C)	Specific conductance (μS/cm)	Temp. (°C)	Specific conductance (μS/cm)	Temp. (°C)	Specific conductance (μS/cm)	Temp. (°C)	Specific conductance (μS/cm)
3.5	1275	3.5		3.5	511	3.5	324
4	1278	4	962	4	511	4	324
4.5	1281	4.5	962	4.5	511	4.5	324
5	1285	5	962	5	511	5	324
5.5	1289	5.5	962	5.5	511	5.5	324
6	1293	6	963	6	511	6	325
6.5	1298	6.5	964	6.5	512	6.5	326
7	1305	7	965	7	516	7	327
7.5	1311	7.5	968	7.5	521	7.5	328
8	1323	8	973	8	527	8	332
8.5	1332	8.5	977	8.5	539	8.5	335

9	1345	9	981	9	547	9	338
9.5	1355	9.5	990	9.5	554	9.5	347
10	1366	10	1001	10	564	10	358
10.5	1378	10.5	1012	10.5	572	10.5	366
11	1394	11	1020	11	586	11	380
11.5	1404	11.5	1035	11.5	599	11.5	397
12	1421	12	1054	12	621	12	408
12.5	1436	12.5	1074	12.5	642	12.5	422
13	1448	13	1085	13	658	13	449
13.5	1458	13.5	1102	13.5	683	13.5	482
14	1471	14	1121	14	698	14	512
14.5	1477	14.5	1131	14.5	726	14.5	545
15	1484	15	1143	15	742	15	570
15.5	1489	15.5	1160	15.5	759	15.5	582
16	1493	16	1172	16	767	16	589
16.5	1497	16.5	1185	16.5	771	16.5	592
17	1502	17	1187	17	771	17	597
17.5	1504	17.5	1189	17.5	771	17.5	600
18	1505	18	1191	18	772	18	600
18.5	1504	18.5	1192	18.5	772	18.5	600
19	1503	19	1193	19	772	19	600
19.5	1502	19.5	1195	19.5	772	19.5	600
20	1501	20	1197	20	772	20	601
20.5	1500	20.5		20.5	772	20.5	602
21	1499	21		21	772	21	602
21.5	1498	21.5		21.5	772	21.5	602
22	1497	22		22	772	22	602
22.5	1496	22.5		22.5	772	22.5	602
23	1495	23		23	772	23	602
23.5		23.5		23.5	772	23.5	603

Table-4.20 Krafft temperature data for aqueous solution of CPC in the presence of KCl

CPC (0.01M)- KCl							
0.0125M KCl		0.01 M KCl		0.005 M KCl		0.0025 M KCl	
Temp. (°C)	Specific conductance (μS/cm)	Temp. (°C)	Specific conductance (μS/cm)	Temp. (°C)	Specific conductance (μS/cm)	Temp. (°C)	Specific conductance (μS/cm)
4		4		4	781	4	414
4.5	--	4.5	1500	4.5	780	4.5	413
5	1800	5	1493	5	777	5	412
5.5	1781	5.5	1481	5.5	775	5.5	411
6	1767	6	1476	6	770	6	410
6.5	1758	6.5	1465	6.5	765	6.5	409
7	1755	7	1459	7	763	7	408
7.5	1750	7.5	1450	7.5	762	7.5	407
8	1746	8	1444	8	760	8	406
8.5	1740	8.5	1441	8.5	757	8.5	405
9	1736	9	1437	9	755	9	405
9.5	1732	9.5	1432	9.5	753	9.5	404
10	1728	10	1430	10	750	10	403
10.5	1725	10.5	1425	10.5	748	10.5	403
11	1721	11	1421	11	746	11	403
11.5	1717	11.5	1417	11.5	745	11.5	403
12	1713	12	1411	12	743	12	404
12.5	1708	12.5	1408	12.5	742	12.5	405
13	1703	13	1405	13	741	13	406
13.5	1698	13.5	1403	13.5	740	13.5	407
14	1693	14	1400	14	739	14	408
14.5	1686	14.5	1397	14.5	738	14.5	411
15	1678	15	1394	15	736	15	416
15.5	1671	15.5	1390	15.5	738	15.5	423
16	1669	16	1388	16	739	16	440
16.5	1665	16.5	1387	16.5	740	16.5	465
17	1662	17	1386	17	755	17	494
17.5	1660	17.5	1385	17.5	772	17.5	540
18	1665	18	1383	18	785	18	601
18.5	1672	18.5	1387	18.5	809	18.5	635



19	1680	19	1393	19	857	19	657
19.5	1691	19.5	1428	19.5	941	19.5	681
20	1732	20	1485	20	967	20	682
20.5	1793	20.5	1575	20.5	991	20.5	681
21	1870	21	1661	21	998	21	681
21.5	1963	21.5	1662	21.5	1001	21.5	681
22	1974	22	1661	22	1003	22	681
22.5	1976	22.5	1660	22.5	1005	22.5	681
23	1974	23	1659	23	1007	23	681
23.5	1972	23.5	1658	23.5	1009	23.5	681
24	1970	24	1659	24	1011	24	681
24.5	1969	24.5	1660	24.5	1012	24.5	681
25	1968	25	1661	25	1013	25	681
25.5	1967	25.5	1661	25.5	--	25.5	--
26	1967	26	1661	26	--	26	--

Table-4.21 Krafft temperature data for aqueous solution of CPC in the presence of KBr

CPC (0.01M)- KBr							
0.0125M KBr		0.01 M KBr		0.005 M KBr		0.0025 M KBr	
Temp. (°C)	Specific conductance (μS/cm)	Temp. (°C)	Specific conductance (μS/cm)	Temp. (°C)	Specific conductance (μS/cm)	Temp. (°C)	Specific conductance (μS/cm)
3.5		3.5		3.5	776	3.5	--
4	--	4	1524	4	772	4	403
4.5	--	4.5	1507	4.5	764	4.5	403
5	1885	5	1500	5	761	5	402
5.5	1876	5.5	1495	5.5	756	5.5	403
6	1861	6	1487	6	752	6	403
6.5	1854	6.5	1479	6.5	750	6.5	400
7	1849	7	1472	7	747	7	398
7.5	1845	7.5	1464	7.5	745	7.5	397
8	1840	8	1456	8	742	8	396
8.5	1834	8.5	1450	8.5	740	8.5	395
9	1827	9	1443	9	738	9	395
9.5	1818	9.5	1440	9.5	736	9.5	395
10	1808	10	1438	10	734	10	395
10.5	1804	10.5	1435	10.5	732	10.5	396
11	1800	11	1432	11	730	11	396
11.5	1795	11.5	1428	11.5	728	11.5	395
12	1787	12	1423	12	725	12	395
12.5	1781	12.5	1419	12.5	724	12.5	395
13	1776	13	1414	13	725	13	395
13.5	1773	13.5	1410	13.5	725	13.5	395
14	1770	14	1408	14	724	14	395
14.5	1765	14.5	1406	14.5	723	14.5	395
15	1758	15	1402	15	723	15	397
15.5	1751	15.5	1400	15.5	723	15.5	399
16	1743	16	1399	16	722	16	404
16.5	1740	16.5	1396	16.5	722	16.5	420
17	1736	17	1393	17	722	17	434
17.5	1734	17.5	1389	17.5	722	17.5	459
18	1733	18	1386	18	722	18	476
18.5	1732	18.5	1385	18.5	723	18.5	491
19	1731	19	1385	19	723	19	507
19.5	1730	19.5	1384	19.5	729	19.5	534
20	1729	20	1384	20	740	20	550
20.5	1728	20.5	1385	20.5	752	20.5	583
21	1727	21	1389	21	777	21	602
21.5	1726	21.5	1394	21.5	803	21.5	648
22	1725	22	1399	22	852	22	651
22.5	1724	22.5	1414	22.5	887	22.5	652
23	1723	23	1421	23	917	23	653
23.5	1725	23.5	1433	23.5	959	23.5	654
24	1729	24	1448	24	960	24	655
24.5	1736	24.5	1480	24.5	961	24.5	656
25	1745	25	1503	25	962	25	657
25.5	1761	25.5	1515	25.5	963	25.5	658

26	1783	26	1528	26	964	26	659
26.5	1806	26.5	1545	26.5	965	26.5	660
27	1833	27	1565	27	966	27	661
27.5	1858	27.5	1591	27.5	967	27.5	--
28	1886	28	1600	28	968	28	--
28.5	1921	28.5	1599	28.5	--	28.5	--
29	1926	29	1598	29	--	29	--
29.5	1925	29.5	1598	29.5	--	29.5	--
30	1924	30	1598	30	--	30	--
30.5	1923	30.5	1598	30.5	--	30.5	--
31	1922	31	1598	31	--	31	--
31.5	1921	31.5	1598	31.5	--	31.5	--
32	1920	32	1598	32	--	32	--
32.5	1919	32.5	1598	32.5	--	32.5	--
33	1918	33	1598	33	--	33	--
33.5	1917	33.5	1598	33.5	--	33.5	--
34	--	34	1598	34	--	34	--

Table-4.22 Krafft temperature data for aqueous solution of CPC in the presence of KI

CPC (0.01M)- KI							
0.0125M KI		0.01 M KI		0.005 M KI		0.0025 M KI	
Temp. (°C)	Specific conductance (μS/cm)	Temp. (°C)	Specific conductance (μS/cm)	Temp. (°C)	Specific conductance (μS/cm)	Temp. (°C)	Specific conductance (μS/cm)
3.5		3.5		3.5		3.5	
4	--	4	--	4	--	4	--
4.5	--	4.5	--	4.5	--	4.5	--
5	1888	5	1509	5	660	5	310
5.5	1881	5.5	1504	5.5	652	5.5	307
6	1873	6	1498	6	639	6	305
6.5	1865	6.5	1492	6.5	628	6.5	303
7	1857	7	1486	7	618	7	301
7.5	1851	7.5	1476	7.5	611	7.5	298
8	1842	8	1468	8	609	8	297
8.5	1833	8.5	1462	8.5	607	8.5	296
9	1825	9	1457	9	604	9	295
9.5	1818	9.5	1452	9.5	601	9.5	296
10	1811	10	1448	10	602	10	296
10.5	1805	10.5	1444	10.5	605	10.5	296
11	1800	11	1442	11	607	11	298
11.5	1793	11.5	1440	11.5	624	11.5	305
12	1787	12	1438	12	635	12	318
12.5	1781	12.5	1436	12.5	662	12.5	328
13	1773	13	1433	13	751	13	377
13.5	1769	13.5	1428	13.5	812	13.5	408
14	1765	14	1423	14	877	14	475
14.5	1762	14.5	1417	14.5	884	14.5	521
15	1758	15	1414	15	890	15	577
15.5	1755	15.5	1410	15.5	891	15.5	586
16	1752	16	1408	16	893	16	595
16.5	1750	16.5	1406	16.5	894	16.5	602
17	1748	17	1404	17	895	17	606
17.5	1746	17.5	1401	17.5	896	17.5	608
18	1743	18	1398	18	895	18	609
18.5	1740	18.5	1396	18.5	895	18.5	610
19	1736	19	1394	19	895	19	610
19.5	1732	19.5	1392	19.5	895	19.5	610
20	1727	20	1390	20	895	20	610
20.5	1723	20.5	1389	20.5	895	20.5	610
21	1720	21	1387	21	895	21	611
21.5	1718	21.5	1385	21.5	895	21.5	612
22	1716	22	1383	22	895	22	613
22.5	1715	22.5	1382	22.5	895	22.5	615
23	1714	23	1382	23	895	23	617
23.5	1713	23.5	1382	23.5	895	23.5	619
24	1712	24	1382	24	895	24	621
24.5	1710	24.5	1382	24.5	895	24.5	622

25	1709	25	1382	25	895	25	624
25.5	1707	25.5	1382	25.5	895	25.5	--
26	1705	26	1381	26	895	26	--
26.5	1703	26.5	1380	26.5	895	26.5	--
27	1701	27	1379	27	895	27	--
27.5	1698	27.5	1378	27.5	895	27.5	--
28	1696	28	1377	28	895	28	--
28.5	1694	28.5	1377	28.5	896	28.5	--
29	1692	29	1378	29	903	29	--
29.5	1691	29.5	1379	29.5	908	29.5	--
30	1690	30	1380	30	912	30	--
30.5	1689	30.5	1381	30.5	915	30.5	--
31	1688	31	1381	31	919	31	--
31.5	1687	31.5	1382	31.5	923	31.5	--
32	1686	32	1384	32	926	32	--
32.5	1686	32.5	1387	32.5	928	32.5	--
33	1686	33	1390	33	931	33	--
33.5	1686	33.5	1393	33.5	936	33.5	--
34	1686	34	1395	34	940	34	--
34.5	1685	34.5	1398	34.5	945	34.5	--
35	1684	35	1400	35	951	35	--
35.5	1684	35.5	1403	35.5	952	35.5	--
36	1684	36	1410	36	953	36	--
36.5	1684	36.5	1414	36.5	953	36.5	--
37	1683	37	1418	37	953	37	--
37.5	1682	37.5	1424	37.5	953	37.5	--
38	1681	38	1430	38	953	38	--
38.5	1680	38.5	1437	38.5	953	38.5	--
39	1681	39	1447	39	953	39	--
39.5	1682	39.5	1458	39.5	953	39.5	--
40	1689	40	1472	40	953	40	--
40.5	1699	40.5	1492	40.5	953	40.5	--
41	1711	41	1512	41	953	41	--
41.5	1727	41.5	1521	41.5	953	41.5	--
42	1759	42	1530	42	--	42	--
42.5	1783	42.5	1531	42.5	--	42.5	--
43	1807	43	1532	43	--	43	--
43.5	1808	43.5	1533	43.5	--	43.5	--
44	1809	44	1534	44	--	44	--
44.5	1810	44.5	1535	44.5	--	44.5	--
45	1811	45	1536	45	--	45	--
45.5	1812	45.5	1537	45.5	--	45.5	--
46	1813	46	1538	46	--	46	--
46.5	1814	46.5	1539	46.5	--	46.5	--
47	1815	47	1540	47	--	47	--
47.5	1816	47.5	1541	47.5	--	47.5	--

Table-4.23 Data of Temperature (°C) vs. Surface tension (mN/m) plots for CPC (0.01M) and CPB (0.01M) in pure water

Surface tension of CPC (0.01M) in different temperature		Surface tension of CPB (0.01M) in different temperature	
Temperature (°C)	Surface tension (mN/m)	Temperature (°C)	Surface tension (mN/m)
2	42.1	4	49.6
4	41.9	6	49.3
6	41.7	8	49
8	41.4	10	48.5
10	41.1	12	47.8
12	40.7	14	46.9
14	40.3	16	46.1
16	39.8	18	45.2
18	39.3	20	44.2
19	39	22	42.9
20	38.7	24	41.5
22	38.7	26	40

24	38.7	28	38.5
26	38.7	29	37.6
28	38.8	30	36.7
30	38.8	32	36.7
		34	36.7
		36	36.8
		38	36.8
		40	36.9
		42	36.9

Table-4.24 Data of specific conductance versus concentration of CPC in pure water at 20, 25, 30, 35 °C

20°C		25°C		30°C		35°C	
Conc. of CPC (M)	Specific conductance (μS/cm)	Conc. of CPC (M)	Specific conductance (μS/cm)	Conc. of CPC (M)	Specific conductance (μS/cm)	Conc. of CPC (M)	Specific conductance (μS/cm)
8.65×10 <sup>-5</sup>	9.42	8.65×10 <sup>-5</sup>	9.87	8.65×10 <sup>-5</sup>	9.51	8.65×10 <sup>-5</sup>	9.6
1.71×10 <sup>-4</sup>	17.77	1.71×10 <sup>-4</sup>	18.13	1.71×10 <sup>-4</sup>	16.6	1.71×10 <sup>-4</sup>	17.92
2.54×10 <sup>-4</sup>	25	2.54×10 <sup>-4</sup>	25.2	2.54×10 <sup>-4</sup>	24.6	2.54×10 <sup>-4</sup>	25.1
3.36×10 <sup>-4</sup>	33.2	3.36×10 <sup>-4</sup>	33	3.36×10 <sup>-4</sup>	32.3	3.36×10 <sup>-4</sup>	32.8
4.16×10 <sup>-4</sup>	41.2	4.16×10 <sup>-4</sup>	40.6	4.16×10 <sup>-4</sup>	39.9	4.16×10 <sup>-4</sup>	40.6
4.95×10 <sup>-4</sup>	48.6	4.95×10 <sup>-4</sup>	48.1	4.95×10 <sup>-4</sup>	47.5	4.95×10 <sup>-4</sup>	48.3
5.72×10 <sup>-4</sup>	56.1	5.72×10 <sup>-4</sup>	55.5	5.72×10 <sup>-4</sup>	54.6	5.72×10 <sup>-4</sup>	55.7
6.47×10 <sup>-4</sup>	63.3	6.47×10 <sup>-4</sup>	62.5	6.47×10 <sup>-4</sup>	61.6	6.47×10 <sup>-4</sup>	63
7.21×10 <sup>-4</sup>	70.6	7.21×10 <sup>-4</sup>	69.6	7.21×10 <sup>-4</sup>	69.1	7.21×10 <sup>-4</sup>	70
7.94×10 <sup>-4</sup>	77.4	7.94×10 <sup>-4</sup>	76.5	7.94×10 <sup>-4</sup>	76.2	7.94×10 <sup>-4</sup>	77.1
8.66×10 <sup>-4</sup>	84.2	8.66×10 <sup>-4</sup>	83.2	8.66×10 <sup>-4</sup>	82	8.66×10 <sup>-4</sup>	83.8
9.36×10 <sup>-4</sup>	89.8	9.36×10 <sup>-4</sup>	89.1	9.36×10 <sup>-4</sup>	89	9.36×10 <sup>-4</sup>	90.2
1×10 <sup>-3</sup>	93.7	1×10 <sup>-3</sup>	93.4	1×10 <sup>-3</sup>	93.6	1×10 <sup>-3</sup>	95.8
0.00107	97.1	0.00107	96.8	0.00107	97.8	0.00107	100
0.00114	99.8	0.00114	99.9	0.00114	101.1	0.00114	103.7
0.0012	102.6	0.0012	103	0.0012	104.2	0.0012	107.2
0.00127	105.3	0.00127	105.7	0.00127	107.3	0.00127	110.2
0.00133	108.7	0.00133	108.8	0.00133	110.2	0.00133	113.5
0.00139	111.1	0.00139	111.3	0.00139	113.2	0.00139	116.4
0.00145	113.3	0.00145	113.7	0.00145	115.6	0.00145	119.3
0.00152	115.6	0.00152	116.1	0.00152	118	0.00152	121.9
0.00157	117.8	0.00157	118.6	0.00157	120.7	0.00157	124.6
0.00163	120.7	0.00163	120.9	0.00163	123.2	0.00163	127.3
0.00169	122.7	0.00169	123.4	0.00169	125.7	0.00169	130
0.0018	127.2	0.0018	127.7	0.0018	130.5	0.0018	134.9
0.00191	131.4	0.00191	132	0.00191	135.1	0.00191	139.4
0.00201	135.2	0.00201	135.9	0.00201	139.4	0.00201	144.3
0.00212	139.3	0.00212	140	0.00212	143.5	0.00212	148.8
0.00222	142.7	0.00222	143.8	0.00222	147.8	0.00222	

Table-4.25 Data of specific conductance versus concentration of CPC in pure water at 40, 45 °C

40°C		45°C	
Concentration of CPC (M)	Specific conductance (μS/cm)	Concentration of CPC (M)	Specific conductance (μS/cm)
8.65×10 <sup>-5</sup>	9.99	8.639×10 <sup>-5</sup>	9.66
1.71×10 <sup>-4</sup>	18.21	1.71×10 <sup>-4</sup>	18.02
2.54×10 <sup>-4</sup>	25.4	2.54×10 <sup>-4</sup>	25.2
3.36×10 <sup>-4</sup>	33.2	3.356×10 <sup>-4</sup>	33.3
4.16×10 <sup>-4</sup>	40.9	4.155×10 <sup>-4</sup>	41.3
4.95×10 <sup>-4</sup>	48.4	4.939×10 <sup>-4</sup>	48.9
5.72×10 <sup>-4</sup>	55.8	5.708×10 <sup>-4</sup>	56.5
6.47×10 <sup>-4</sup>	63.2	6.463×10 <sup>-4</sup>	63.8
7.21×10 <sup>-4</sup>	70.3	7.2×10 <sup>-4</sup>	71.1
7.94×10 <sup>-4</sup>	77.2	7.932×10 <sup>-4</sup>	78.3
8.66×10 <sup>-4</sup>	84.1	8.64×10 <sup>-4</sup>	85.2
9.36×10 <sup>-4</sup>	90.6	9.349×10 <sup>-4</sup>	92.2
1×10 <sup>-3</sup>	96.8	1×10 <sup>-3</sup>	98.7
0.00107	101.5	0.00107	104.7
0.00114	106.1	0.00113	109.8
0.0012	109.9	0.0012	114.4

0.00127	113.8	0.00126	118
0.00133	116.9	0.00133	122
0.00139	120.2	0.00139	125.3
0.00145	123.2	0.00145	128.8
0.00152	125.9	0.00151	131.8
0.00157	128.9	0.00157	134.9
0.00163	131.7	0.00163	137.5
0.00169	134.3	0.00168	140.6
0.0018	139.4	0.0018	145.8
0.00191	144.2	0.0019	150.8
0.00201	148.9	0.00201	155.7
0.00212	154.3	0.00211	160.8

Table-4.26 Data of specific conductance versus concentration of CPC in the presence of KF, KSCN, KBr and KI at 45°C

KF (0.005M)		KBr(0.005M)		KI (0.005M)		KSCN (0.005M)	
Concentration of CPC (M)	Specific conductance ( $\mu\text{S}/\text{cm}$ )	Concentration of CPC (M)	Specific conductance ( $\mu\text{S}/\text{cm}$ )	Concentration of CPC (M)	Specific conductance ( $\mu\text{S}/\text{cm}$ )	Concentration of CPC (M)	Specific conductance ( $\mu\text{S}/\text{cm}$ )
$6.862 \times 10^{-5}$	525	$3.289 \times 10^{-5}$	704	$6.578 \times 10^{-6}$	697	$6.578 \times 10^{-6}$	649
$1.346 \times 10^{-4}$	531	$6.493 \times 10^{-5}$	707	$1.298 \times 10^{-5}$	699	$1.298 \times 10^{-5}$	651
$1.98 \times 10^{-4}$	537	$9.615 \times 10^{-5}$	710	$1.923 \times 10^{-5}$	701	$1.923 \times 10^{-5}$	653
$2.59 \times 10^{-4}$	543	$1.265 \times 10^{-4}$	713	$2.531 \times 10^{-5}$	703	$2.531 \times 10^{-5}$	655
$3.181 \times 10^{-4}$	550	$1.562 \times 10^{-4}$	716	$3.125 \times 10^{-5}$	705	$3.125 \times 10^{-5}$	657
$3.75 \times 10^{-4}$	555	$1.851 \times 10^{-4}$	719	$3.703 \times 10^{-5}$	707	$3.703 \times 10^{-5}$	658
$4.29 \times 10^{-4}$	561	$2.134 \times 10^{-4}$	721	$4.268 \times 10^{-5}$	708	$4.268 \times 10^{-5}$	659
$4.827 \times 10^{-4}$	567	$2.409 \times 10^{-4}$	724	$4.819 \times 10^{-5}$	709	$4.819 \times 10^{-5}$	660
$5.33 \times 10^{-4}$	573	$2.678 \times 10^{-4}$	726	$5.357 \times 10^{-5}$	710	$5.357 \times 10^{-5}$	661
$5.83 \times 10^{-4}$	578	$2.941 \times 10^{-4}$	728	$5.882 \times 10^{-5}$	711	$5.882 \times 10^{-5}$	662
$6.311 \times 10^{-4}$	584	$3.197 \times 10^{-4}$	729	$6.395 \times 10^{-5}$	712	$6.395 \times 10^{-5}$	663
$6.77 \times 10^{-4}$	588	$3.448 \times 10^{-4}$	730	$6.896 \times 10^{-5}$	713	$6.896 \times 10^{-5}$	664
$7.22 \times 10^{-4}$	593	$3.693 \times 10^{-4}$	731	$7.386 \times 10^{-5}$	714	$7.386 \times 10^{-5}$	665
$7.65 \times 10^{-4}$	597	$3.932 \times 10^{-4}$	732	$7.865 \times 10^{-5}$	715	$7.865 \times 10^{-5}$	666
$8.07 \times 10^{-4}$	600	$4.166 \times 10^{-4}$	733	$8.333 \times 10^{-5}$	716	$8.333 \times 10^{-5}$	667
$8.484 \times 10^{-4}$	603	$4.395 \times 10^{-4}$	734	$8.791 \times 10^{-5}$		$8.791 \times 10^{-5}$	668
$8.88 \times 10^{-4}$	606	$4.619 \times 10^{-4}$	735	$9.239 \times 10^{-5}$		$9.239 \times 10^{-5}$	--
$9.26 \times 10^{-4}$	609	$4.838 \times 10^{-4}$	736	$9.677 \times 10^{-5}$		$9.677 \times 10^{-5}$	--
$9.63 \times 10^{-4}$	611	$5.053 \times 10^{-4}$	737	$1.019 \times 10^{-4}$		$1.019 \times 10^{-4}$	--
$1 \times 10^{-3}$	613	$5.263 \times 10^{-4}$	738	$1.052 \times 10^{-4}$		$1.052 \times 10^{-4}$	--
0.00103	616		--	$1.093 \times 10^{-4}$		$1.093 \times 10^{-4}$	--
0.00107	619		--	--		--	--
0.0011	621		--	--		--	--

Table-4.27 Data of specific conductance versus concentration of CPC in the presence of  $\text{KNO}_3$ ,  $\text{K}_2\text{CO}_3$ , and  $\text{K}_2\text{HPO}_4$  at 45°C

$\text{KNO}_3(0.005\text{M})$		$\text{K}_2\text{CO}_3(0.005 \text{ ionic strength})$		$\text{K}_2\text{HPO}_4(0.005 \text{ ionic strength})$	
Concentration of CPC (M)	Specific conductance ( $\mu\text{S}/\text{cm}$ )	Concentration of CPC (M)	Specific conductance ( $\mu\text{S}/\text{cm}$ )	Concentration of CPC (M)	Specific conductance ( $\mu\text{S}/\text{cm}$ )
0	666	0	435	0	381
$2.94 \times 10^{-5}$	669	$3.92 \times 10^{-5}$	437	$3.92 \times 10^{-5}$	385
$5.76 \times 10^{-5}$	673	$7.69 \times 10^{-5}$	440	$7.69 \times 10^{-5}$	389
$8.49 \times 10^{-5}$	677	$1.13 \times 10^{-4}$	443	$1.13 \times 10^{-4}$	392
$1.11 \times 10^{-4}$	679	$1.48 \times 10^{-4}$	446	$1.48 \times 10^{-4}$	394
$1.36 \times 10^{-4}$	682	$1.81 \times 10^{-4}$	448	$1.81 \times 10^{-4}$	397
$1.6 \times 10^{-4}$	685	$2.14 \times 10^{-4}$	450	$2.14 \times 10^{-4}$	401
$1.84 \times 10^{-4}$	687	$2.45 \times 10^{-4}$	452	$2.45 \times 10^{-4}$	403
$2.06 \times 10^{-4}$	689	$2.75 \times 10^{-4}$	453	$2.75 \times 10^{-4}$	406
$2.28 \times 10^{-4}$	690	$3.05 \times 10^{-4}$	453	$3.05 \times 10^{-4}$	408
$2.5 \times 10^{-4}$	691	$3.33 \times 10^{-4}$	453	$3.33 \times 10^{-4}$	410
$2.7 \times 10^{-4}$	692	$3.6 \times 10^{-4}$	453	$3.6 \times 10^{-4}$	412
$2.9 \times 10^{-4}$	693	$3.87 \times 10^{-4}$	453	$3.87 \times 10^{-4}$	413
$3.09 \times 10^{-4}$	694	$4.12 \times 10^{-4}$	453	$4.12 \times 10^{-4}$	414
$3.28 \times 10^{-4}$	695	$4.37 \times 10^{-4}$	453	$4.37 \times 10^{-4}$	415
$3.46 \times 10^{-4}$	696	$4.61 \times 10^{-4}$	453	$4.61 \times 10^{-4}$	416
$3.63 \times 10^{-4}$	697	$4.84 \times 10^{-4}$	453	$4.84 \times 10^{-4}$	417

$3.8 \times 10^{-4}$		$5.07 \times 10^{-4}$	453	$5.07 \times 10^{-4}$	418
$3.97 \times 10^{-4}$		$5.29 \times 10^{-4}$	453	$5.29 \times 10^{-4}$	419
$4.13 \times 10^{-4}$		$5.5 \times 10^{-4}$	453	$5.5 \times 10^{-4}$	420
$4.28 \times 10^{-4}$		$5.71 \times 10^{-4}$	--	$5.71 \times 10^{-4}$	421

Table-4.28 Data of specific conductance versus concentration of CPC in the presence of KCl at 25, 30, 35, 40 and 45 °C

Concentration of CPC (M)	KCl (0.005M)				
	25 °C Specific conductance (μS/cm)	30 °C Specific conductance (mS/cm)	35 °C Specific conductance (mS/cm)	40 °C Specific conductance (μS/cm)	45 °C Specific conductance (mS/cm)
$3.92 \times 10^{-5}$	702	702	705	703	694
$7.69 \times 10^{-5}$	705	706	708	708	698
$1.13 \times 10^{-4}$	708	710	712	711	703
$1.48 \times 10^{-4}$	712	713	716	714	707
$1.81 \times 10^{-4}$	716	715	719	718	711
$2.14 \times 10^{-4}$	719	718	722	721	714
$2.45 \times 10^{-4}$	721	721	725	725	718
$2.75 \times 10^{-4}$	723	724	728	728	722
$3.05 \times 10^{-4}$	725	726	730	730	726
$3.33 \times 10^{-4}$	727	728	732	732	729
$3.6 \times 10^{-4}$	728	729	734	734	733
$3.87 \times 10^{-4}$	729	730	735	736	735
$4.12 \times 10^{-4}$	730	731	736	738	737
$4.37 \times 10^{-4}$	731	732	737	739	739
$4.61 \times 10^{-4}$	732	733	738	740	741
$4.84 \times 10^{-4}$	733	734	739	741	743
$5.07 \times 10^{-4}$	734	735	740	742	745
$5.29 \times 10^{-4}$	735	736	741	743	747
$5.50 \times 10^{-4}$	736	737	742	744	749
$5.71 \times 10^{-4}$	737	738	743	745	751

Table4.29 Data of specific conductance versus concentration of CPC in the presence of K<sub>2</sub>SO<sub>4</sub> 15, 20, 25 and 30 °C

Concentration of CPC (M)	K <sub>2</sub> SO <sub>4</sub> (0.005 ionic strength)			
	15 °C Specific conductance (μS/cm)	20 °C Specific conductance (mS/cm)	25 °C Specific conductance (mS/cm)	30 °C Specific conductance (μS/cm)
0	476	469	464	462
$1.31 \times 10^{-5}$	477	470	465	463
$2.59 \times 10^{-5}$	478	471	466	464
$3.84 \times 10^{-5}$	479	472	467	465
$5.06 \times 10^{-5}$	480	473	468	466
$6.26 \times 10^{-5}$	481	474	469	467
$7.4 \times 10^{-5}$	482	475	470	468
$8.53 \times 10^{-5}$	483	476	471	469
$9.63 \times 10^{-5}$	484	477	472	470
$1.07 \times 10^{-4}$	485	478	473	471
$1.176 \times 10^{-4}$	486	479	474	472
$1.27 \times 10^{-4}$	487	480	475	473
$1.37 \times 10^{-4}$	487	481	476	474
$1.47 \times 10^{-4}$	488	481	476	475
$1.57 \times 10^{-4}$	488	481	477	476
$1.66 \times 10^{-4}$	489	482	477	476
$1.75 \times 10^{-4}$	489	482	477	477
$1.84 \times 10^{-4}$	489	482	478	477
$1.93 \times 10^{-4}$	490	483	478	477
$2.02 \times 10^{-4}$	490	483	478	478
$2.1 \times 10^{-4}$	490	483	479	478
$2.18 \times 10^{-4}$	491	484	479	478
$2.26 \times 10^{-4}$	491	484	479	479
$2.34 \times 10^{-4}$	491	484	480	479
$2.42 \times 10^{-4}$	492	485	480	479

Table-4.30 Data of specific conductance versus concentration of CPC in the presence of K<sub>2</sub>SO<sub>4</sub> 35, 40 and 45 °C

K <sub>2</sub> SO <sub>4</sub> (0.005 ionic strength)			
Concentration of CPC (M)	35 °C	40 °C	45 °C
	Specific conductance (μS/cm)	Specific conductance (mS/cm)	Specific conductance (mS/cm)
0	460	460	462
1.96×10 <sup>-5</sup>	462	462	464
3.84×10 <sup>-5</sup>	464	464	466
5.66×10 <sup>-5</sup>	465	466	468
7.4×10 <sup>-5</sup>	467	468	470
9.09×10 <sup>-5</sup>	469	470	472
1.07×10 <sup>-4</sup>	471	471	474
1.22×10 <sup>-4</sup>	472	472	476
1.37×10 <sup>-4</sup>	473	473	477
1.52×10 <sup>-4</sup>	474	474	479
1.66×10 <sup>-4</sup>	475	475	480
1.8×10 <sup>-4</sup>	476	476	481
1.93×10 <sup>-4</sup>	476	477	482
2.06×10 <sup>-4</sup>	476	477	483
2.18×10 <sup>-4</sup>	477	478	484
2.3×10 <sup>-4</sup>	477	478	485
2.42×10 <sup>-4</sup>	477	479	485
2.53×10 <sup>-4</sup>	478	479	486
2.64×10 <sup>-4</sup>	478	480	
2.75×10 <sup>-4</sup>	478	480	
2.85×10 <sup>-4</sup>	479	481	
2.95×10 <sup>-4</sup>	479	481	
3.05×10 <sup>-4</sup>	479	482	
3.15×10 <sup>-4</sup>	480	482	
3.24×10 <sup>-4</sup>	480	483	
3.33×10 <sup>-4</sup>	480	483	
3.42×10 <sup>-4</sup>	480	484	

Table-4.31 Data of specific conductance versus concentration of CPB in pure water at 30, 35, 40, 45 °C

Concentration of CPB (M)	30 °C	35 °C	40 °C	45 °C
	Specific conductance (μS/cm)	Specific conductance (μS/cm)	Specific conductance (μS/cm)	Specific conductance (μS/cm)
6.86×10 <sup>-5</sup>	7.36	7.38	7.39	7.4
1.346×10 <sup>-4</sup>	13.33	13.4	13.41	13.52
1.98×10 <sup>-4</sup>	19.16	19.24	19.25	19.37
2.592×10 <sup>-4</sup>	24.4	24.7	24.8	25.1
3.18×10 <sup>-4</sup>	29.7	30.1	30.2	30.5
3.75×10 <sup>-4</sup>	34.9	35.3	35.4	35.8
4.298×10 <sup>-4</sup>	39.8	40.2	40.4	40.9
4.827×10 <sup>-4</sup>	44.7	44.9	45.2	45.9
5.338×10 <sup>-4</sup>	49.2	49.4	49.9	50.5
5.83×10 <sup>-4</sup>	53.6	53.9	54.3	55.1
6.311×10 <sup>-4</sup>	58	58.3	58.8	59.3
6.774×10 <sup>-4</sup>	62	62.2	62.9	63.7
7.222×10 <sup>-4</sup>	65.3	66.3	66.9	67.8
7.656×10 <sup>-4</sup>	67.1	69.2	70.7	71.9
8.0769×10 <sup>-4</sup>	68.7	71.1	73.7	75.5
8.48×10 <sup>-4</sup>	69.9	72.7	75.4	78.5
8.88×10 <sup>-4</sup>	71.1	73.9	77.2	80.7
9.26×10 <sup>-4</sup>	72.1	75.1	78.7	82.5
9.63×10 <sup>-4</sup>	73.1	76.1	79.7	83.6
1×10 <sup>-3</sup>	74.1	77.1	80.8	85
0.00103	75	78.2	82.1	86.2
0.00107	76	79.1	83.1	87.8
0.0011	77	80.2	84.2	89.1
0.00113	77.9	81.2	85.1	90.1
0.00117	78.9	82.1	86.2	91.1

Table-4.32 Data of specific conductance versus concentration of CPB in the presence of KF, KCl, KI, and KSCN at 45°C

KF (0.005M)		KCl(0.005M)		KI(0.005M)		KSCN(0.005M)	
Concentration of CPB (M)	Specific conductance ( $\mu\text{S}/\text{cm}$ )	Concentration of CPB (M)	Specific conductance ( $\mu\text{S}/\text{cm}$ )	Concentration of CPB (M)	Specific conductance ( $\mu\text{S}/\text{cm}$ )	Concentration of CPB (M)	Specific conductance ( $\mu\text{S}/\text{cm}$ )
$6.862 \times 10^{-5}$	527	$3.92 \times 10^{-5}$	692	0	694	0	648
$1.346 \times 10^{-4}$	535	$7.69 \times 10^{-5}$	695	$6.578 \times 10^{-6}$	696	$6.578 \times 10^{-6}$	650
$1.98 \times 10^{-4}$	541	$1.13 \times 10^{-4}$	699	$1.298 \times 10^{-5}$	698	$1.298 \times 10^{-5}$	652
$2.59 \times 10^{-4}$	547	$1.48 \times 10^{-4}$	703	$1.923 \times 10^{-5}$	700	$1.923 \times 10^{-5}$	654
$3.18 \times 10^{-4}$	553	$1.81 \times 10^{-4}$	707	$2.531 \times 10^{-5}$	702	$2.531 \times 10^{-5}$	656
$3.75 \times 10^{-4}$	558	$2.14 \times 10^{-4}$	710	$3.125 \times 10^{-5}$	704	$3.125 \times 10^{-5}$	658
$4.29 \times 10^{-4}$	563	$2.45 \times 10^{-4}$	714	$3.703 \times 10^{-5}$	706	$3.703 \times 10^{-5}$	659
$4.82 \times 10^{-4}$	568	$2.75 \times 10^{-4}$	718	$4.268 \times 10^{-5}$	708	$4.268 \times 10^{-5}$	660
$5.33 \times 10^{-4}$	573	$3.05 \times 10^{-4}$	722	$4.819 \times 10^{-5}$	710	$4.819 \times 10^{-5}$	661
$5.83 \times 10^{-4}$	579	$3.33 \times 10^{-4}$	724	$5.357 \times 10^{-5}$	711	$5.357 \times 10^{-5}$	662
$6.31 \times 10^{-4}$	583	$3.6 \times 10^{-4}$	726	$5.882 \times 10^{-5}$	712	$5.882 \times 10^{-5}$	663
$6.77 \times 10^{-4}$	586	$3.87 \times 10^{-4}$	728	$6.395 \times 10^{-5}$	713	$6.395 \times 10^{-5}$	664
$7.22 \times 10^{-4}$	589	$4.12 \times 10^{-4}$	730	$6.896 \times 10^{-5}$	714	$6.896 \times 10^{-5}$	665
$7.65 \times 10^{-4}$	591	$4.37 \times 10^{-4}$	732	$7.386 \times 10^{-5}$	715	$7.386 \times 10^{-5}$	666
$8.07 \times 10^{-4}$	593	$4.61 \times 10^{-4}$	734	$7.865 \times 10^{-5}$	716	$7.865 \times 10^{-5}$	667
$8.48 \times 10^{-4}$	596	$4.84 \times 10^{-4}$	736	$8.333 \times 10^{-5}$	717		
$8.88 \times 10^{-4}$	599	$5.07 \times 10^{-4}$	738	$8.791 \times 10^{-5}$	718		
$9.26 \times 10^{-4}$	601	$5.29 \times 10^{-4}$	740	$9.239 \times 10^{-5}$	719		
$9.63 \times 10^{-4}$	603	$5.5 \times 10^{-4}$	742	$9.677 \times 10^{-5}$	720		
$1 \times 10^{-3}$	605	$5.71 \times 10^{-4}$	744	$1.019 \times 10^{-4}$	721		

Table-4.33 Data of specific conductance versus concentration of CPB in the presence of  $\text{K}_2\text{SO}_4$ ,  $\text{K}_2\text{CO}_3$ , and  $\text{K}_2\text{HPO}_4$  at 45°C

$\text{K}_2\text{SO}_4$ (0.005 ionic strength)		$\text{K}_2\text{CO}_3$ (0.005 ionic strength)		$\text{K}_2\text{HPO}_4$ (0.005 ionic strength)	
Concentration of CPB (M)	Specific conductance ( $\mu\text{S}/\text{cm}$ )	Concentration of CPC (M)	Specific conductance ( $\mu\text{S}/\text{cm}$ )	Concentration of CPC (M)	Specific conductance ( $\mu\text{S}/\text{cm}$ )
$1.973 \times 10^{-5}$	469	0	435	0	391
$3.896 \times 10^{-5}$	471	$3.92 \times 10^{-5}$	438	$3.92 \times 10^{-5}$	394
$5.769 \times 10^{-5}$	473	$7.69 \times 10^{-5}$	440	$7.69 \times 10^{-5}$	397
$7.594 \times 10^{-5}$	476	$1.13 \times 10^{-4}$	442	$1.13 \times 10^{-4}$	400
$9.345 \times 10^{-5}$	478	$1.48 \times 10^{-4}$	444	$1.48 \times 10^{-4}$	403
$1.111 \times 10^{-4}$	480	$1.81 \times 10^{-4}$	446	$1.81 \times 10^{-4}$	406
$1.28 \times 10^{-4}$	482	$2.14 \times 10^{-4}$	448	$2.14 \times 10^{-4}$	409
$1.445 \times 10^{-4}$	484	$2.45 \times 10^{-4}$	450	$2.45 \times 10^{-4}$	411
$1.607 \times 10^{-4}$	486	$2.75 \times 10^{-4}$	452	$2.75 \times 10^{-4}$	412
$1.764 \times 10^{-4}$	488	$3.05 \times 10^{-4}$	452	$3.05 \times 10^{-4}$	413
$1.918 \times 10^{-4}$	489	$3.33 \times 10^{-4}$	452	$3.33 \times 10^{-4}$	414
$2.068 \times 10^{-4}$	490	$3.6 \times 10^{-4}$	452	$3.6 \times 10^{-4}$	415
$2.215 \times 10^{-4}$	491	$3.87 \times 10^{-4}$	452	$3.87 \times 10^{-4}$	416
$2.359 \times 10^{-4}$	492	$4.12 \times 10^{-4}$	452	$4.12 \times 10^{-4}$	417
$2.5 \times 10^{-4}$	493	$4.37 \times 10^{-4}$	452	$4.37 \times 10^{-4}$	418
$2.637 \times 10^{-4}$	494	$4.61 \times 10^{-4}$	452	$4.61 \times 10^{-4}$	419
$2.771 \times 10^{-4}$	494	$4.84 \times 10^{-4}$	452	$4.84 \times 10^{-4}$	420
$2.903 \times 10^{-4}$	495	$5.07 \times 10^{-4}$	452		
$3.0319 \times 10^{-4}$	495	$5.29 \times 10^{-4}$	452		
$3.157 \times 10^{-4}$	496	$5.5 \times 10^{-4}$	452		
$3.281 \times 10^{-4}$	496				
$3.402 \times 10^{-4}$	497				
$3.52 \times 10^{-4}$	497				
$3.636 \times 10^{-4}$	498				
$3.75 \times 10^{-4}$	498				



Table-4.34 Data of specific conductance versus concentration of CPB in the presence of KBr at 25, 30, 35, 40 and 45°C

KBr (0.005M)			
Concentration of CPB (M)	35°C	40°C	45°C
	Specific conductance ( $\mu\text{S}/\text{cm}$ )	Specific conductance (mS/cm)	Specific conductance (mS/cm)
$1.973 \times 10^{-5}$	701	703	700
$3.896 \times 10^{-5}$	703	705	702
$5.769 \times 10^{-5}$	705	707	704
$7.594 \times 10^{-5}$	707	709	706
$9.345 \times 10^{-5}$	709	711	708
$1.111 \times 10^{-4}$	711	713	710
$1.28 \times 10^{-4}$	713	715	712
$1.445 \times 10^{-4}$	715	717	714
$1.607 \times 10^{-4}$	717	719	716
$1.764 \times 10^{-4}$	718	721	718
$1.918 \times 10^{-4}$	719	723	720
$2.068 \times 10^{-4}$	720	724	722
$2.215 \times 10^{-4}$	721	725	724
$2.359 \times 10^{-4}$	722	726	725
$2.5 \times 10^{-4}$	723	727	726
$2.637 \times 10^{-4}$	724	728	727
$2.771 \times 10^{-4}$	725	729	728
$2.903 \times 10^{-4}$	726	730	729
$3.0319 \times 10^{-4}$		731	730
$3.157 \times 10^{-4}$		732	731
$3.281 \times 10^{-4}$		733	732
$3.402 \times 10^{-4}$			733
$3.52 \times 10^{-4}$			734

Table-4.35 Data of specific conductance versus concentration of CPB in the presence of  $\text{KNO}_3$  at 15, 20, 25 and 30°C

$\text{KNO}_3$ (0.005M)				
Concentration of CPB (M)	20°C	25°C	30°C	35°C
	Specific conductance ( $\mu\text{S}/\text{cm}$ )	Specific conductance (mS/cm)	Specific conductance (mS/cm)	Specific conductance ( $\mu\text{S}/\text{cm}$ )
0	681	674	669	667
$2.94 \times 10^{-5}$	683	677	672	670
$5.76 \times 10^{-5}$	686	680	675	673
$8.49 \times 10^{-5}$	688	682	678	675
$1.11 \times 10^{-4}$	690	685	680	677
$1.36 \times 10^{-4}$	691	686	682	679
$1.6 \times 10^{-4}$	692	687	683	680
$1.84 \times 10^{-4}$	693	688	684	681
$2.06 \times 10^{-4}$	694	689	685	682
$2.28 \times 10^{-4}$	695	690	686	683
$2.5 \times 10^{-4}$	696	691	687	684
$2.7 \times 10^{-4}$	697	692	688	685
$2.9 \times 10^{-4}$			689	
$3.09 \times 10^{-4}$			690	
$3.28 \times 10^{-4}$			691	

Table-4.36 Data of specific conductance versus concentration of CPB in the presence of  $\text{KNO}_3$  35, 40, and 45°C

$\text{KNO}_3$ (0.005M)			
40°C		45°C	
Concentration of CPB (M)	Specific conductance ( $\mu\text{S}/\text{cm}$ )	Concentration of CPB (M)	Specific conductance (mS/cm)
0	664	0	661
$1.973 \times 10^{-5}$	667	$1.973 \times 10^{-5}$	664
$3.896 \times 10^{-5}$	669	$3.896 \times 10^{-5}$	667
$5.769 \times 10^{-5}$	672	$5.769 \times 10^{-5}$	669
$7.594 \times 10^{-5}$	674	$7.594 \times 10^{-5}$	671
$9.345 \times 10^{-5}$	676	$9.345 \times 10^{-5}$	673
$1.111 \times 10^{-4}$	678	$1.111 \times 10^{-4}$	675
$1.28 \times 10^{-4}$	681	$1.28 \times 10^{-4}$	677
$1.445 \times 10^{-4}$	684	$1.445 \times 10^{-4}$	680
$1.607 \times 10^{-4}$	686	$1.607 \times 10^{-4}$	682

$1.764 \times 10^{-4}$	688	$1.764 \times 10^{-4}$	684
$1.918 \times 10^{-4}$	689	$1.918 \times 10^{-4}$	686
$2.068 \times 10^{-4}$	690	$2.068 \times 10^{-4}$	688
$2.215 \times 10^{-4}$	691	$2.215 \times 10^{-4}$	689
$2.359 \times 10^{-4}$	692	$2.359 \times 10^{-4}$	690
$2.5 \times 10^{-4}$	693	$2.5 \times 10^{-4}$	691
$2.637 \times 10^{-4}$	694	$2.637 \times 10^{-4}$	692
$2.771 \times 10^{-4}$	695	$2.771 \times 10^{-4}$	693
$2.903 \times 10^{-4}$	696	$2.903 \times 10^{-4}$	694
$3.0319 \times 10^{-4}$	697	$3.0319 \times 10^{-4}$	695
$3.157 \times 10^{-4}$	--	$3.157 \times 10^{-4}$	696
$3.281 \times 10^{-4}$	--	$3.281 \times 10^{-4}$	697
$3.402 \times 10^{-4}$	--	$3.402 \times 10^{-4}$	698

## Surface tensiometric method

Table-4.37 Data of surface tension versus logarithm of concentration of aqueous solution of CPC at 20, 25, 30, 35, 40, and 45 °C

Log <sub>10</sub> C	20 °C	25 °C	30 °C	35 °C	40 °C	45 °C
	Surface tension (mN/m)	Surface tension (mN/m)	Surface tension (mN/m)	Surface tension (mN/m)	Surface tension (mN/m)	Surface tension (mN/m)
-3.929	62.1	62.8	63.1	63.8	64.4	65.1
-3.636	57.9	59.3	58.8	59.6	60.5	60.9
-3.469	53.7	54.2	55.2	55.7	56.4	57.2
-3.352	50.1	50.9	51.9	52.3	53.1	54.1
-3.263	46.7	47.7	49.3	49.4	50.6	51.6
-3.191	44.1	45.6	47.1	47.3	48.5	49.5
-3.132	42.2	43.3	45.4	45.5	46.8	47.8
-3.082	42	42.6	44.2	44.2	45.5	46.5
-3.038	42	42.4	42.7	43.1	44.4	45.3
-3	42	42.2	42.5	42.9	43.2	44.3
-2.965	42	42.2	42.5	42.8	43	43.3
-2.935	42	42.2	42.5	42.8	43	43.3
-2.907	42	42.2	42.5	42.8	43	43.3
-2.881	42	42.2	42.5	42.8	43	43.3
-2.858	42	42.2	42.5	42.8	43	43.3
-2.837	42	42.2	42.5	42.8	43	43.3
-2.817	42	42.2	42.5	42.8	43	43.3
-2.799	42	42.2	42.5	42.8	43	43.3
-2.781	42	42.2	42.5	42.8	43	43.3
-2.765	42	42.2	42.5	42.8	43	43.3

Table-4.38 Data of surface tension versus logarithm of concentration of aqueous solution of CPC in the presence of KF, KBr, KI at 45 °C

KF (0.005M)		KBr (0.005M)		KI (0.005M)	
Log <sub>10</sub> C	Surface tension (mN/m)	Log <sub>10</sub> C	Surface tension (mN/m)	Log <sub>10</sub> C	Surface tension (mN/m)
-4.054	51.9	-4.531	50.3	-5.406	45.1
-3.761	48.1	-4.238	44	-5.113	40.2
-3.593	45.6	-4.071	40.5	-4.946	37.3
-3.477	43.9	-3.954	37.9	-4.829	35.1
-3.388	42.6	-3.865	36.2	-4.74	33.7
-3.316	41.5	-3.793	34.6	-4.669	32.5
-3.257	40.6	-3.734	33.7	-4.609	31.6
-3.207	39.9	-3.684	33.6	-4.559	30.8
-3.163	39.3	-3.64	33.5	-4.515	30
-3.124	38.9	-3.602	33.5	-4.477	29.4
-3.09	38.9	-3.567	33.5	-4.442	28.8
-3.059	38.9	-3.537	33.5	-4.412	28.5
-3.032	38.9	-3.509	33.5	-4.384	28.5
-3	38.9	-3.483	33.5	-4.359	28.5
-2.98	38.9	-3.46	33.5	-4.335	28.5
-2.96	38.9	-3.439	33.5	-4.314	28.5

-2.94	38.9	-3.419	33.5	-4.29	28.5
-2.924	38.9	-3.401	33.5	-4.276	28.5

Table-4.39 Data of surface tension versus logarithm of concentration of aqueous solution of CPC in the presence of KSCN, K<sub>2</sub>CO<sub>3</sub>, K<sub>2</sub>HPO<sub>4</sub> at 45 °C

KSCN 0.005M		K <sub>2</sub> CO <sub>3</sub> 0.005 ionic strength		K <sub>2</sub> HPO <sub>4</sub> 0.005 ionic strength		KNO <sub>3</sub> 0.005M	
Log <sub>10</sub> C	Surface tension (mN/m)	Log <sub>10</sub> C	Surface tension (mN/m)	Log <sub>10</sub> C	Surface tension (mN/m)	Log <sub>10</sub> C	Surface tension (mN/m)
-5.4	45.7	-4.53	50.9	-4.7	49.4	-4.815	53.6
-5.113	40.2	-4.238	46.7	-4.4	43.7	-4.522	48.9
-4.946	36.8	-4.071	43.1	-4.23	40.6	-4.355	45.4
-4.829	34.6	-3.954	39.9	-4.11	38.1	-4.238	42.7
-4.74	32.9	-3.865	37.7	-4.02	36.6	-4.149	40.6
-4.669	31.7	-3.793	35.8	-3.946	35.2	-4.077	38.8
-4.609	31.6	-3.734	34.4	-3.88	35.3	-4.018	37.2
-4.559	31.6	-3.684	33.7	-3.82	35.3	-3.968	35.8
-4.515	31.6	-3.64	33.5	-3.78	35.3	-3.924	34.4
-4.477	31.6	-3.6	33.6	-3.74	35.3	-3.886	33.2
-4.442	31.6	-3.567	33.6	-3.7	35.3	-3.851	31.8
-4.412	31.6	-3.537	33.6	-3.66	35.3	-3.821	31.8
-4.384	31.6	-3.509	33.6	-3.6	35.3	-3.793	31.8
-4.359	31.6	-3.483	33.6	-3.55	35.3	-3.767	31.8
-4.335	31.6	-3.46	33.6	-3.51	35.3	-3.744	31.8
-4.314	31.6	-3.439	33.6	-3.47	35.3	-3.723	31.8
-4.29	31.6	-3.419	33.6	-3.44	35.3	-3.697	31.8
-4.276	31.6	-3.4	33.6	-3.41	35.3	-3.685	31.8
		-3.38	33.6	-3.38	35.3	-3.668	31.8
		-3.36	33.6	-3.35	35.3	-3.651	31.8

Table-4.40 Data of surface tension versus logarithm of concentration of aqueous solution of CPC in the presence of K<sub>2</sub>SO<sub>4</sub> at 20, 25, 30, 35, 40, and 45 °C

Log <sub>10</sub> C	K <sub>2</sub> SO <sub>4</sub> at 0.005 ionic strength					
	20 °C Surface tension (mN/m)	25 °C Surface tension (mN/m)	30 °C Surface tension (mN/m)	35 °C Surface tension (mN/m)	40 °C Surface tension (mN/m)	45 °C Surface tension (mN/m)
-4.707	51.5	52.3	52.9	53	53.6	53.6
-4.414	46.8	46.9	48.5	49	48.6	48.4
-4.247	43.4	43.5	45.7	46.4	45.4	45.3
-4.13	40.8	41.3	43.7	44.2	43.2	43.2
-4.041	39.2	39.5	41.8	42.2	41.4	41.4
-3.97	37.8	38.1	40.4	40.8	40.1	40.2
-3.91	37.8	38.1	39.2	39.7	39	39.3
-3.86	37.8	38.1	38.4	38.6	38.8	39
-3.816	37.8	38.1	38.4	38.5	38.8	39
-3.778	37.8	38.1	38.4	38.5	38.8	39
-3.743	37.8	38.1	38.3	38.5	38.8	39
-3.713	37.8	38.1	38.3	38.5	38.8	39
-3.685	37.8	38.1	38.3	38.5	38.8	39
-3.66	37.8	38.1	38.3	38.5	38.8	39
-3.636	37.8	38.1	38.3	38.5	38.8	39
-3.606	37.8	38.1	38.3	38.5	38.8	39
-3.595	37.8	38.1	38.3	38.5	38.8	39
-3.577	37.8	38.1	38.3	38.5	38.8	39

Table-4.41 Data of surface tension versus logarithm of concentration of aqueous solution of CPC in the presence of KCl at 25, 30, 35, 40, and 45°C

Log <sub>10</sub> C	KCl (0.005M)				
	25°C	30°C	35°C	40°C	45°C
	Surface tension (mN/m)	Surface tension (mN/m)	Surface tension (mN/m)	Surface tension (mN/m)	Surface tension (mN/m)
-4.406	49.8	51.8	52.3	52.9	53.9
-4.113	46	47.4	47.7	47.5	49.1
-3.946	43.4	44.2	44.2	44.3	45.3
-3.829	41.2	41.7	41.8	42.1	42.9
-3.74	39.5	39.9	39.9	40.5	40.7
-3.669	38	38.4	38.3	39	39.3
-3.609	36.7	37.1	37	37.7	38.1
-3.559	35.6	36	36	36.7	37.1
-3.515	35.6	35.8	36	36.5	36.8
-3.477	35.6	35.8	36	36.5	36.8
-3.442	35.6	35.8	36	36.5	36.8
-3.412	35.6	35.8	36	36.5	36.8
-3.384	35.6	35.8	36	36.5	36.8
-3.359	35.6	35.8	36	36.5	36.8
-3.335	35.6	35.8	36	36.5	36.8
-3.314	35.6	35.8	36	36.5	36.8
-3.294	35.6	35.8	36	36.5	36.8
-3.276	35.6	35.8	36	36.5	36.8
-3.259	35.6	35.8	36	36.5	36.8
-3.243	35.6	35.8	36	36.5	36.8

Table-4.42 Data of surface tension versus logarithm of concentration of aqueous solution of CPB at 30, 35, 40, and 45°C

Log <sub>10</sub> C	30°C	35°C	40°C	45°C
	Surface tension (mN/m)	Surface tension (mN/m)	Surface tension (mN/m)	Surface tension (mN/m)
-4.105	65	65.2	65.3	65.6
-3.812	59	60.1	60.5	61.2
-3.645	54	55.2	55.7	57.6
-3.528	50.3	51.3	52.3	54.8
-3.439	47	48	49.5	52.3
-3.367	44.2	45.7	46.6	50
-3.308	41.9	43	44.1	47.7
-3.258	39.9	41.4	41.9	45.6
-3.214	38.4	39.2	40.1	43.5
-3.176	37.1	38.1	38.7	41.6
-3.141	37	37.5	37.8	40.2
-3.111	37	37.4	37.5	39.1
-3.083	37	37.3	37.5	38.5
-3.057	37	37.3	37.5	38.4
-3.034	37	37.3	37.5	38.4
-3.013	37	37.3	37.5	38.4
-2.993	37	37.3	37.5	38.4
-2.97	37	37.3	37.5	38.4
-2.95	37	37.3	37.5	38.4
-2.94	37	37.3	37.5	38.4

Table-4.43 Data of surface tension versus logarithm of concentration of aqueous solution of CPB in the presence of KF, KCl, KI at 45°C

KF (0.005M)		KCl (0.005M)		KI(0.005M)	
Log <sub>10</sub> C	Surface tension (mN/m)	Log <sub>10</sub> C	Surface tension (mN/m)	Log <sub>10</sub> C	Surface tension (mN/m)
-4.15	54	-4.406	51.5	-5.23	49.9
-3.858	48.5	-4.113	46.4	-4.93	44
-3.69	45.2	-3.946	43.6	-4.77	40.9
-3.57	42.8	-3.829	41.5	-4.653	37.8

-3.485	41.1	-3.74	40	-4.564	35.9
-3.413	39.8	-3.669	38.8	-4.492	34.4
-3.35	38.5	-3.609	37.8	-4.383	32.1
-3.304	37.6	-3.559	37.5	-4.339	31.1
-3.26	36.8	-3.515	37.4	-4.3	30.4
-3.221	36.5	-3.477	37.4	-4.266	30.4
-3.187	36.4	-3.442	37.4	-4.236	30.3
-3.156	36.4	-3.412	37.4	-4.208	30.3
-3.129	36.3	-3.384	37.4	-4.182	30.3
-3.103	36.3	-3.359	37.4	-4.159	30.3
-3.08	36.3	-3.335	37.4		
-3.059	36.3	-3.314	37.4		
-3.039	36.3	-3.294	37.4		
-3.02	36.3	-3.276	37.4		
		-3.259	37.4		
		-3.243	37.4		

Table-4.44 Data of surface tension versus logarithm of concentration of aqueous solution of CPB in the presence of KSCN, K<sub>2</sub>CO<sub>3</sub>, K<sub>2</sub>HPO<sub>4</sub>, and K<sub>2</sub>SO<sub>4</sub> at 45 °C

KSCN 0.005 ionic strength		K <sub>2</sub> CO <sub>3</sub> 0.005 ionic strength		K <sub>2</sub> HPO <sub>4</sub> 0.005 ionic strength		K <sub>2</sub> SO <sub>4</sub> 0.005 ionic strength	
Log <sub>10</sub> C	Surface tension (mN/m)	Log <sub>10</sub> C	Surface tension (mN/m)	Log <sub>10</sub> C	Surface tension (mN/m)	Log <sub>10</sub> C	Surface tension (mN/m)
-5.4	44.1	-4.53	53.6	-4.53	45.3	-4.82	49.6
-5.113	38.8	-4.238	46.9	-4.238	40.6	-4.53	44.9
-4.946	35.5	-4.071	42.5	-4.071	37.8	-4.35	41.8
-4.829	32.6	-3.954	39.6	-3.954	35.5	-4.23	39.9
-4.74	30.9	-3.865	37.4	-3.865	34.1	-4.14	38.5
-4.669	29.3	-3.793	35.5	-3.793	34.2	-4.07	37.6
-4.609	28.9	-3.734	34	-3.734	34.2	-4	37.4
-4.559	28.9	-3.684	33.6	-3.684	34.2	-3.954	37.3
-4.515	28.8	-3.64	33.5	-3.64	34.2	-3.907	37.3
-4.477	28.8	-3.6	33.5	-3.6	34.2	-3.865	37.3
-4.442	28.8	-3.567	33.5	-3.567	34.2	-3.827	37.3
-4.412	28.8	-3.537	33.5	-3.537	34.2	-3.793	37.3
-4.384	28.8	-3.509	33.5	-3.509	34.2	-3.76	37.3
-4.359	28.8	-3.483	33.5	-3.483	34.2	-3.734	37.3
-4.335	28.8	-3.46	33.5	-3.46	34.2	-3.684	37.3
-4.314	28.8	-3.439	33.5	-3.439	34.2	-3.64	37.3
-4.29	28.8	-3.419	33.5	-3.419	34.2	-3.6	37.3
-4.276	28.8	-3.4	33.5	-3.4	34.2	-3.567	37.3
		-3.38	33.5	-3.38	34.2	-3.537	37.3
		-3.36	33.5	-3.36	34.2		

Table-4.45 Data of surface tension versus logarithm of concentration of aqueous solution of CPB in the presence of KNO<sub>3</sub> at 20, 25, 30, 35, 40, and 45 °C

Log <sub>10</sub> C	KNO <sub>3</sub> (0.005 M)					
	20 °C Surface tension (mN/m)	25 °C Surface tension (mN/m)	30 °C Surface tension (mN/m)	35 °C Surface tension (mN/m)	40 °C Surface tension (mN/m)	45 °C Surface tension (mN/m)
-4.804	48.9	49.3	51	52.8	53.7	55.1
-4.511	42.7	43.3	45.3	47.4	48.6	49.6
-4.344	38.8	39.5	42.1	43.9	45.3	46.1
-4.227	35.9	36.9	39.6	41.1	42.6	43.5
-4.138	34	35	37.6	38.9	40.5	41.3
-4.066	32.6	33.4	36	37.3	38.6	39.5
-4.007	32	32.5	34.7	35.7	37	37.9
-3.957	31.9	32.2	33.5	34.3	35.6	36.6
-3.913	31.9	32.2	32.6	33	34.3	35.7
-3.875	31.8	32.2	32.5	32.9	33.3	34.7
-3.84	31.8	32.2	32.5	32.8	33.3	33.9
-3.81	31.8	32.2	32.5	32.8	33.3	33.6
-3.782	31.8	32.2	32.5	32.8	33.3	33.5

-3.756	31.8	32.2	32.5	32.8	33.3	33.5
-3.733	31.8	32.2	32.5	32.8	33.3	33.5
-3.712	31.8	32.2	32.5	32.8	33.3	33.5
-3.692	31.8	32.2	32.5	32.8	33.3	33.5

Table-4.46 Data of surface tension versus logarithm of concentration of aqueous solution of CPB in the presence of KBr at 35, 40, and 45°C

Log <sub>10</sub> C	KBr (0.005M)		
	35°C	40°C	45°C
	Surface tension (mN/m)	Surface tension (mN/m)	Surface tension (mN/m)
-4.531	49.9	50.9	50.5
-4.238	44.4	45.4	45.6
-4.071	40.4	41.7	41.8
-3.954	37.8	39.2	39.4
-3.865	35.9	37.1	37.4
-3.793	34	35.6	35.8
-3.734	33.5	34.5	34.6
-3.684	33.4	33.9	33.6
-3.64	33.4	33.6	33.5
-3.602	33.4	33.6	33.5
-3.567	33.4	33.5	33.5
-3.537	33.4	33.5	33.5
-3.509	33.4	33.5	33.5
-3.483	33.4	33.5	33.5
-3.46	33.4	33.5	33.5
-3.439	33.4	33.5	33.5
-3.419	33.4	33.5	33.5
-3.401	33.4	33.5	33.5

Table-4.47 Data of surface excess concentration vs. temperature plots of CPC in pure water and in presence of KCl and K<sub>2</sub>SO<sub>4</sub> at 0.005 ionic strength

Temperature (°C)	Surface excess concentration ( $\times 10^{-6}$ molm <sup>-2</sup> )		
	CPC in pure water	CPC in the presence of 0.005 M KCl	CPC in the presence of K <sub>2</sub> SO <sub>4</sub> at 0.005 ionic strength
20	3.21	--	1.81
25	2.98	1.887	1.73
30	2.49	1.856	1.675
35	2.38	1.81	1.67
40	2.317	1.758	1.63
45	2.314	1.63	1.48

Table-4.48 Data of surface excess concentration vs. temperature plots of CPB in pure water and in presence of 0.005 M KNO<sub>3</sub> and KBr

Temperature (°C)	Surface excess concentration ( $\times 10^{-6}$ molm <sup>-2</sup> )		
	CPB in pure water	CPB in the presence of 0.005 M KBr	CPB in the presence of 0.005M KNO <sub>3</sub>
293	--	--	2.14
298	--	--	2.08
303	3.24	--	2
308	3.14	1.84	1.98
313	3.07	1.76	1.95
318	2.93	1.72	1.82

**Solubilization data**

Table-4.49 Data of calibration curve of PAN in aqueous solution of CPB

Concentration of PAN	Absorbance
$6.41 \times 10^{-6}$	0.105
$1.925 \times 10^{-5}$	0.297
$3.209 \times 10^{-5}$	0.524
$4.49 \times 10^{-5}$	0.733
$5.77 \times 10^{-5}$	0.924
$9.628 \times 10^{-5}$	1.538
$1.28 \times 10^{-4}$	2.004
$1.6 \times 10^{-4}$	2.355

Table-4.50 Data of calibration curve of PAN in aqueous solution of CPB

Concentration of CPB	Absorbance of PAN
0.0000	0.013
$4.23 \times 10^{-4}$	0.033
$5.23 \times 10^{-4}$	0.035
$6.23 \times 10^{-4}$	0.037
$7.23 \times 10^{-4}$	0.093
$8.23 \times 10^{-4}$	0.124
$9.23 \times 10^{-4}$	0.18
0.00123	0.375
0.00223	1.088
0.00323	1.732

Table-4.51 Data of calibration curve of PAN in aqueous solution of CPB in the presence of  $\text{KNO}_3$ 

Concentration of CPB	Absorbance of PAN(in the presence of 0.005M $\text{KNO}_3$ )
0.000	0.078
$1 \times 10^{-5}$	0.084
$5 \times 10^{-5}$	0.092
$1 \times 10^{-4}$	0.094
$1.5 \times 10^{-4}$	0.101
$2 \times 10^{-4}$	0.145
$2.5 \times 10^{-4}$	0.179
$3.5 \times 10^{-4}$	0.251
$4 \times 10^{-4}$	0.305

Table-4.52 Data of calibration curve of curcumin in aqueous solution of CPC in aqueous solution

Concentration of curcumin	Absorbance
$5.42 \times 10^{-6}$	0.115
$1.085 \times 10^{-5}$	0.228
$1.628 \times 10^{-5}$	0.334
$2.171 \times 10^{-5}$	0.461
$2.71 \times 10^{-5}$	0.594

Table-4.53 Data of calibration curve of curcumin in aqueous solution of CPC in the presence of  $\text{KNO}_3$ 

Concentration of CPC	Absorbance of curcumin
0	0.03
$6 \times 10^{-5}$	0.071
$1 \times 10^{-4}$	0.091
$1.2 \times 10^{-4}$	0.095
$1.4 \times 10^{-4}$	0.097
$1.6 \times 10^{-4}$	0.301
$2 \times 10^{-4}$	0.494
$3 \times 10^{-4}$	0.925
$4 \times 10^{-4}$	1.551
$6 \times 10^{-4}$	2.587
$8 \times 10^{-4}$	3.355

Table-4.54 Data of calibration curve of curcumin in aqueous solution of CPC in the presence of  $K_2SO_4$  at 0.005 ionic strength

Concentration of CPC	Absorbance of curcumin(in the presence of $K_2SO_4$ )
0.000	000
$1.4 \times 10^{-4}$	1.698
$1.5 \times 10^{-4}$	1.731
$1.6 \times 10^{-4}$	1.743
$1.8 \times 10^{-4}$	1.791
$1.9 \times 10^{-4}$	2.048
$2.0 \times 10^{-4}$	2.278
$2.2 \times 10^{-4}$	2.8

Table-4.55 Data of  $Cu^{2+}$ - curcumin complex in aqueous solution of CPC when concentration of Curcumin is constant

Concentration of $CuSO_4$ (M) when concentration of Curcumin is constant	Absorbance
$7.9776 \times 10^{-6}$	0.244
$9.3072 \times 10^{-6}$	0.302
$1.063 \times 10^{-5}$	0.333
$1.1966 \times 10^{-5}$	0.386
$1.329 \times 10^{-5}$	0.432
$1.9944 \times 10^{-5}$	0.754
$2.659 \times 10^{-5}$	0.823
$3.324 \times 10^{-5}$	0.95
$3.9888 \times 10^{-5}$	0.981
$4.6536 \times 10^{-5}$	1.012
$5.318 \times 10^{-5}$	1.098

Table-4.56 Data of  $Cu^{2+}$ - curcumin complex in aqueous solution of CPC when concentration of  $CuSO_4$  is constant

Concentration of Curcumin (M) when concentration of $CuSO_4$ is constant	Absorbance
$5.4565 \times 10^{-6}$	0.052
$1.0912 \times 10^{-5}$	0.142
$2.182 \times 10^{-5}$	0.341
$3.2736 \times 10^{-5}$	0.535
$4.3648 \times 10^{-5}$	0.715

Table-4.57 Data of calibration curve of  $Cu^{2+}$ - curcumin complex in aqueous solution of CPC

Concentration of $CuSO_4$ (M) at constant concentration of Curcumin ( $8.148 \times 10^{-3} M$ )	Absorbance
$8.4 \times 10^{-6}$	0.317
$1.008 \times 10^{-5}$	0.383
$1.176 \times 10^{-5}$	0.461
$1.344 \times 10^{-5}$	0.523
$1.512 \times 10^{-5}$	0.565
$1.68 \times 10^{-5}$	0.638
$2.016 \times 10^{-5}$	0.692
$2.52 \times 10^{-5}$	0.849
$3.024 \times 10^{-5}$	0.919
$3.36 \times 10^{-5}$	0.951

Table-4.58 Data of  $Cu^{2+}$ - PAN complex in aqueous solution of CPB when concentration of PAN is constant ( $2 \times 10^{-5} M$ )

Concentration of $CuSO_4$ (M) when concentration of PAN is constant	Absorbance
$2 \times 10^{-6}$	0.043
$4 \times 10^{-6}$	0.096
$6 \times 10^{-6}$	0.147
$8 \times 10^{-6}$	0.188
$1 \times 10^{-5}$	0.235
$1.2 \times 10^{-5}$	0.278
$1.4 \times 10^{-5}$	0.328
$2 \times 10^{-5}$	0.043
$4 \times 10^{-5}$	0.096
$6 \times 10^{-5}$	0.147



$8 \times 10^{-5}$	0.188
$1 \times 10^{-5}$	0.235
$1.2 \times 10^{-5}$	0.278
$1.4 \times 10^{-5}$	0.328

Table-4.59 Data of  $\text{Cu}^{2+}$ - PAN complex in aqueous solution of CPB when concentration of  $\text{CuSO}_4$  is constant ( $2 \times 10^{-5} \text{M}$ )

Concentration of $\text{CuSO}_4$ (M)	Absorbance
$2 \times 10^{-6}$	0.072
$4 \times 10^{-6}$	0.12
$6 \times 10^{-6}$	0.173
$8 \times 10^{-6}$	0.226
$1 \times 10^{-5}$	0.259
$1.2 \times 10^{-5}$	0.31
$1.4 \times 10^{-5}$	0.349

Table-4.60 Data of calibration curve of  $\text{Cu}^{2+}$ - PAN complex in aqueous solution of CPB

Concentration of $\text{CuSO}_4$ (M) when concentration of PAN is constant ( $2.5 \times 10^{-4} \text{M}$ )	Absorbance
$8 \times 10^{-7}$	0.015
$1.6 \times 10^{-6}$	0.035
$2 \times 10^{-6}$	0.045
$4 \times 10^{-6}$	0.101
$8 \times 10^{-6}$	0.188
$1.2 \times 10^{-5}$	0.278
$1.6 \times 10^{-5}$	0.357

Table-4.61 Data of  $\text{Ni}^{2+}$ - PAN complex in aqueous solution of CPB when concentration of PAN is constant

Concentration of $\text{NiSO}_4$ (M) when concentration of PAN is constant	Absorbance
$4 \times 10^{-6}$	0.168
$8 \times 10^{-6}$	0.301
$1.2 \times 10^{-5}$	0.409
$1.6 \times 10^{-5}$	0.523
$1.8 \times 10^{-5}$	0.582

Table-4.62 Data of  $\text{Ni}^{2+}$ - PAN complex in aqueous solution of CPC when concentration of  $\text{NiSO}_4$  is constant

Concentration of PAN (M) when concentration of $\text{NiSO}_4$ is constant	Absorbance
$4 \times 10^{-6}$	0.043
$8 \times 10^{-6}$	0.159
$1.2 \times 10^{-5}$	0.265
$1.6 \times 10^{-5}$	0.364
$2 \times 10^{-5}$	0.461

Table-4.63 Data of calibration curve of  $\text{Ni}^{2+}$ - PAN complex in aqueous solution of CPB

Concentration of $\text{NiSO}_4$ (M) at constant concentration of PAN ( $1.25 \times 10^{-4} \text{M}$ )	Absorbance
$1.276 \times 10^{-6}$	0.055
$2.552 \times 10^{-6}$	0.119
$3.828 \times 10^{-6}$	0.174
$5.104 \times 10^{-6}$	0.24
$6.38 \times 10^{-6}$	0.291
$7.656 \times 10^{-6}$	0.345
$1.0208 \times 10^{-5}$	0.461
$1.276 \times 10^{-5}$	0.569

Table-4.64 Data of  $Zn^{2+}$  - PAN complex in aqueous solution of CPB when concentration of PAN is constant

Concentration of $ZnSO_4$ (M) when concentration of PAN is constant	Absorbance
$4 \times 10^{-6}$	0.153
$8 \times 10^{-6}$	0.209
$1.2 \times 10^{-5}$	0.287
$1.6 \times 10^{-5}$	0.35
$2 \times 10^{-5}$	0.409
$2.4 \times 10^{-5}$	0.506
$4 \times 10^{-5}$	0.153
$8 \times 10^{-5}$	0.209
$1.2 \times 10^{-5}$	0.287
$1.6 \times 10^{-5}$	0.35
$2 \times 10^{-5}$	0.409
$2.4 \times 10^{-5}$	0.506

Table-4.65 Data of  $Zn^{2+}$  - PAN complex in aqueous solution of CPB when concentration of  $ZnSO_4$  is constant

Concentration of PAN (M) when concentration of $ZnSO_4$ is constant	Absorbance
$8 \times 10^{-6}$	0.078
$1.2 \times 10^{-5}$	0.152
$1.6 \times 10^{-5}$	0.234
$2 \times 10^{-5}$	0.294
$2.4 \times 10^{-5}$	0.364

Table-4.66 Data of calibration curve of  $Zn^{2+}$  - PAN complex in aqueous solution of CPB

Concentration of $ZnSO_4$ (M) at constant concentration of PAN ( $2.5 \times 10^{-4} M$ )	Absorbance
$1.251 \times 10^{-6}$	0.071
$2.503 \times 10^{-6}$	0.126
$3.7548 \times 10^{-6}$	0.198
$5.264 \times 10^{-6}$	0.26
$6.258 \times 10^{-6}$	0.305
$7.5 \times 10^{-6}$	0.375
$1.001 \times 10^{-5}$	0.505

## CALCULATION

### Micellization

#### Counter ion binding calculation

$$\beta = (1 - \alpha)$$

$$\alpha = \frac{\text{Slope of postmicellar zone}}{\text{Slope of premicellar zone}}$$

Example: At 303K in aqueous solution of CPC

The value of post-micellar region = 28572.13 (by taking the Fit Linear)

The value of pre-micellar region = 89390.68 (by taking the Fit Linear)

$$\text{Now, } \alpha = \frac{42436.38767}{94259.446} = 0.4502$$

$$\text{So, } \beta = 0.549$$

**Note:** In all temperatures and in all medium  $\alpha$  values were calculated in the same way.

### Thermodynamic parameters calculation for CPC in aqueous solution

#### Mole fraction calculation

At 303K, the CMC of CPC in aqueous solution = 1 mM. During this CMC value the total volume of the solution is (50+6.5) mL = 56.5 ml.

1000 ml 1M CPC solution contains = 358.01 gm CPC

$$\text{So, 56.5 ml 1mM CPC solution contains} = \frac{358.01 \times 56.5 \times 0.001}{1000} = 0.0202 \text{ gm CPC}$$

$$\text{Mole of CPC} = \frac{0.0202}{358.01} = 5.65 \times 10^{-5}$$

$$\text{Mole of water} = \frac{56.5}{18} = 3.1388$$

$$\text{Total mole} = 3.1388 + 5.65 \times 10^{-5} = 3.1389$$

$$\text{Mole fraction of CPC at CMC} = (5.65 \times 10^{-5}) / 3.1389 = 1.7999 \times 10^{-5}$$

$$\text{At 303K, } \ln X_{\text{CMC}} = -10.9251$$

**Note:** All the calculation for mole fraction has been calculated in the same way for CPC and CPB in aqueous solution.

### Free energy of micellization ( $\Delta G_{mic}^o$ )

$$\begin{aligned} \text{At } 303\text{K, } (\Delta G_{mic}^o)_{303} &= (1 + \beta) RT \ln(\text{CMC}) = (1+0.549) \times 8.314 \times 303 \times (-10.9251) \\ &= -42.465 \text{ kJmol}^{-1} \end{aligned}$$

**Note:** All the calculation for free energy of micellization ( $\Delta G_{mic}^o$ ) has been calculated in the same way for CPC and CPB in aqueous solution.

### Entropy ( $\Delta S_{mic}^o$ ) Calculation

$$\text{We know } (\Delta S_{mic}^o) = - \left\{ \frac{\partial(\Delta G_{mic}^o)}{\partial T} \right\}_P$$

Now, plotting the T vs.  $\Delta G_{mic}^o$  graph for aqueous solution of CPC in excel sheet we get an equation like

$$\Delta G_{mic}^o = 0.0267 T^2 - 16.689 T + 2566.8$$

$$\frac{\partial(\Delta G_{mic}^o)}{\partial T} = 2 \times 0.0267 \times T - 16.689$$

$$\text{When } T = 303\text{K then } \frac{\partial(\Delta G_{mic}^o)}{\partial T} = -1.0428$$

So for T = 303K

$$(\Delta S_{mic}^o)_{303} = 1.0428 \text{ kJmol}^{-1}\text{K}^{-1}$$

**Note:** The same way has been followed for all calculations at different temperatures for CPC and CPB in aqueous solution.

### Enthalpy ( $\Delta H_{mic}^o$ )<sub>303</sub> Calculation

$$\text{We know, } \Delta G_{mic}^o = \Delta H_{mic}^o - T \Delta S_{mic}^o$$

$$\text{At } 303\text{K, } \Delta H_{mic}^o = \frac{303 \times 1.0428 - 42.465}{1000} = 111.70 \text{ kJ/mol}$$

$$\text{So, } \Delta H_{mic}^o = 111.70 \text{ kJ/mol}$$

Note: In such a way we can calculate the value of  $\Delta H_{mic}^o$  for CPC and CPB in aqueous solutions at different temperatures.

### Adsorption

#### Thermodynamic parameters calculation for aqueous CPC solution

#### Surface Excess Concentration: (from surface tension data)

$$\Gamma_{\max.} = - \frac{1}{2RT} \left( \frac{\partial \gamma}{\partial \ln C} \right)_{T,P} = - \frac{1}{2.303 \times 2RT} \left( \frac{\partial \gamma}{\partial \log C} \right)_{T,P}$$

In aqueous solution and in salt solution the way of calculation of Surface Excess Concentration  $\Gamma_{\max}$  is same.

Example: At 303K in aqueous CPC solution

Here the value of  $(\frac{\partial\gamma}{\partial\log c}) = -28.891$  ( from the slope of the surface tension data, calculated by Fit Linear)

$$\Gamma_{\max} = -\frac{1 \times (-28.891)}{2.303 \times 2 \times 8.314 \times 303 \times 1000} = 2.49 \times 10^{-6} \text{ mol/m}^2$$

**Note:** In all temperatures and in all medium  $\Gamma_{\max}$  value is calculated in the same way.

### **Equilibrium surface pressure**

$$\pi_{\text{cmc}} = \gamma_o - \gamma_{\text{cmc}}$$

At 303K for aqueous CPC solution

$$\gamma_o = 72.0 \text{ mN/m, and } \gamma_{\text{cmc}} = 43 \text{ mN/m}$$

$$\text{So, } \pi_{\text{cmc}} = 29 \text{ mN/m}$$

**Note:** In all temperatures and in all medium  $\pi_{\text{cmc}}$  value is calculated in the same way.

### **Free energy of adsorption ( $\Delta G_{ad}^o$ )**

$$\Delta G_{ad}^o = (\Delta G_{mic}^o) - (\pi_{\text{cmc}} / \Gamma_{\max})$$

At 303K for aqueous solution of CPC

$$\Delta G_{ad}^o = (-42.465 - 11.646) = -54.111 \text{ kJ/mol}$$

**Note:** In all temperatures and in all medium ( $\Delta G_{ad}^o$ ) value is calculated in the same way.

### **Entropy ( $\Delta S_{ad}^o$ ) calculation**

This calculation is done in the same way as micellization of CPC in aqueous solution.

### **Enthalpy ( $\Delta H_{ad}^o$ ) calculation**

This calculation is done in the same way as micellization of CPC in aqueous solution.

## **Solubilization**

### **Calculation of MSR at 298K for CPB**

To get a calibration curve, at first, a fixed amount of dye was dissolved in a fixed amount of CPB but several times higher concentration than CMC. The amount of dye to be like that it remains below to that of the solubilization equilibrium with surfactant micelle. Then carrying out the UV-spectra, we get the following data-

**Table-4.67 Data of calibration curve of PAN in aqueous solution of CPB**

Concentration of CPB	Absorbance of PAN
0.0000	0.013
$4.23 \times 10^{-4}$	0.033
$5.23 \times 10^{-4}$	0.035
$6.23 \times 10^{-4}$	0.037
$7.23 \times 10^{-4}$	0.093
$8.23 \times 10^{-4}$	0.124
$9.23 \times 10^{-4}$	0.18
0.00123	0.375
0.00223	1.088
0.00323	1.732

Molar mass of PAN is 249.27 g

249.27 g 1000 ml = 1 M

By solubilizing PAN (fixed amount) at different concentration (above and below CMC value) of CPB we get the following data from UV-spectrophotogram

**Table-4.68 Data of calibration curve of PAN in aqueous solution of CPB**

Concentration of PAN	Absorbance
6.41E-6	0.105
1.925E-5	0.297
3.209E-5	0.524
4.49E-5	0.733
5.77E-5	0.924
9.628E-5	1.538
1.28E-4	2.004
1.6E-4	2.355

Using absorbance data from Table-4.68, we can calculate corresponding concentration of dye that is absorbed from Table-4.67 with the help of a plot.

## Complexation

### Calculation of formation constant, Molar absorptivity, and the Sandell's sensitivity for Cu(ii)-PAN complex in the micelle of CPB in aqueous media

#### Calculation of Molar absorptivity of Cu(II)-PAN complex

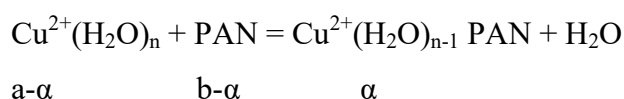
The value of  $\epsilon$  is calculated using the following equation

$$\begin{aligned}\epsilon &= \frac{A}{cl} \\ &= \frac{0.278}{1.2 \times 10^{-5} \times 1} \quad [\text{Where „A“ is 0.278, „c“ is } 1.2 \times 10^{-5} M, \text{ and „l“ is 1 cm}] \\ &= 2.316666 \times 10^4 \text{ L/mol/cm}\end{aligned}$$

Moreover, the mean value of the molar absorptivity ( $\epsilon$ ) calculated by the method of least squares as the slope of the straight line going through the origin. The mean value of the molar absorptivity ( $\epsilon$ ) of Cu(II)-PAN complex was found to be  $2.32249 \times 10^4$  L/mol/cm.

#### Calculation of formation constant of Cu(ii)-PAN complex

Formation constant or stability constant is the equilibrium constant for the formation of a complex in solution. The formation of a complex between Cu(II) ion, and PAN is usually a substitution reaction. Cu(II) ion stays in solution as hydrated, so the reaction for the formation of complex is written as;



The equilibrium constant for this reaction is given by

$$K_f = \frac{[\text{Cu}^{2+}(\text{H}_2\text{O})_{n-1}(\text{PAN})][\text{H}_2\text{O}]}{[\text{Cu}^{2+}(\text{H}_2\text{O})_n][\text{PAN}]}$$

In dilute solution the concentration of water is effectively constant. The expression becomes

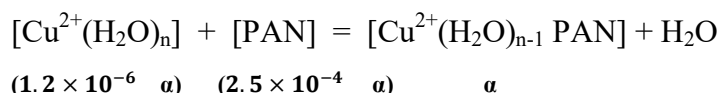
$$K_f = \frac{[\text{Cu}^{2+}(\text{PAN})]}{[\text{Cu}^{2+}][\text{PAN}]}$$

$$\text{so, } K_f = \frac{\alpha}{[a-\alpha][b-\alpha]}$$

We calculated the value of  $\alpha$  for the [Cu(II)-(PAN)] complex using the following equation

$$A = \epsilon cl$$

$$\text{Or, } c = \frac{A}{\epsilon l}$$



When absorbance „A“ is 0.278, we found the value of  $\alpha = 1.19699 \times 10^{-5}$  M using the equation  $c = \frac{A}{\epsilon l}$

$$\text{So, } K_{f1} = \frac{\alpha}{[a-\alpha][b-\alpha]}$$

$$= \frac{1.19699 \times 10^{-5}}{(1.2 \times 10^{-6} - 1.19699 \times 10^{-5})(2.5 \times 10^{-4} - 1.19699 \times 10^{-5})}$$

$$= \frac{1.19699 \times 10^{-5}}{3.01 \times 10^{-8} \times 2.38 \times 10^{-4}}$$

$$= \frac{1.19699 \times 10^{-5}}{(7.1647 \times 10^{-12})}$$

$$= 1.670677 \times 10^6$$

$K_{f2} = 1.6809 \times 10^4$  When absorbance „A“ is 0.015, we found the value of  $\alpha = 1.19699 \times 10^{-5}$  M

$K_{f3} = 6.5210 \times 10^4$  When absorbance „A“ is 0.035, we found the value of  $\alpha = 1.19699 \times 10^{-5}$  M

$K_{f4} = 1.111437 \times 10^5$  When absorbance „A“ is 0.045, we found the value of  $\alpha = 1.19699 \times 10^{-5}$  M

**The average formation constant ( $K_f$ ) of Cu(II)-PAN complex is  $4.659599 \times 10^5$**

### The Sandell's sensitivity calculation

The Sandell's sensitivity is the concentration of the analyte (in  $\mu\text{g mL}^{-1}$ ) which will give an absorbance of 0.001 in a cell of path length 1cm and is expressed as  $\mu\text{g cm}^{-2}$ .

$$\text{Sandell's sensitivity} = \frac{[M] \times M_w \times 10^6 \times 0.001}{\text{Abs} \times 1000 \text{ml}}$$

$$= \frac{2 \times 10^{-6} \times 63.546 \times 10^6 \times 0.001}{0.045 \times 1000}$$

$$= 0.00282 \mu\text{g cm}^{-2} \text{ Cu(II) ion}$$

Average Sandell's sensitivity of Cu(II)-PAN complex is  $2.84 \times 10^{-3} \mu\text{g cm}^{-2}$ .